8

NOAA ATLAS No. 8

Atlas of Tropical Sea Surface Temperature and Surface Winds

Silver Spring, Md.
June 1989

U.S. DEPARTMENT OF COMMERCE
National Oceanic and Atmospheric Administration
National Weather Service

C 55.22:

NOAA ATLAS No. 8

Atlas of Tropical Sea Surface Temperature and Surface Winds

Michael S. Halpert, C.F. Ropelewski
Climate Analysis Center
National Meteorological Center
National Weather Service

Silver Spring, MD.
June 1989

U.S. DEPARTMENT OF COMMERCE
Robert Mosbacher, Secretary
National Oceanic and Atmospheric Administration
William E. Evans, Under Secretary
National Weather Service
Dr. Elbert W. Friday, Jr., Assistant Administrator

TABLE OF CONTENTS

ABSTRACT 1

INTRODUCTION 1

DATA AND ANALYSIS 3

DISCUSSION 4

1. SST Means and Variances 4

2. Surface Wind Means and Variances 5

3. El Niño/Southern Oscillation Composites 6

4. Equatorial Time-Longitude Cross Sections 7

5. Harmonic Analysis 7

APPENDIX A 10

APPENDIX B 11

REFERENCES 12

FIGURES 14

COPIES MAY BE OBTAINED FROM:

Climate Analysis Center
W/NMC52
5200 Auth Road
Washington, D. C. 20233

Atlas of Tropical Sea Surface Temperatures and Surface Winds

Abstract

An atlas of sea surface temperatures (SSTs) and surface winds over the global tropical oceans based on the Comprehensive Ocean Atmosphere Data Set (COADS) is presented. The emphasis of the atlas is the evolution of the annual cycle and variations about it. Mean sea surface temperature, zonal and meridional wind means, standard deviations, differences from the annual mean and differences from the zonal mean are presented for the period 1950-1979, along with the vector wind means and differences from the annual mean. Time-longitude cross sections from 1950-1987 are shown for the mean, anomaly and difference from the annual mean for the zonal wind, meridional wind and SST. Mean and anomalous ENSO composites for the vector wind and SST based on the years 1951, 1953, 1957, 1965, 1969, 1972, and 1976 are presented. The first and second harmonic of the SST, the zonal wind and meridional wind are also shown. The first and second harmonic of the 200 mb zonal wind and the outgoing longwave radiation (OLR) are included in order to give an indication of the circulation throughout the tropical troposphere.

INTRODUCTION

This atlas contains descriptions of the annual cycle of sea surface temperatures (SSTs) and surface winds over the global tropical oceans from 30^{o}N to 30^{o}S. It differs from other recent similar efforts--Sadler et al. (1987), Wright (1988), Shea (1986) and Levitus (1982)--in that its emphasis is on the progression of the annual cycle and variations about the annual cycle. Also included are composite analyses for the principal El Niño/Southern Oscillation (ENSO) episodes occurring during the period 1950 to 1979. The intent of this atlas is to provide a more complete description of the annual cycle in the tropical ocean basins. None of the individual sets of analyses presented here are unique. However, taken as a whole, the atlas provides an integrated description of tropical variability in the context of global ocean-atmosphere interactions. The various analyses, described below, were selected to emphasize different aspects of annual variability.

The atlas contains standard climatological fields: the 1950-1979 mean and interannual standard deviation, by month, for the sea surface temperature (SST), zonal and meridional wind components and mean vector wind maps (derived from the wind components). In addition, analyses are presented depicting mean monthly differences from the annual mean for the SST, vector wind and wind components, as well as monthly means with the zonal mean removed (asymmetric component) for the SST and the wind components. These representations of the annual cycle, along with maps of the annual means, provide a different perspective from which to examine the characteristic variability in the tropical belt. The annual and semi-annual

cycles for the SST and the wind components are also shown as the first and second harmonics of the 12 monthly 30-year means, following the analysis of Horel (1982). The relative magnitudes of the semi-annual and annual cycles are also given for each of the variables of interest.

In order to get a better indication of the atmospheric circulation through the depth of the tropical troposphere, the first and second harmonics of the 200 mb zonal wind are also shown. Finally, the annual and semi-annual cycles of the outgoing longwave radiation (OLR) are included as indications of convective activity and diabatic forcing (Richards and Arkin, 1981) in the tropics and also to depict the relationship of their annual cycle to the SST and winds.

In addition to the mean fields and harmonic analysis, equatorial time-longitude cross sections for the period 1950-1987 are presented for the SST and wind components. A unique feature of this atlas is the presentation of three sets of time-longitude cross sections. These are based on 1) the observed monthly mean fields, 2) anomalies from the 1950-1979 period monthly means, and 3) monthly deviations from the 1950-1979 annual mean. Cross sections depicting the mean annual cycle are also presented for comparison. Mean and anomalous composites of the vector wind and SST for ENSO events beginning two seasons before until two seasons after the episode are also shown.

The data used to compute the fields presented in this atlas come from the Comprehensive Ocean-Atmosphere Data Set (COADS) (Slutz et al., 1985). Other atlases have been published based on this extensive data set (Sadler et al. 1987; Wright, 1988). Depending on their purpose, atlases can be prepared in a number of different ways. Sadler's atlas was based on data from the 1900-1979 period and used a subjective analysis to present monthly fields for sea level pressure, wind, wind stress and SST. The subjective analysis enabled them to use other available information (coastal effects, persistent patterns, etc.) to produce a climatology that includes small-scale features. In the analysis presented here, the interest is focused more towards large-scale climate anomalies consistent with other Climate Analysis Center (CAC) climate diagnostics.

Ramage (1987) points out that the COADS wind data has larger mean scalar winds during the 1950-1979 period than for the earlier 1900-1939 period. This trend is probably due to changes in measurement techniques. Because of this trend and other possible inaccuracies, as well as the limited amount of data available before 1950, this atlas is based on only the 1950-1979 period. The monthly fields presented here are computer generated from the monthly data on a 2^0 latitude by 2^0 longitude grid. A modified Cressman (1959) interpolation scheme was used to fill in areas where data are missing.

This atlas is designed to be a practical reference for use in conjunction with other CAC climate monitoring products and tools. A multiplicity of techniques were utilized for the analysis and display of the annual cycle and ENSO composites to facilitate the usefulness of the atlas and to stimulate and support climate diagnostics research and real-time climate monitoring.

DATA AND ANALYSIS

The COADS is one of the largest and most complete data sets of marine data available today. The first release consisted of global ship reports from 1854-1979. Release 2 extends the data set until 1987. Initially about 100 million observations, the first release of COADS was reduced to about 72 million reports after the elimination of duplicate entries. These were summarized into 2^{0} latitude by 2^{0} longitude squares. Data used to prepare this atlas came from the COADS monthly summary trimmed file, which was formed by eliminating observations that were more than 3.5 standard deviations away from the mean. More detail about the processing of the COADS can be obtained in Slutz et al. (1985) and Woodruff et al. (1987).

Although there are a tremendous number of observations (over 72 million) in the original data set, large areas of the ocean basins contain very little data. Several regions of the southern Indian ocean, the South Atlantic, and large areas of the equatorial Pacific have less than 20 years of data, except along the principal shipping routes. More detail about the distribution and amount of data may be found in Appendix A. To produce representative field analyses, given the uneven distribution of data, the following procedures were followed:

1. A preliminary 30-year climatology for each surface variable (SST, zonal wind and meridional wind) was computed using all available data for the 1950-1979 period with an interpolation scheme (Cressman, 1959) to create completely filled 2^{0} latitude by 2^{0} longitude fields.

2. Individual monthly fields were then formed using the same interpolation scheme, except individual values were screened against the mean fields to eliminate outliers. Details concerning the various tests used to screen the data and an indication of the amount of data eliminated can be found in Appendix B.

3. A nonlinear filter based on medians, which was developed by Tukey (see Rabiner et al., 1975), was applied spatially to the monthly fields. The algorithm may be found in Reynolds (1989). This filter objectively eliminates extreme values instead of smoothing the extreme values over large areas.

4. The monthly fields were then smoothed with a two-dimensional binomial 1-2-1 filter.

5. After formation of the smoothed monthly fields for the period 1950-1979, the climatology was recomputed by averaging the 30 years of monthly fields.

After recomputation of the monthly climatology, anomaly fields for the 30 years of data were formed and stored. The standard deviations for the SST and the wind components were then computed from the variance of the monthly anomaly fields. The monthly mean vector wind was constructed from the monthly mean wind components. The annual means of all variables were computed by averaging the monthly means.

In addition to the traditional charts depicting the means and standard deviations, a number of supplemental analyses are displayed. These include

a harmonic analysis, in which the phase and amplitude for the annual cycle (12-month harmonic) is presented using the technique shown in Hsu and Wallace (1976). Equatorial time-longitude cross sections for the wind components and SST are also presented. These were computed by averaging the individual monthly data fields in the latitude band from $5^{o}S$ to $5^{o}N$ in 5^{o} longitude segments. The cross sections of the equatorial annual cycles were prepared similarly, except the base period mean was used. Finally, the eight season ENSO composites were computed by averaging data for the following seven ENSO episodes: 1951, 1953, 1957, 1965, 1969, 1972, and 1976.

The OLR data used in the harmonic analyses are derived from AVHRR window channel radiances. A description of the data processing may be found in Gruber and Winston (1978). OLR means and variances can be found in the Atlas of Outgoing Longwave Radiation Derived from NOAA Satellite Data (Janowiak et al., 1985). The 200 mb zonal winds are derived from the NMC operational analysis. Details about the different analyses used through February 1979 can be found in Arkin (1982). Other details through 1982 can be found in Kistler and Parrish (1982). Means and variances for the 200 mb zonal wind can be found in the Atlas of the Tropical and Subtropical Circulation Derived from National Meteorological Center Operational Analyses (Arkin et al., 1986).

DISCUSSION

The purpose of this discussion is not to present a detailed description of all of the figures shown in this atlas, but rather to serve as a quick reference to some of the major features of the annual cycle.

1. SST Means and Variances

Figures 2a through 17a show the monthly and seasonal mean SST and figures 2b through 17b show the monthly and seasonal SST standard deviations. In the equatorial regions, SSTs show a relatively small annual range, except in the coastal upwelling regions of the tropical eastern Pacific and Atlantic Oceans. In the eastern South Pacific region, temperatures reach their maximum in March along the South American coast, then fall rapidly. A tongue of relatively cold water develops and extends westward along the equator from this region. This westward extension of cooler water also provides greater variability in the SST as far west as the date line. The occurrences of the El Niño (7 out of 30 years) also increases the variability in this region. In the eastern equatorial Atlantic, SSTs reach their maximum in April and May. Away from the equator, the annual cycle of SSTs is dominated by the solar annual cycle, with maximum temperatures occurring one or two months after the summer solstice. While the annual range of SST increases poleward, the interannual variability, as expressed in the standard deviation charts, remains largest in equatorial regions.

Some aspects of the annual SST cycle can be seen more easily through examination of the mean monthly differences from the annual mean (Figs. 2c-13c). In the subtropics, the Northern Hemisphere SSTs vary by as much as 5 or 6 degrees from the annual mean, with the largest differences occurring in

the Gulf of Mexico and in the western Pacific. These differences are greatest around February and August, indicative of the lagged response to solar heating in the SSTs. The Southern Hemisphere subtropical SSTs follow a similar pattern, although the magnitudes of the differences are somewhat less. The equatorial regions tend to follow the Southern Hemisphere seasons, but the maximum amplitude of the annual cycle is lagged even more with respect to the solar cycle, with relative maxima in March and minima in September. The extremes in the annual cycle of equatorial SST, thus, tend to occur near the high-latitude transition seasons. The areas of upwelling along the west coast of South America and Africa show up as the only areas along the equator with an amplitude in the annual cycle greater than $2^{o}C$.

2. Surface Wind Means and Variances

Figures 19a-34a and 36a-51a show the monthly and seasonal mean zonal and meridional wind components, while Figs. 19b-34b and 36b-51b show their standard deviations. The mean monthly and seasonal vector winds are found in Figs. 53a-64a and 65-68. The Southwest Monsoon circulation over India and Indochina is evident, with a complete reversal of the wind from the winter season to the summer season. The annual cycle in both the zonal and meridional wind components is greatest in the eastern Indian Ocean, where the Somali Jet reaches a maximum in the northern summer. The shift in the mean position of the Intertropical Convergence Zone (ITCZ) and its strength is depicted by the position of the implied convergence in the meridional component over the eastern Pacific and Atlantic Oceans. This can also be seen in Figs. 19c-30c and 36c-47c, which show the monthly differences from the annual mean for the zonal and meridional winds.

The near equatorial zonal winds are characterized by mean easterlies throughout the Atlantic and Pacific basins for the months of June through October. Mean zonal winds remain near zero throughout the year in the Indian Ocean, with the exception of the Somali Jet region discussed above. Weak equatorial westerlies appear in the Indonesian and New Guinea region in November and extend as far as $160^{o}E$ in December and January. A lobe of zonal westerlies extends to the east-southeast, south of the equator, during this period.

The mean meridional wind pattern shows cross-equatorial flow from the Southern to the Northern Hemisphere over all of the Atlantic basin, with the exception of the extreme western region, and for the eastern Pacific for each month of the year, Figs. 36a-47a. This is a reflection of the preferred positions of the ITCZs north of the equator. Only the western Pacific shows any tendency for mean meridional flow in the opposite sense over the equatorial regions, and then only during the months of December through April. Monthly mean deviations from the annual mean, Figs. 36c-47c, clearly illustrate the large amplitudes of the meridional wind annual cycle in the Atlantic Ocean and eastern Pacific. Both regions show relative northerlies, with respect to the annual mean, in the first half of the calendar year and relative southerlies during the second half of the year. In the Arabian Sea region, relative northerlies from October through April are present to balance the intense southerly flow associated with the June through September monsoon.

The annual mean vector wind, Fig. 52, is characterized by easterlies throughout the analysis domain, except for the Indian Ocean, north of the equator where the summer monsoon dominates the annual mean. Significant mean meridional wind components are reflected in the vector winds in the eastern sections of the ocean basins. In the Pacific, the mean axis of the transition from northeast to southeast trade winds lies north of the equator from Central America to 160°W. West of this longitude, the annual mean trades decrease in magnitude and become almost completely zonal.

Several features of the surface vector wind annual cycle are illustrated in the monthly vector wind differences from the annual vector wind, Figs. 53b-64b. This series of charts illustrates the relative importance of the meridional winds compared to the zonal winds in equatorial regions. One of the most striking features is the January through May (July to October) evolution of relative northerlies (southerlies) north of the equator in the Atlantic and the eastern Pacific basins. As the ITCZs move from their southernmost position in the late Northern Hemisphere winter and early spring, the vector wind differences in these regions indicate a stronger northerly component than the annual mean. In the late Northern Hemisphere summer or fall, when the convergence zone reaches its northernmost position, the meridional wind differences show a southerly maximum. The largest magnitudes of these vector differences from the annual mean wind occur in the transition months of March and September and represent an oceanic monsoonal circulation.

The Indian and southern Asian monsoon circulation is illustrated by the relative southwesterly flow during the months of May through September and the relative northeast winds from October to March. The complete reversal of the relative vector wind over most of the region illustrates the monsoonal character of the circulation throughout the equatorial tropical oceans. The well known Indian and Asian monsoons can be understood in terms of direct thermal circulations arising from the oceanic-continental temperature differences. An examination of the annual cycle of SST, also expressed as deviations from the annual mean, suggests that the monsoonal character of the east Pacific and equatorial Atlantic winds may also be interpreted in terms of direct thermal circulations consistent with theoretical arguments of Lindzen and Nigam,(1987). The evolution of the annual cycle through an examination of the monthly mean SST and wind charts where the zonal means have been removed is shown in Figs. 2d-13d, 19d-30d, and 36d-47d. The monthly means presented in this way, as asymmetrical components, also suggest a direct thermal circulation of the winds near the South Pacific Convergence Zone (SPCZ).

3. El Niño/Southern Oscillation Composites

Sea surface temperatures and anomalies for an eight season ENSO cycle are presented in Figs. 69a-76a and 69b-76b. The seven ENSO years used to compute the composites, listed above, are from Rasmusson and Carpenter (1982). The anomaly composites show general agreement with other published work, although the magnitudes of the anomalies in the Pacific are slightly smaller. This is probably due to the ways the original data were filtered and smoothed. ENSO composites for the mean vector wind and anomaly (Figs. 77a-84a and 77b-84b) show the equatorial Pacific westerly anomalies beginning in the March (0) to May (0) season, reaching a maximum in the

December (0) to February (+1) season, and then quickly dying out so that by the June (+1) to August (+1) season, the westerly anomalies have disappeared. Over the eastern Indian Ocean, strong westerly anomalies appear in the September (-1) to November (-1) season, lasting for just that season. This feature is indicative of a stronger than normal monsoon circulation. One year later, anomalies in that same region become easterly, lasting through the December (0) to February (+1) season.

4. Equatorial Time-Longitude Cross Sections

Time-longitude cross sections of SST and zonal and meridional wind components provide yet another way to examine the annual cycle in equatorial regions (Figs. 85-150). The relatively large amplitude of the SST annual cycle in the equatorial eastern Pacific and Atlantic Oceans, with a range of $3^{o}C$ to $4^{o}C$, compared to the Indian Ocean and western Pacific Ocean, with a range of near $1^{o}C$, is clearly illustrated in Fig. 85. The time-longitude cross section of the zonal wind component (Fig. 107) shows the largest annual cycle in the western Pacific and Indian Oceans, with relatively small amplitudes elsewhere--an annual cycle amplitude pattern which is, in many ways, opposite to that observed in the SST. The meridional wind component cross section (Fig. 129) illustrates the annual cycle of cross equatorial flow as a function of longitude. The Indian Ocean, western Pacific, and western Atlantic equatorial regions experience northerly (southerly) flow in Northern Hemisphere winter (summer), while the meridional component remains southerly over the rest of the Atlantic and Pacific Ocean basins throughout the year.

Time-longitude cross sections of equatorial SST and winds are among the standard analysis tools used for the study of interannual variability and ENSO evolution. We present equatorial cross sections of SST and zonal and meridional wind components from 1950-1987 for the mean (Figs. 86-92, 108-114, and 130-136) and anomalies (Figs. 93-99, 115-121, and 137-143). Cross sections of the monthly differences from the annual mean (Figs. 100-106, 122-128, and 144-150) emphasize the annual cycle and, thus, provide a complementary analysis to the other cross sections. Each of the analyses is useful in describing the evolution of the major swings in the Southern Oscillation, including the 9 major ENSO episodes which occurred during the 1950 to 1987 period. Of particular interest in the monthly differences from the annual mean cross sections is the suggestion that the ENSO episodes (1951, 1953, 1957, 1965, 1969, 1972, 1976/7, 1982/3, 1986/7) are associated with a slight enhancement of the amplitudes in the annual cycle, while the high Southern Oscillation Index years: 1950, 1955, 1956, 1964, 1970, 1973, 1971, and 1975, (Ropelewski and Jones, 1987), show relatively low amplitudes in the annual cycle of SST and winds along the equator.

5. Harmonic Analysis

Harmonic vector diagrams, Figs. 154-158, are yet another way to examine the annual cycle of SST and winds. The first harmonic of the annual cycle of SST, Fig. 154a, shows the clear tendency for the higher latitude SST maxima to occur during the summer seasons in each hemisphere. Near the equator, the maxima tend to occur during March or April (a transition season in both hemispheres), particularly in the eastern ocean basins. The

amplitude of the annual cycle of SST is virtually zero in the central and western equatorial Pacific, as well as being relatively small in the western equatorial Atlantic and all of the equatorial Indian Ocean.

The first harmonics of the annual cycle of the surface wind components, Figs. 155a and 156a, show interesting similarities and differences. The first harmonics of both wind components have large amplitudes in the Indian Ocean north of the equator, a region with a very small annual cycle in SST (Fig. 154a). In the southern Indian Ocean, the first harmonics of the zonal and meridional surface wind components are six months out of phase with each other. The zonal winds are strongest in the southern summer, with maxima around February, while the meridional winds have maxima in August to September. The equatorial zonal surface winds generally have relatively small amplitudes in the annual cycle, while the meridional surface winds in the Atlantic and eastern Pacific north of the equator show strong maxima in northern summer to fall. For the 200 mb level, only the harmonics for the zonal wind are presented, Fig. 157a and 157b. The general pattern of the annual cycle amplitudes tends to resemble that of the SST more closely than either of the surface wind components. The amplitudes of the annual harmonic increase poleward from south of the equator in each ocean basin. There appears to be little or no annual cycle of zonal 200 mb winds in the central and western equatorial Pacific.

The first harmonic of the OLR (Fig. 158a) can be thought of as representing the annual cycle of convective precipitation in the tropics. Since lower values of OLR are associated with convective precipitation, the plotting convention for these harmonic vectors is reversed; the phase of the vectors represents the season with minimum OLR values. The largest amplitudes of the OLR annual cycle occur over the continental areas. Over the oceans, the largest amplitudes of the OLR annual cycle tend to occur near and east of the mean position of the SPCZ. The SPCZ-related maximum in the amplitude of the annual cycle is roughly coincident with the maximum in SST over that region of the Pacific. This area also shows a relative maximum in the amplitude of both the zonal and meridional surface wind annual cycles. The OLR minima occur roughly during the same season as relative minima (maxima) in the surface meridional (zonal) winds. The relative maxima in the OLR annual cycle amplitudes occur slightly south of the axis of minimum 200 mb annual harmonic zonal wind amplitude.

The second harmonics of the annual cycle for these variables, in general, show much smaller amplitudes than the first harmonics, Figs 154b-158b. For SST the amplitudes of the semi-annual harmonics are very small almost everywhere. Only the Arabian Sea area shows significant semi-annual variability. The relative amplitude of the semi-annual surface zonal wind component is a significant fraction of the annual cycle amplitude over large areas of the analysis domain (Fig. 154b) but for the most part, these regions have relatively small amplitudes in both the annual and semi-annual components. Areas of the western North Pacific and the Arabian Sea, however, show semi-annual surface zonal wind variability in the 1 ms^{-1} to 2 ms^{-1} range. The surface meridional wind component (Fig. 156b) shows very little amplitude in the semi-annual components, except in the Arabian Sea and just north of the equator in the eastern Pacific. The plot of the 200 mb zonal wind semi-annual component shows large areas of the western equatorial Pacific and southern Indian Ocean with relatively large amplitudes (Fig. 157b). However, these are regions of relatively weak 200 mb flow, e.g., Arkin et al (1986). There

appears to be no easily perceived relationship between the OLR second harmonic (Fig. 158b) and the second harmonics in the wind fields or SST. Unlike the first harmonic, the largest values of the second OLR harmonic tend to occur over the oceans, particularly in the western Pacific north of the equator and the eastern Pacific south of the equator. The OLR second harmonic is also relatively large in portions of the north Atlantic and Indian Oceans.

ACKNOWLEDGMENTS

The authors wish to thank John Kopman for his help in preparing the large volume of figures and Kathy Stevenson for her help in preparing the text. Dick Reynolds was most helpful in devising the filtering techniques, and he and Tony Barnston provided useful comments about the text. The authors also wish to thank Mary Jo Nath and Bram Oort for providing the 1950-1979 data and Steven Worley for providing the 1980-1987 data. We also owe a debt of gratitude to Gene Rasmusson for suggesting several of the analyses and for providing the initial encouragement to produce this atlas.

APPENDIX A

DATA QUANTITY AND DISTRIBUTION

Despite the very large number of total observations available in the COADS, large areas of the Southern Hemisphere oceans have very little data available throughout the decade of the 1950s. Figure A1 shows which grid squares had any SST data during any January of the 1950s, Fig. A2 shows those squares that had data for more than half of the years, and Fig. A3 shows where data was available for all ten Januaries in the decade. It is evident that although most squares had some data during this decade, only the primary ship tracks and areas of the north Atlantic and Indian Oceans had complete data.

The total number of observations increased dramatically from the 1950s to the 1970s. During the 1950s, the number of observations ranged from about 20,000 per month in the early part of the decade to about 50,000 by the end of the decade. By the late 1960s, over 90,000 observations per month were available during some months. There were somewhat less data during the 1970s, with most months having between 55,000 and 70,000 observations per month. Figure A4 shows which grid squares had data for more than five of the Januaries during the 1970s, while Fig. A5 shows which grid squares had data for all ten years. Even during the 1970s, large parts of the Southern Hemisphere and of the Pacific Ocean did not have complete coverage. Small areas of the central Pacific near the date line and off the coast of South America had data for less than half of the years. Figure A6 shows those locations where data were available for at least 10 Januaries during the 30-year period, Fig. A7 where data were available for at least 20, and Fig. A8 where data were available for all 30 Januaries. While most areas had data for more than 10 years, large holes develop in the coverage of the Pacific when looking at areas with greater than 20 years of data. The data coverage is similar for other months and also for the zonal and meridional wind components.

APPENDIX B

DATA SCREENING PROCEDURES

The data used to produce the smoothed SST and wind fields were screened in order to filter out bad data. An SST data value for a grid square was rejected if it failed any of the following tests (values used for 1980-1987 are in parenthesis):

1. The absolute value of the anomaly is greater than $5^{o}C$ ($8^{o}C$).

2. The absolute value of the anomaly is greater than $3.5^{o}C$ ($6^{o}C$) and the number of observations is 2.

3. The absolute value of the anomaly is greater than $2.5^{o}C$ ($4^{o}C$) and the number of observations is 1.

4. The number of observations is 1, and there are no observations in any of the four neighboring boxes to the north, south, east, or west.

5. The magnitude of the difference between the gridded 2^{o} anomaly value and the nearest grid point in a separate analysis of the anomaly field on a 4^{o} grid was greater than $2^{o}C$.

The following tests were used for the wind data (the same tests were used for all 38 years):

1. The absolute value of the anomaly is greater than 20 m/s.

2. The absolute value of the anomaly is greater than 15 m/s and the number of observations is 2.

3. The absolute value of the anomaly is greater than 10 m/s and the number of observations is 1.

4. The number of observations is 1, and there are no observations in any of the four neighboring boxes to the north, south, east, or west.

5. The magnitude of the difference between the gridded 2^{o} anomaly value and the nearest grid point in a separate analysis of the anomaly field on a 4^{o} grid was greater than 4 m/s.

These data screening techniques were used mainly to filter out misplaced points or data that is clearly incorrect. Generally less than one percent of the data were eliminated by the above screening techniques. The 2^{o} grid comparison to the 4^{o} grid was the test that removed about 90% of the data which were eliminated. The other tests generally eliminated less than 50 observations per month.

REFERENCES

Arkin, P. A., 1982: The relationship between interannual variability in the 200 mb tropical wind field and the Southern Oscillation. Mon. Wea. Rev., 110, 1393-1404.

_____, V. E. Kousky, J. E. Janowiak, and E. A. O'Lenic, 1986: Atlas of the Tropical and Subtropical Circulation Derived from National Meteorological Center Operational Analyses. NOAA Atlas No. 7, U. S. Department of Commerce, National Oceanic and Atmospheric Administration, National Weather Service, Silver Spring, MD, 59 pp.

Cressman, G. P., 1959: An operational objective analysis system. Mon. Wea. Rev., 87, 367-374.

Gruber, A. and A. F. Krueger, 1984: The status of the NOAA outgoing longwave radiation data set. Bull. Amer. Meteor. Soc., 65, 958-962.

Horel, J. D., 1982: On the Annual Cycle of the Tropical Atmosphere and Ocean. Mon. Wea. Rev., 110, 1863-1878.

Hsu, C. F. and J. M. Wallace, 1976: The global distribution of the annual and semiannual cycles in precipitation. Mon. Wea. Rev., 104, 1093-1101.

Janowiak, J. E., A. F. Krueger, P. A. Arkin, and A. Gruber, 1985: Atlas of Outgoing Longwave Radiation Derived from NOAA Satellite Data. NOAA Atlas No. 6, U. S. Department of Commerce, National Oceanic and Atmospheric Administration, National Weather Service, Silver Spring, MD, 44 pp.

Kistler, R. E. and D. F. Parrish, 1982: Evolution of the NMC Data Assimilation System: September 1978-January 1982. Mon. Wea. Rev., 110, 1335-1346.

Levitus, S., 1982: Climatological Atlas of the World Ocean. NOAA Professional Paper No. 13, U. S. Government Printing Office, 173 pp.

Lindzen, R. S. and S. Nigam, 1987: On the role of sea surface temperature gradients in forcing low-level winds and convergence in the tropics. J. Atmos. Sci. 44, 2418-2436.

Rabiner, L. R., M. R. Sambar and C. E. Schmidt, 1975: Applications of nonlinear smoothing algorithm to speech processing. IEEE Trans. on Acoust. Speech Signal Process, ASSP-23, 552-557.

Ramage, C. S., 1987: Secular changes in reported surface wind speeds over the ocean. J. Climat. Appl. Meteor., 26, 525-528.

Rasmusson, E. M. and T. H. Carpenter, 1982: Variations in tropical sea surface temperature and surface wind fields associated with the Southern Oscillation/El Niño. Mon. Wea. Rev., 111, 517-528.

Reynolds, R. W., 1989: A real-time global sea surface temperature analysis. J. of Clim., 1, 75-86.

Richards, F., and P. Arkin, 1981: On the relationship between satellite-observed cloud cover and precipitation. Mon. Wea. Rev., 109, 1081-1093.

Ropelewski, C. F. and P. D. Jones, 1987: An extension of the Tahiti-Darwin Southern Oscillation Index. Mon. Wea. Rev., 115, 2161-2165.

Sadler, J. C., M. A. Lander, A. M. Hori, and L. K. Oda, 1987: Tropical Marine Climatic Atlas. Volume I: Indian and Atlantic Ocean. Department of Meteorology, University of Hawaii, Report No. UHMET 87-01, 51 pp.

Sadler, J. C., M. A. Lander, A. M. Hori, and L. K. Oda, 1987: Tropical Marine Climatic Atlas. Volume II: Pacific Ocean. Department of Meteorology, University of Hawaii, Report No. UHMET 87-02, 27 pp.

Slutz, R. J., S. J. Lubker, J. D. Hiscox, S. D. Woodruff, R. L. Jenne, D. H. Joseph, P. M. Steurer and J. D. Elms. 1985: COADS, Comprehensive Ocean-Atmosphere Data Set, Release 1. Climate Research Program, Environmental Research Laboratory, Boulder, CO, 262 pp.

Wright, P., 1988: An Atlas based on the "COADS" data set: Fields of mean wind, cloudiness and humidity at the surface of the global ocean. Max-Planck-Institute for Meteorology, Hamburg, Federal Republic of Germany, Report 14.

Woodruff, S. D., R. J. Slutz, R. L. Jenne, and P. M. Steurer, 1987: A Comprehensive Ocean-Atmosphere Data Set. Bull. Amer. Met. Soc., 68, 1239-1250.

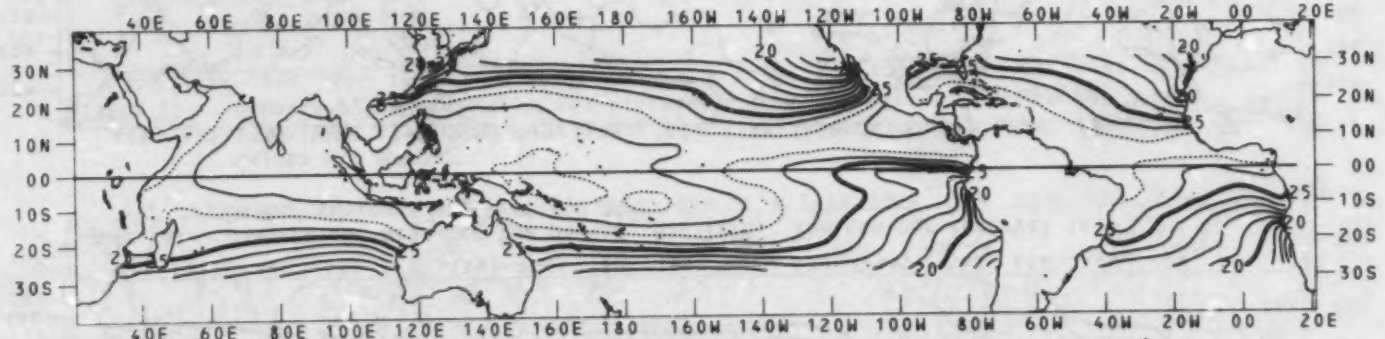

Figure 1. Annual SST mean for the period 1950-1979. The contour interval is 1.0°C. Dashed contours are 27°C and 29°C.

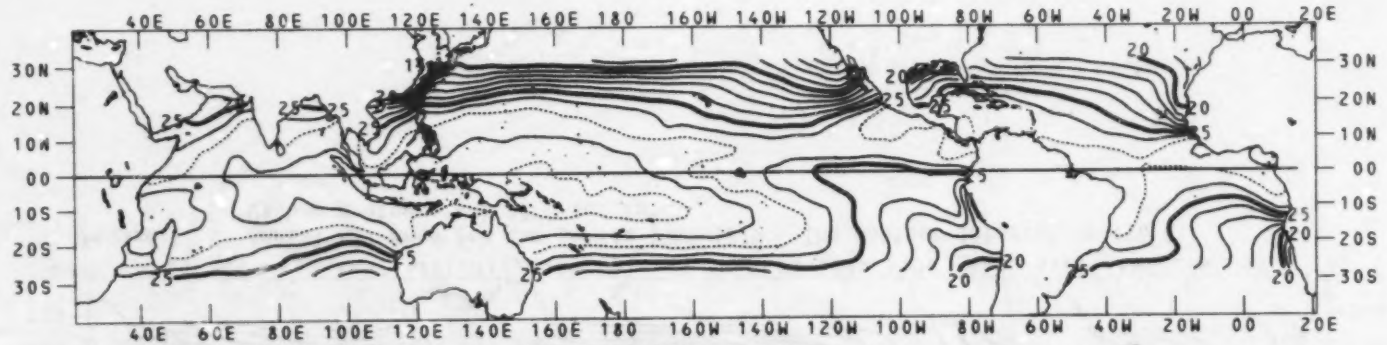

Figure 2a. January SST mean for the period 1950-1979. The contour interval is 1°C. Dashed contours are 27°C and 29°C.

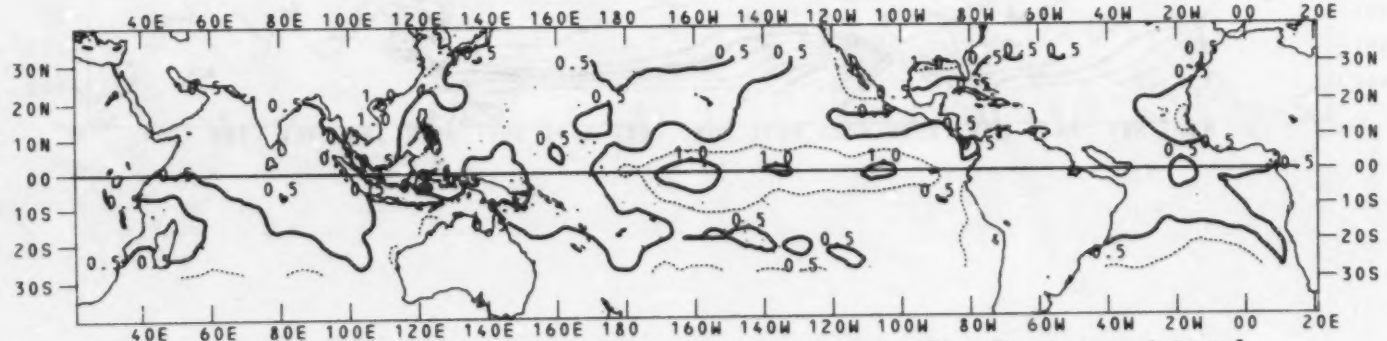

Figure 2b. January SST standard deviation for the period 1950-1979. The contour interval is .25°C. Dashed contours are .75°C and 1.25°C.

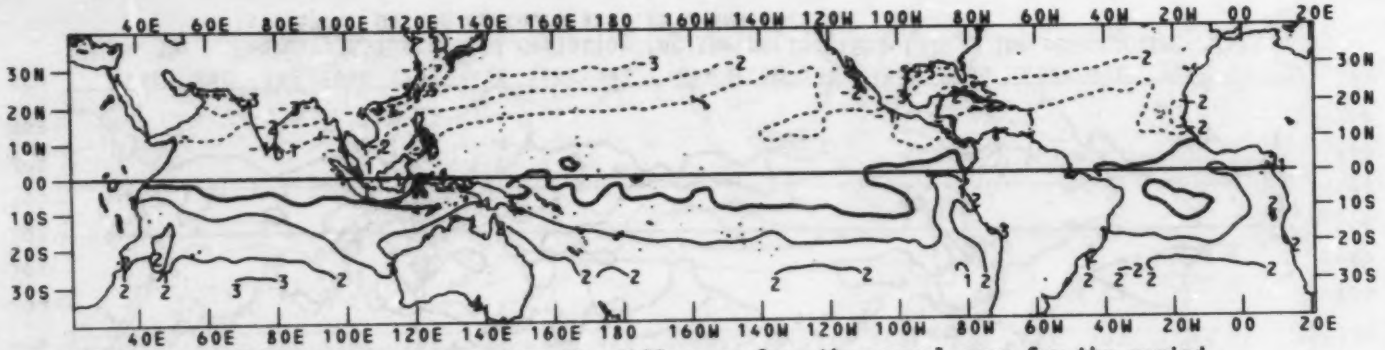

Figure 2c. January SST expressed as the difference from the annual mean for the period 1950-1979. The contour interval is 1°C. The dark line is zero. Negative values are dashed.

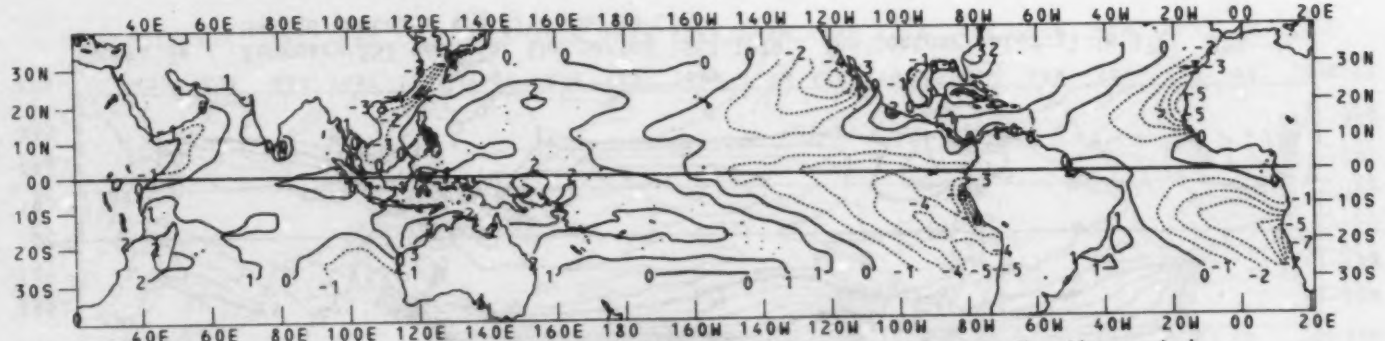

Figure 2d. January SST expressed as the difference from the zonal mean for the period 1950-1979. The contour interval is 1°C. Negative values are dashed.

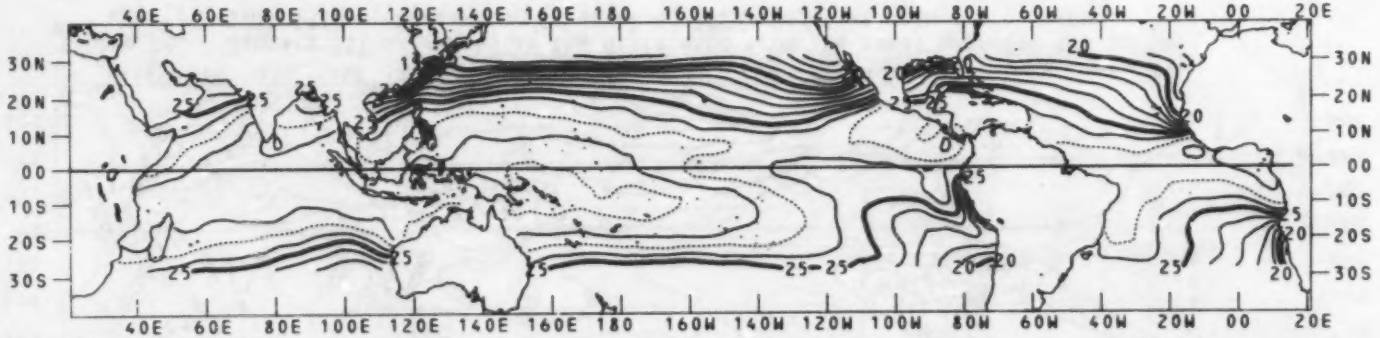

Figure 3a. February SST mean for the period 1950-1979. The contour interval is 1°C. Dashed contours are 27°C and 29°C.

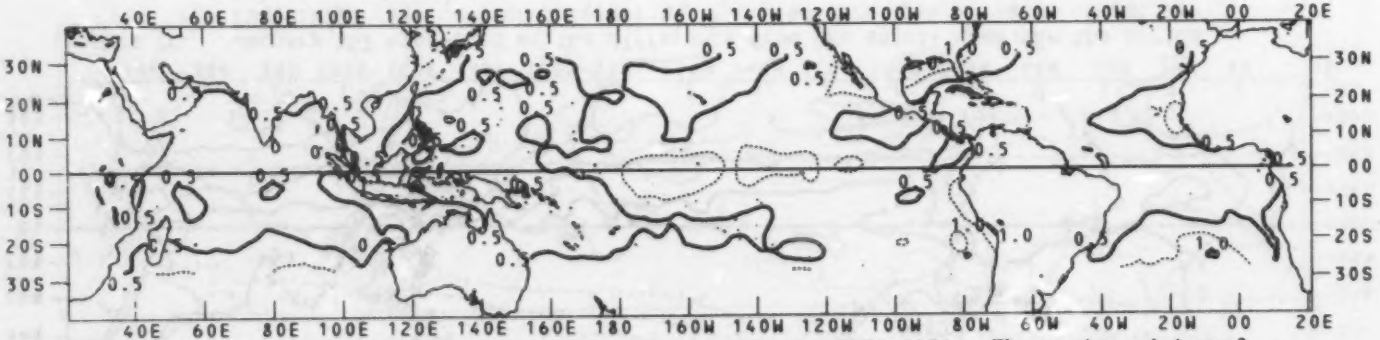

Figure 3b. February SST standard deviation for the period 1950-1979. The contour interval is .25°C. Dashed contours are .75°C and 1.25°C.

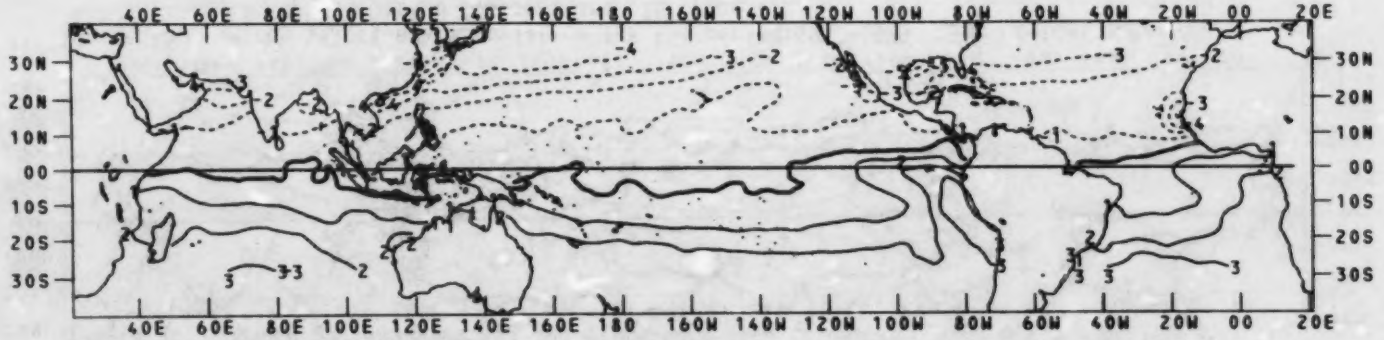

Figure 3c. February SST expressed as the difference from the annual mean for the period 1950-1979. The contour interval is 1°C. The dark line is zero. Negative values are dashed.

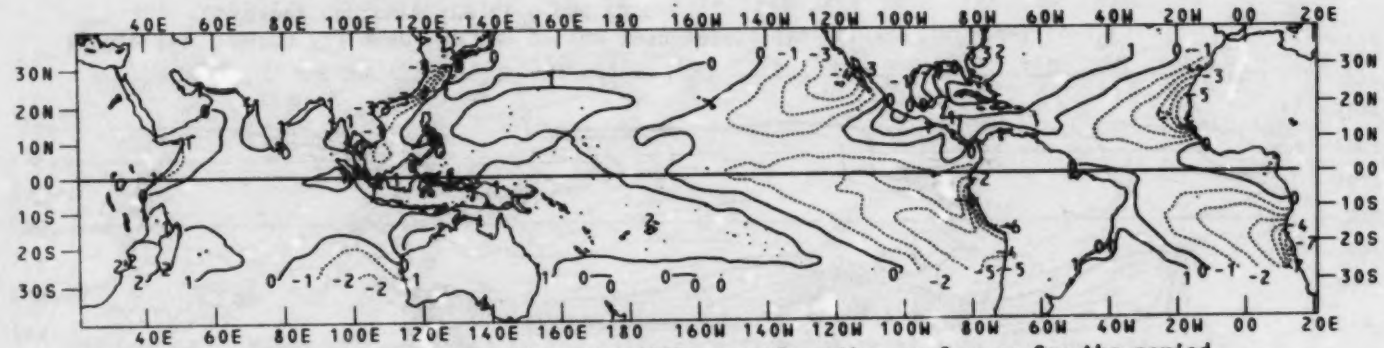

Figure 3d. February SST expressed as the difference from the zonal mean for the period 1950-1979. The contour interval is 1°C. Negative values are dashed.

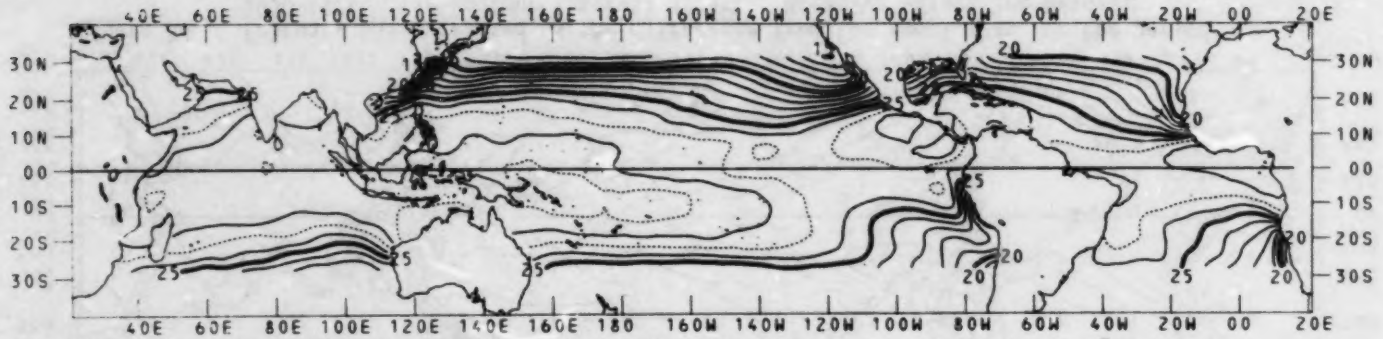

Figure 4a. March SST mean for the period 1950-1979. The contour interval is 1°C. Dashed contours are 27°C and 29°C.

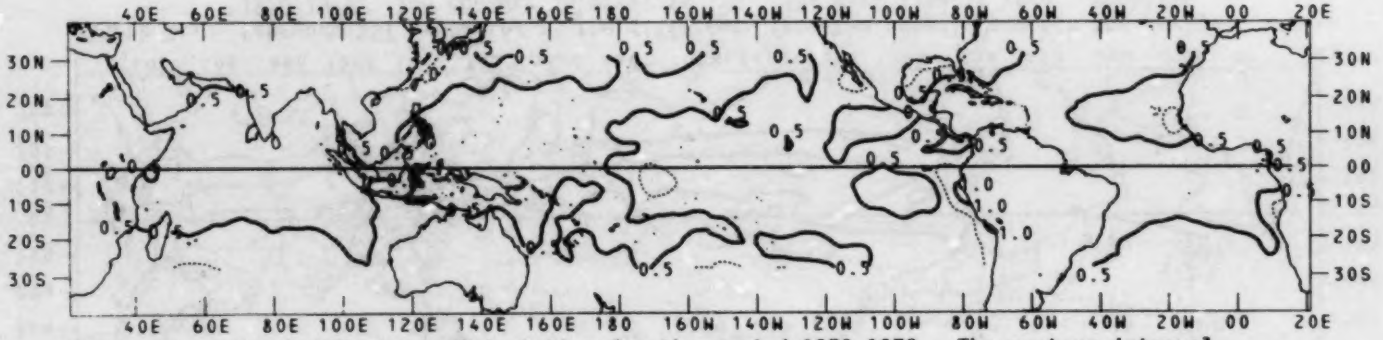

Figure 4b. March SST standard deviation for the period 1950-1979. The contour interval is .25°C. Dashed contours are .75°C and 1.25°C.

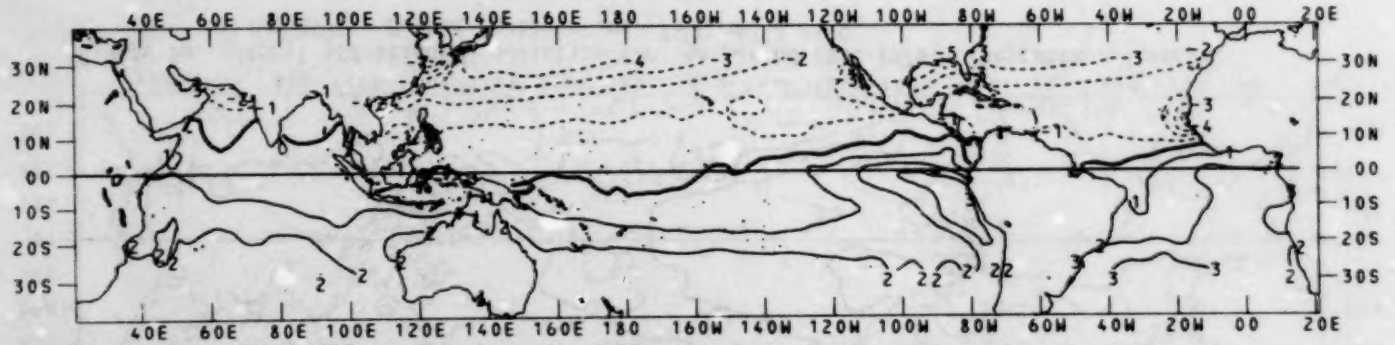

Figure 4c. March SST expressed as the difference from the annual mean for the period 1950-1979. The contour interval is 1°C. The dark line is zero. Negative values are dashed.

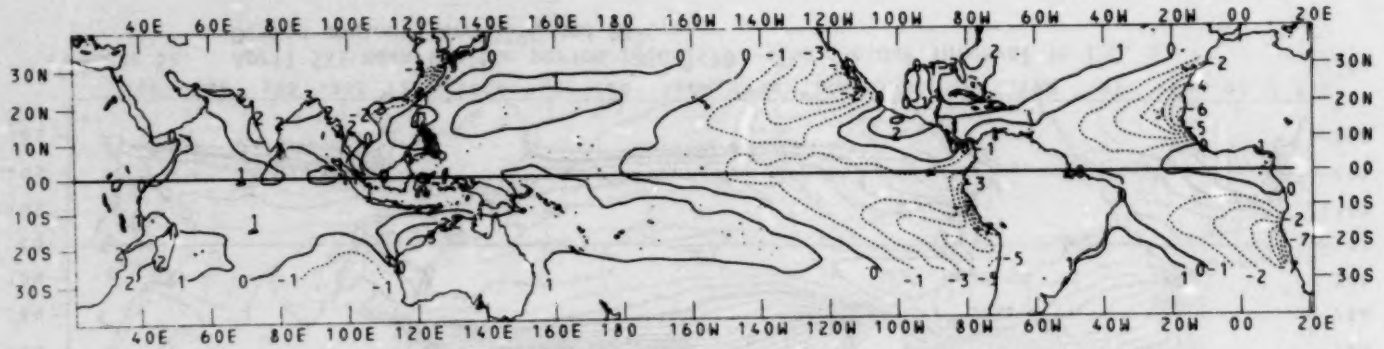

Figure 4d. March SST expressed as the difference from the zonal mean for the period 1950-1979. The contour interval is 1°C. Negative values are dashed.

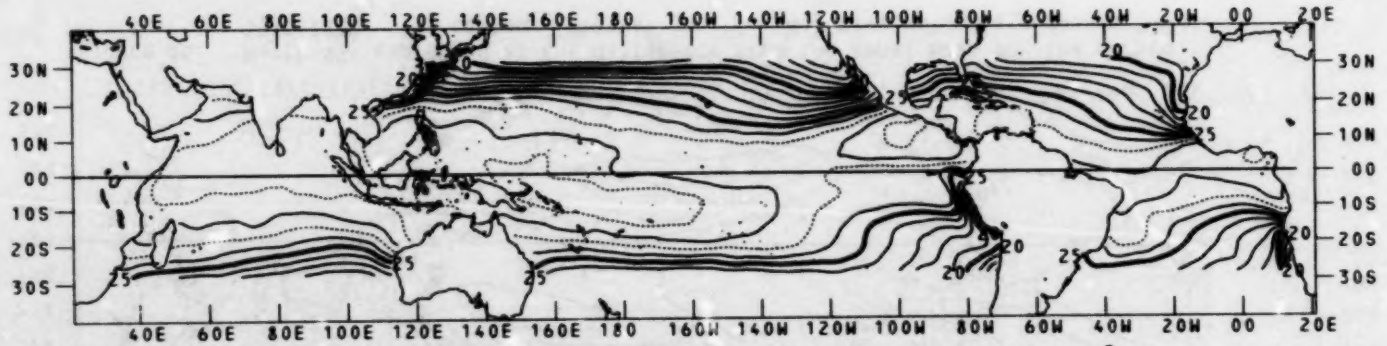

Figure 5a. April SST mean for the period 1950-1979. The contour interval is 1°C. Dashed contours are 27°C and 29°C.

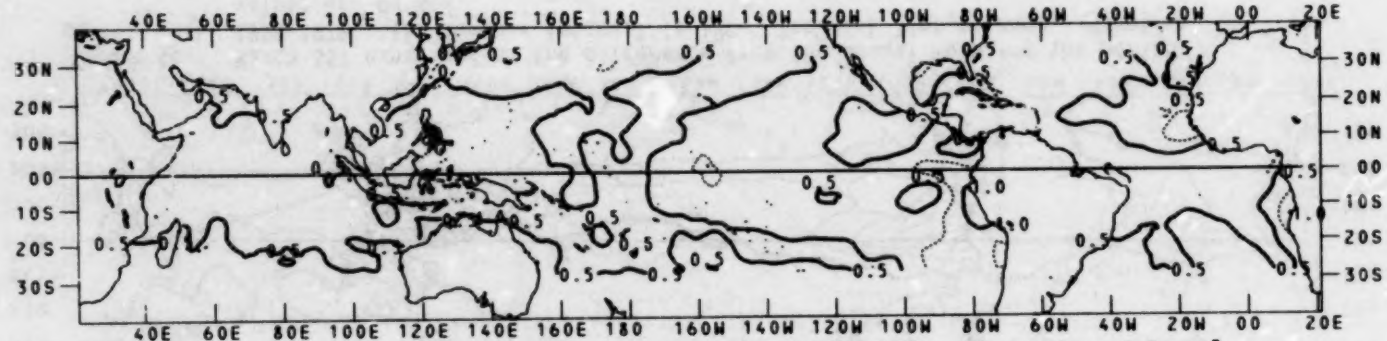

Figure 5b. April SST standard deviation for the period 1950-1979. The contour interval is .25°C. Dashed contours are .75°C and 1.25°C.

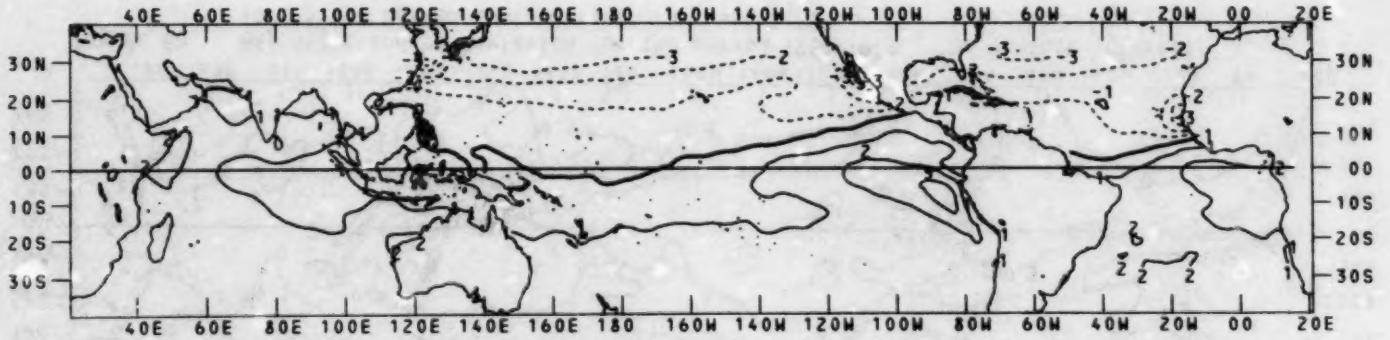

Figure 5c. April SST expressed as the difference from the annual mean for the period 1950-1979. The contour interval is 1°C. The dark line is zero. Negative values are dashed.

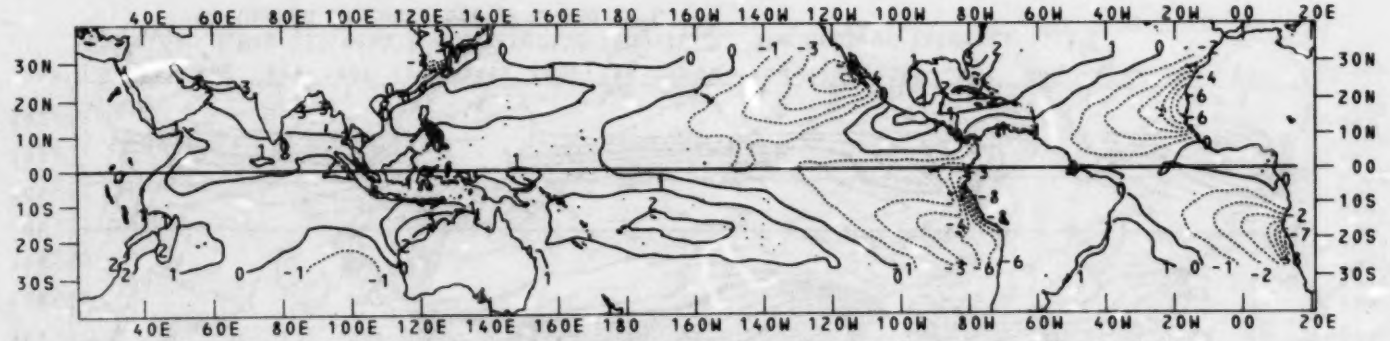

Figure 5d. April SST expressed as the difference from the zonal mean for the period 1950-1979. The contour interval is 1°C. Negative values are dashed.

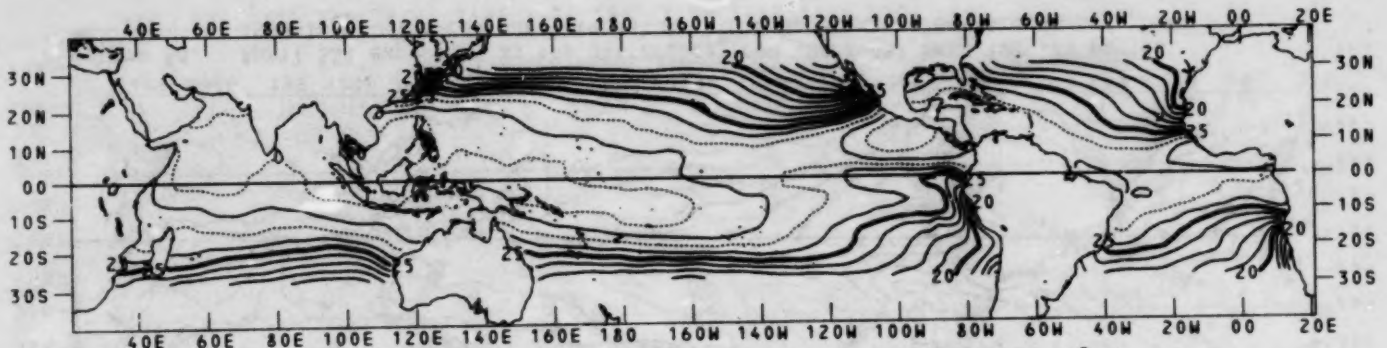

Figure 6a. May SST mean for the period 1950-1979. The contour interval is 1°C. Dashed contours are 27°C and 29°C.

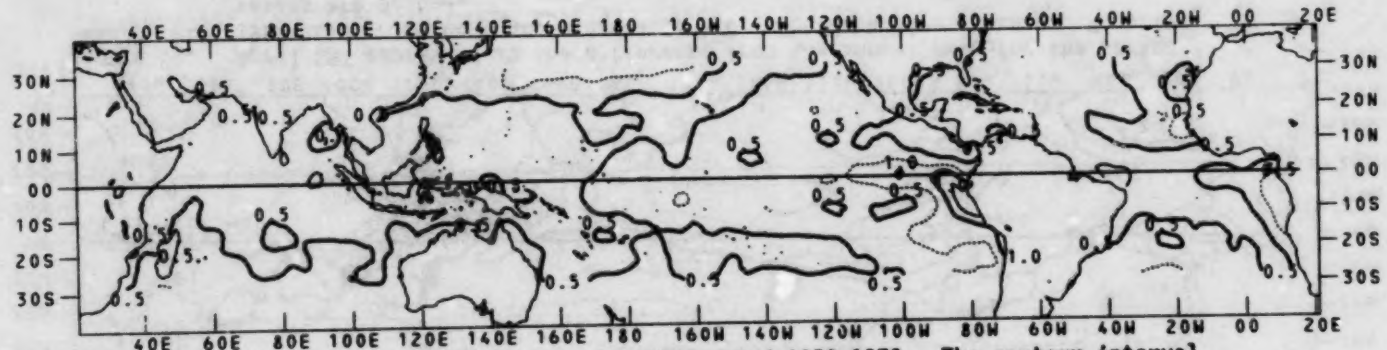

Figure 6b. May SST standard deviation for the period 1950-1979. The contour interval is .25°C. Dashed contours are .75°C and 1.25°C.

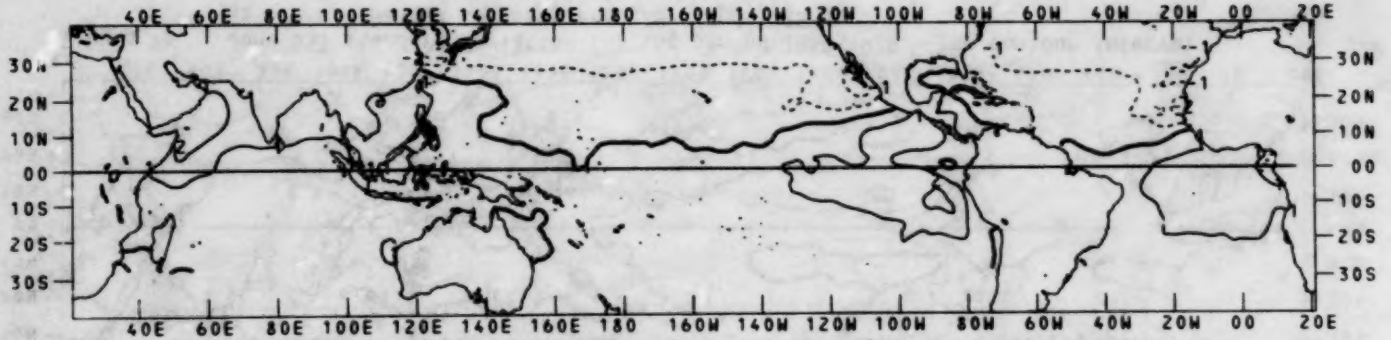

Figure 6c. May SST expressed as the difference from the annual mean for the period 1950-1979. The contour interval is 1°C. The dark line is zero. Negative values are dashed.

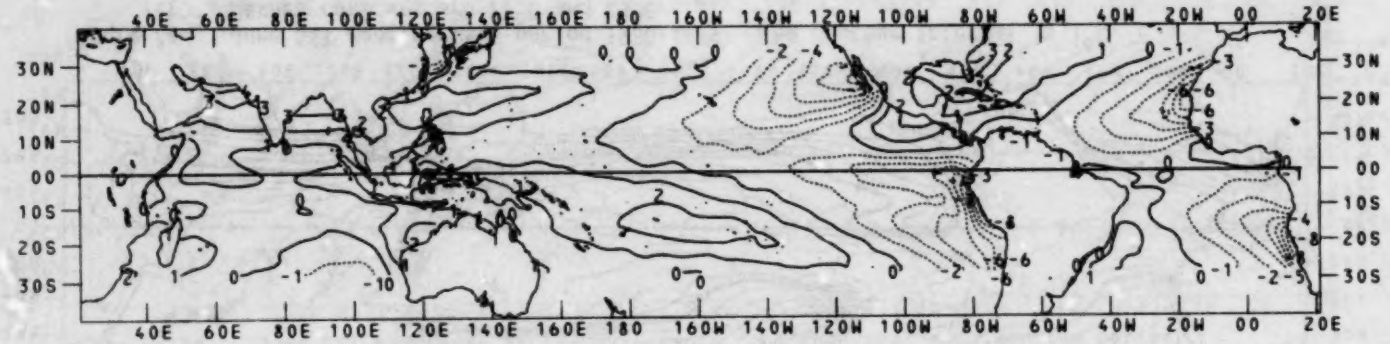

Figure 6d. May SST expressed as the difference from the zonal mean for the period 1950-1979. The contour interval is 1°C. Negative values are dashed.

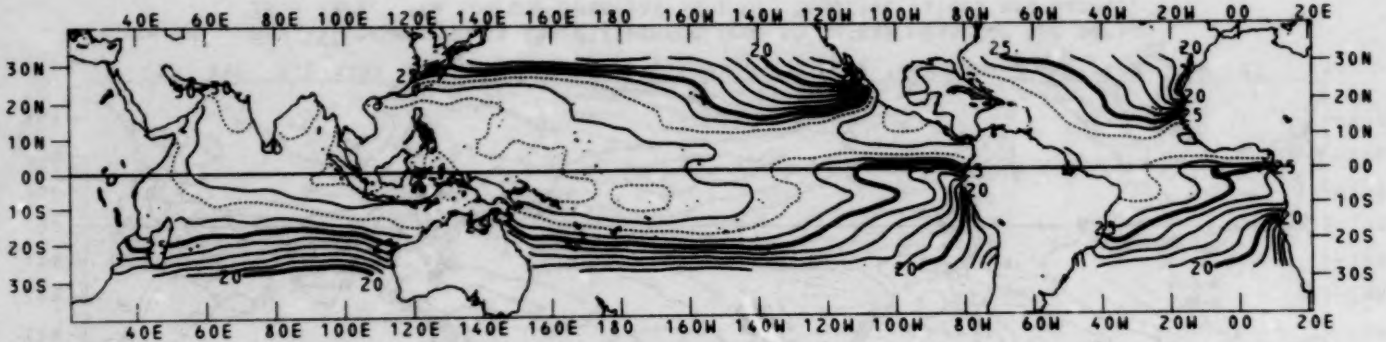

Figure 7a. June SST mean for the period 1950-1979. The contour interval is 1°C. Dashed contours are 27°C and 29°C.

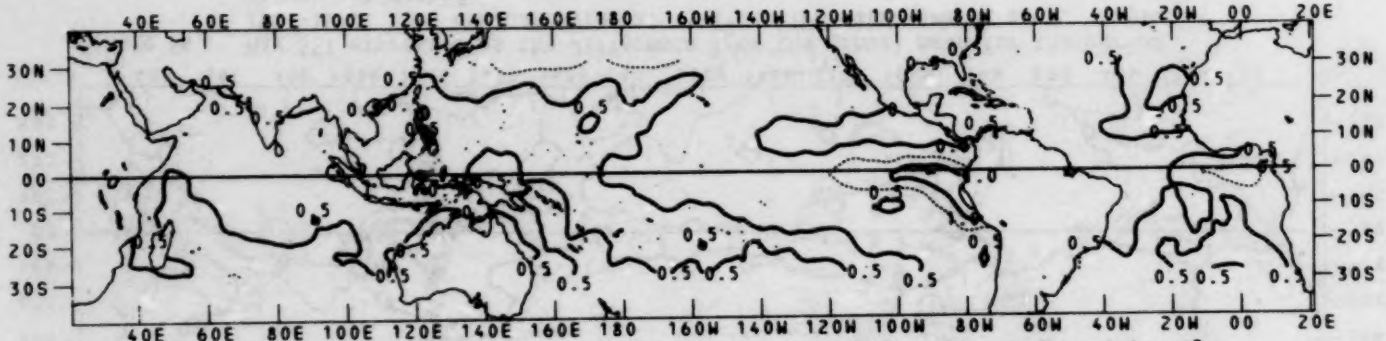

Figure 7b. June SST standard deviation for the period 1950-1979. The contour interval is .25°C. Dashed contours are .75°C and 1.25°C.

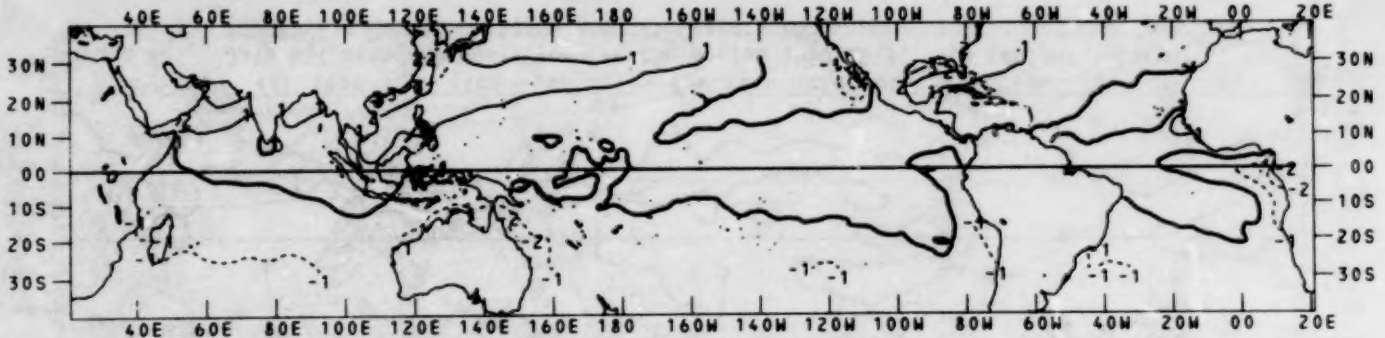

Figure 7c. June SST expressed as the difference from the annual mean for the period 1950-1979. The contour interval is 1°C. The dark line is zero. Negative values are dashed.

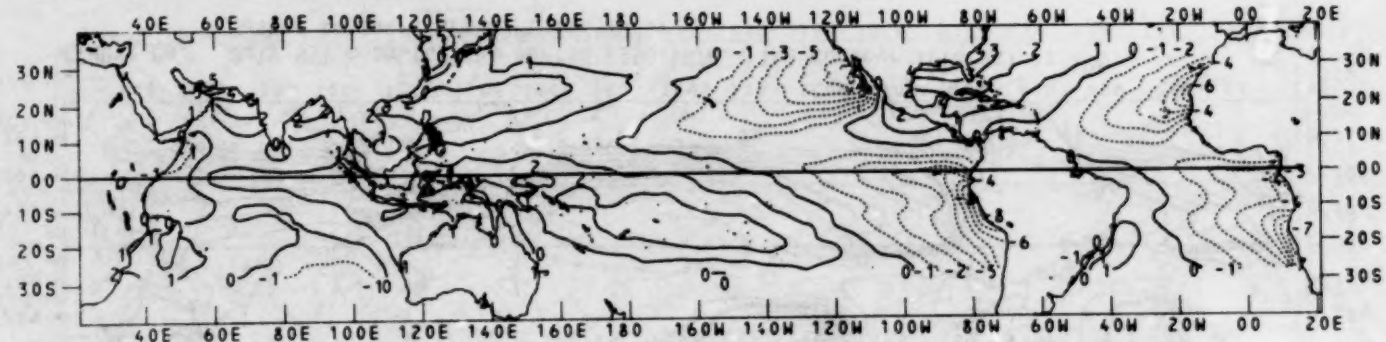

Figure 7d. June SST expressed as the difference from the zonal mean for the period 1950-1979. The contour interval is 1°C. Negative values are dashed.

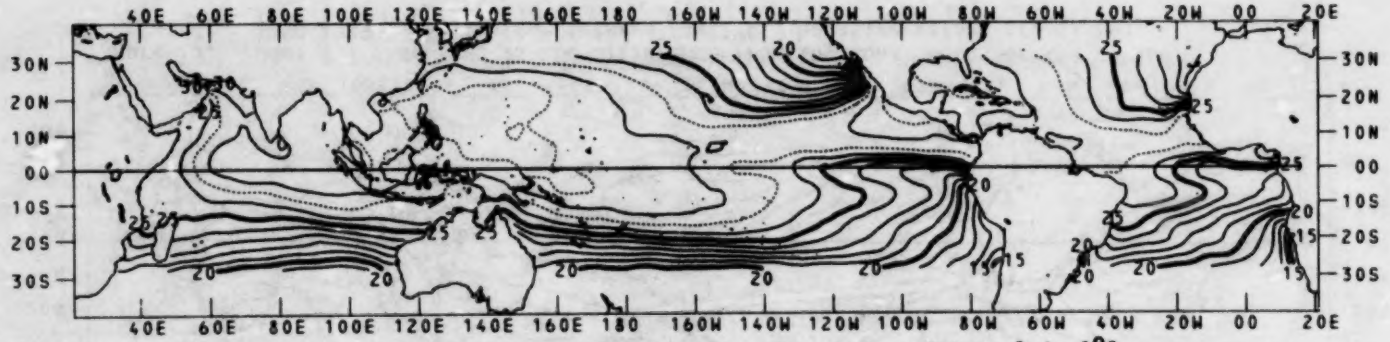

Figure 8a. July SST mean for the period 1950-1979. The contour interval is 1°C. Dashed contours are 27°C and 29°C.

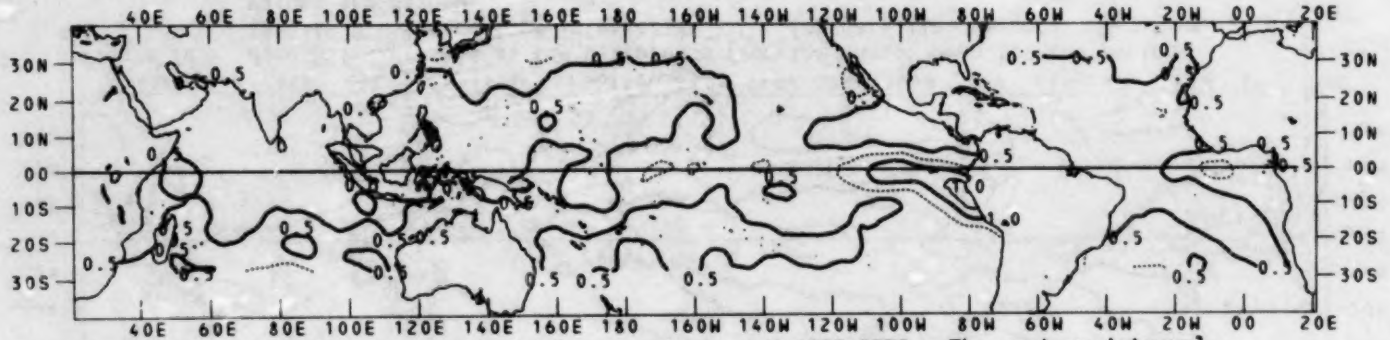

Figure 8b. July SST standard deviation for the period 1950-1979. The contour interval is .25°C. Dashed contours are .75°C and 1.25°C.

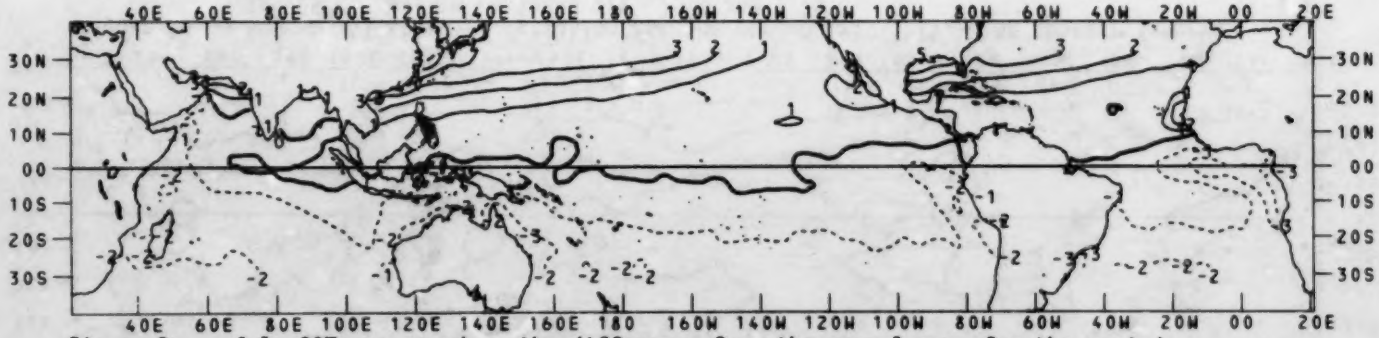

Figure 8c. July SST expressed as the difference from the annual mean for the period 1950-1979. The contour interval is 1°C. The dark line is zero. Negative values are dashed.

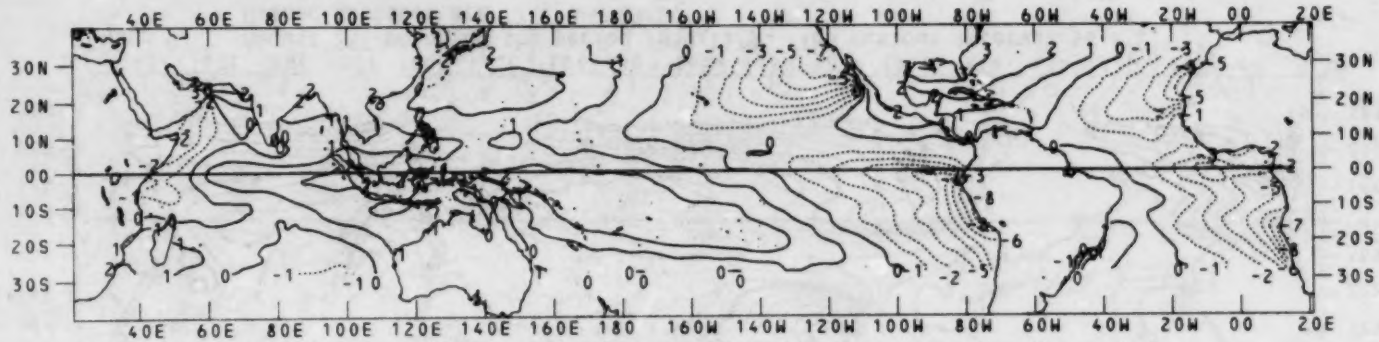

Figure 8d. July SST expressed as the difference from the zonal mean for the period 1950-1979. The contour interval is 1°C. Negative values are dashed.

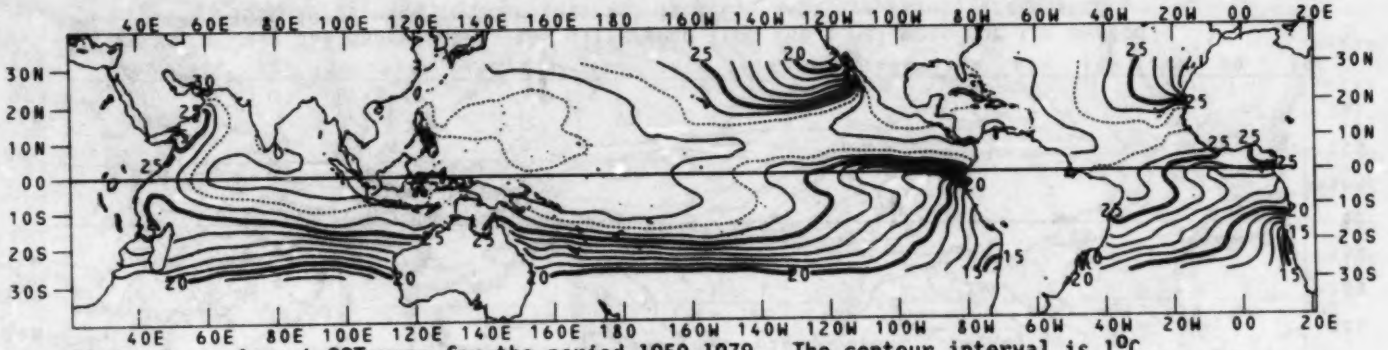

Figure 9a. August SST mean for the period 1950-1979. The contour interval is 1°C. Dashed contours are 27°C and 29°C.

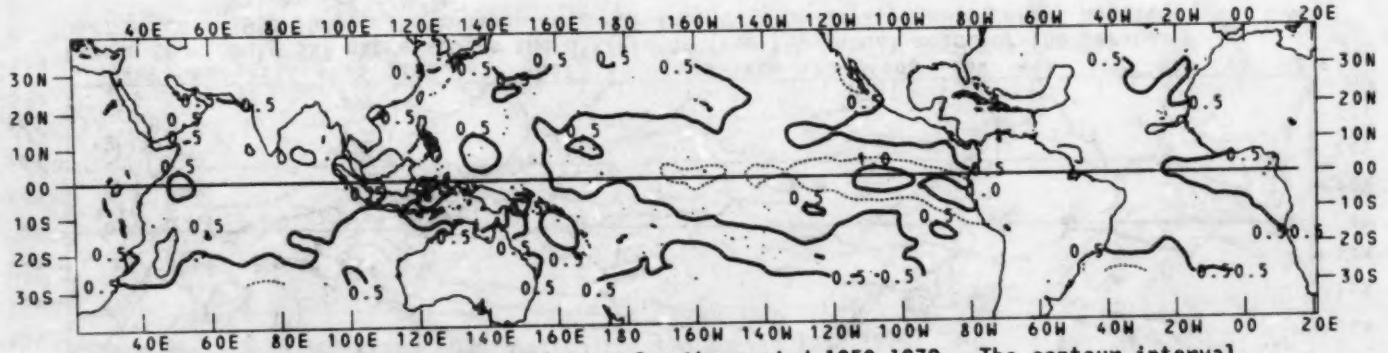

Figure 9b. August SST standard deviation for the period 1950-1979. The contour interval is .25°C. Dashed contours are .75°C and 1.25°C.

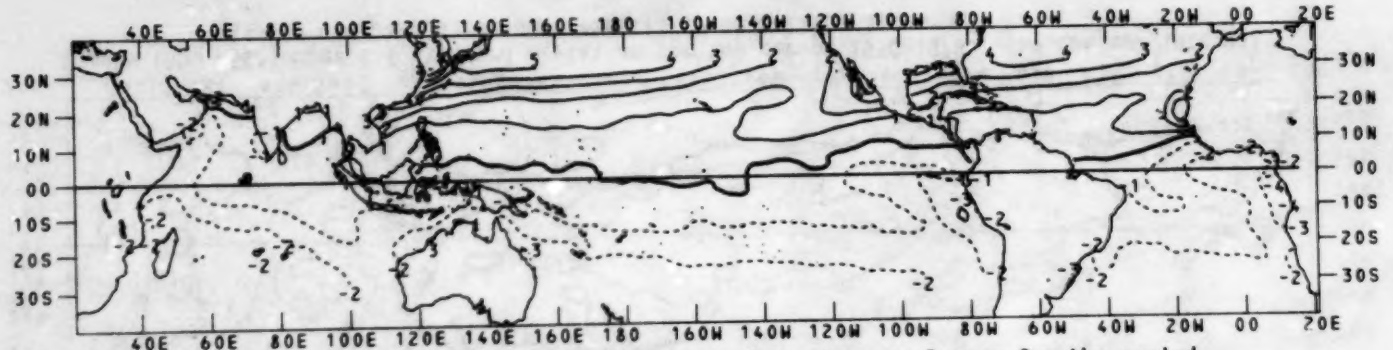

Figure 9c. August SST expressed as the difference from the annual mean for the period 1950-1979. The contour interval is 1°C. The dark line is zero. Negative values are dashed.

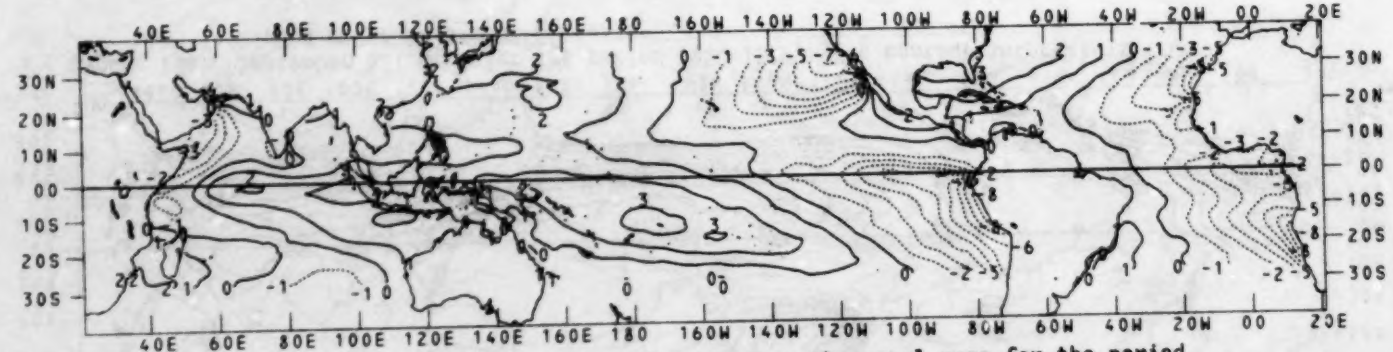

Figure 9d. August SST expressed as the difference from the zonal mean for the period 1950-1979. The contour interval is 1°C. Negative values are dashed.

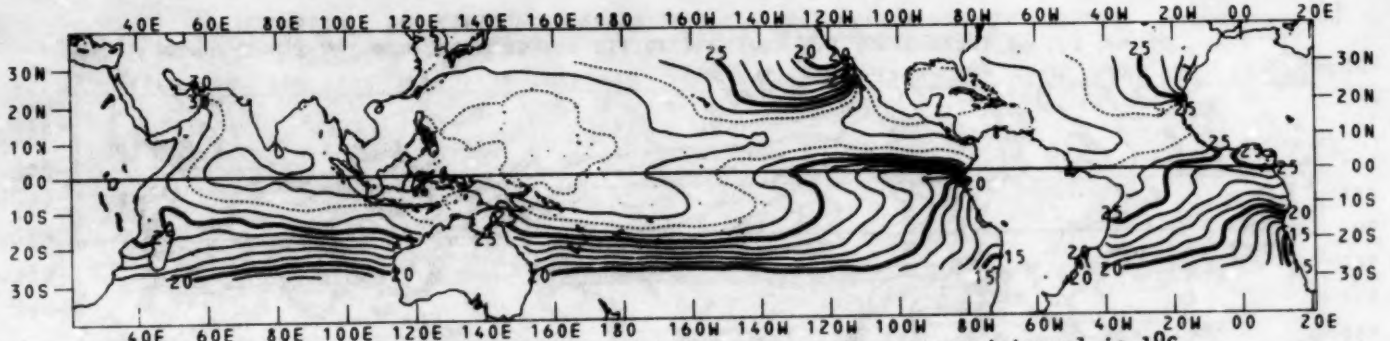

Figure 10a. September SST mean for the period 1950-1979. The contour interval is 1°C. Dashed contours are 27°C and 29°C.

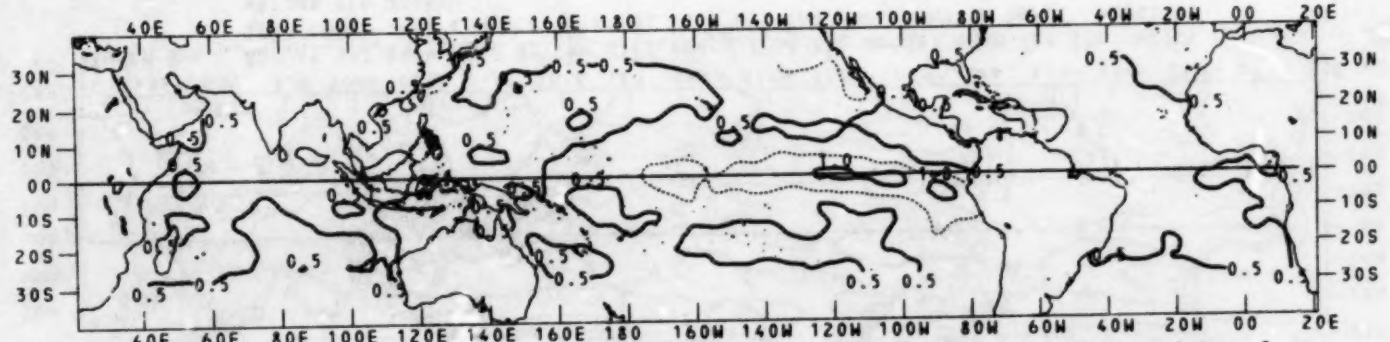

Figure 10b. September SST standard deviation for the period 1950-1979. The contour interval is .25°C. Dashed contours are .75°C and 1.25°C.

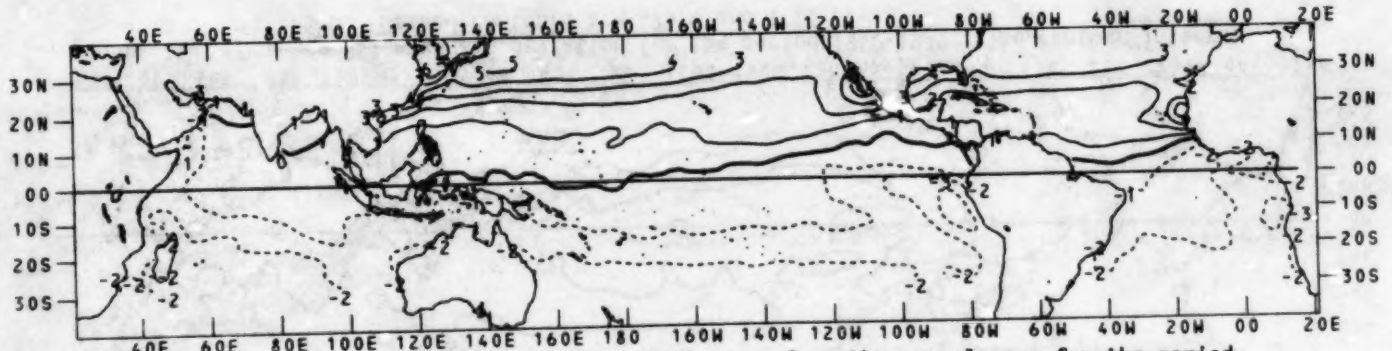

Figure 10c. September SST expressed as the difference from the annual mean for the period 1950-1979. The contour interval is 1°C. The dark line is zero. Negative values are dashed.

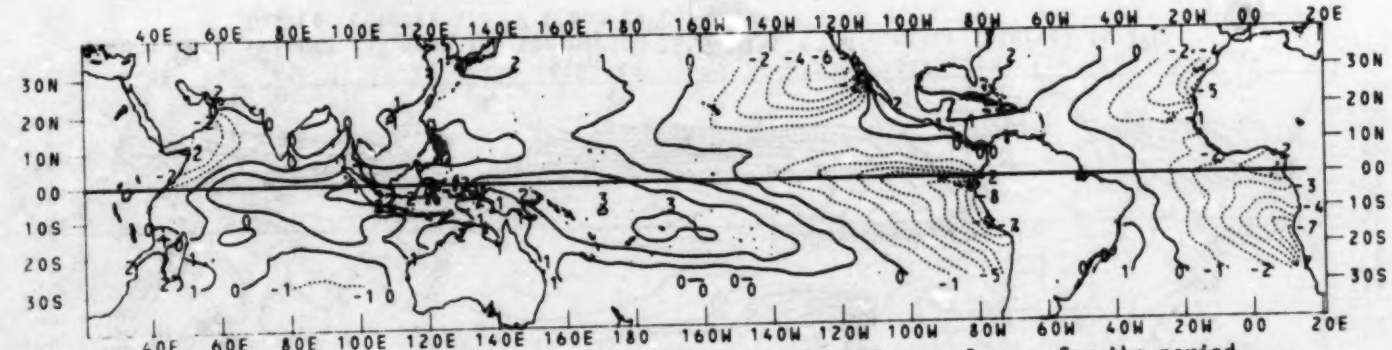

Figure 10d. September SST expressed as the difference from the zonal mean for the period 1950-1979. The contour interval is 1°C. Negative values are dashed.

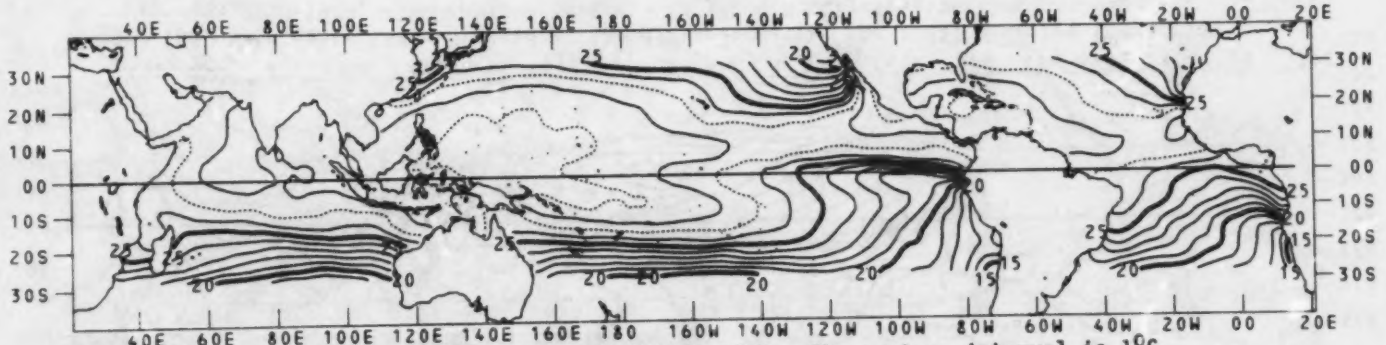

Figure 11a. October SST mean for the period 1950-1979. The contour interval is 1°C. Dashed contours are 27°C and 29°C.

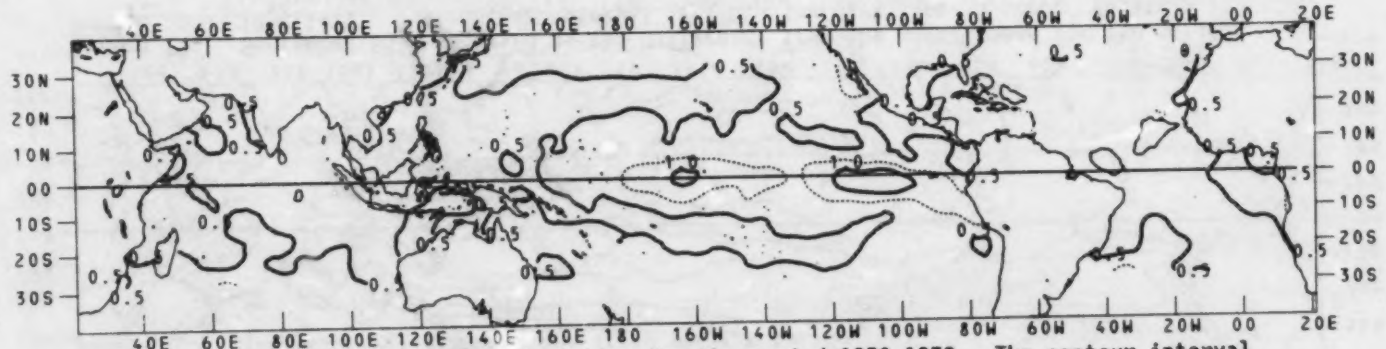

Figure 11b. October SST standard deviation for the period 1950-1979. The contour interval is .25°C. Dashed contours are .75°C and 1.25°C.

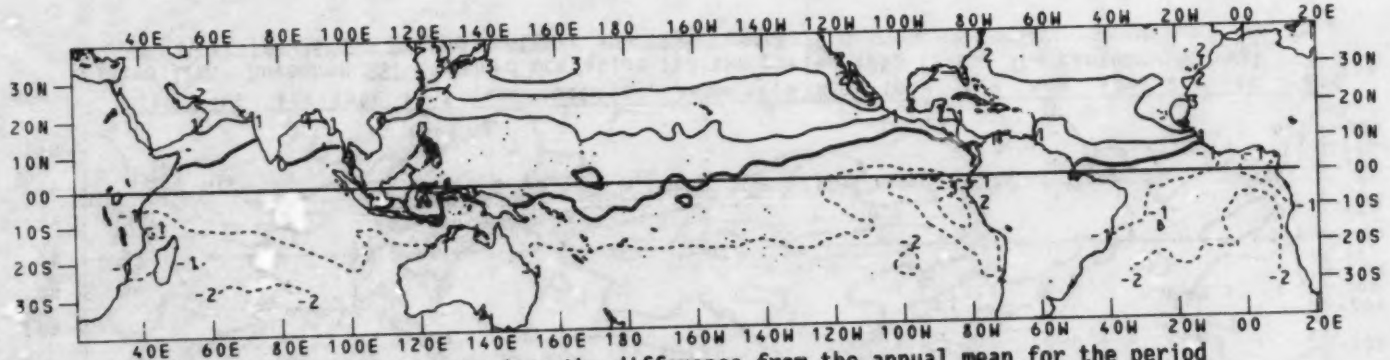

Figure 11c. October SST expressed as the difference from the annual mean for the period 1950-1979. The contour interval is $1^{0}C$. The dark line is zero. Negative values are dashed.

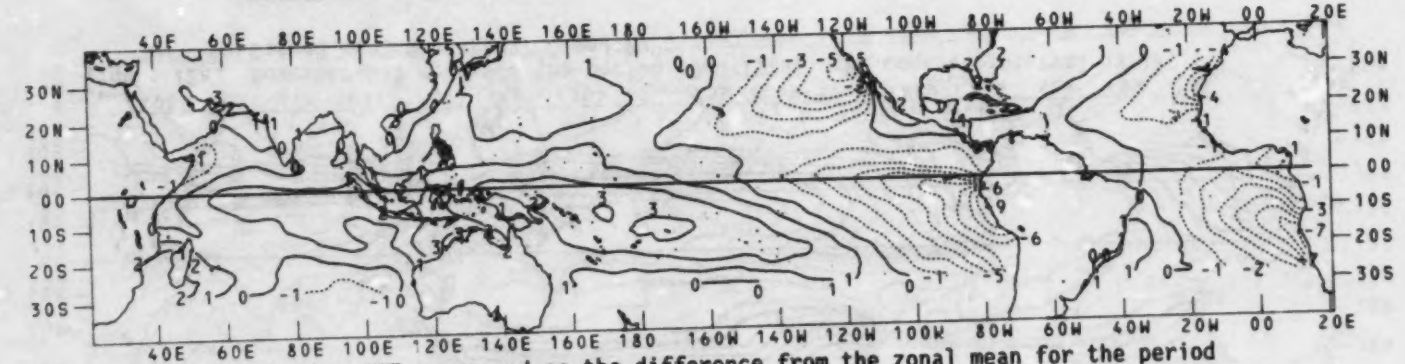

Figure 11d. October SST expressed as the difference from the zonal mean for the period 1950-1979. The contour interval is $1^{0}C$. Negative values are dashed.

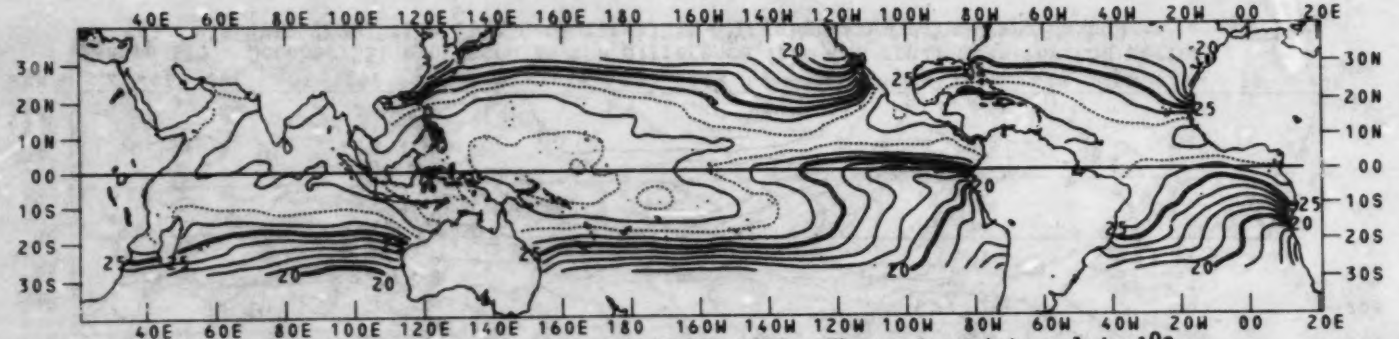

Figure 12a. November SST mean for the period 1950-1979. The contour interval is 1°C. Dashed contours are 27°C and 29°C.

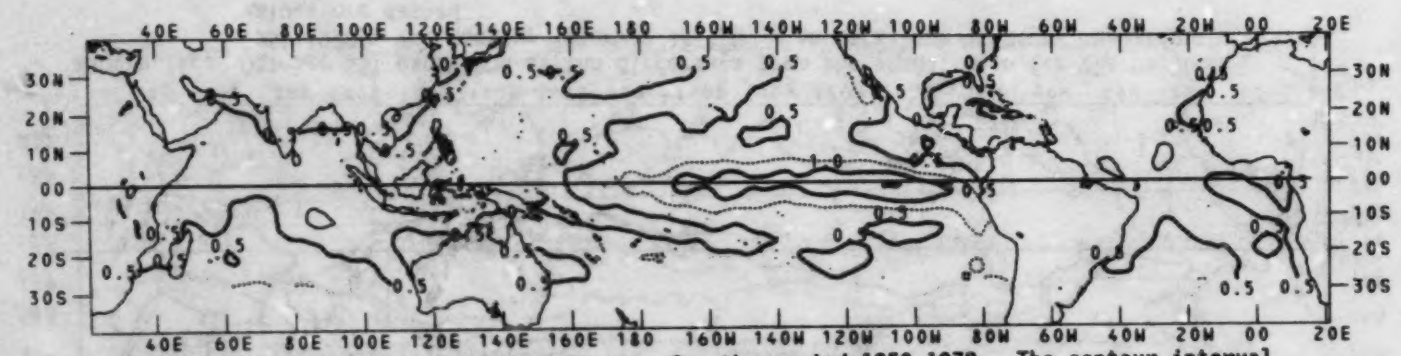

Figure 12b. November SST standard deviation for the period 1950-1979. The contour interval is .25°C. Dashed contours are .75°C and 1.25°C.

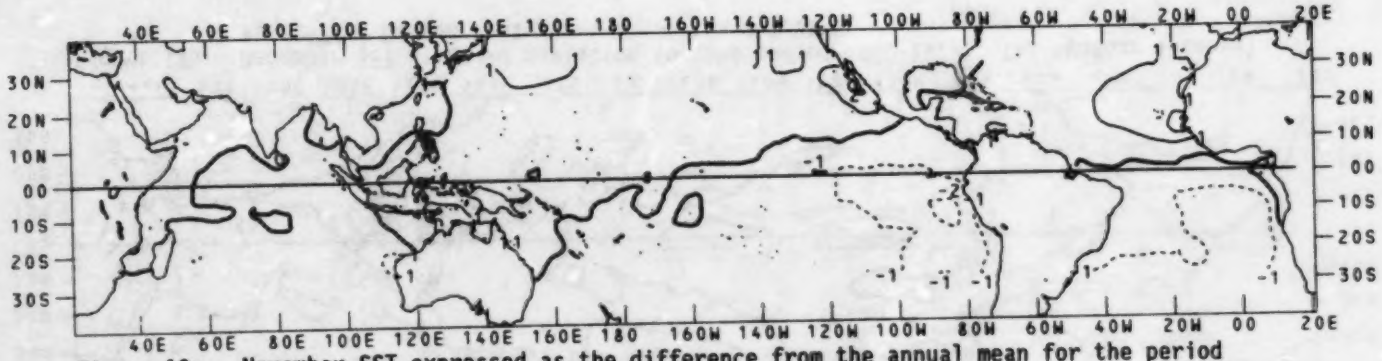

Figure 12c. November SST expressed as the difference from the annual mean for the period 1950-1979. The contour interval is 1°C. The dark line is zero. Negative values are dashed.

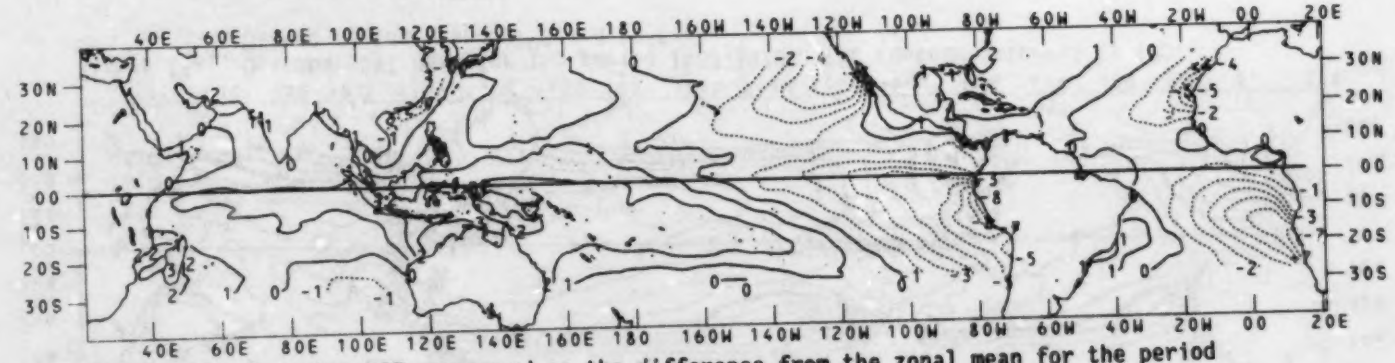

Figure 12d. November SST expressed as the difference from the zonal mean for the period 1950-1979. The contour interval is 1°C. Negative values are dashed.

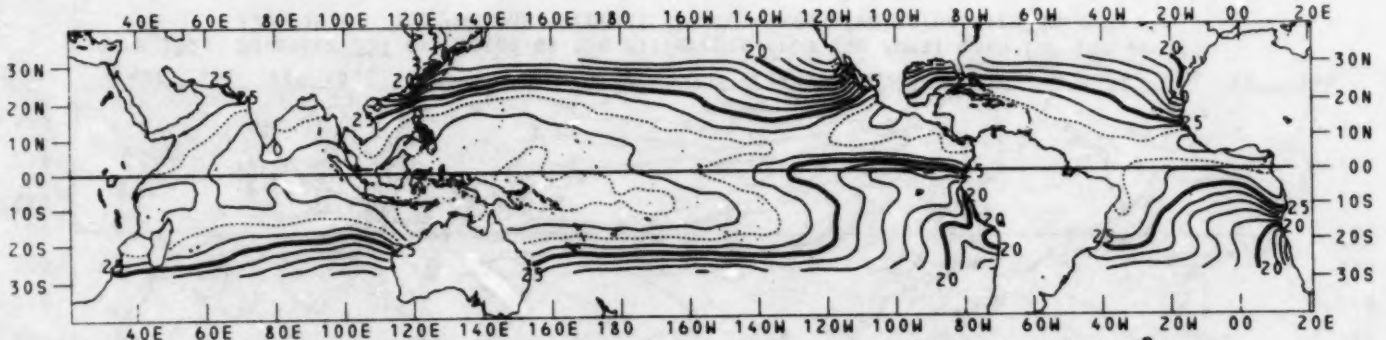

Figure 13a. December SST mean for the period 1950-1979. The contour interval is 1°C. Dashed contours are 27°C and 29°C.

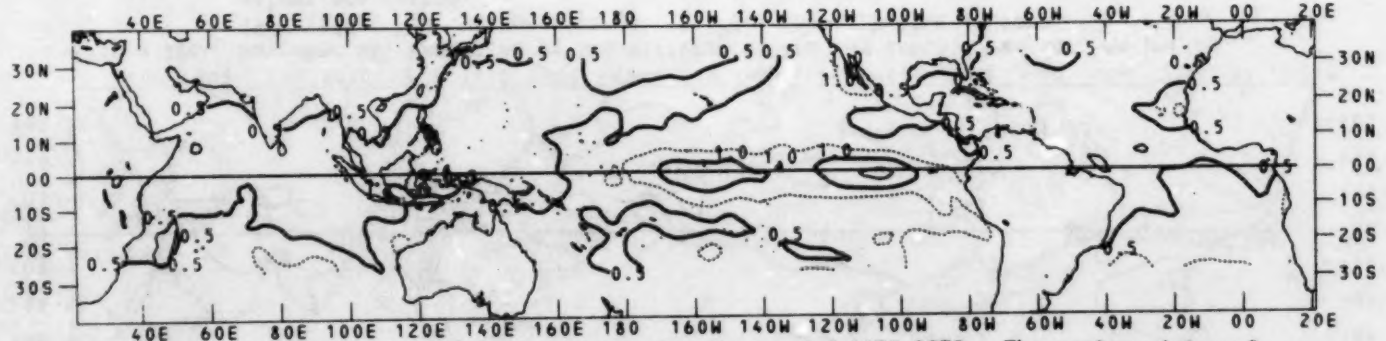

Figure 13b. December SST standard deviation for the period 1950-1979. The contour interval is .25°C. Dashed contours are .75°C and 1.25°C.

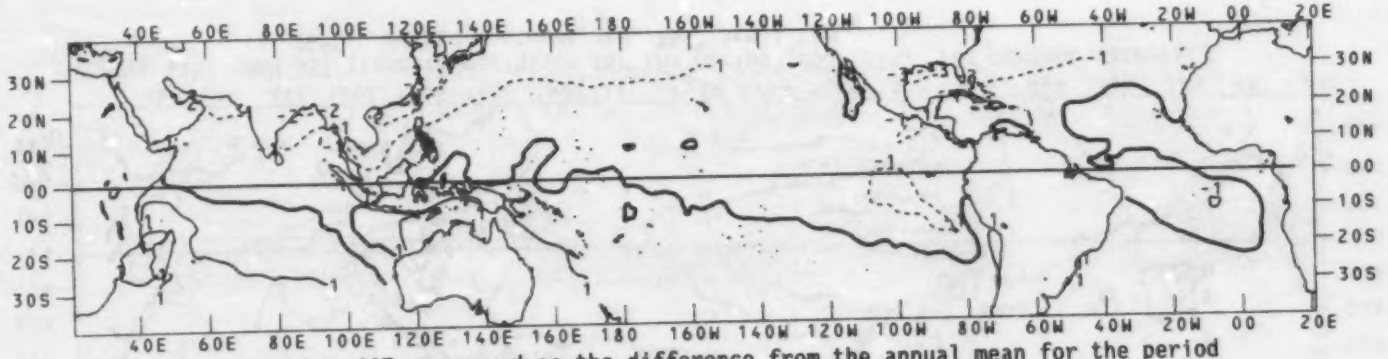

Figure 13c. December SST expressed as the difference from the annual mean for the period 1950-1979. The contour interval is 1°C. The dark line is zero. Negative values are dashed.

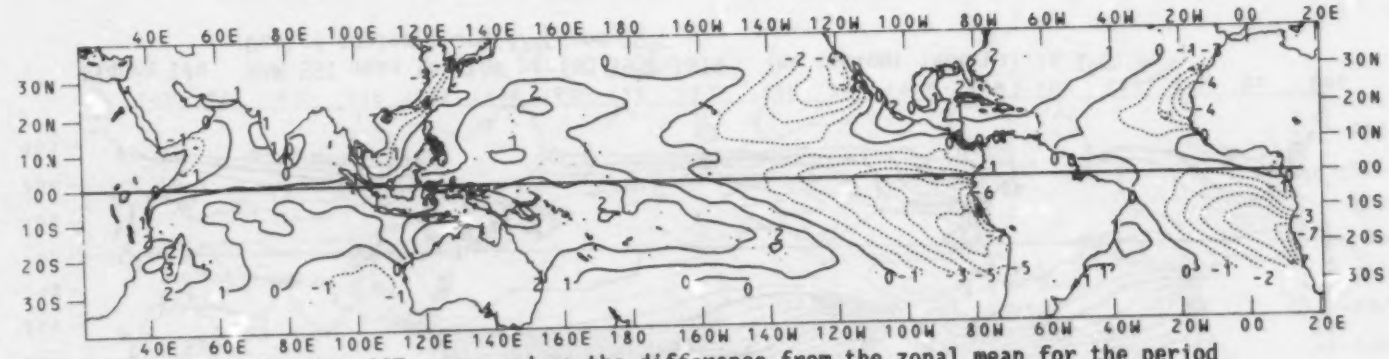

Figure 13d. December SST expressed as the difference from the zonal mean for the period 1950-1979. The contour interval is 1°C. Negative values are dashed.

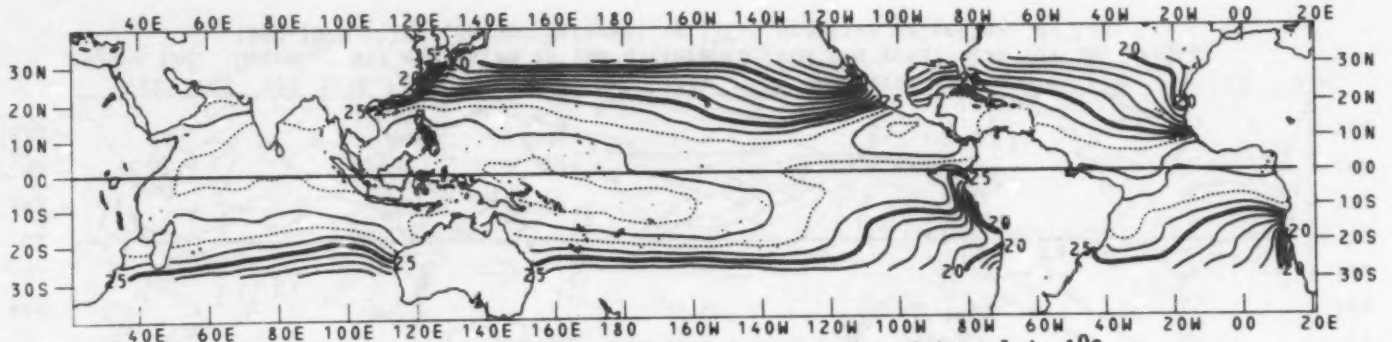

Figure 14a. MAM SST mean for the period 1950-1979. The contour interval is 1°C. Dashed contours are 27°C and 29°C.

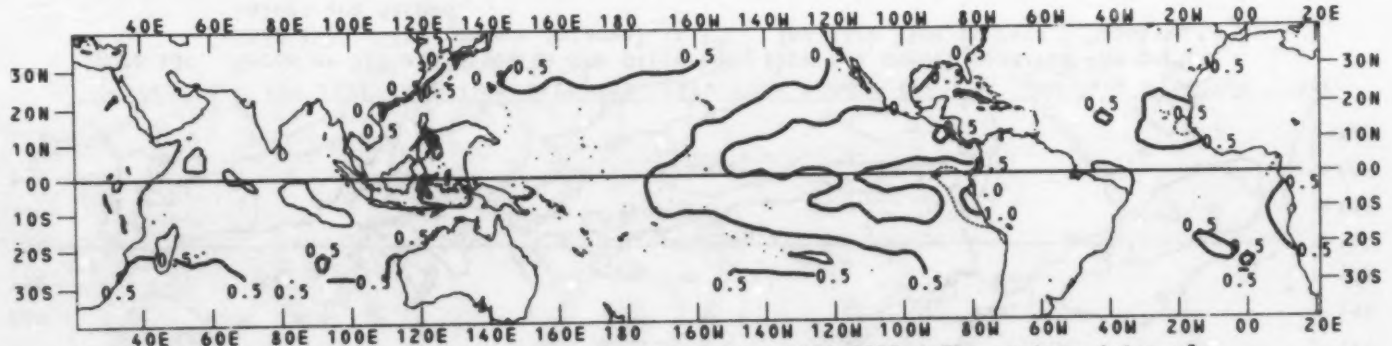

Figure 14b. MAM SST standard deviation for the period 1950-1979. The contour interval is .25°C. Dashed contours are .75°C and 1.25°C.

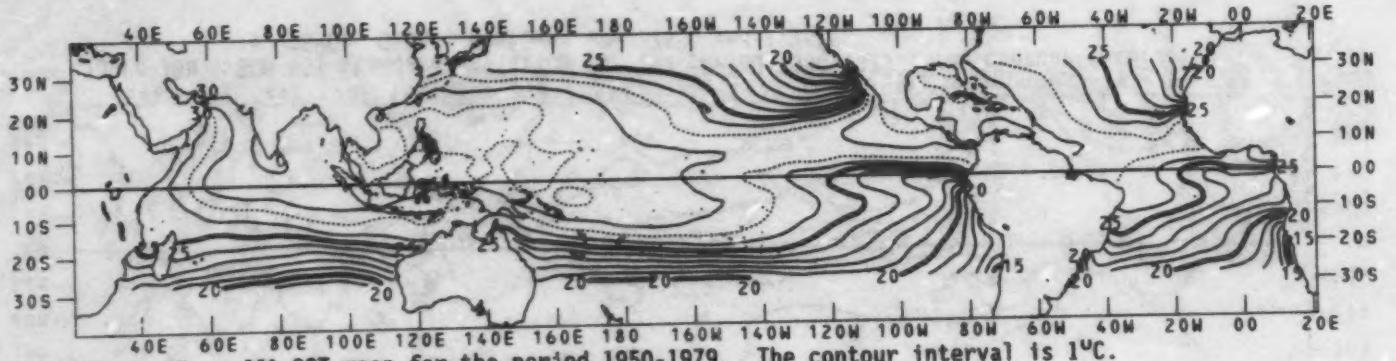

Figure 15a. JJA SST mean for the period 1950-1979. The contour interval is 1°C. Dashed contours are 27°C and 29°C.

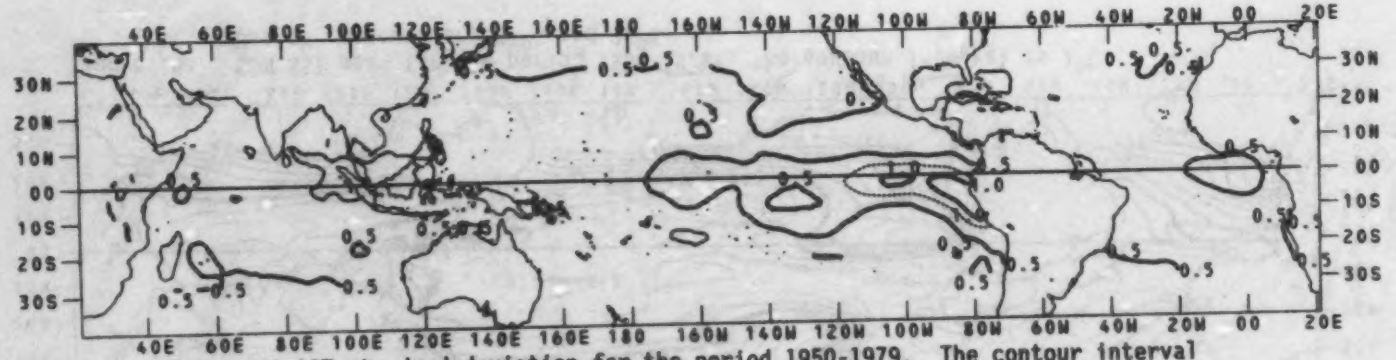

Figure 15b. JJA SST standard deviation for the period 1950-1979. The contour interval is .25°C. Dashed contours are .75°C and 1.25°C.

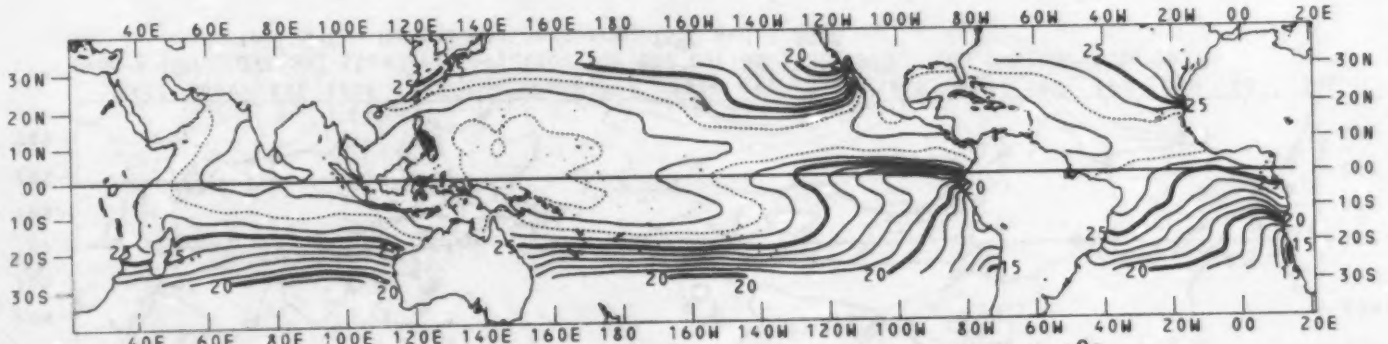

Figure 16a. SON SST mean for the period 1950-1979. The contour interval is 1°C. Dashed contours are 27°C and 29°C.

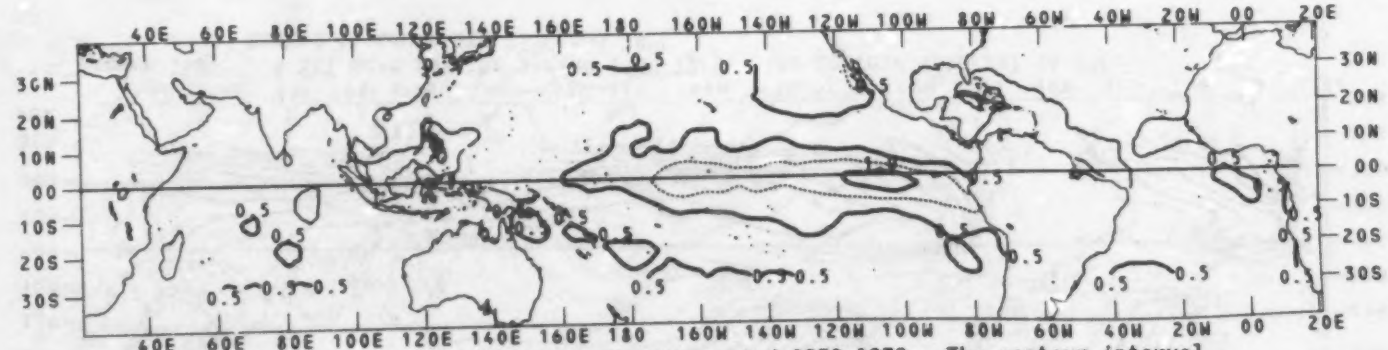

Figure 16b. SON SST standard deviation for the period 1950-1979. The contour interval is .25°C. Dashed contours are .75°C and 1.25°C.

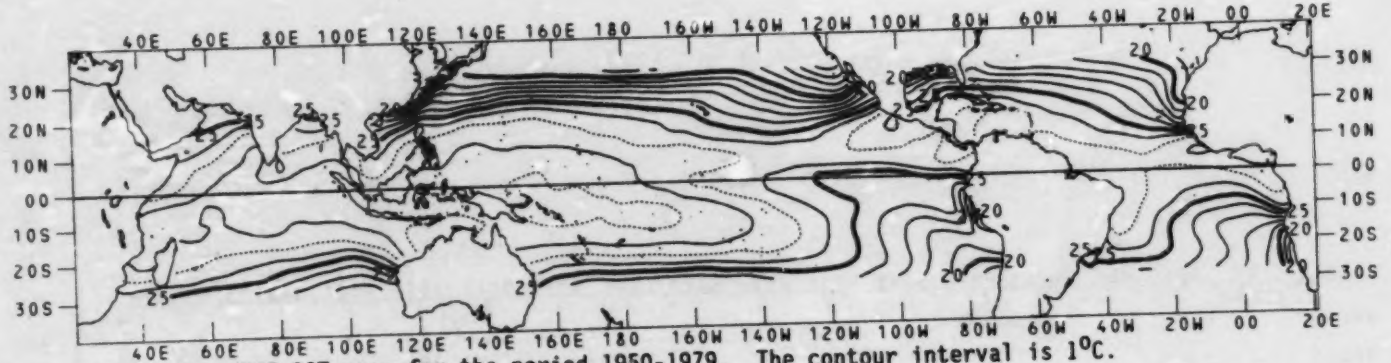

Figure 17a. DJF SST mean for the period 1950-1979. The contour interval is 1°C. Dashed contours are 27°C and 29°C.

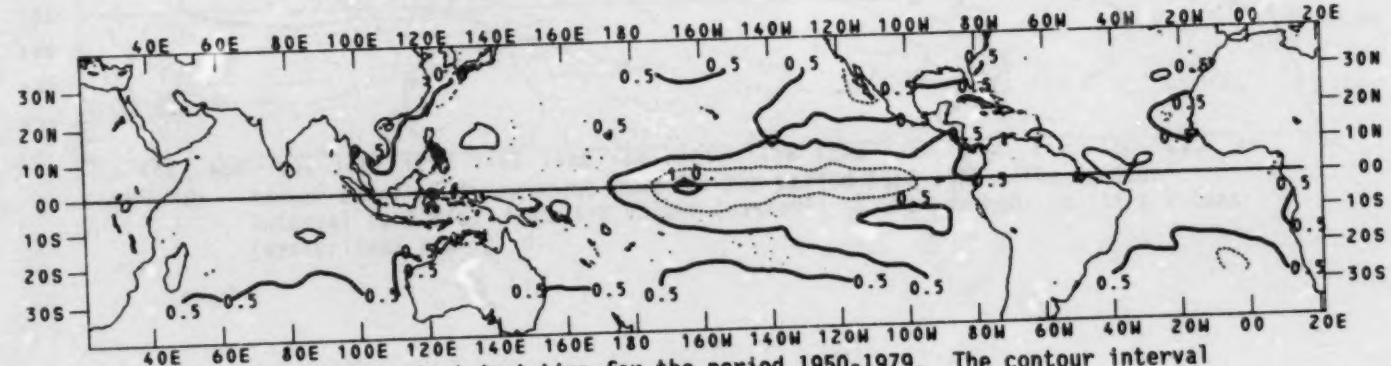

Figure 17b. DJF SST standard deviation for the period 1950-1979. The contour interval is .25°C. Dashed contours are .75°C and 1.25°C.

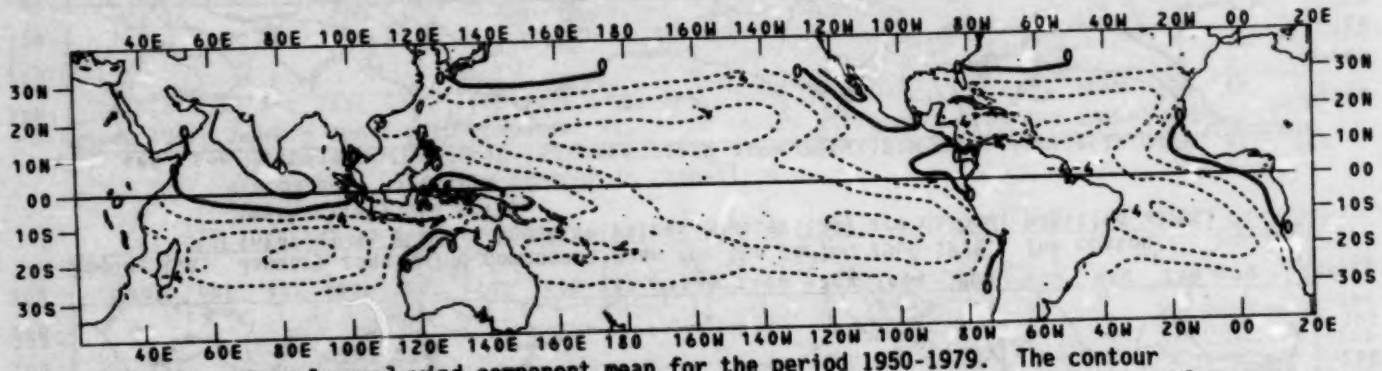

Figure 18. Annual zonal wind component mean for the period 1950-1979. The contour interval is 2 m/s. Negative values (easterlies) are dashed; positive values (westerlies) are solid.

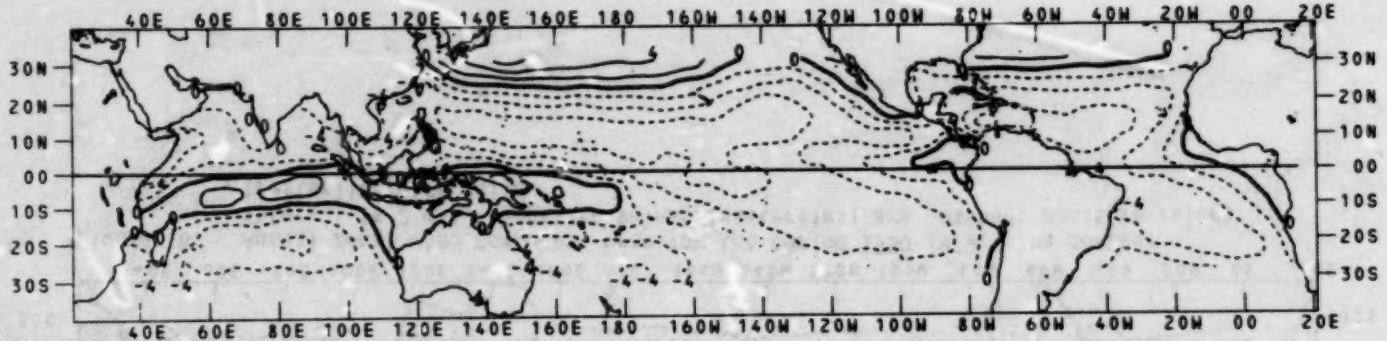

Figure 19a. January zonal wind component mean for the period 1950-1979. The contour interval is 2 m/s. Negative values (easterlies) are dashed; positive values (westerlies) are solid.

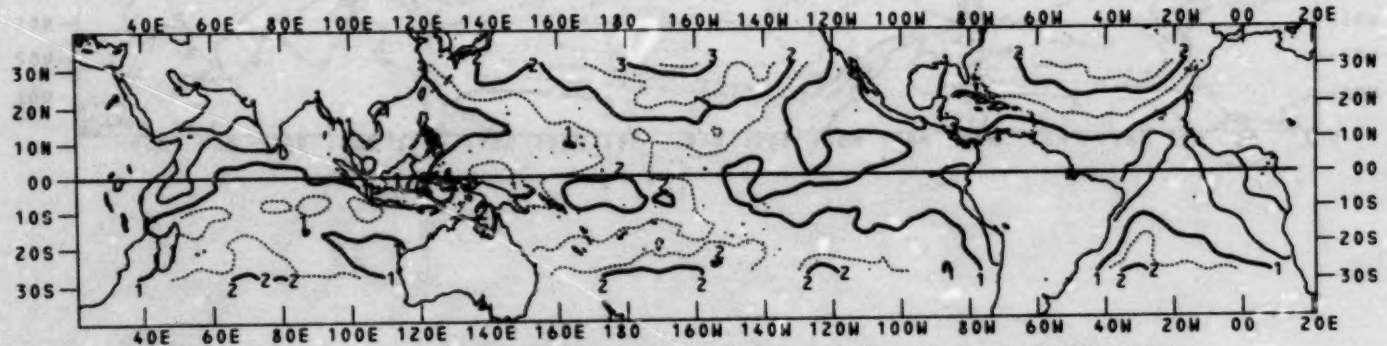

Figure 19b. January zonal wind component standard deviation for the period 1950-1979. The contour interval is .5 m/s.

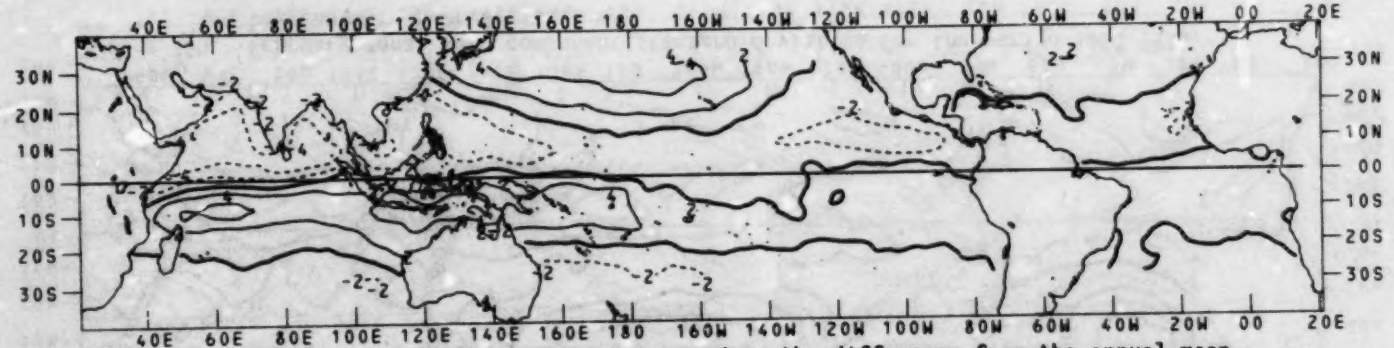

Figure 19c. January zonal wind component expressed as the difference from the annual mean for the period 1950-1979. The contour interval is 2 m/s. Negative values are dashed. The zero contour is emphasized.

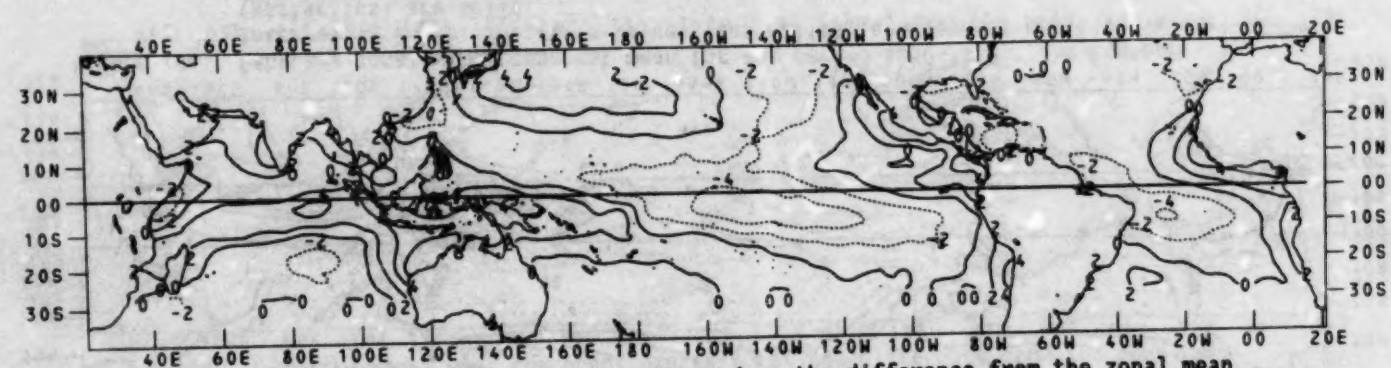

Figure 19d. January zonal wind component expressed as the difference from the zonal mean for the period 1950-1979. The contour interval is 2 m/s. Negative values are dashed.

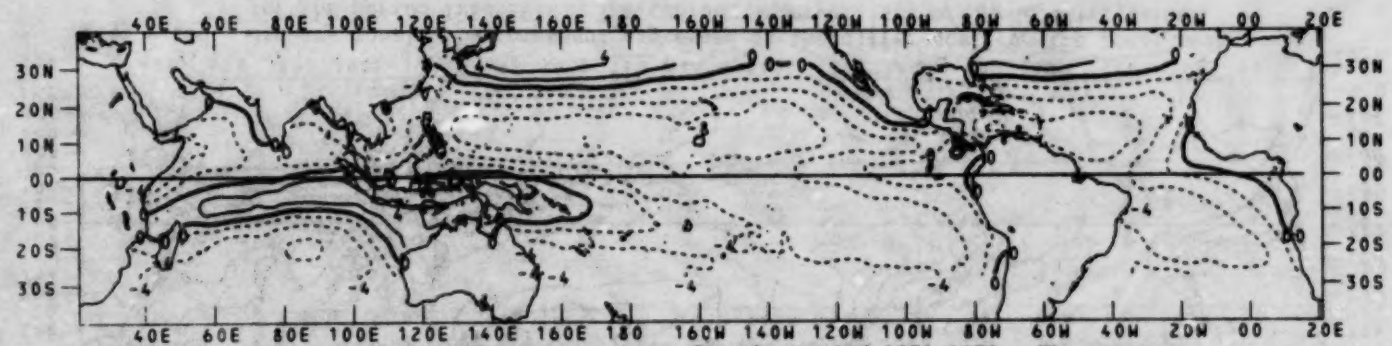

Figure 20a. February zonal wind component mean for the period 1950-1979. The contour interval is 2 m/s. Negative values (easterlies) are dashed; positive values (westerlies) are solid.

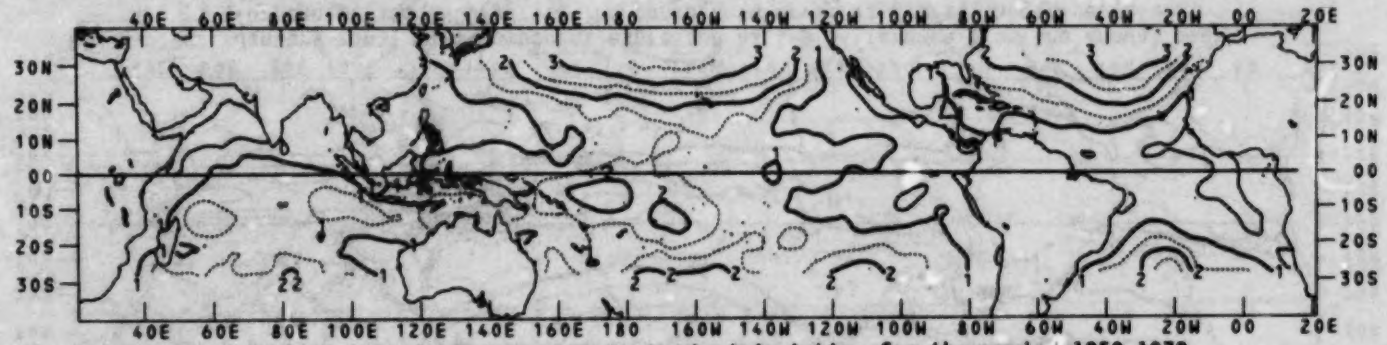

Figure 20b. February zonal wind component standard deviation for the period 1950-1979. The contour interval is .5 m/s.

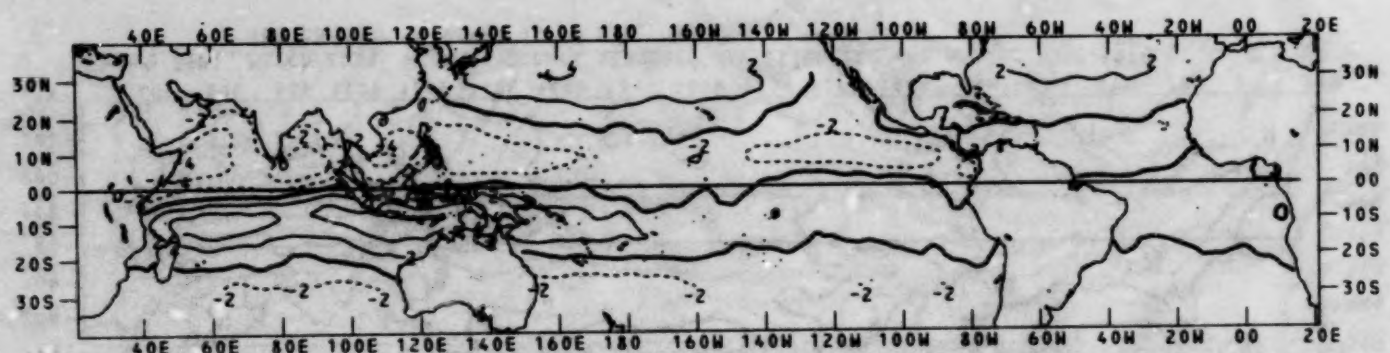

Figure 20c. February zonal wind component expressed as the difference from the annual mean for the period 1950-1979. The contour interval is 2 m/s. Negative values are dashed. The zero contour is emphasized.

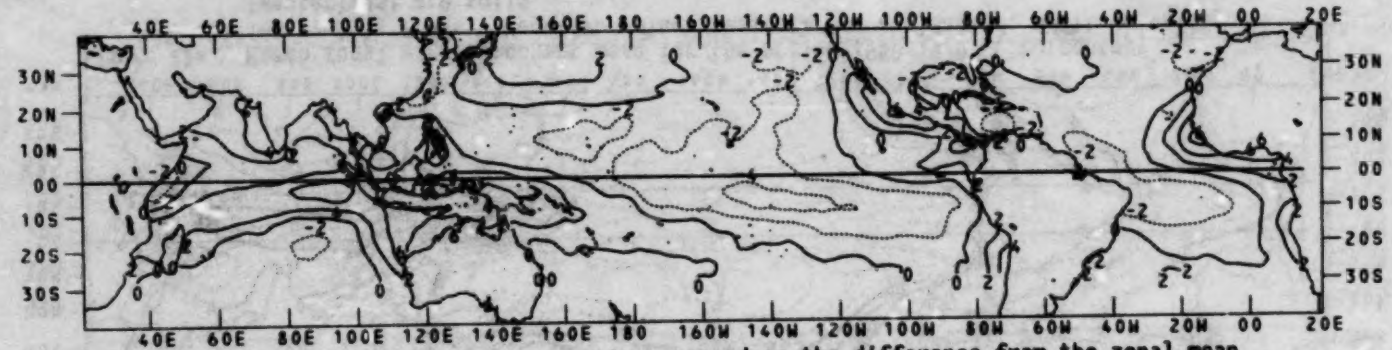

Figure 20d. February zonal wind component expressed as the difference from the zonal mean for the period 1950-1979. The contour interval is 2 m/s. Negative values are dashed.

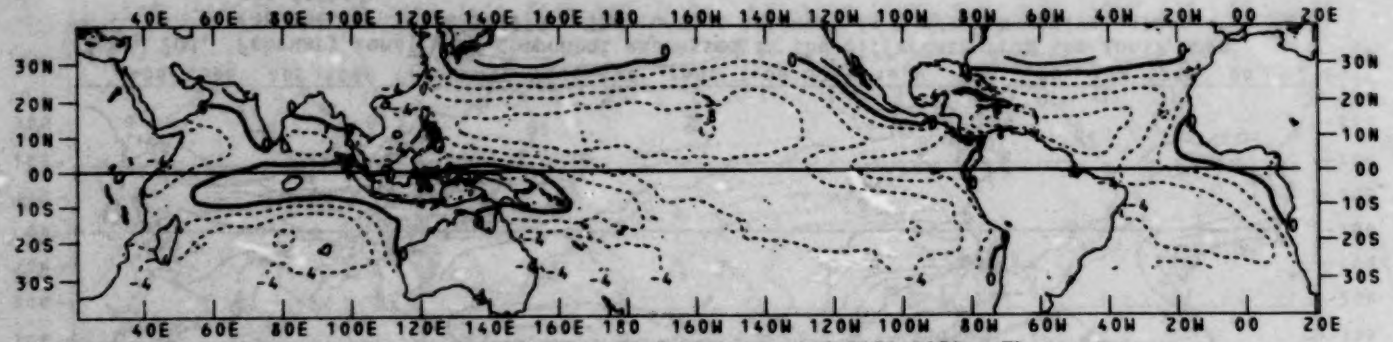

Figure 21a. March zonal wind component mean for the period 1950-1979. The contour interval is 2 m/s. Negative values (easterlies) are dashed; positive values (westerlies) are solid.

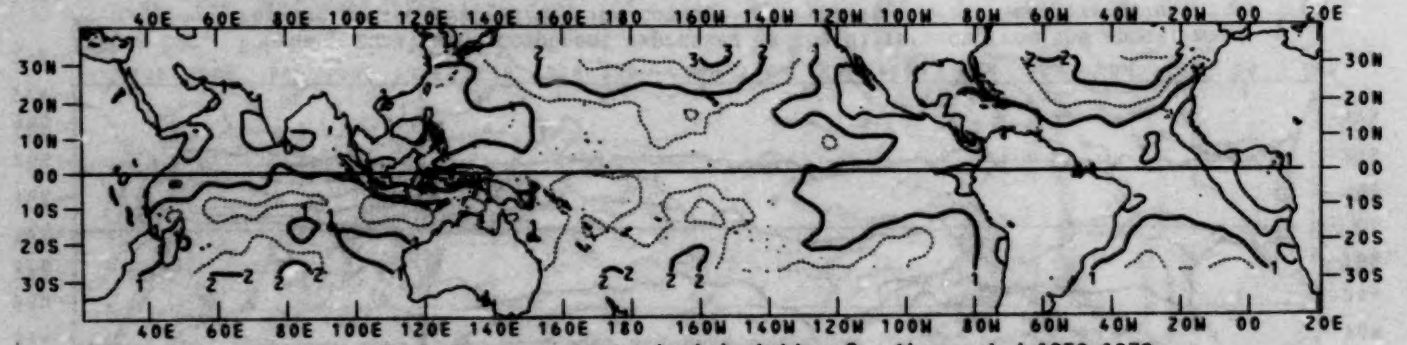

Figure 21b. March zonal wind component standard deviation for the period 1950-1979. The contour interval is .5 m/s.

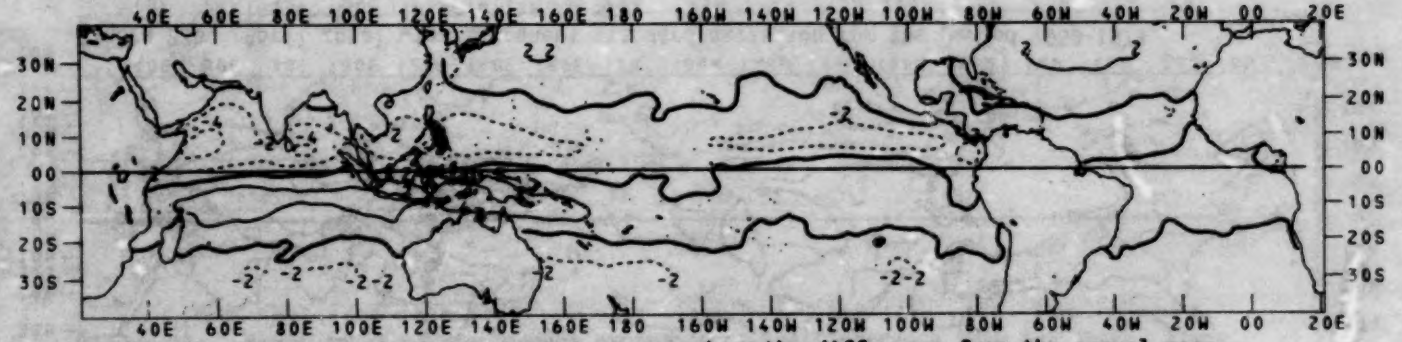

Figure 21c. March zonal wind component expressed as the difference from the annual mean for the period 1950-1979. The contour interval is 2 m/s. Negative values are dashed. The zero contour is emphasized.

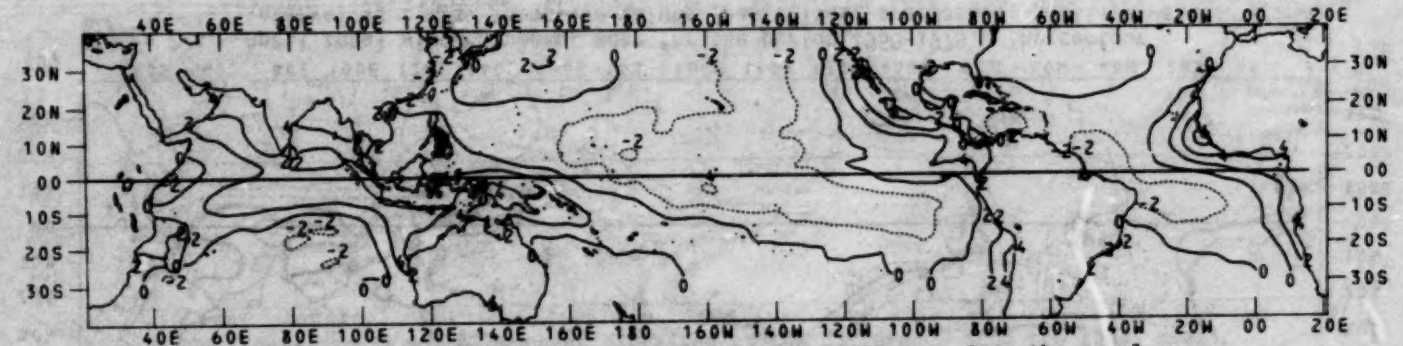

Figure 21d. March zonal wind component expressed as the difference from the zonal mean for the period 1950-1979. The contour interval is 2 m/s. Negative values are dashed.

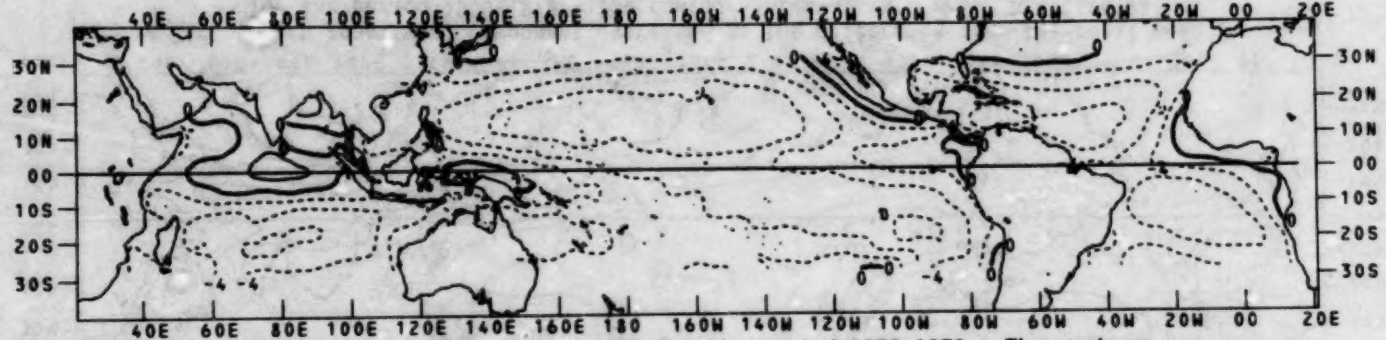

Figure 22a. April zonal wind component mean for the period 1950-1979. The contour interval is 2 m/s. Negative values (easterlies) are dashed; positive values (westerlies) are solid.

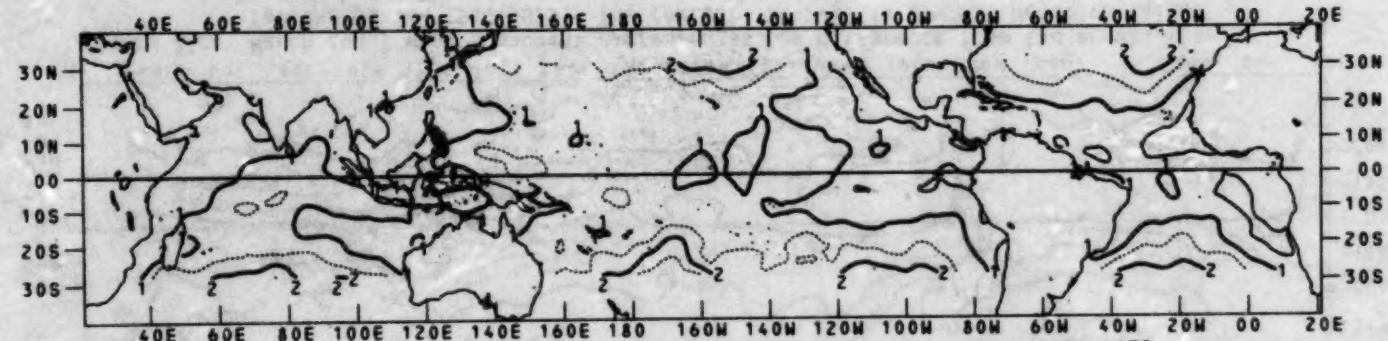

Figure 22b. April zonal wind component standard deviation for the period 1950-1979. The contour interval is .5 m/s.

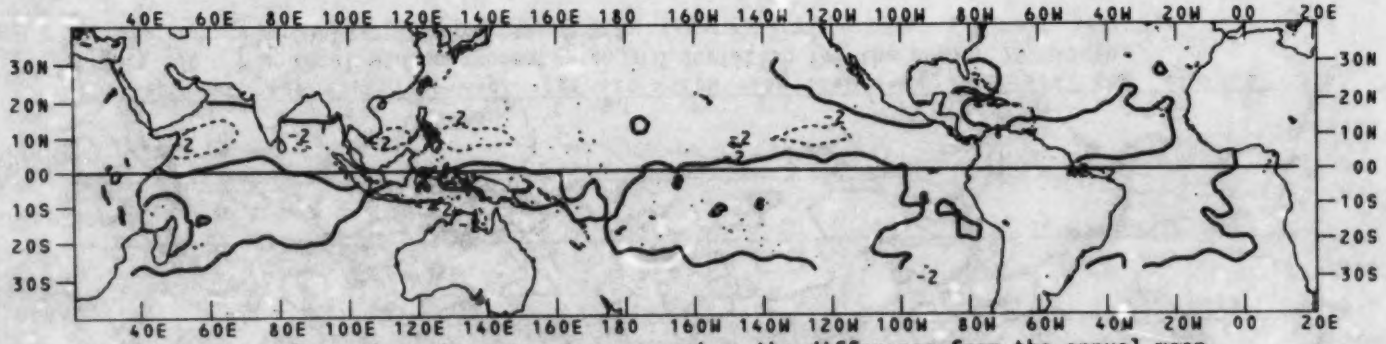

Figure 22c. April zonal wind component expressed as the difference from the annual mean for the period 1950-1979. The contour interval is 2 m/s. Negative values are dashed. The zero contour is emphasized.

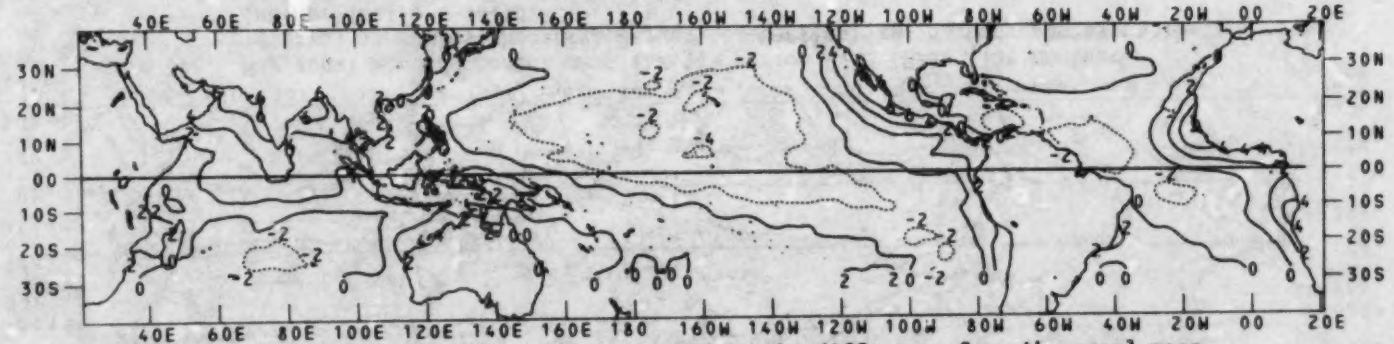

Figure 22d. April zonal wind component expressed as the difference from the zonal mean for the period 1950-1979. The contour interval is 2 m/s. Negative values are dashed.

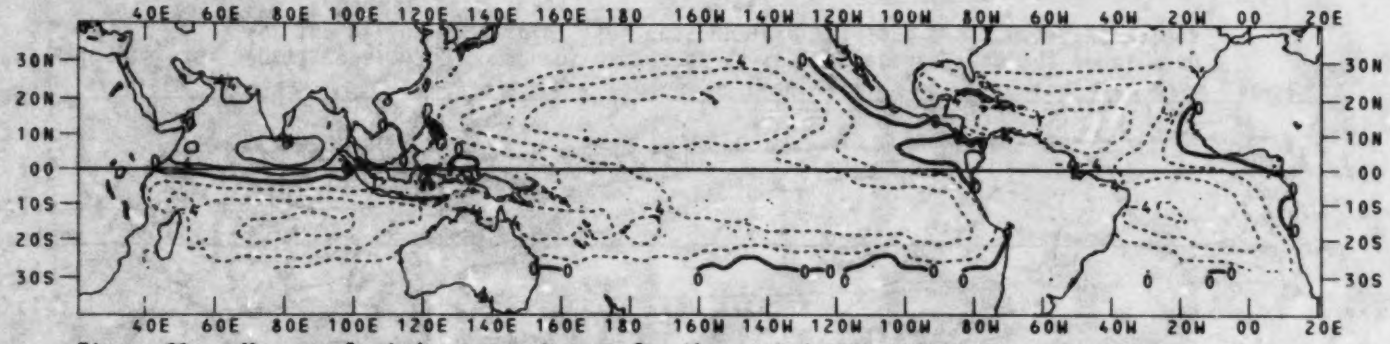

Figure 23a. May zonal wind component mean for the period 1950-1979. The contour interval is 2 m/s. Negative values (easterlies) are dashed; positive values (westerlies) are solid.

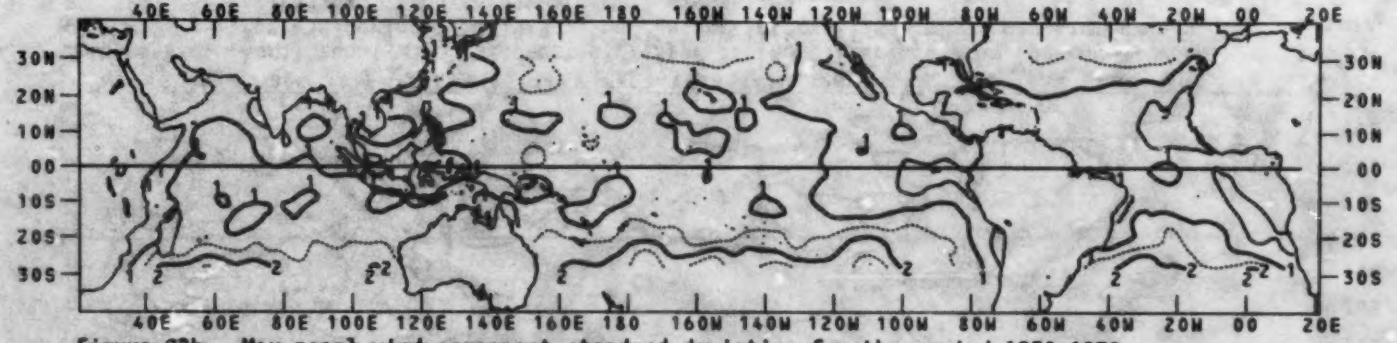

Figure 23b. May zonal wind component standard deviation for the period 1950-1979. The contour interval is .5 m/s.

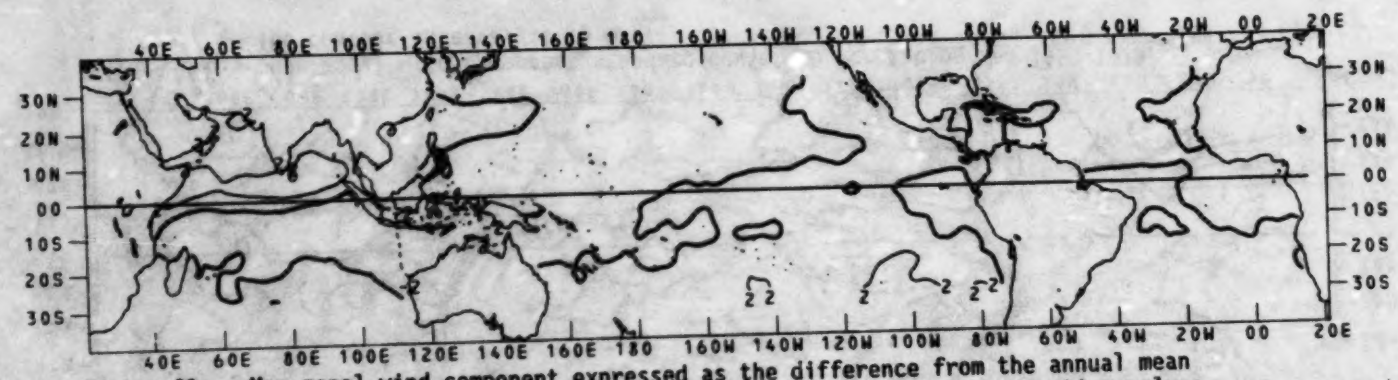

Figure 23c. May zonal wind component expressed as the difference from the annual mean for the period 1950-1979. The contour interval is 2 m/s. Negative values are dashed. The zero contour is emphasized.

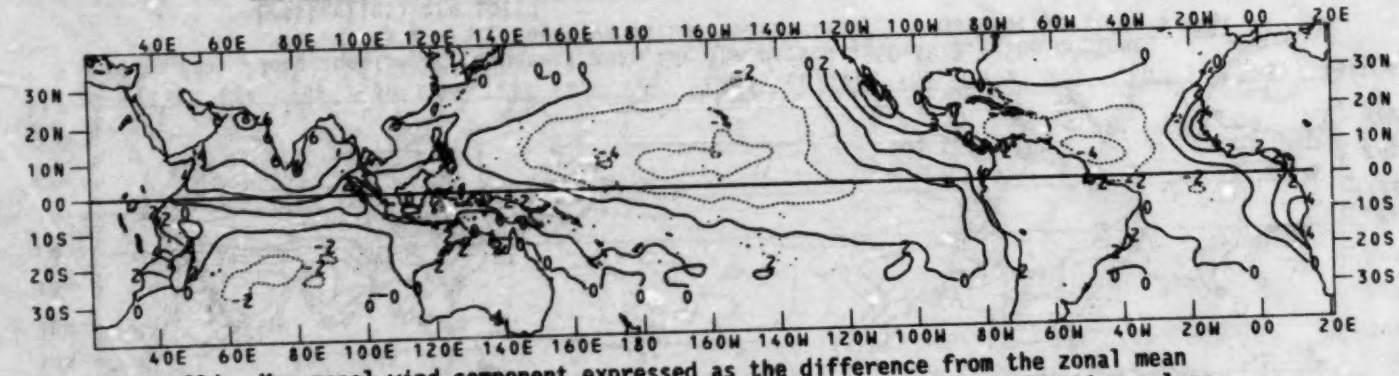

Figure 23d. May zonal wind component expressed as the difference from the zonal mean for the period 1950-1979. The contour interval is 2 m/s. Negative values are dashed.

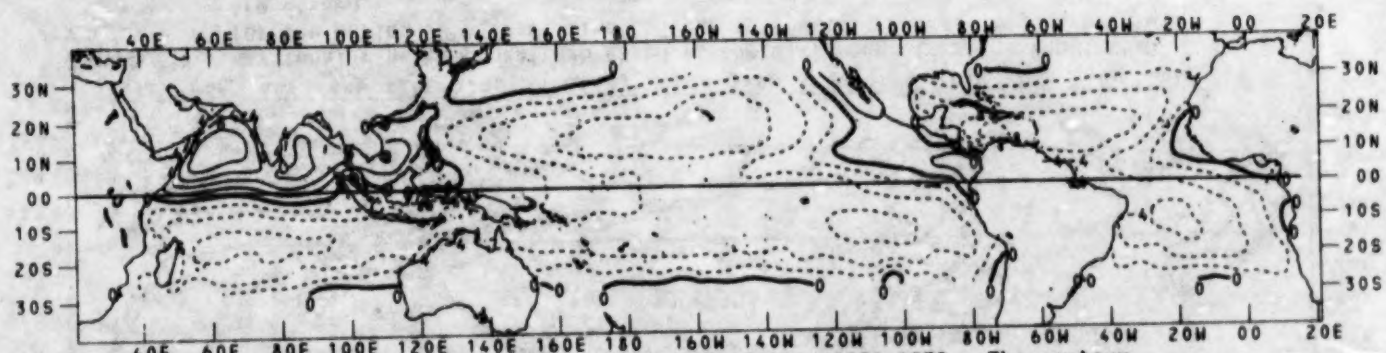

Figure 24a. June zonal wind component mean for the period 1950-1979. The contour interval is 2 m/s. Negative values (easterlies) are dashed; positive values (westerlies) are solid.

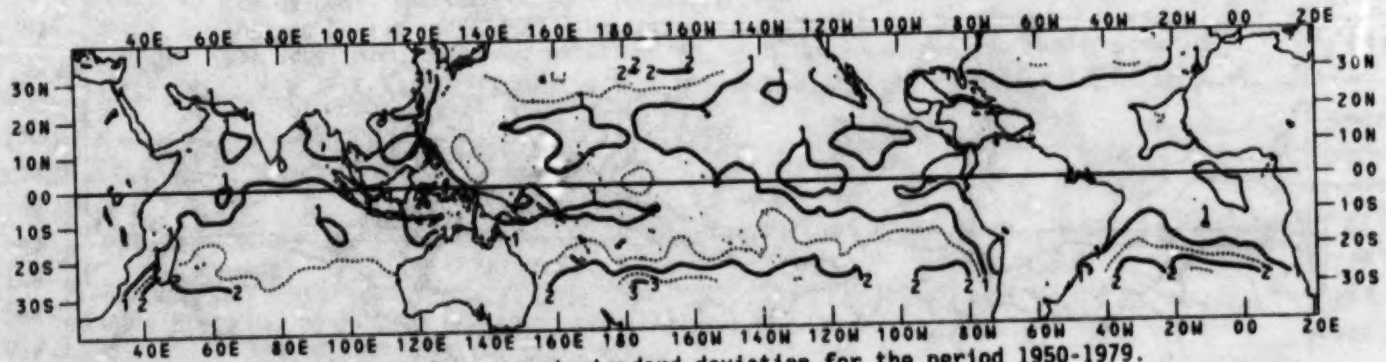

Figure 24b. June zonal wind component standard deviation for the period 1950-1979. The contour interval is .5 m/s.

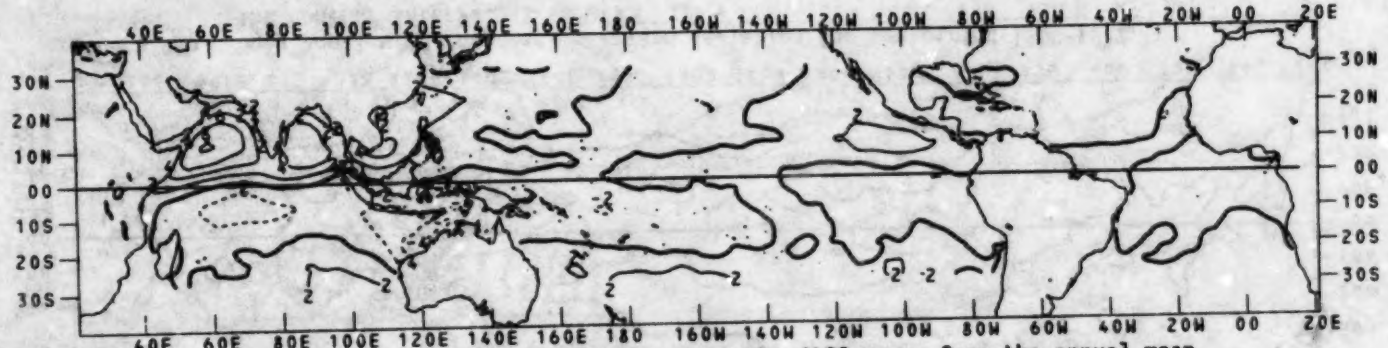

Figure 24c. June zonal wind component expressed as the difference from the annual mean for the period 1950-1979. The contour interval is 2 m/s. Negative values are dashed. The zero contour is emphasized.

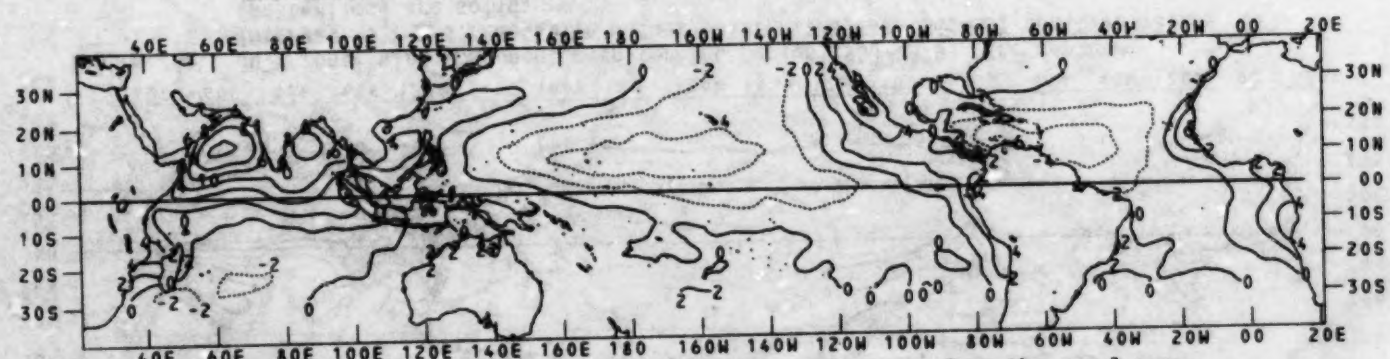

Figure 24d. June zonal wind component expressed as the difference from the zonal mean for the period 1950-1979. The contour interval is 2 m/s. Negative values are dashed.

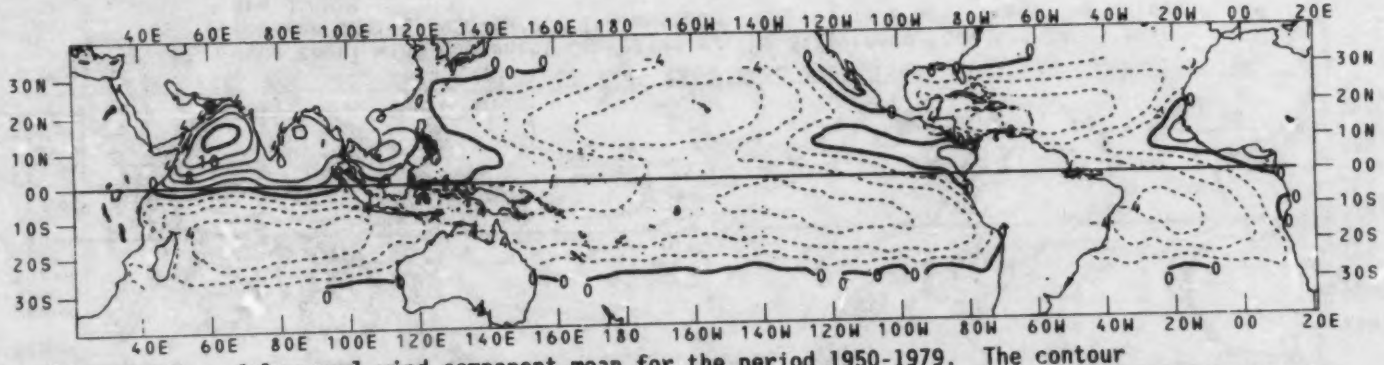

Figure 25a. July zonal wind component mean for the period 1950-1979. The contour interval is 2 m/s. Negative values (easterlies) are dashed; positive values (westerlies) are solid.

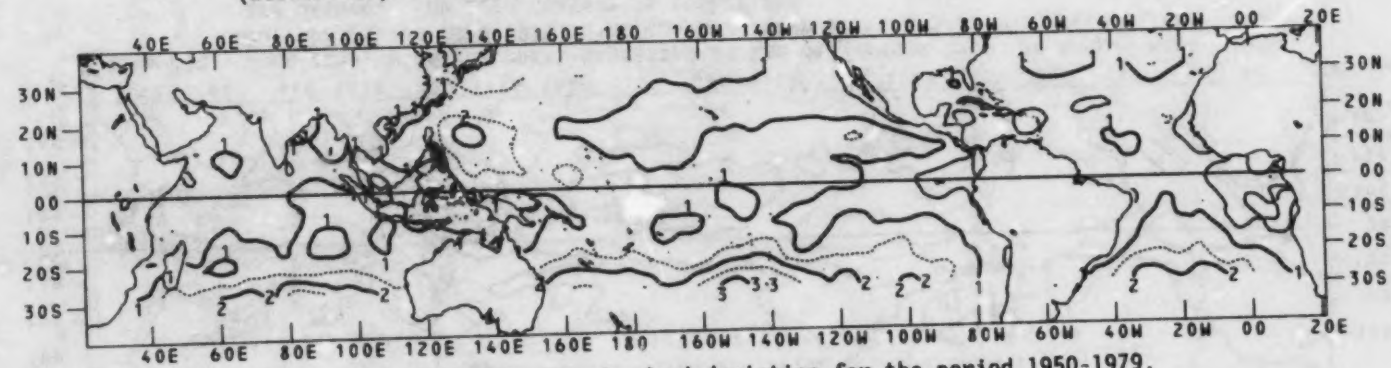

Figure 25b. July zonal wind component standard deviation for the period 1950-1979. The contour interval is .5 m/s.

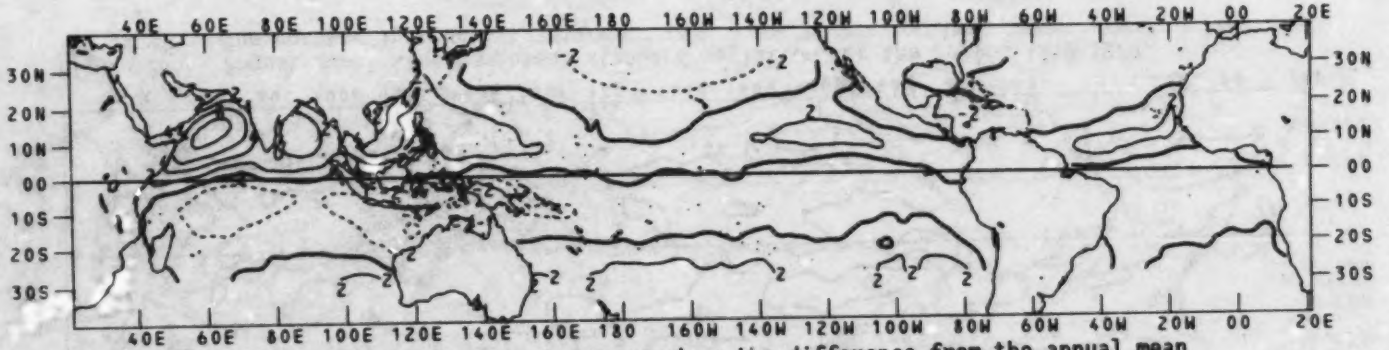

Figure 25c. July zonal wind component expressed as the difference from the annual mean for the period 1950-1979. The contour interval is 2 m/s. Negative values are dashed. The zero contour is emphasized.

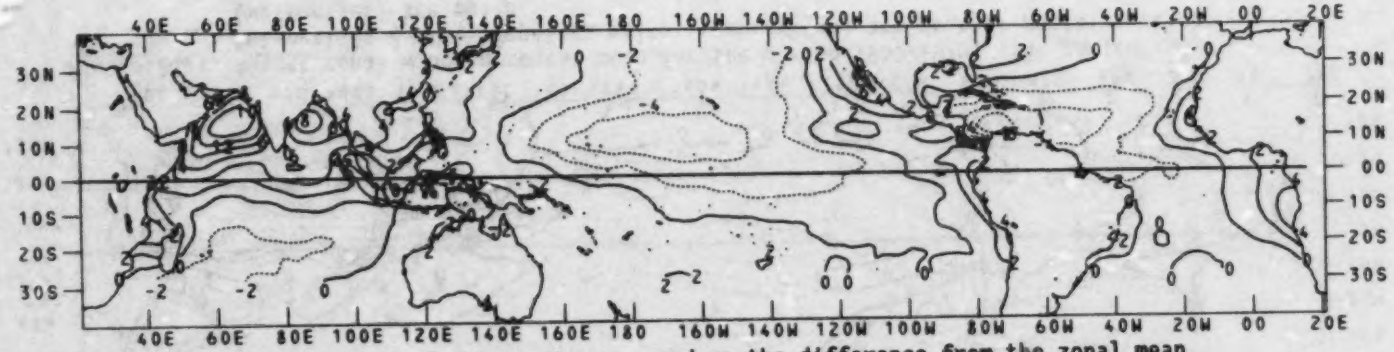

Figure 25d. July zonal wind component expressed as the difference from the zonal mean for the period 1950-1979. The contour interval is 2 m/s. Negative values are dashed.

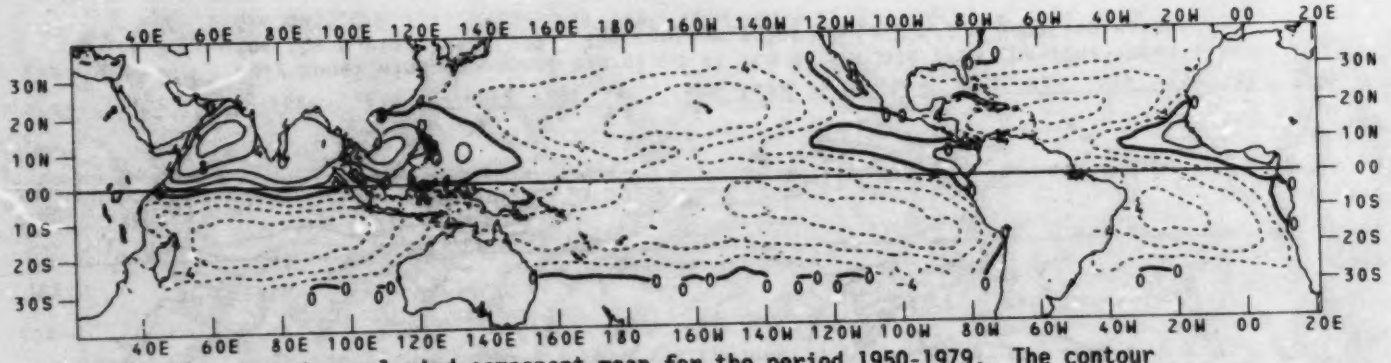

Figure 26a. August zonal wind component mean for the period 1950-1979. The contour interval is 2 m/s. Negative values (easterlies) are dashed; positive values (westerlies) are solid.

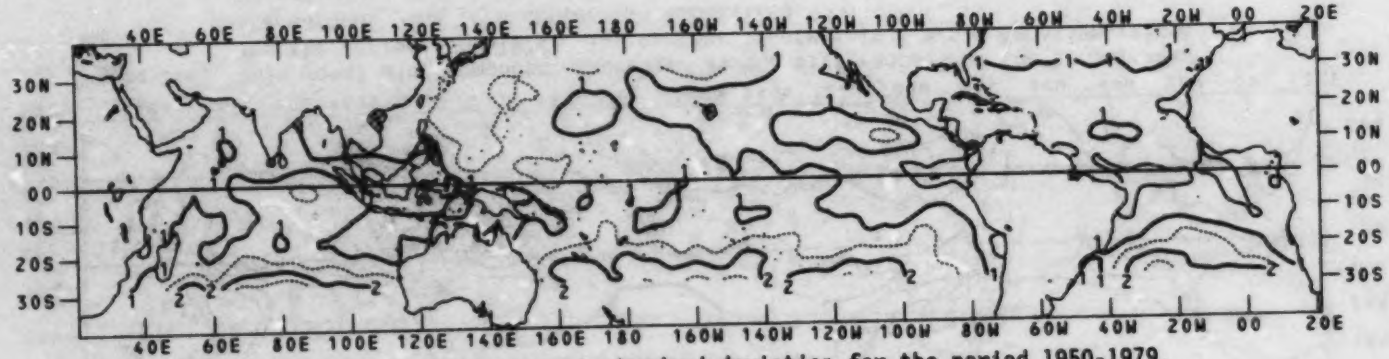

Figure 26b August zonal wind component standard deviation for the period 1950-1979. The contour interval is .5 m/s.

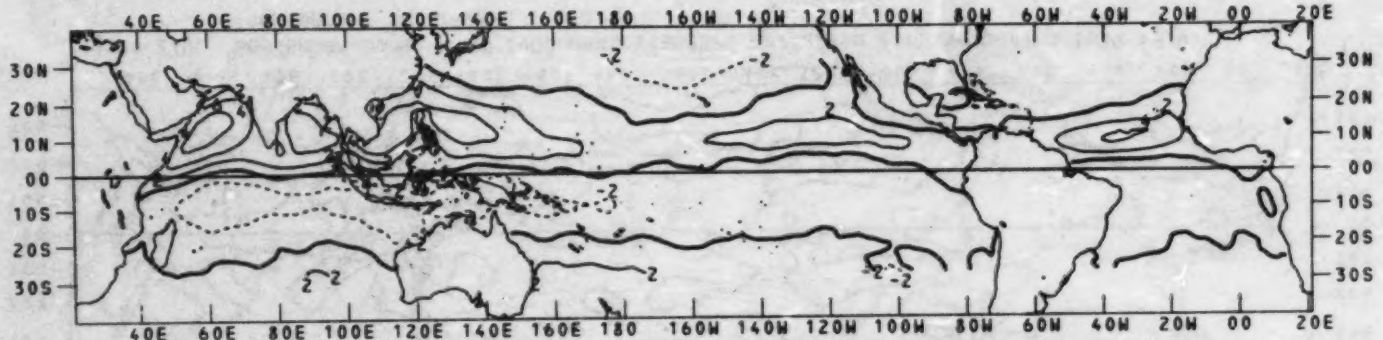

Figure 26c. August zonal wind component expressed as the difference from the annual mean for the period 1950-1979. The contour interval is 2 m/s. Negative values are dashed. The zero contour is emphasized.

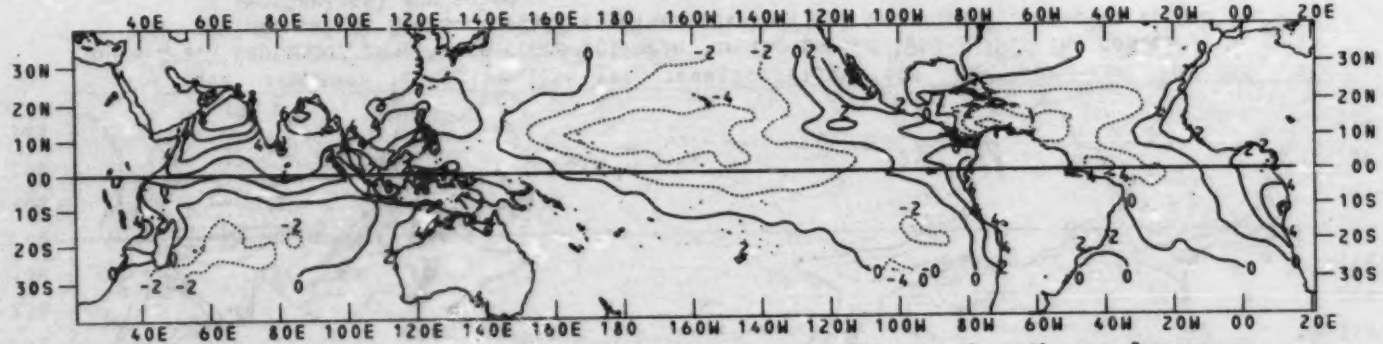

Figure 26d. August zonal wind component expressed as the difference from the zonal mean for the period 1950-1979. The contour interval is 2 m/s. Negative values are dashed.

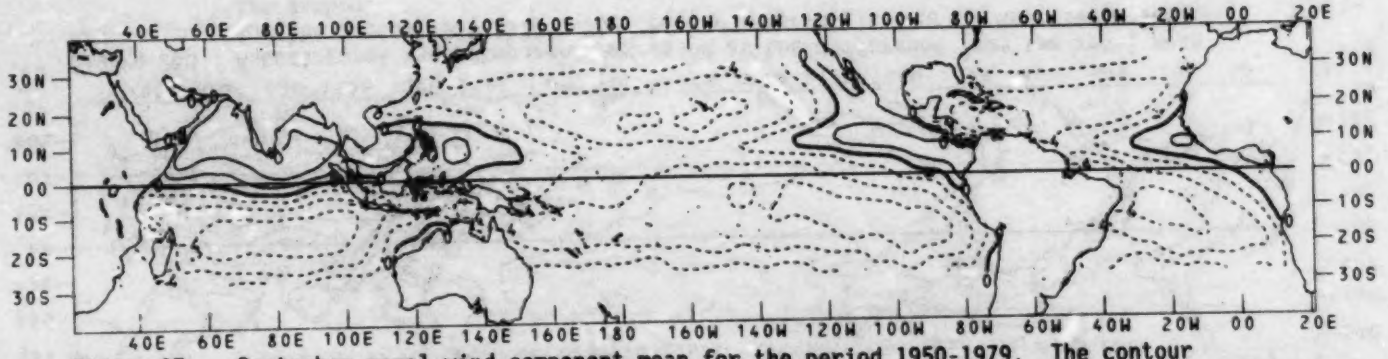

Figure 27a. September zonal wind component mean for the period 1950-1979. The contour interval is 2 m/s. Negative values (easterlies) are dashed; positive values (westerlies) are solid.

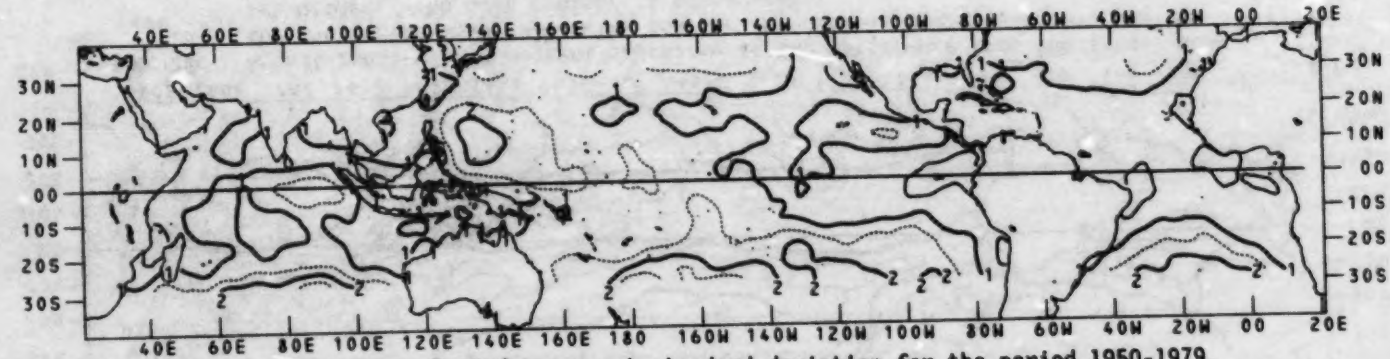

Figure 27b. September zonal wind component standard deviation for the period 1950-1979. The contour interval is .5 m/s.

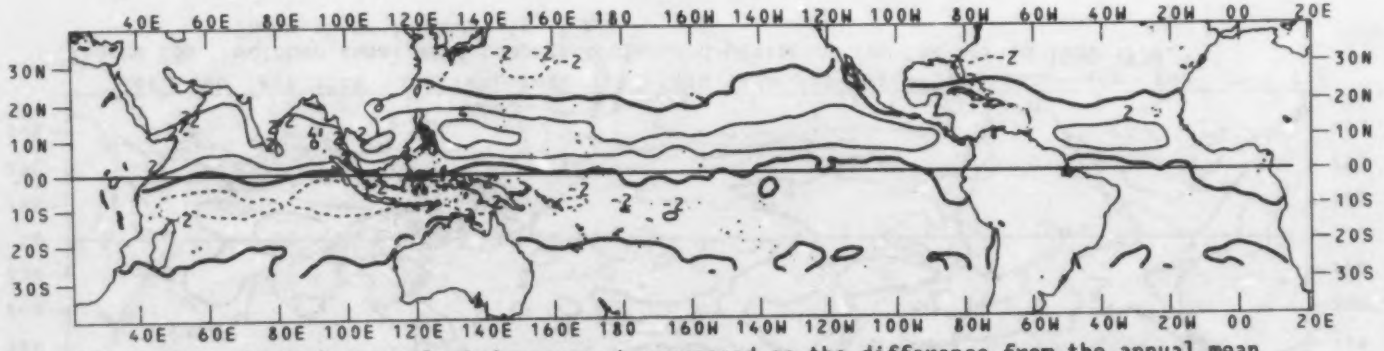

Figure 27c. September zonal wind component expressed as the difference from the annual mean for the period 1950-1979. The contour interval is 2 m/s. Negative values are dashed. The zero contour is emphasized.

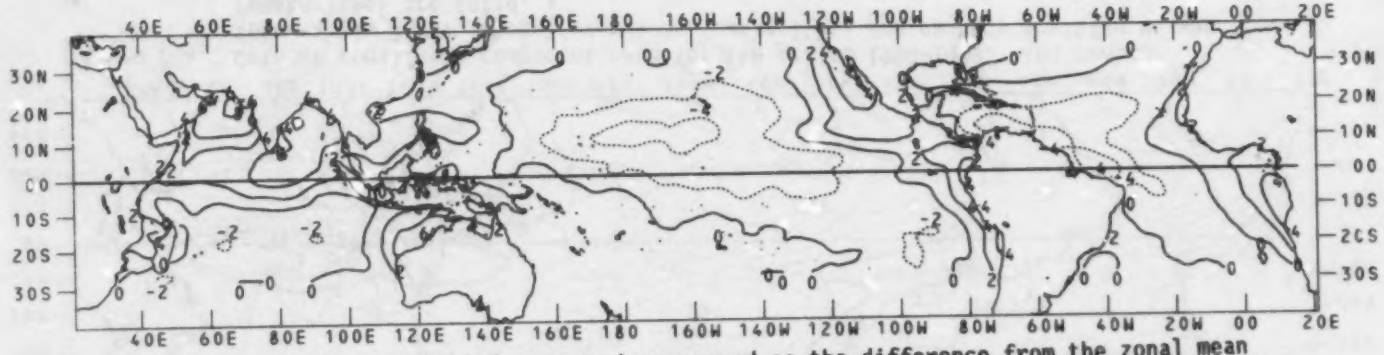

Figure 27d. September zonal wind component expressed as the difference from the zonal mean for the period 1950-1979. The contour interval is 2 m/s. Negative values are dashed.

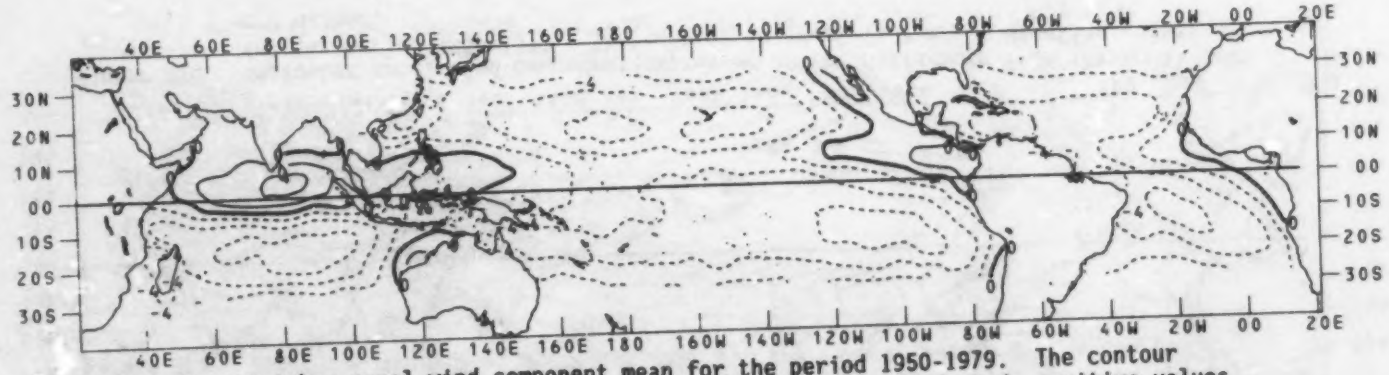

Figure 28a. October zonal wind component mean for the period 1950-1979. The contour interval is 2 m/s. Negative values (easterlies) are dashed; positive values (westerlies) are solid.

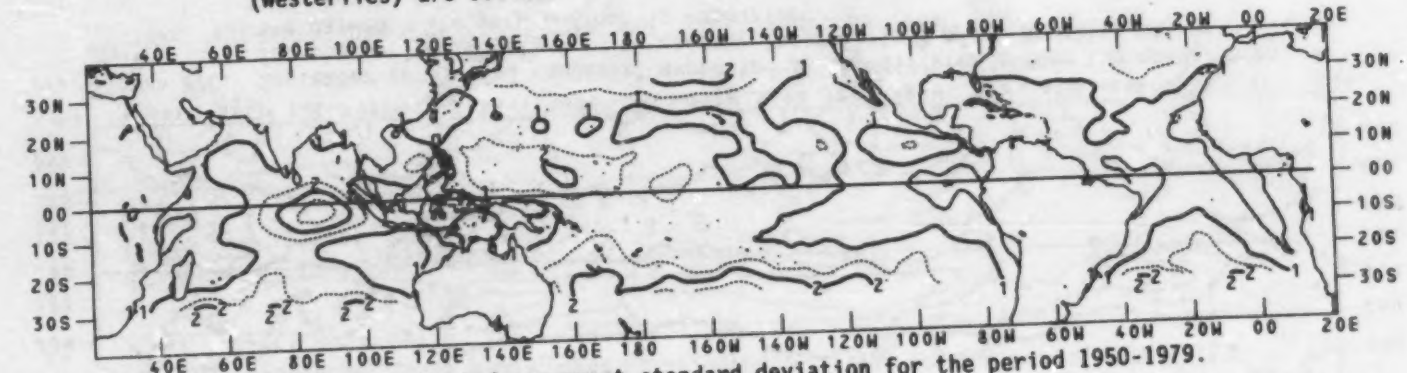

Figure 28b. October zonal wind component standard deviation for the period 1950-1979. The contour interval is .5 m/s.

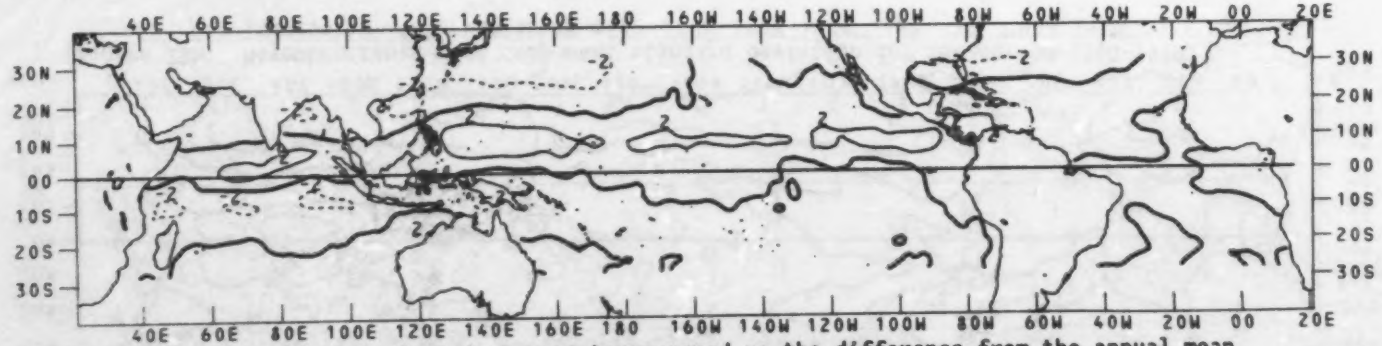

Figure 28c. October zonal wind component expressed as the difference from the annual mean for the period 1950-1979. The contour interval is 2 m/s. Negative values are dashed. The zero contour is emphasized.

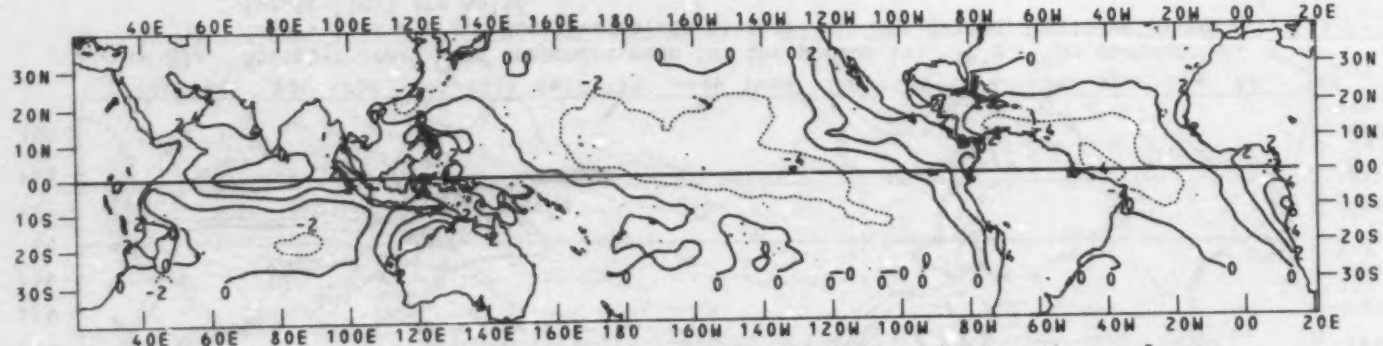

Figure 28d. October zonal wind component expressed as the difference from the zonal mean for the period 1950-1979. The contour interval is 2 m/s. Negative values are dashed.

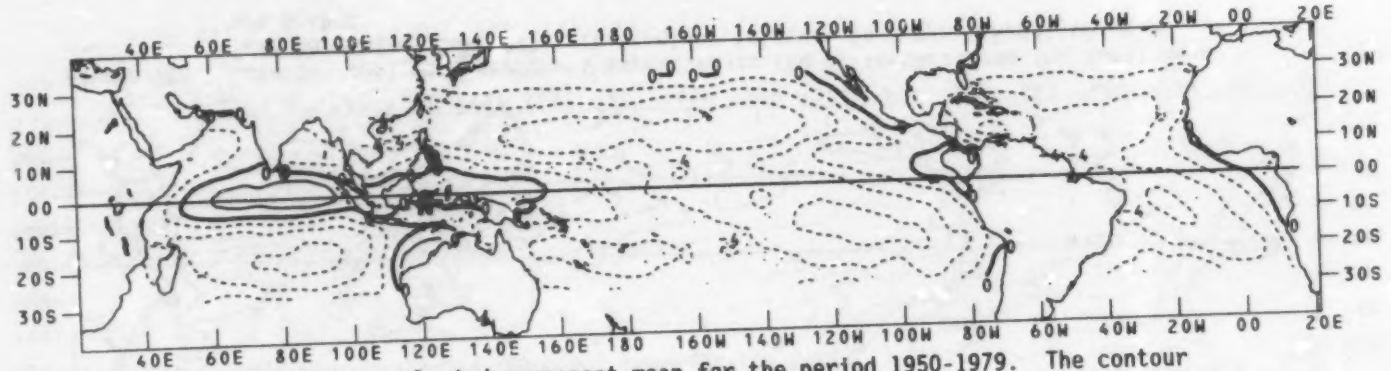

Figure 29a. November zonal wind component mean for the period 1950-1979. The contour interval is 2 m/s. Negative values (easterlies) are dashed; positive values (westerlies) are solid.

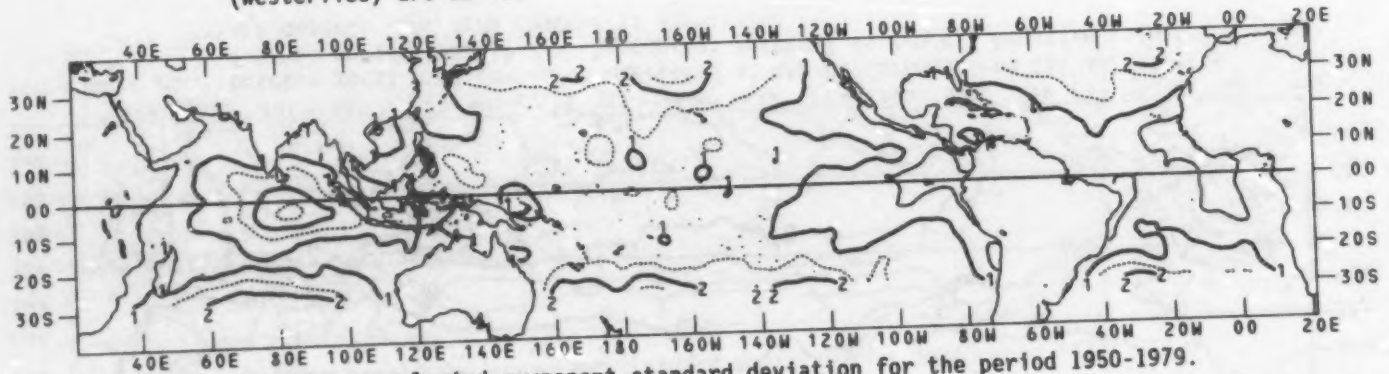

Figure 29b. November zonal wind component standard deviation for the period 1950-1979. The contour interval is .5 m/s.

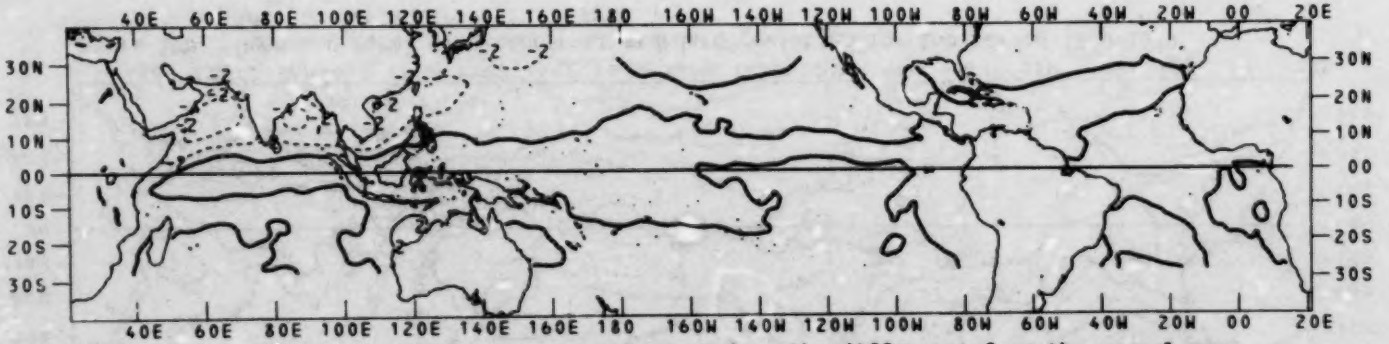

Figure 29c. November zonal wind component expressed as the difference from the annual mean for the period 1950-1979. The contour interval is 2 m/s. Negative values are dashed. The zero contour is emphasized.

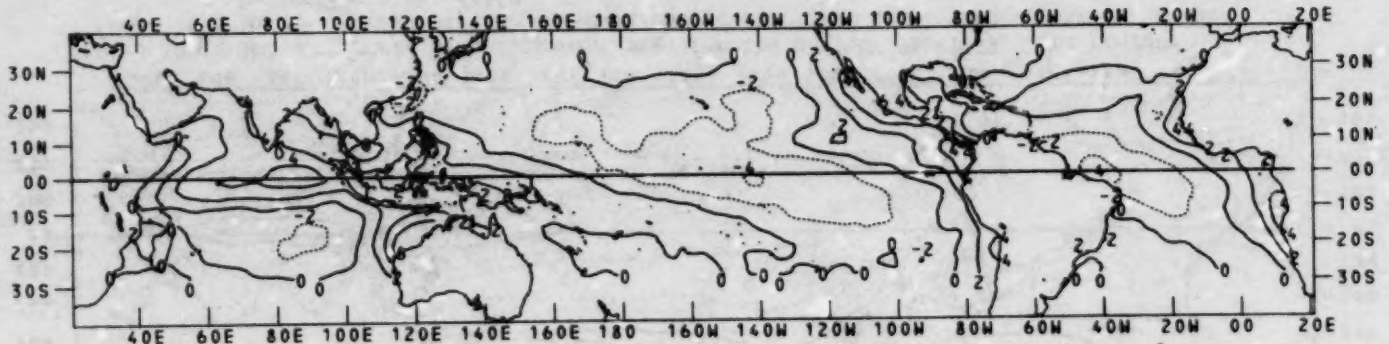

Figure 29d. November zonal wind component expressed as the difference from the zonal mean for the period 1950-1979. The contour interval is 2 m/s. Negative values are dashed.

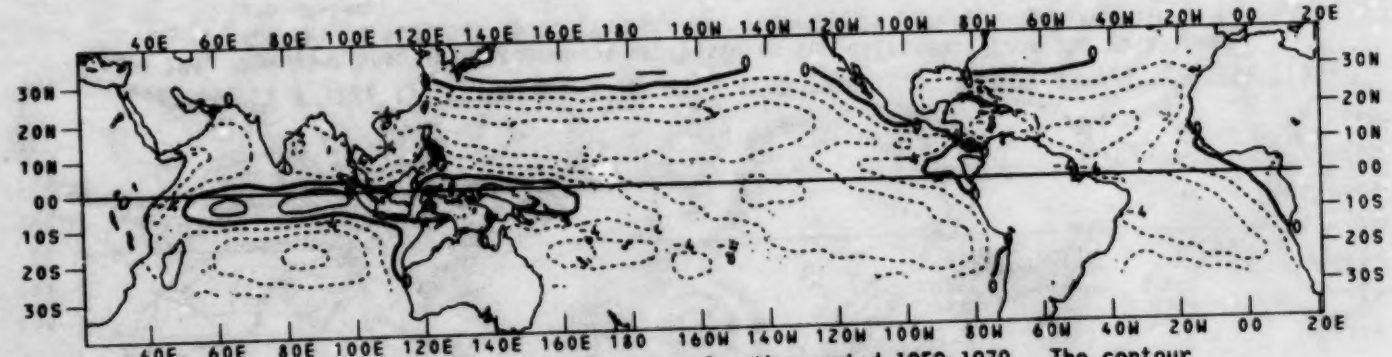

Figure 30a. December zonal wind component mean for the period 1950-1979. The contour interval is 2 m/s. Negative values (easterlies) are dashed; positive values (westerlies) are solid.

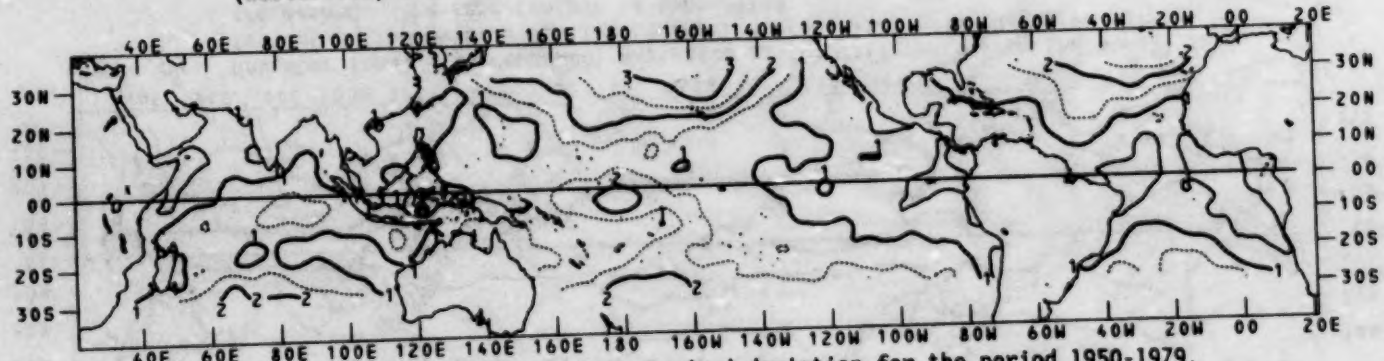

Figure 30b. December zonal wind component standard deviation for the period 1950-1979. The contour interval is .5 m/s.

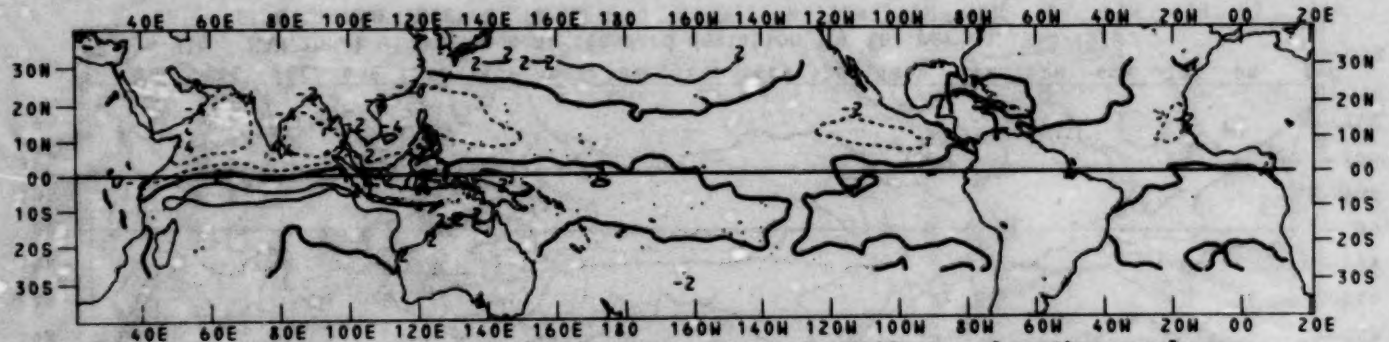

Figure 30c. December zonal wind component expressed as the difference from the annual mean for the period 1950-1979. The contour interval is 2 m/s. Negative values are dashed. The zero contour is emphasized.

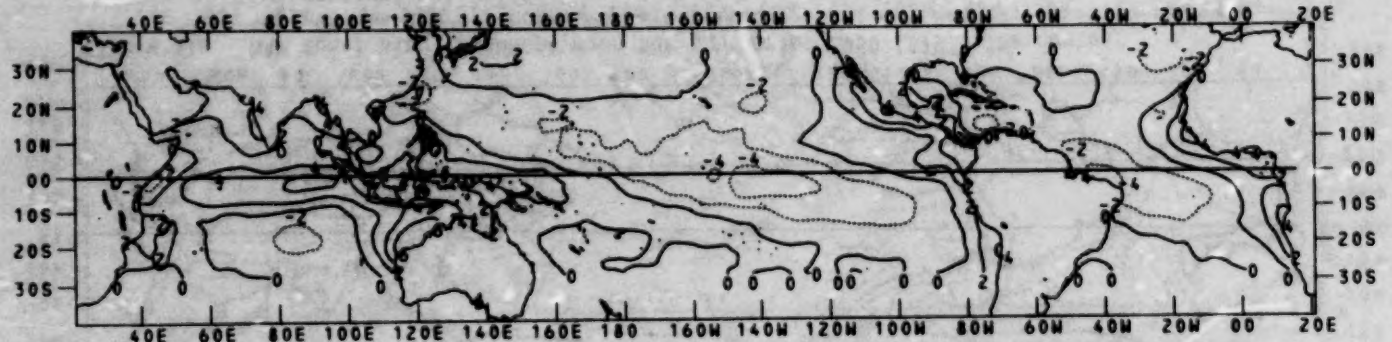

Figure 30d. December zonal wind component expressed as the difference from the zonal mean for the period 1950-1979. The contour interval is 2 m/s. Negative values are dashed.

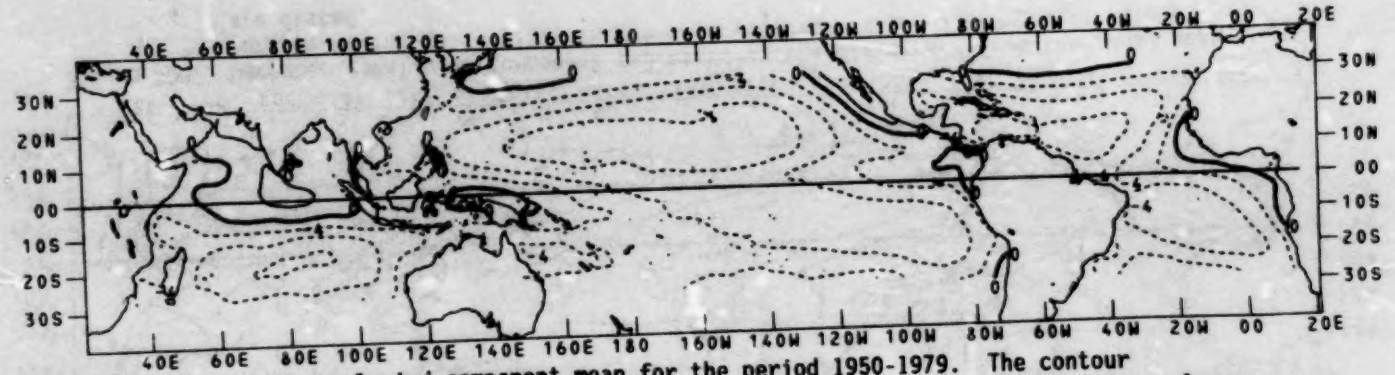

Figure 31a. MAM zonal wind component mean for the period 1950-1979. The contour interval is 2 m/s. Negative values (easterlies) are dashed; positive values (westerlies) are solid.

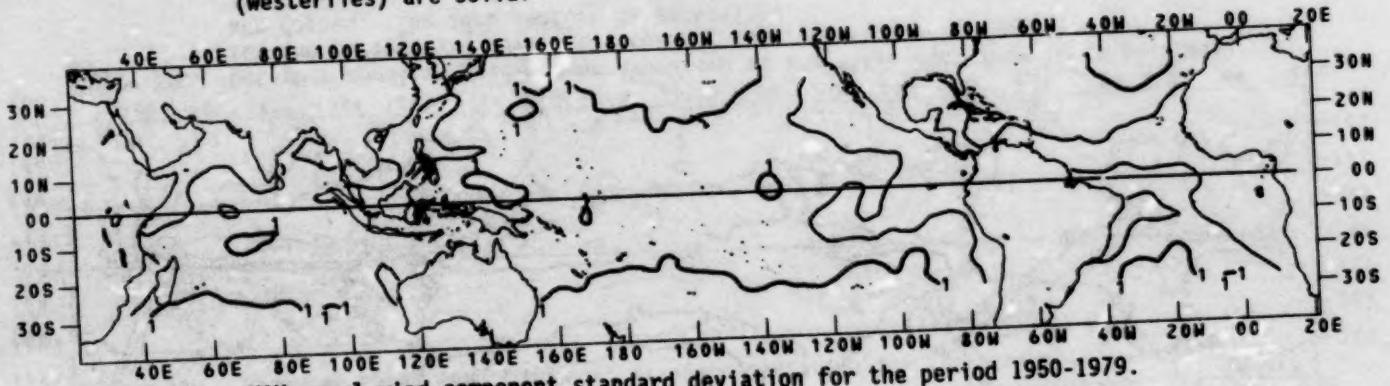

Figure 31b. MAM zonal wind component standard deviation for the period 1950-1979. The contour interval is .5 m/s.

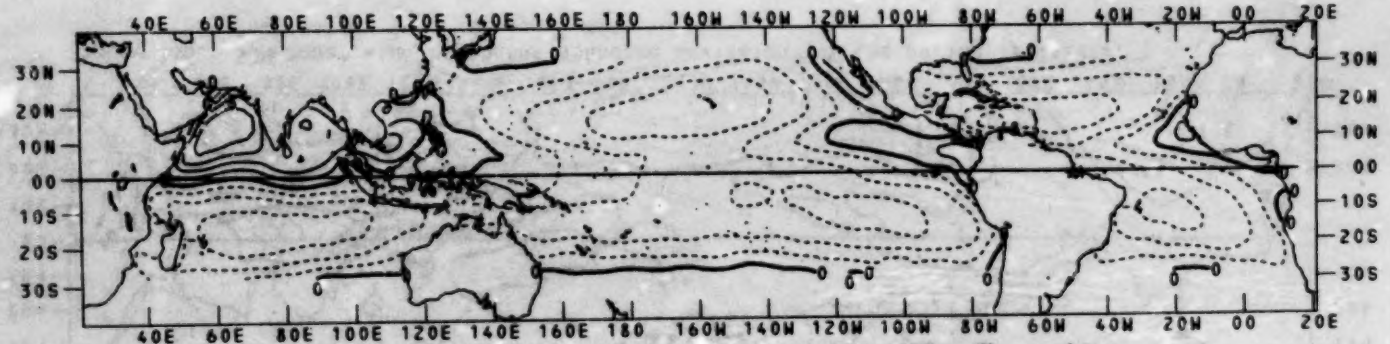

Figure 32a. JJA zonal wind component mean for the period 1950-1979. The contour interval is 2 m/s. Negative values (easterlies) are dashed; positive values (westerlies) are solid.

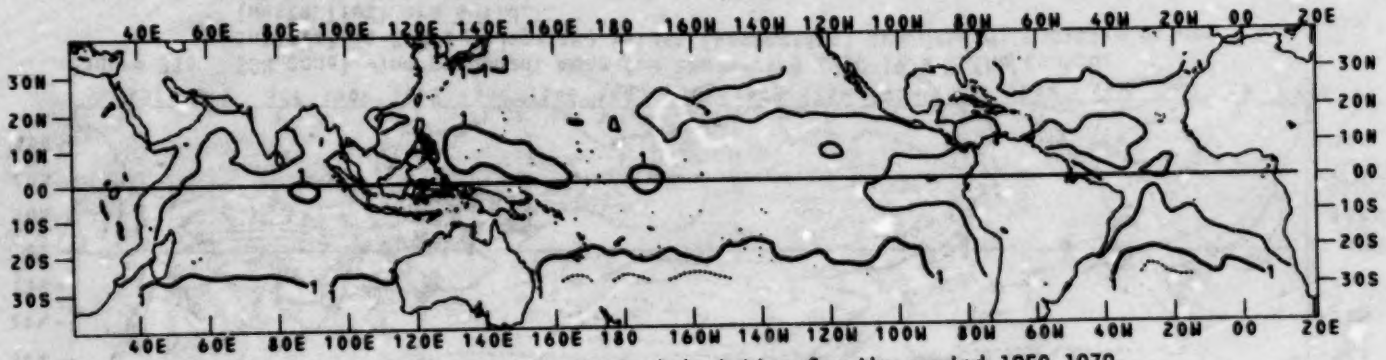

Figure 32b. JJA zonal wind component standard deviation for the period 1950-1979. The contour interval is .5 m/s.

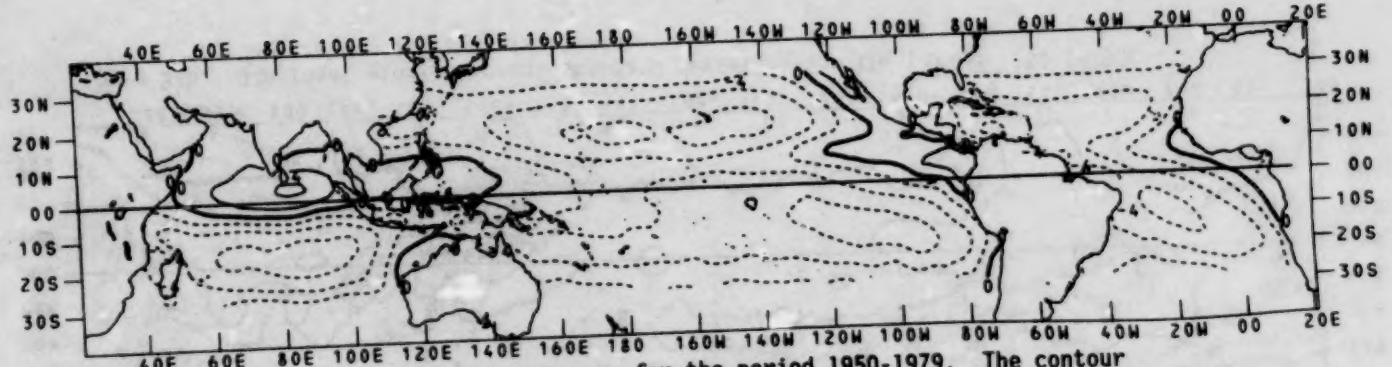

Figure 33a. SON zonal wind component mean for the period 1950-1979. The contour interval is 2 m/s. Negative values (easterlies) are dashed; positive values (westerlies) are solid.

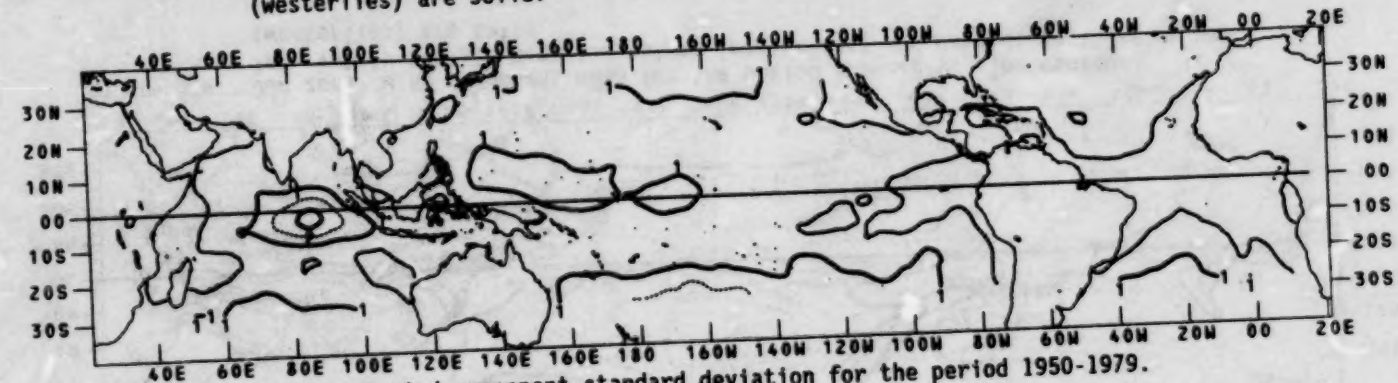

Figure 33b. SON zonal wind component standard deviation for the period 1950-1979. The contour interval is .5 m/s.

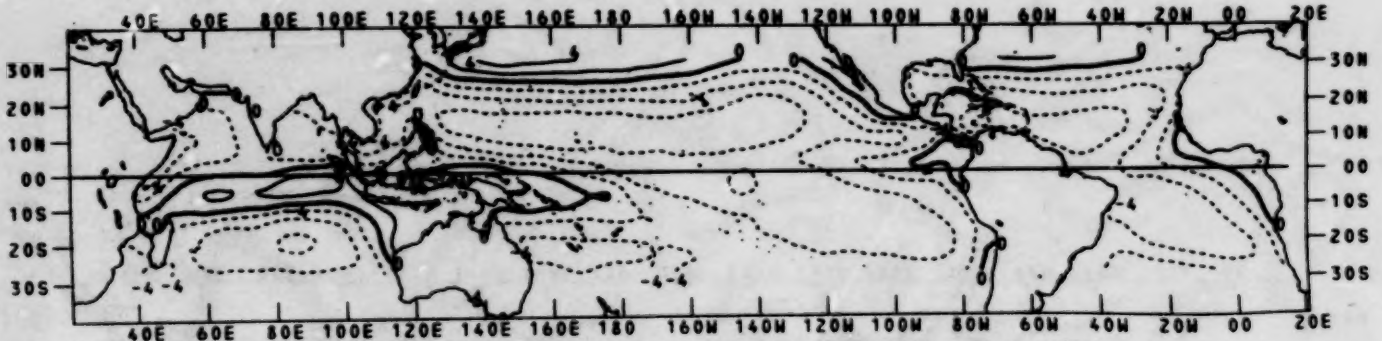

Figure 34a. DJF zonal wind component mean for the period 1950-1979. The contour interval is 2 m/s. Negative values (easterlies) are dashed; positive values (westerlies) are solid.

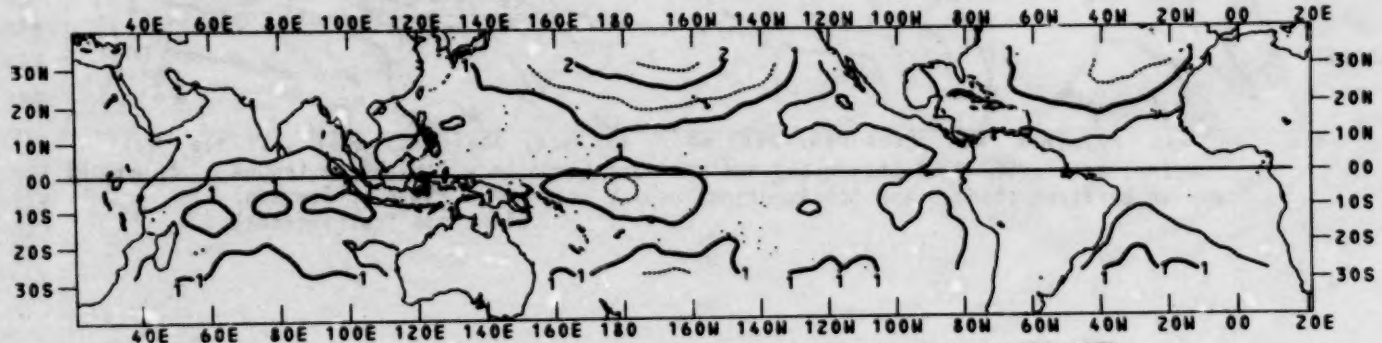

Figure 34b. DJF zonal wind component standard deviation for the period 1950-1979. The contour interval is .5 m/s.

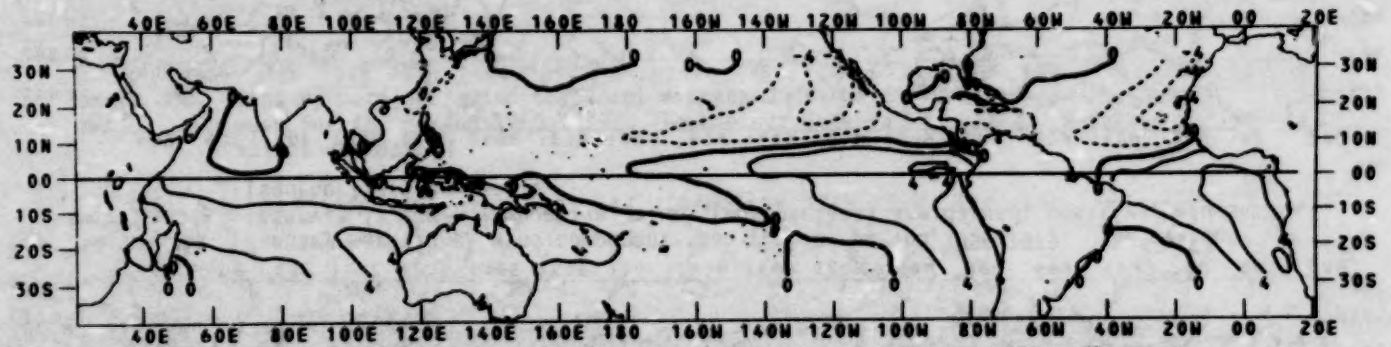

Figure 35. Annual meridional wind component mean for the period 1950-1979. The contour interval is 2 m/s. Negative values (northerlies) are dashed; positive values (southerlies) are solid.

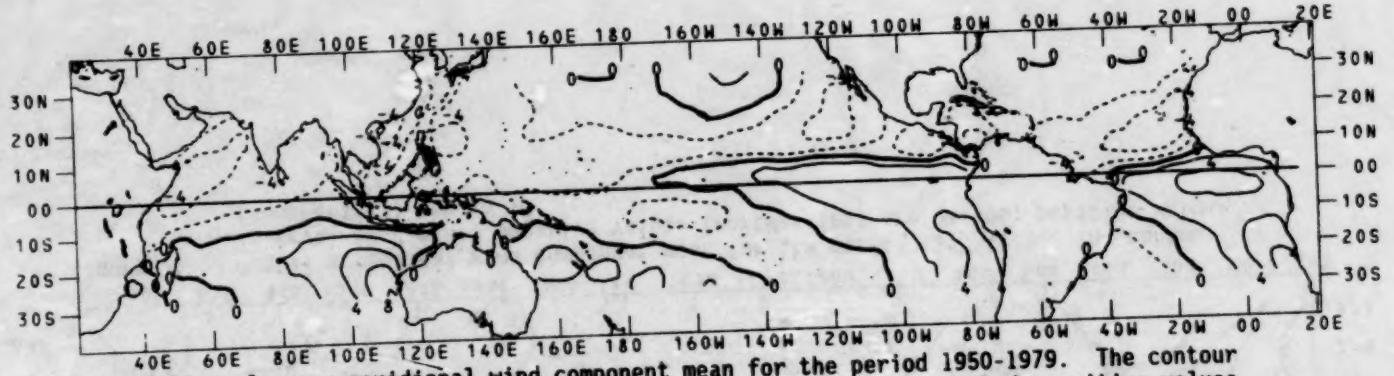

Figure 36a. January meridional wind component mean for the period 1950-1979. The contour interval is 2 m/s. Negative values (northerlies) are dashed; positive values (southerlies) are solid.

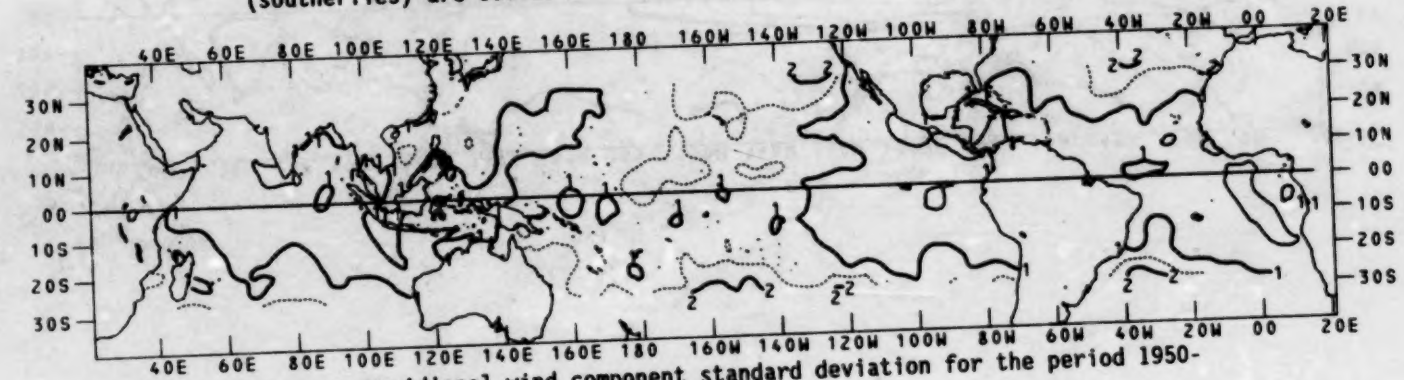

Figure 36b. January meridional wind component standard deviation for the period 1950-1979. The contour interval is .5 m/s.

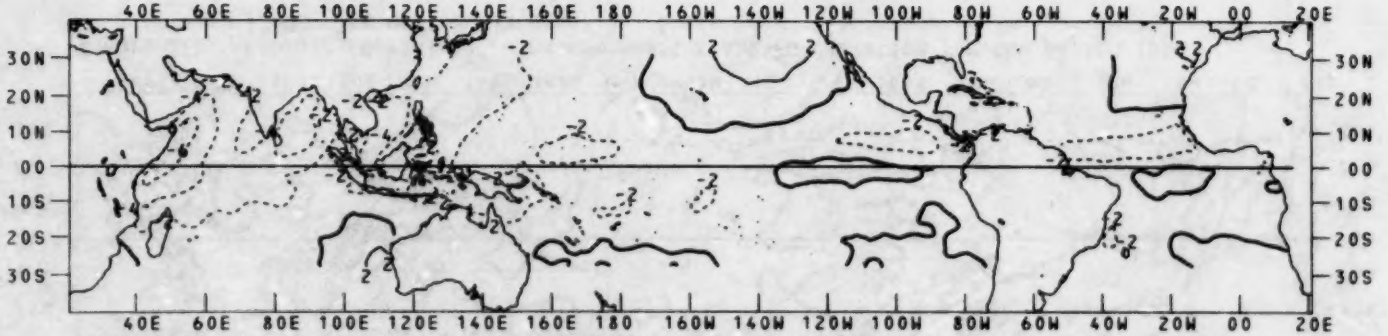

Figure 36c. January merdional wind component expressed as the difference from the annual mean for the period 1950-1979. The contour interval is 2 m/s. Negative values are dashed.

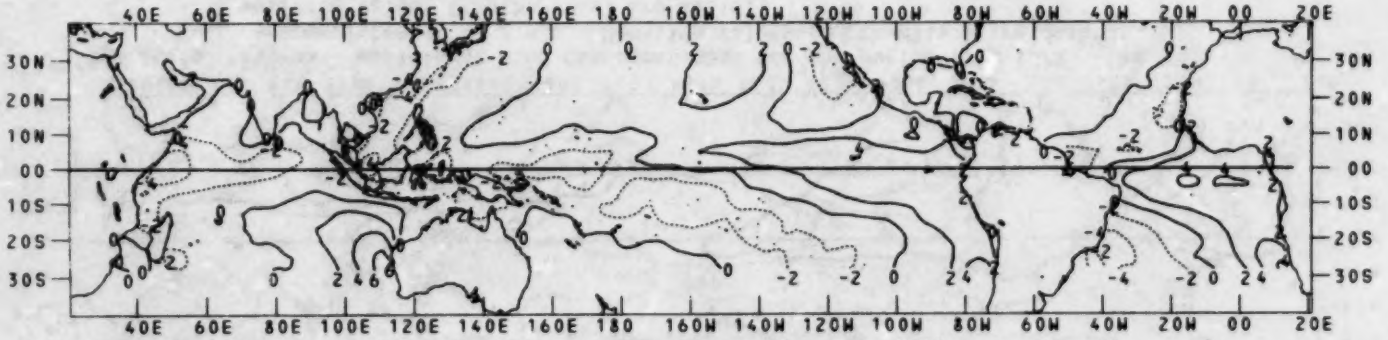

Figure 36d. January meridional wind component expressed as the difference from the zonal mean for the period 1950-1979. The contour interval is 2 m/s. Negative values are dashed.

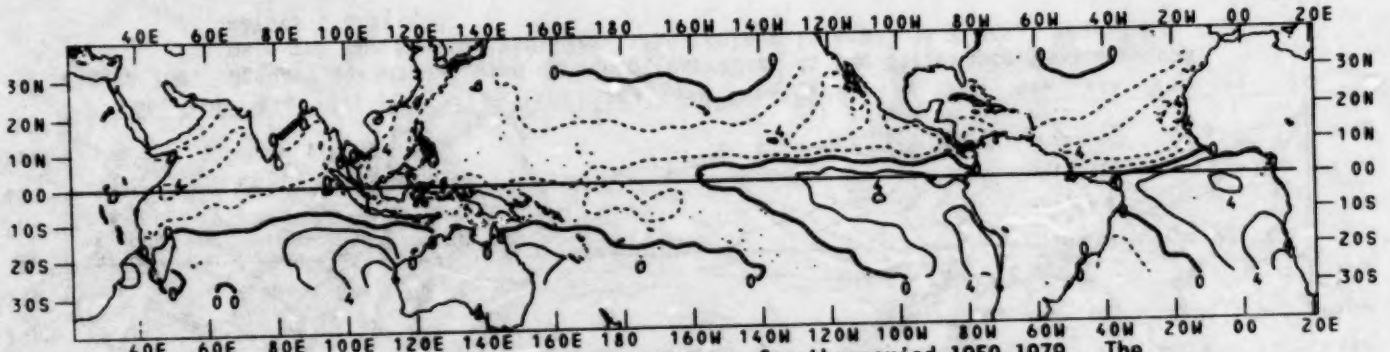

Figure 37a. February meridional wind component mean for the period 1950-1979. The contour interval is 2 m/s. Negative values (northerlies) are dashed; positive values (southerlies) are solid.

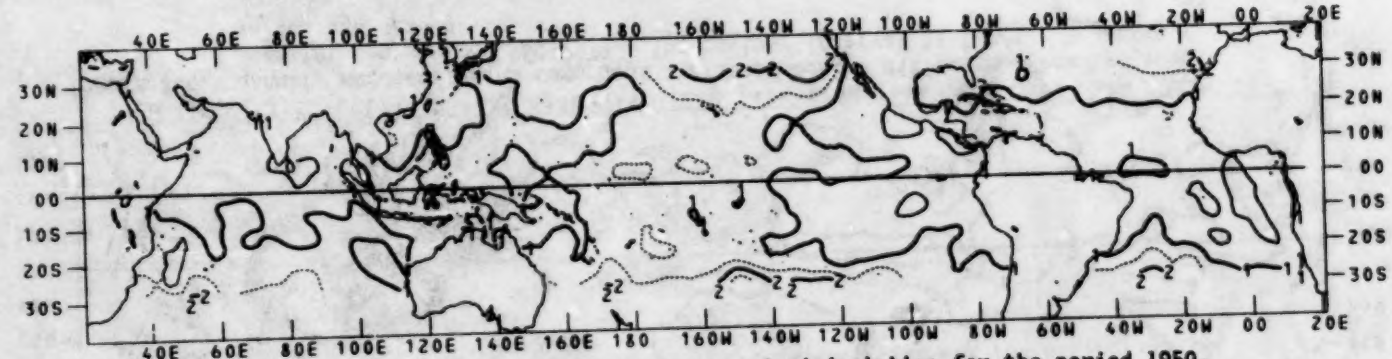

Figure 37b. February meridional wind component standard deviation for the period 1950-1979. The contour interval is .5 m/s.

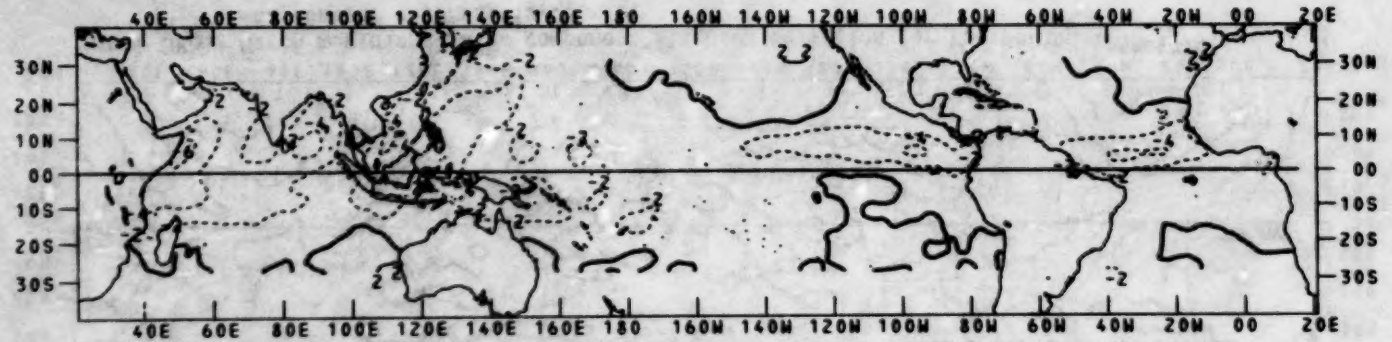

Figure 37c. February merdional wind component expressed as the difference from the annual mean for the period 1950-1979. The contour interval is 2 m/s. Negative values are dashed.

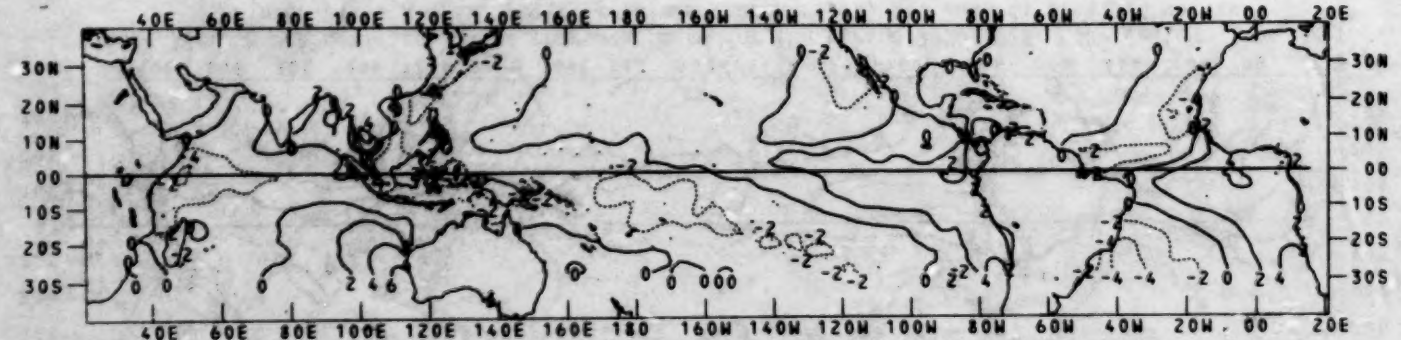

Figure 37d. February meridional wind component expressed as the difference from the zonal mean for the period 1950-1979. The contour interval is 2 m/s. Negative values are dashed.

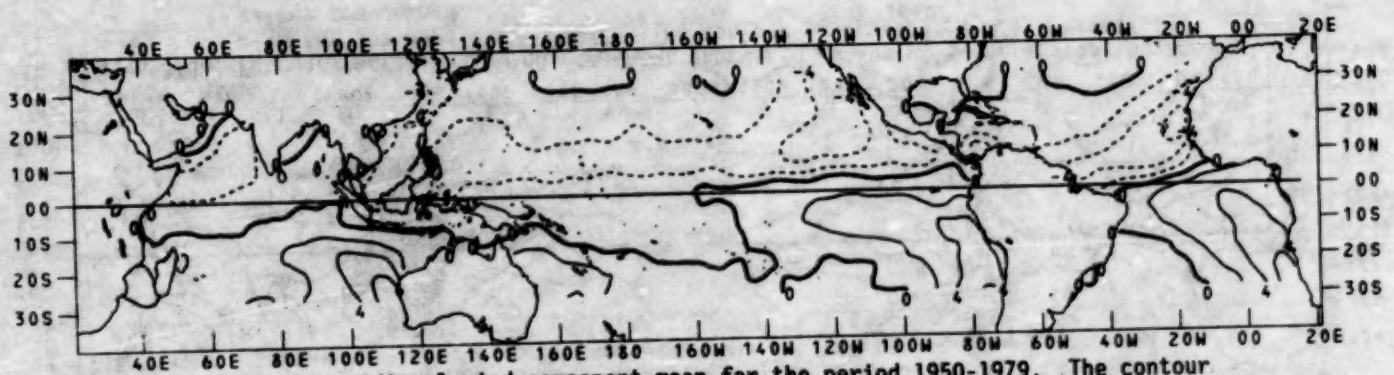

Figure 38a. March meridional wind component mean for the period 1950-1979. The contour interval is 2 m/s. Negative values (northerlies) are dashed; positive values (southerlies) are solid.

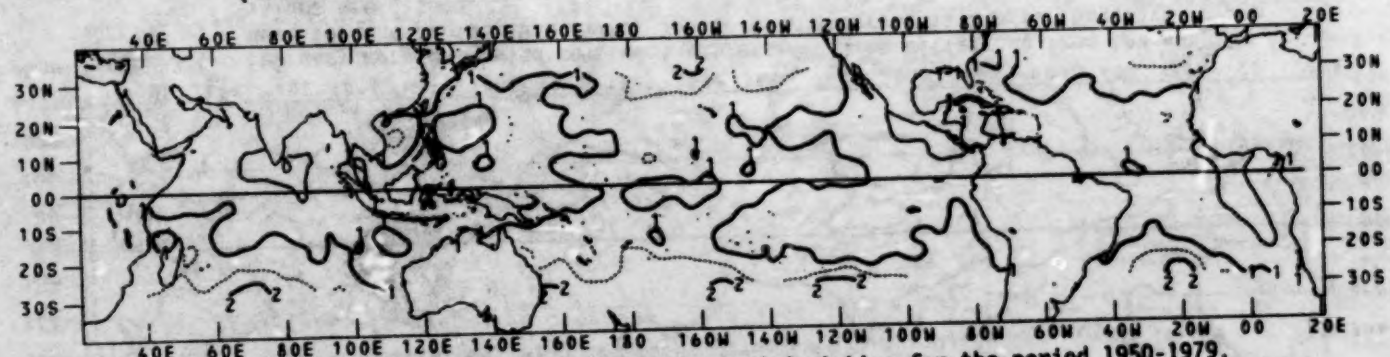

Figure 38b. March meridional wind component standard deviation for the period 1950-1979. The contour interval is .5 m/s.

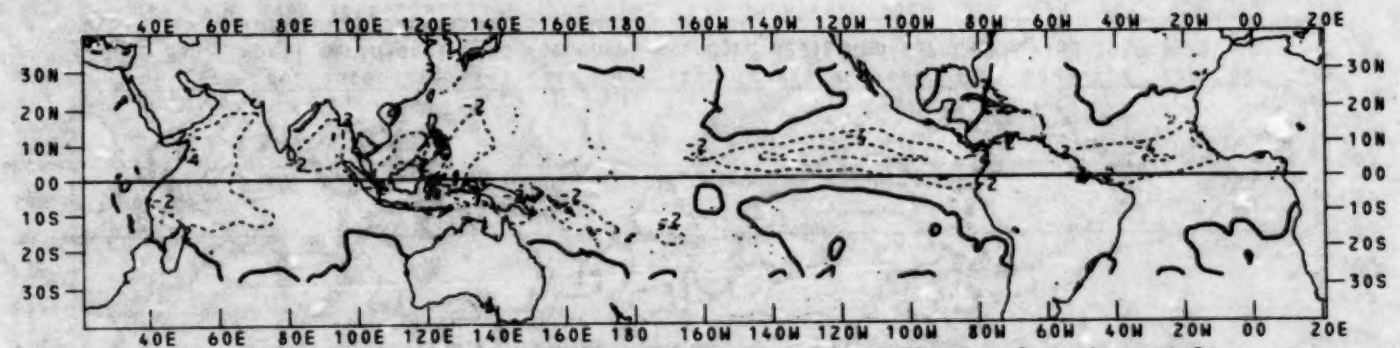

Figure 38c. March merdional wind component expressed as the difference from the annual mean for the period 1950-1979. The contour interval is 2 m/s. Negative values are dashed.

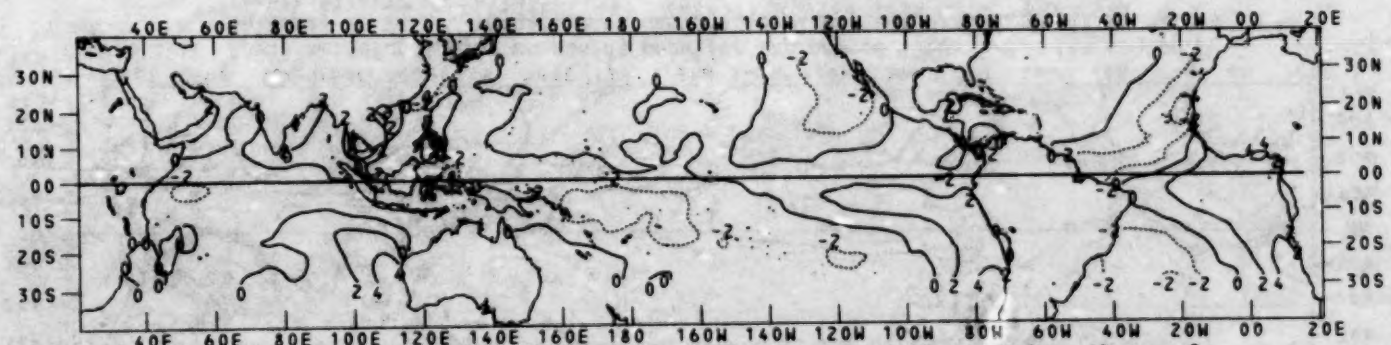

Figure 38d. March meridional wind component expressed as the difference from the zonal mean for the period 1950-1979. The contour interval is 2 m/s. Negative values are dashed.

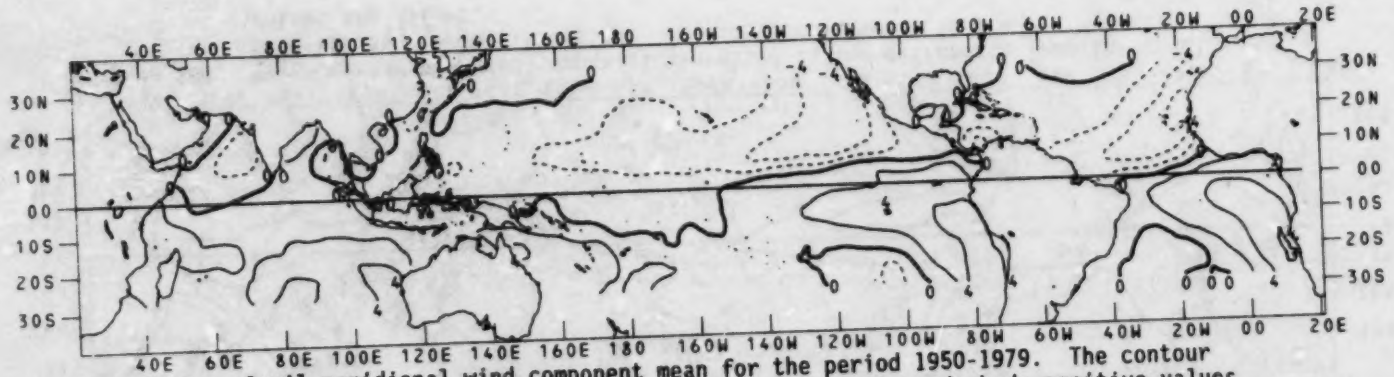

Figure 39a. April meridional wind component mean for the period 1950-1979. The contour interval is 2 m/s. Negative values (northerlies) are dashed; positive values (southerlies) are solid.

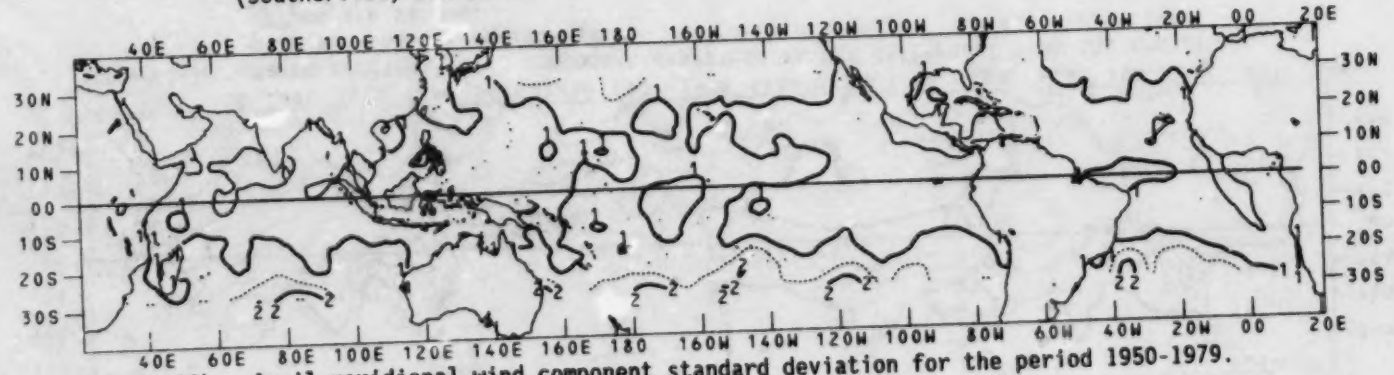

Figure 39b. April meridional wind component standard deviation for the period 1950-1979. The contour interval is .5 m/s.

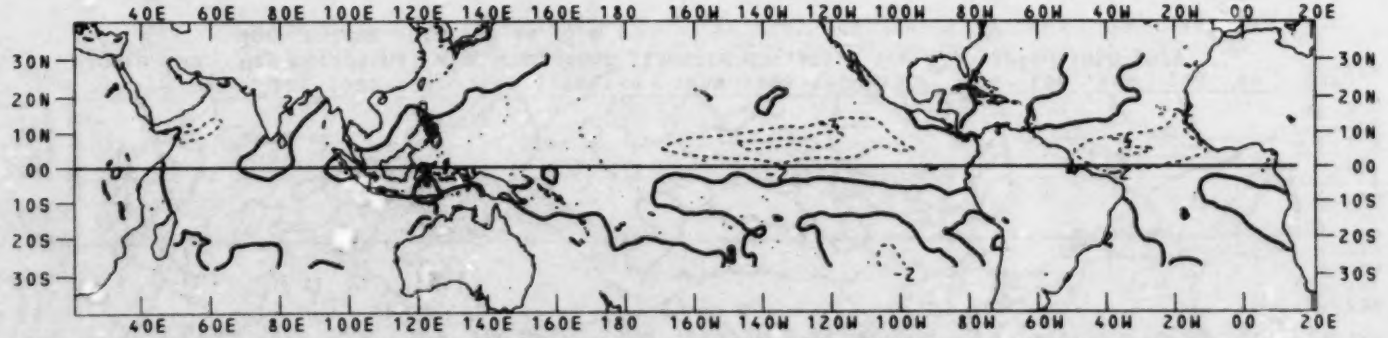

Figure 39c. April merdional wind component expressed as the difference from the annual mean for the period 1950-1979. The contour interval is 2 m/s. Negative values are dashed.

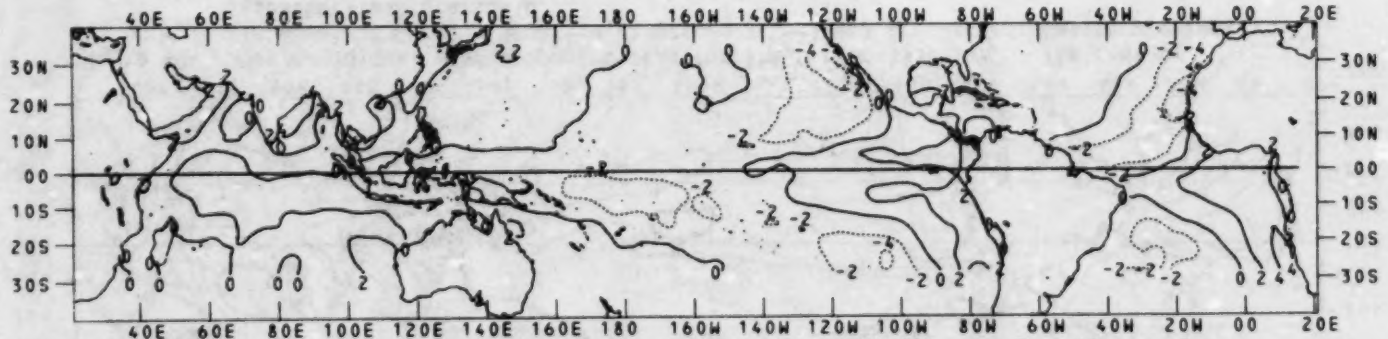

Figure 39d. April meridional wind component expressed as the difference from the zonal mean for the period 1950-1979. The contour interval is 2 m/s. Negative values are dashed.

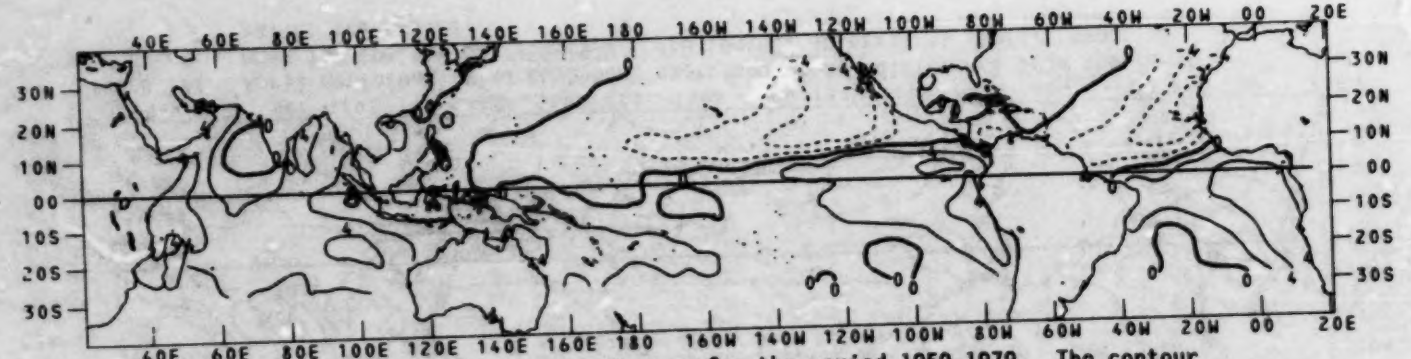

Figure 40a May meridional wind component mean for the period 1950-1979. The contour interval is 2 m/s. Negative values (northerlies) are dashed; positive values (southerlies) are solid.

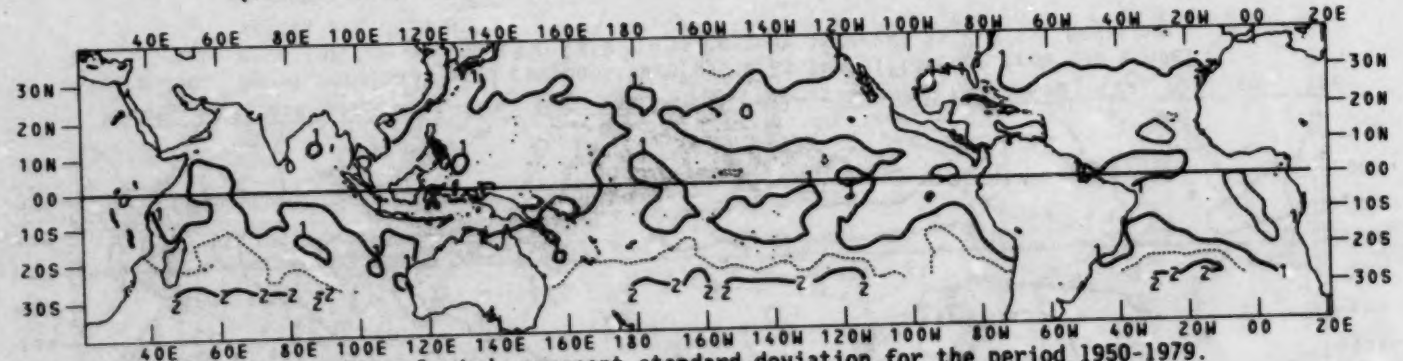

Figure 40b. May meridional wind component standard deviation for the period 1950-1979. The contour interval is .5 m/s.

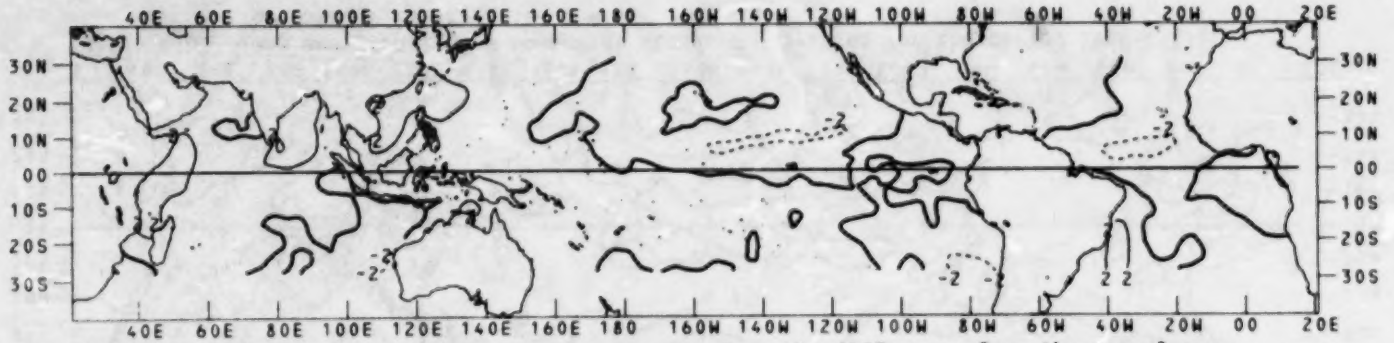

Figure 40c. May merdional wind component expressed as the difference from the annual mean for the period 1950-1979. The contour interval is 2 m/s. Negative values are dashed.

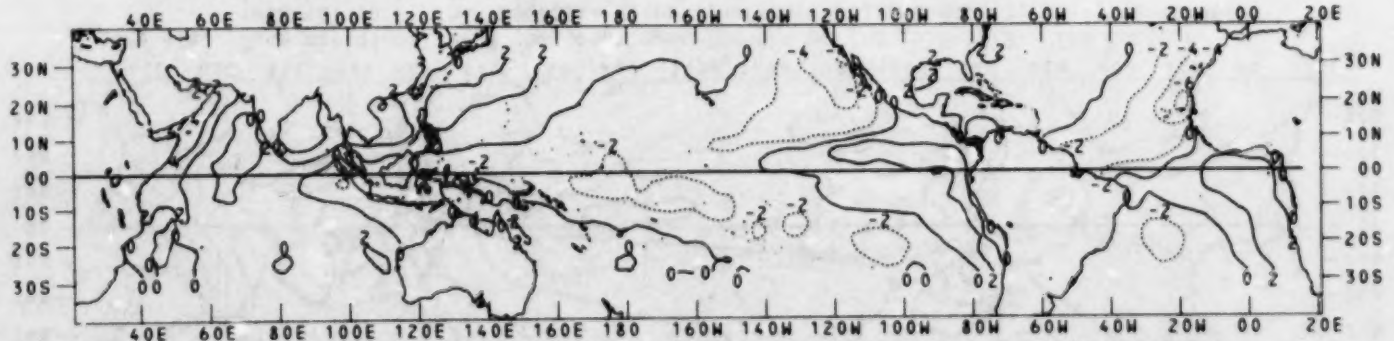

Figure 40d. May meridional wind component expressed as the difference from the zonal mean for the period 1950-1979. The contour interval is 2 m/s. Negative values are dashed.

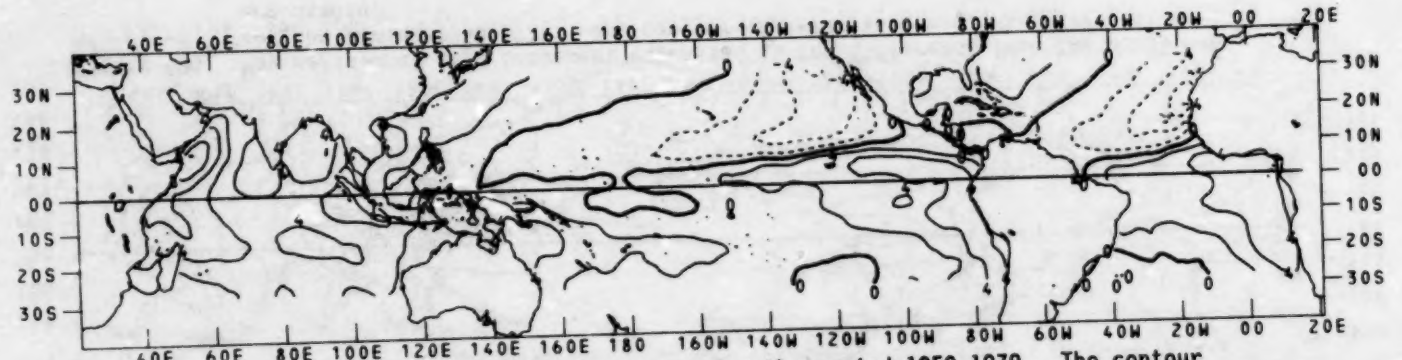

Figure 41a. June meridional wind component mean for the period 1950-1979. The contour interval is 2 m/s. Negative values (northerlies) are dashed; positive values (southerlies) are solid.

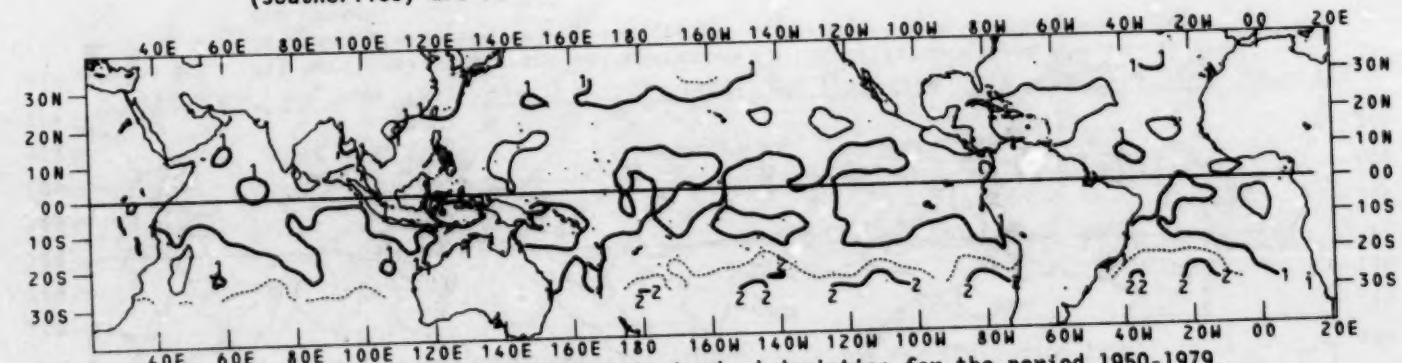

Figure 41b. June meridional wind component standard deviation for the period 1950-1979. The contour interval is .5 m/s.

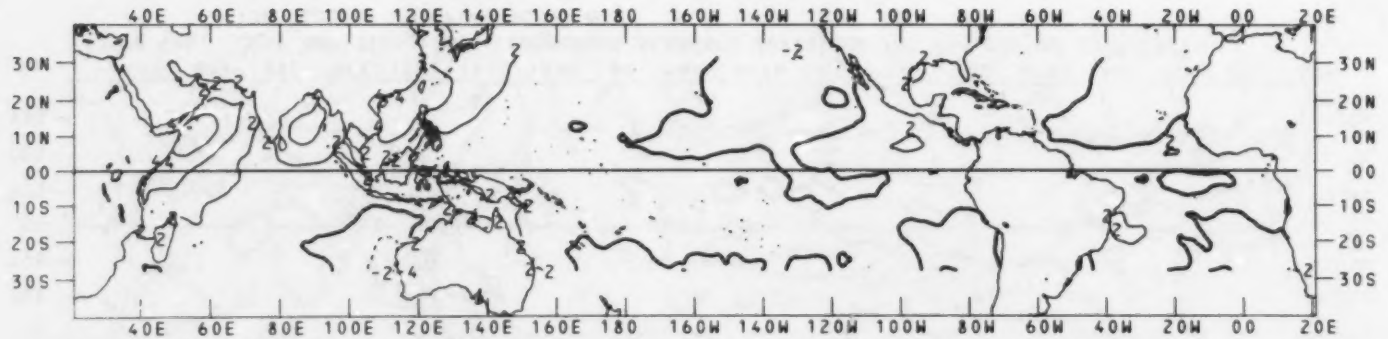

Figure 41c. June merdional wind component expressed as the difference from the annual mean for the period 1950-1979. The contour interval is 2 m/s. Negative values are dashed.

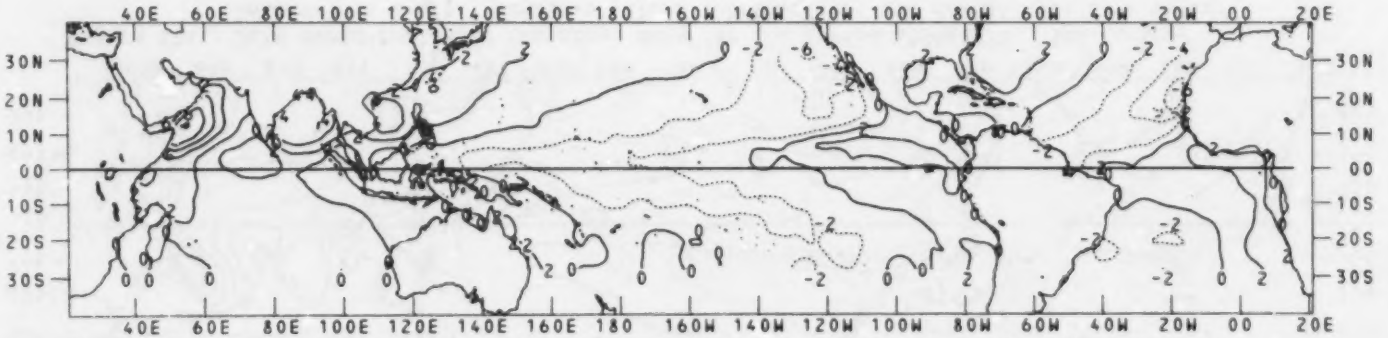

Figure 41d. June meridional wind component expressed as the difference from the zonal mean for the period 1950-1979. The contour interval is 2 m/s. Negative values are dashed.

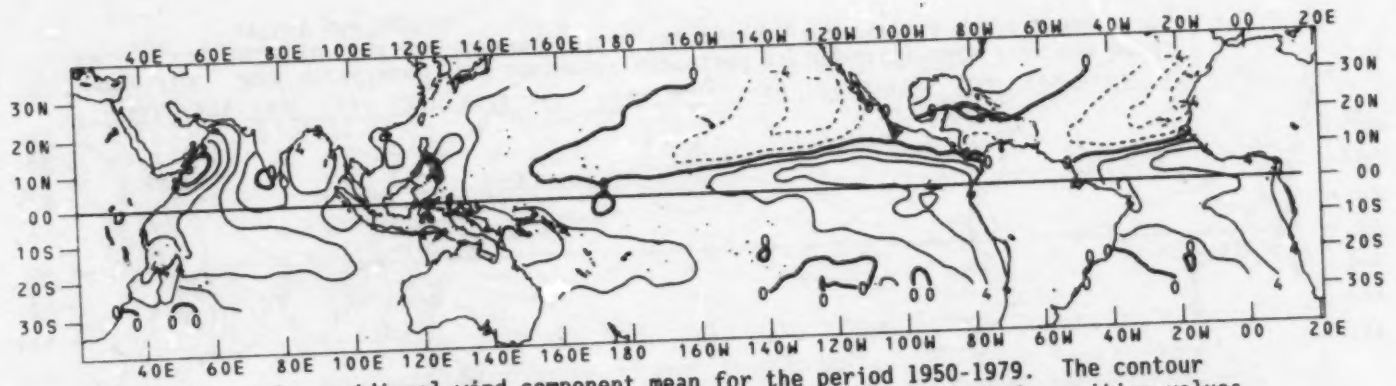

Figure 42a. July meridional wind component mean for the period 1950-1979. The contour interval is 2 m/s. Negative values (northerlies) are dashed; positive values (southerlies) are solid.

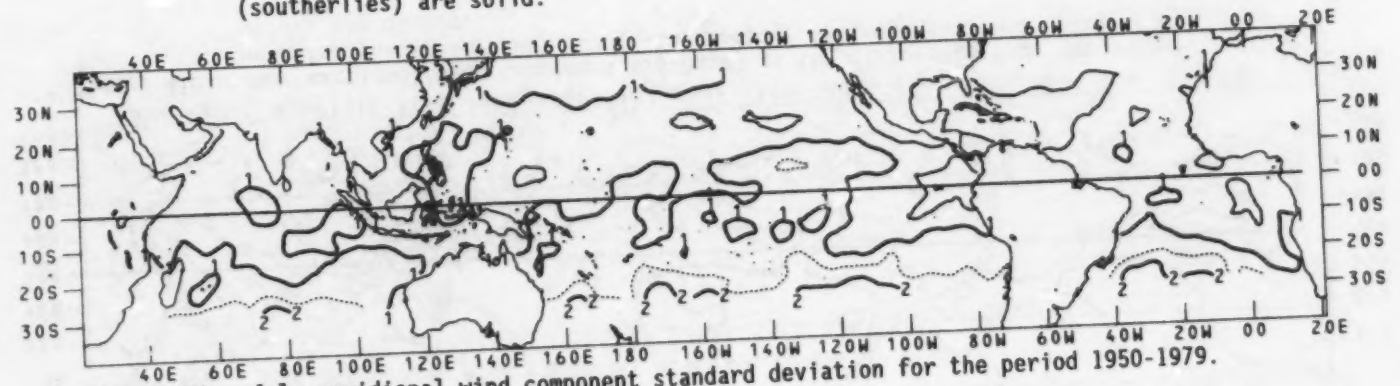

Figure 42b. July meridional wind component standard deviation for the period 1950-1979. The contour interval is .5 m/s.

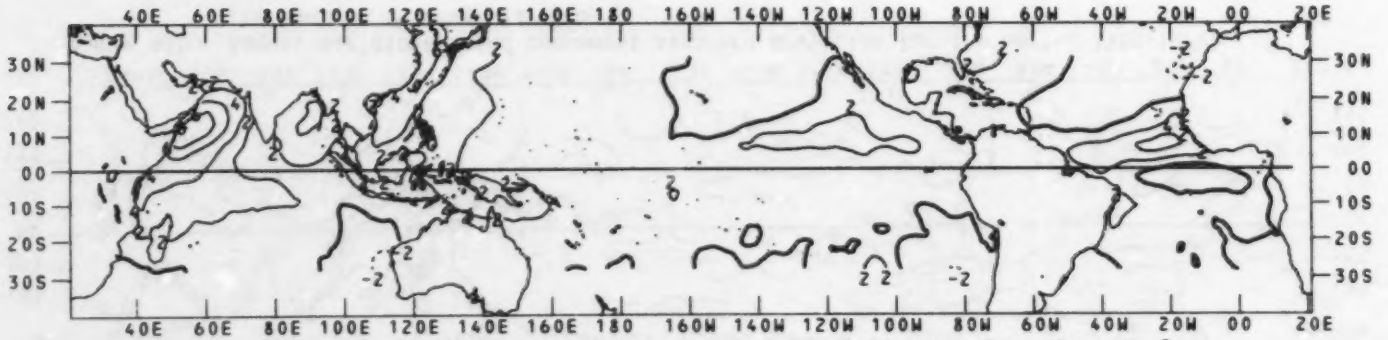

Figure 42c. July merdional wind component expressed as the difference from the annual mean for the period 1950-1979. The contour interval is 2 m/s. Negative values are dashed.

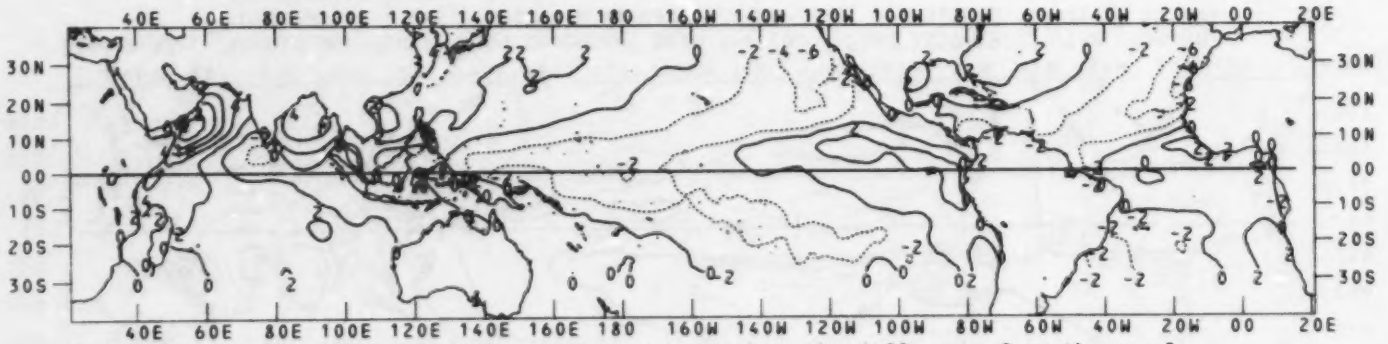

Figure 42d. July meridional wind component expressed as the difference from the zonal mean for the period 1950-1979. The contour interval is 2 m/s. Negative values are dashed.

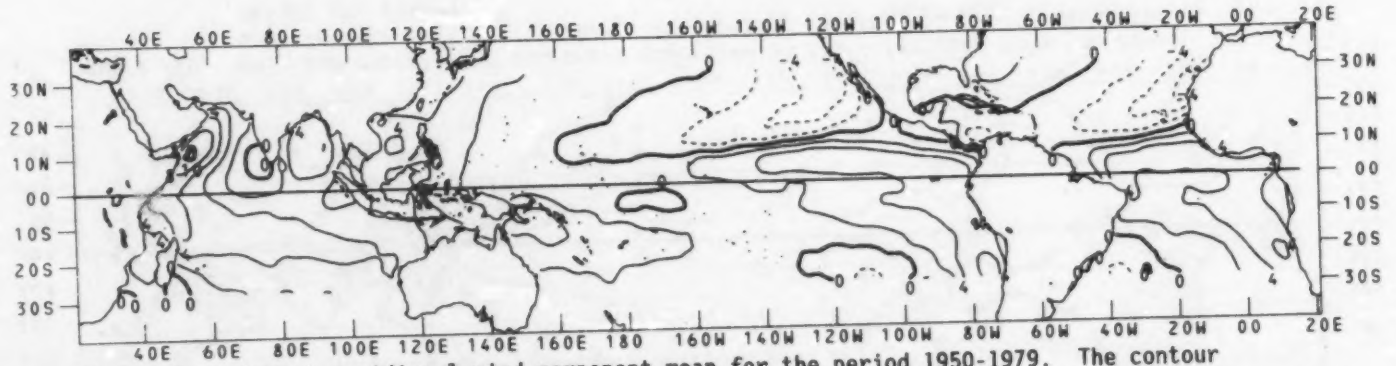

Figure 43a. August meridional wind component mean for the period 1950-1979. The contour interval is 2 m/s. Negative values (northerlies) are dashed; positive values (southerlies) are solid.

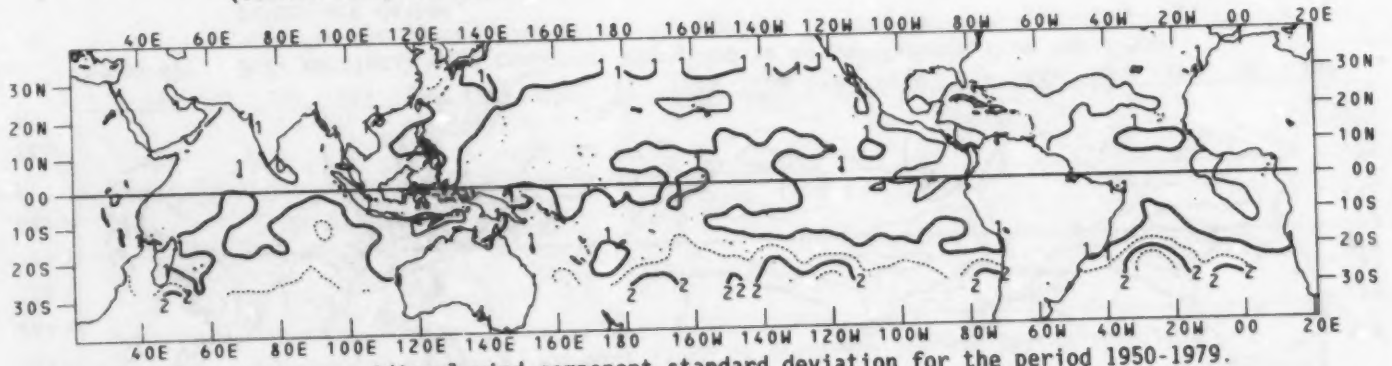

Figure 43b. August meridional wind component standard deviation for the period 1950-1979. The contour interval is .5 m/s.

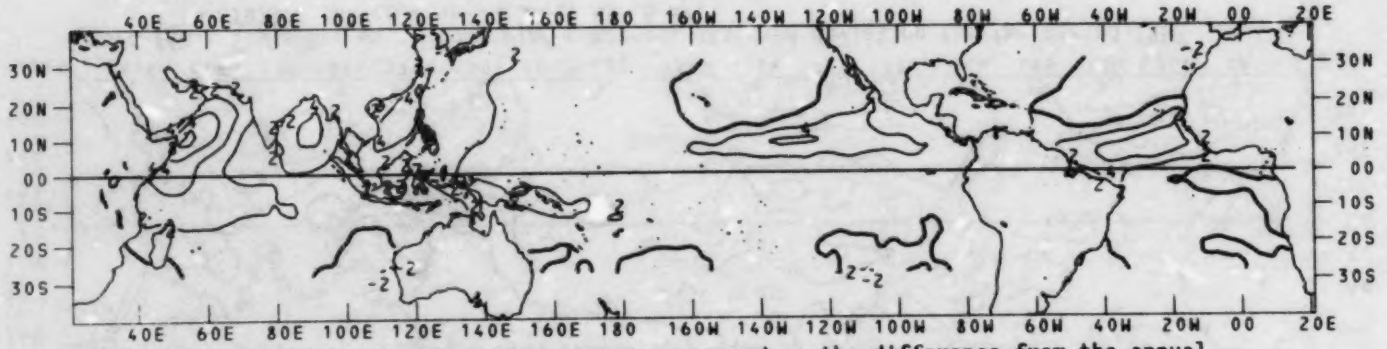

Figure 43c. August merdional wind component expressed as the difference from the annual mean for the period 1950-1979. The contour interval is 2 m/s. Negative values are dashed.

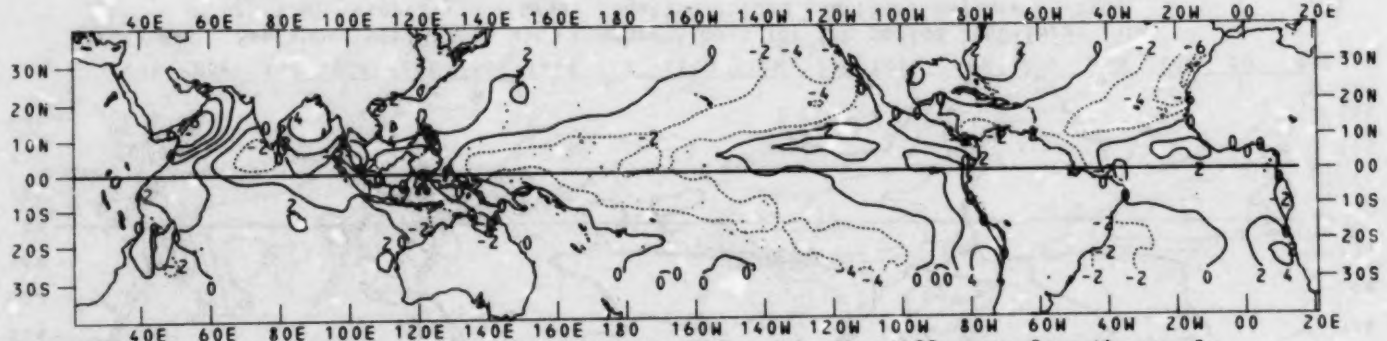

Figure 43d. August meridional wind component expressed as the difference from the zonal mean for the period 1950-1979. The contour interval is 2 m/s. Negative values are dashed.

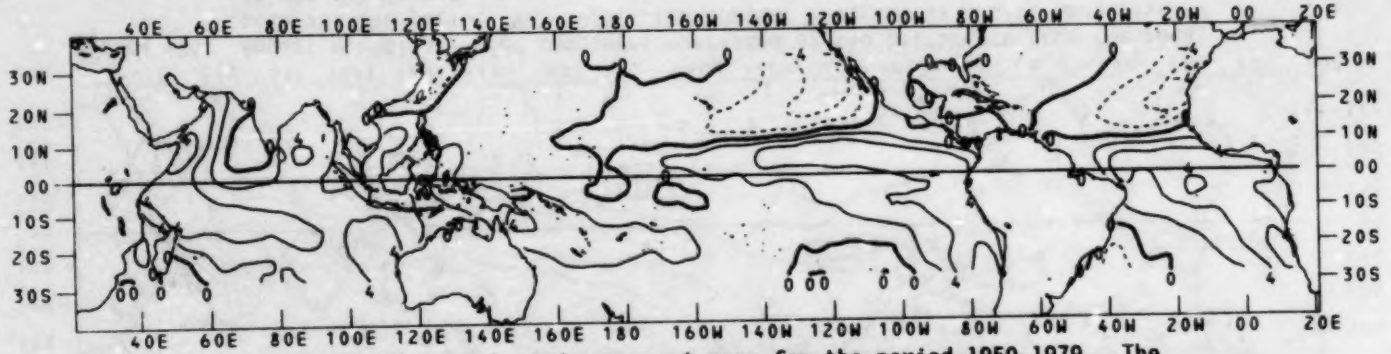

Figure 44a. September meridional wind component mean for the period 1950-1979. The contour interval is 2 m/s. Negative values (northerlies) are dashed; positive values (southerlies) are solid.

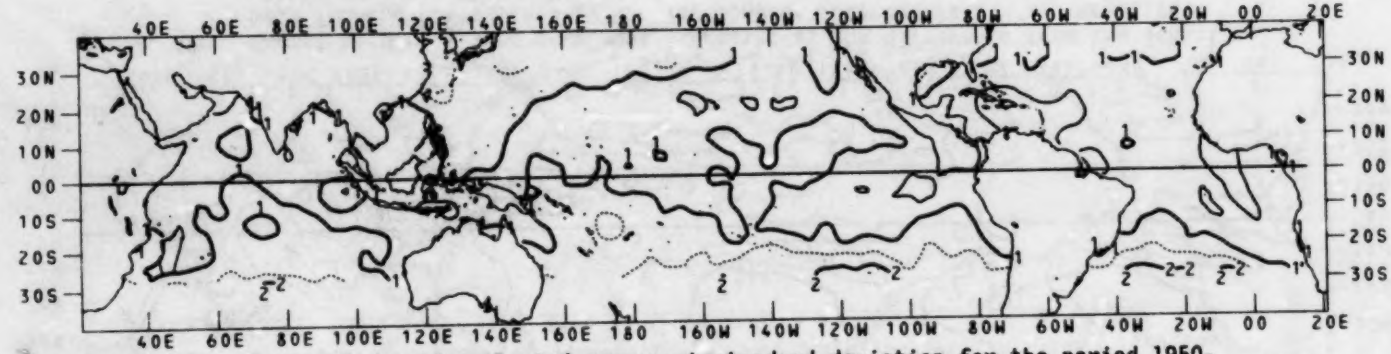

Figure 44b. September meridional wind component standard deviation for the period 1950-1979. The contour interval is .5 m/s.

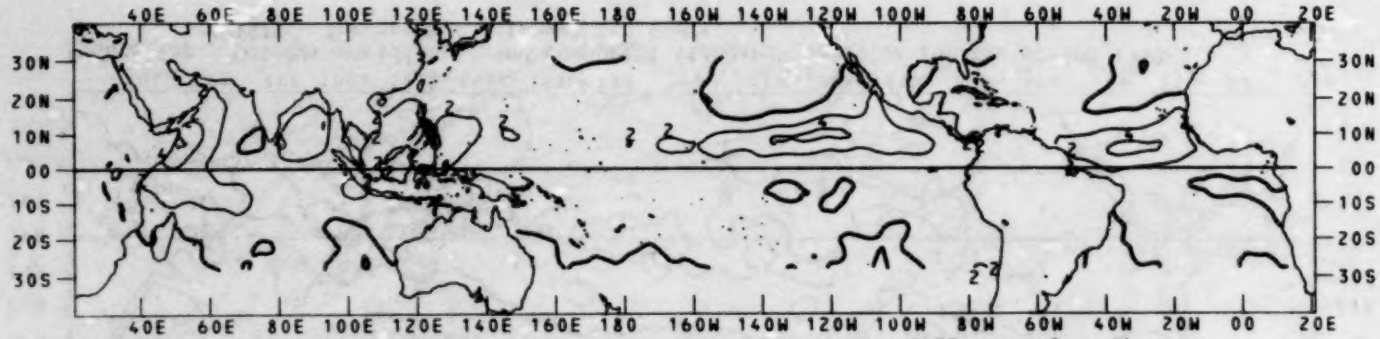

Figure 44c. September merdional wind component expressed as the difference from the annual mean for the period 1950-1979. The contour interval is 2 m/s. Negative values are dashed.

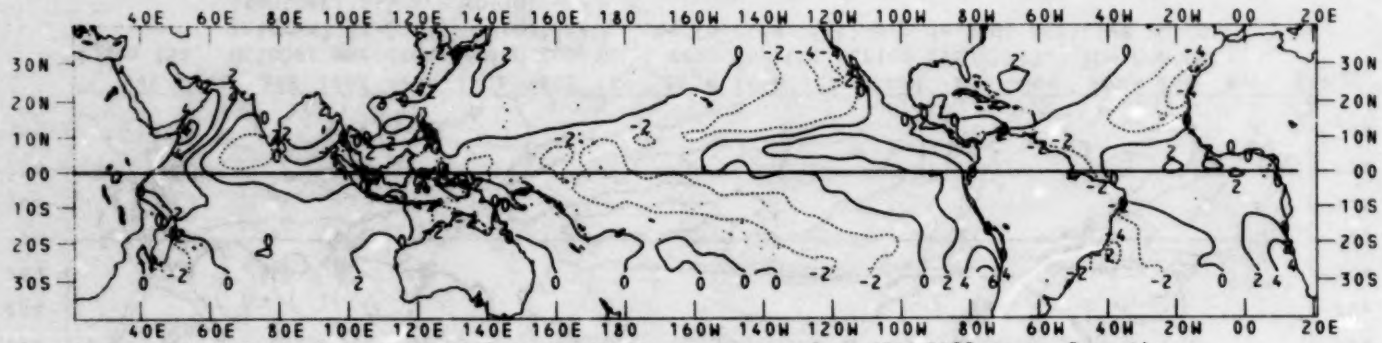

Figure 44d. September meridional wind component expressed as the difference from the zonal mean for the period 1950-1979. The contour interval is 2 m/s. Negative values are dashed.

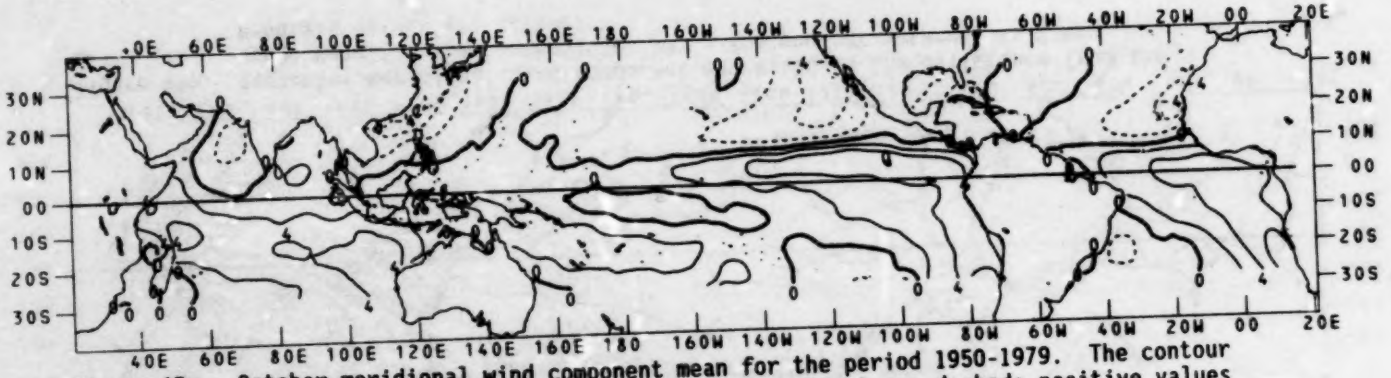

Figure 45a. October meridional wind component mean for the period 1950-1979. The contour interval is 2 m/s. Negative values (northerlies) are dashed; positive values (southerlies) are solid.

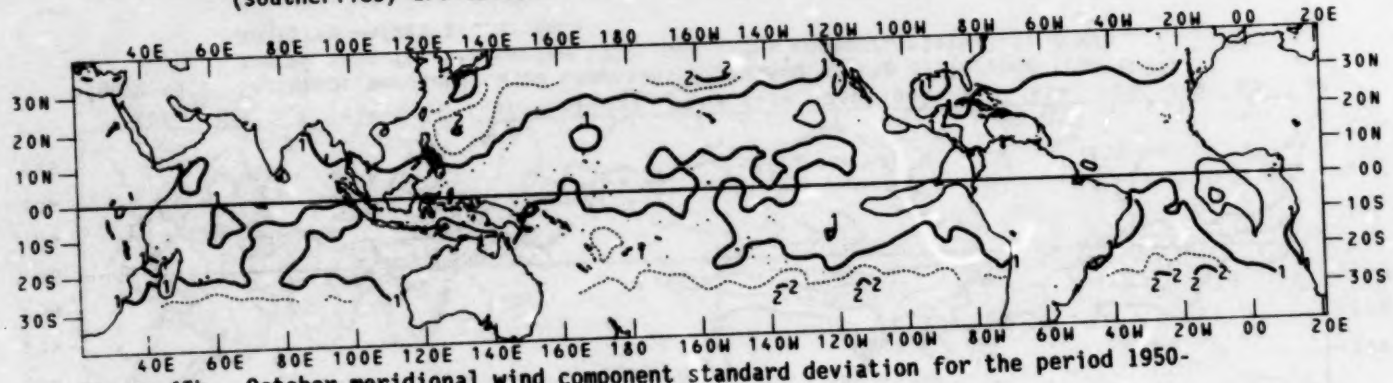

Figure 45b. October meridional wind component standard deviation for the period 1950-1979. The contour interval is .5 m/s.

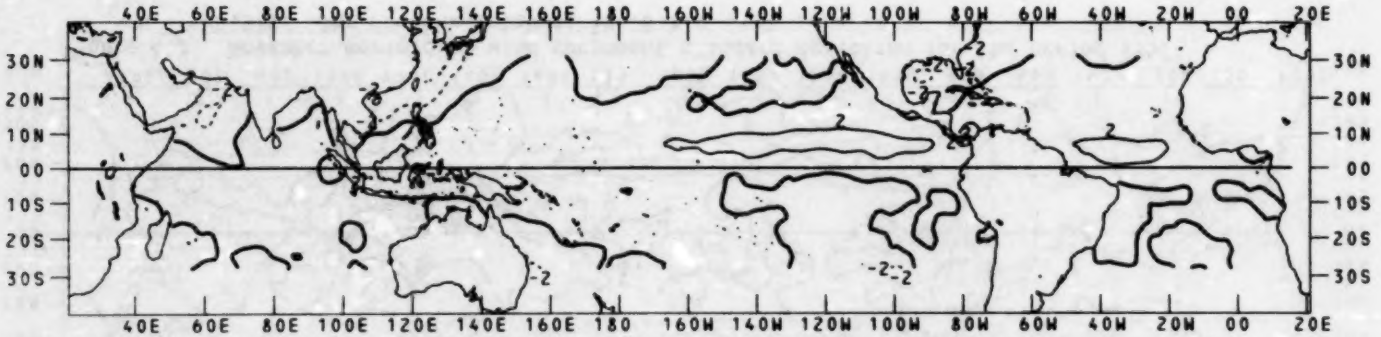

Figure 45c. October merdional wind component expressed as the difference from the annual mean for the period 1950-1979. The contour interval is 2 m/s. Negative values are dashed.

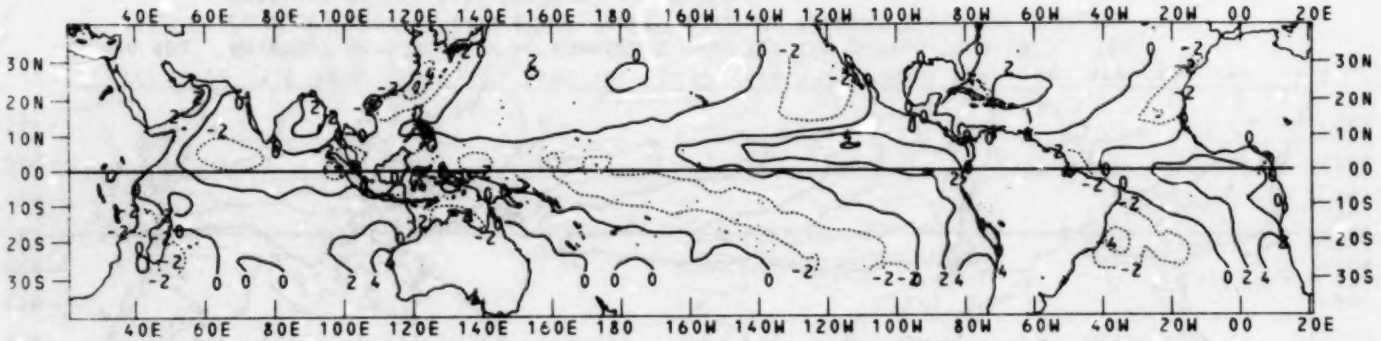

Figure 45d. October meridional wind component expressed as the difference from the zonal mean for the period 1950-1979. The contour interval is 2 m/s. Negative values are dashed.

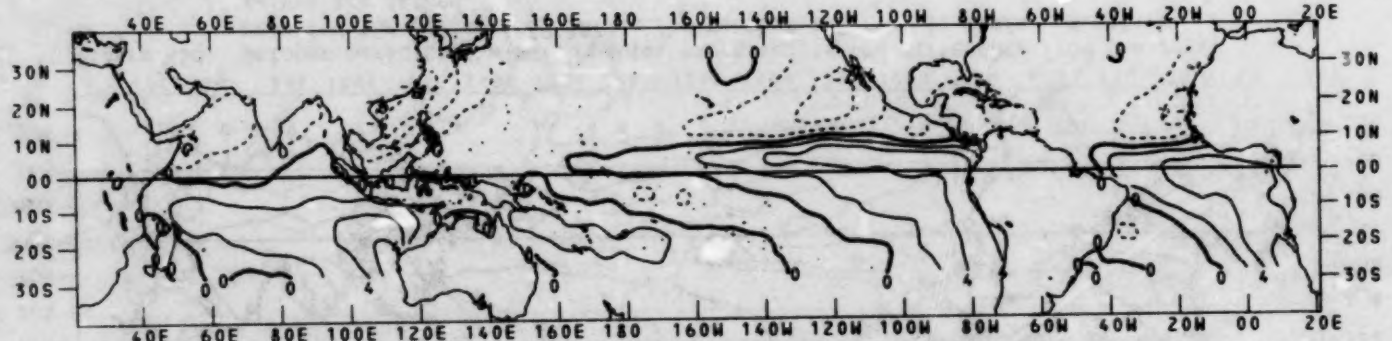

Figure 46a. November meridional wind component mean for the period 1950-1979. The contour interval is 2 m/s. Negative values (northerlies) are dashed; positive values (southerlies) are solid.

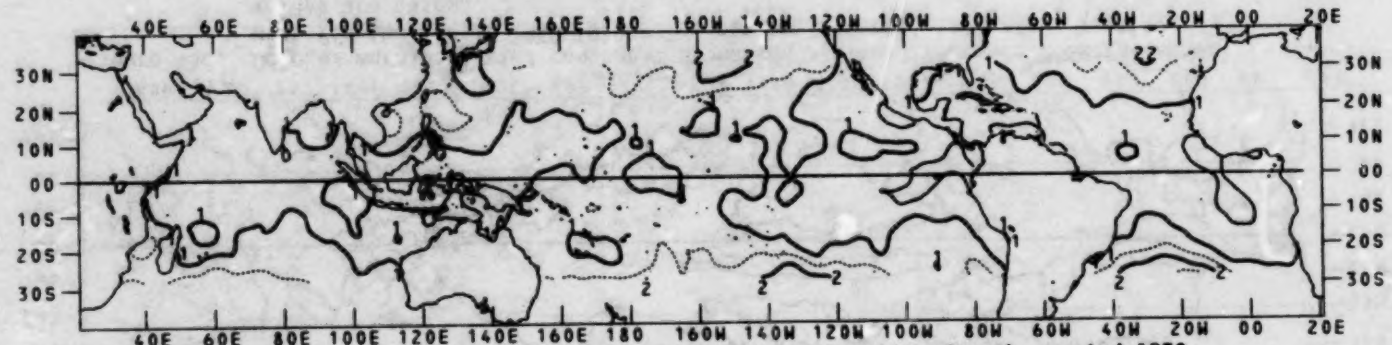

Figure 46b. November meridional wind component standard deviation for the period 1950-1979. The contour interval is .5 m/s.

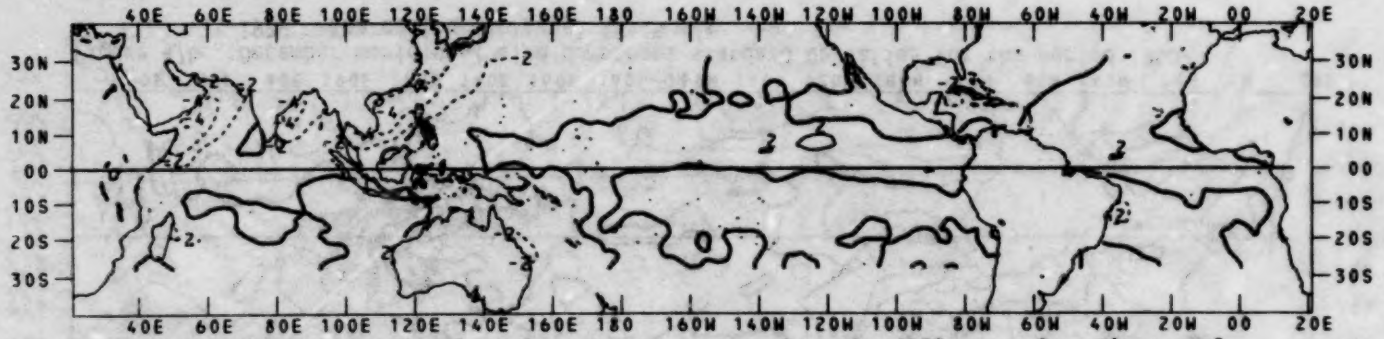

Figure 46c. November merdional wind component expressed as the difference from the annual mean for the period 1950-1979. The contour interval is 2 m/s. Negative values are dashed.

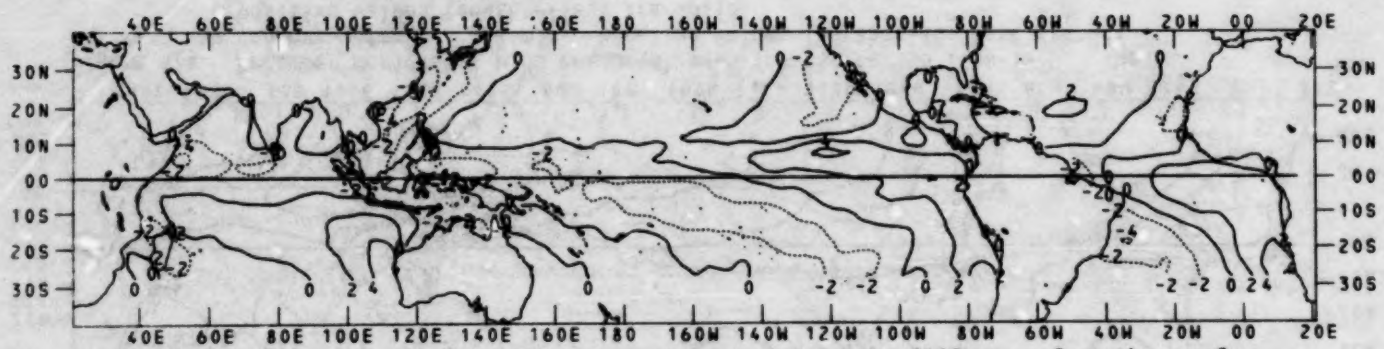

Figure 46d. November meridional wind component expressed as the difference from the zonal mean for the period 1950-1979. The contour interval is 2 m/s. Negative values are dashed.

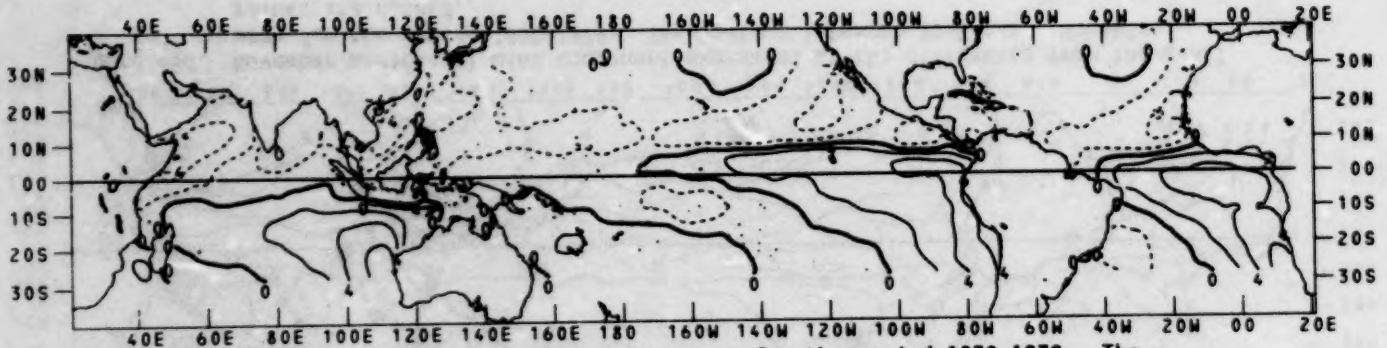

Figure 47a. December meridional wind component mean for the period 1950-1979. The contour interval is 2 m/s. Negative values (northerlies) are dashed; positive values (southerlies) are solid.

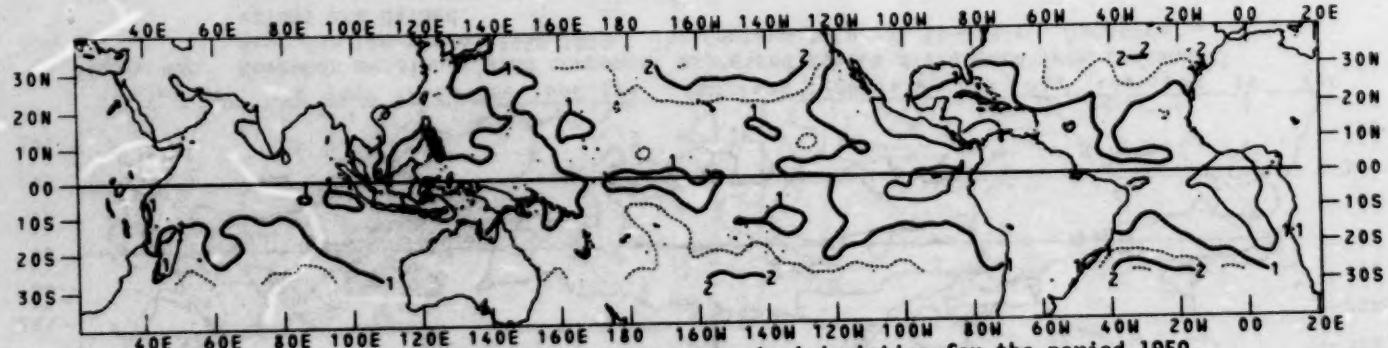

Figure 47b. December meridional wind component standard deviation for the period 1950-1979. The contour interval is .5 m/s.

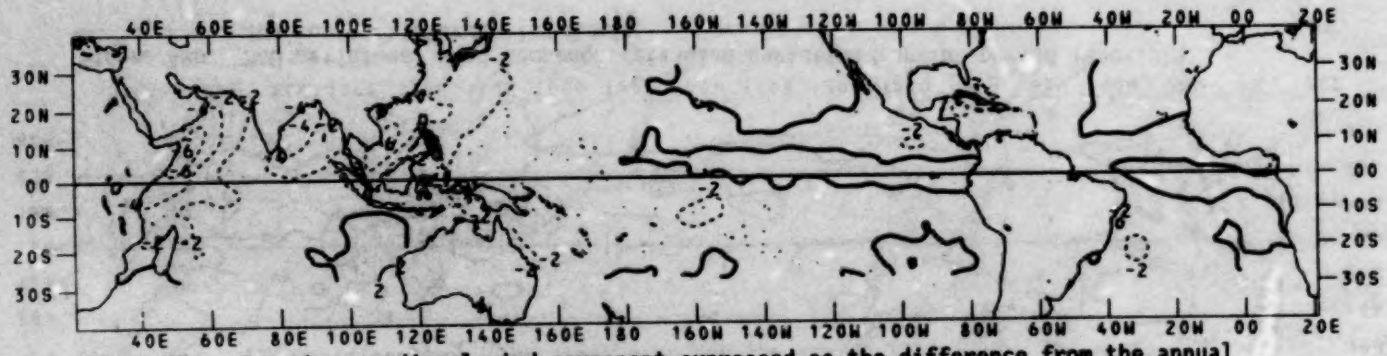

Figure 47c. December merdional wind component expressed as the difference from the annual mean for the period 1950-1979. The contour interval is 2 m/s. Negative values are dashed.

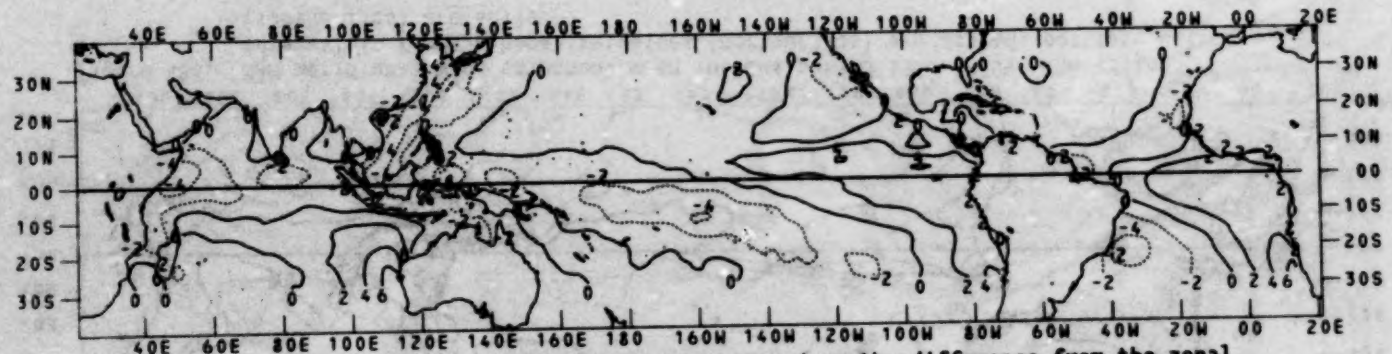

Figure 47d. December meridional wind component expressed as the difference from the zonal mean for the period 1950-1979. The contour interval is 2 m/s. Negative values are dashed.

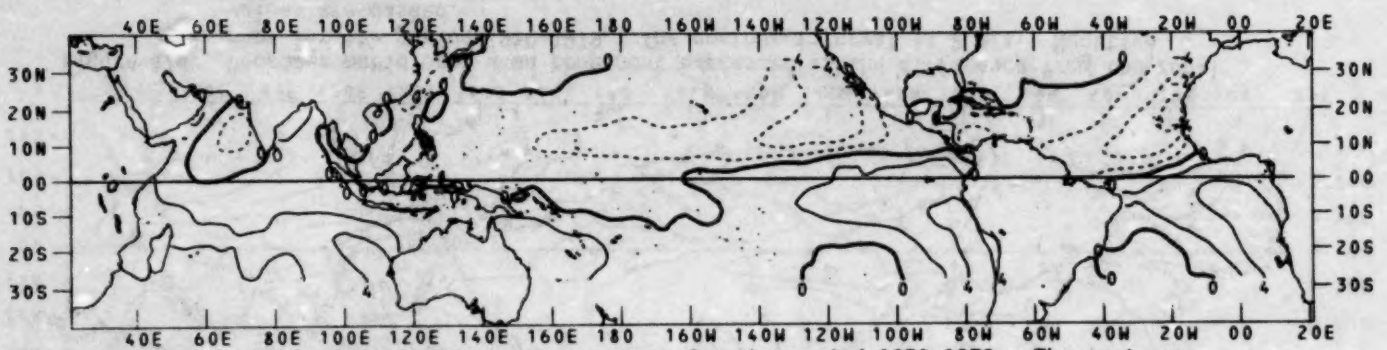

Figure 48a. MAM meridional wind component mean for the period 1950-1979. The contour interval is 2 m/s. Negative values (northerlies) are dashed; positive values (southerlies) are solid.

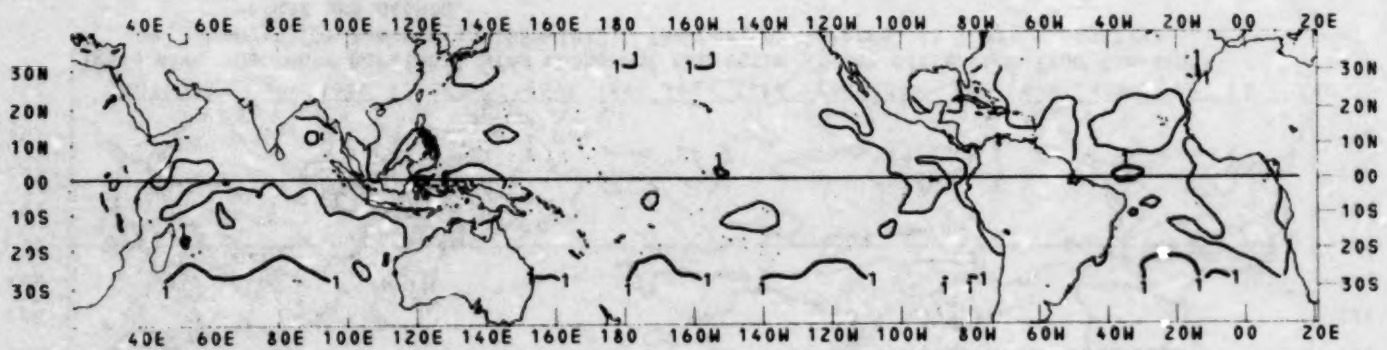

Figure 48b. MAM meridional wind component standard deviation for the period 1950-1979. The contour interval is .5 m/s.

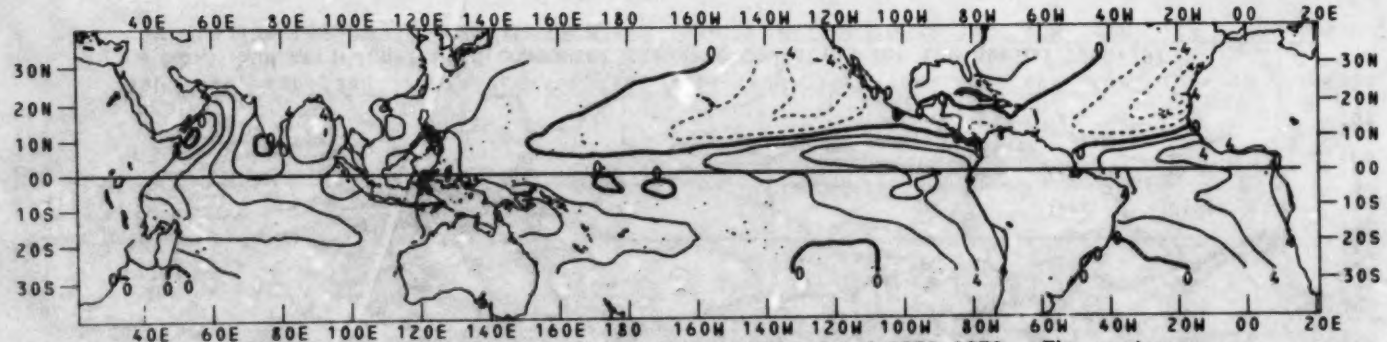

Figure 49a. JJA meridional wind component mean for the period 1950-1979. The contour interval is 2 m/s. Negative values (northerlies) are dashed, positive values (southerlies) are solid.

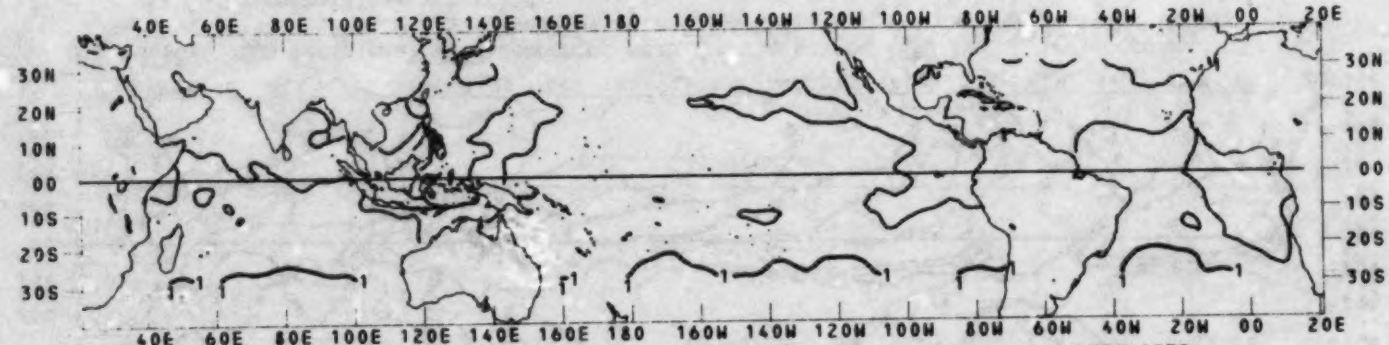

Figure 49b. JJA meridional wind component standard deviation for the period 1950-1979. The contour interval is .5 m/s.

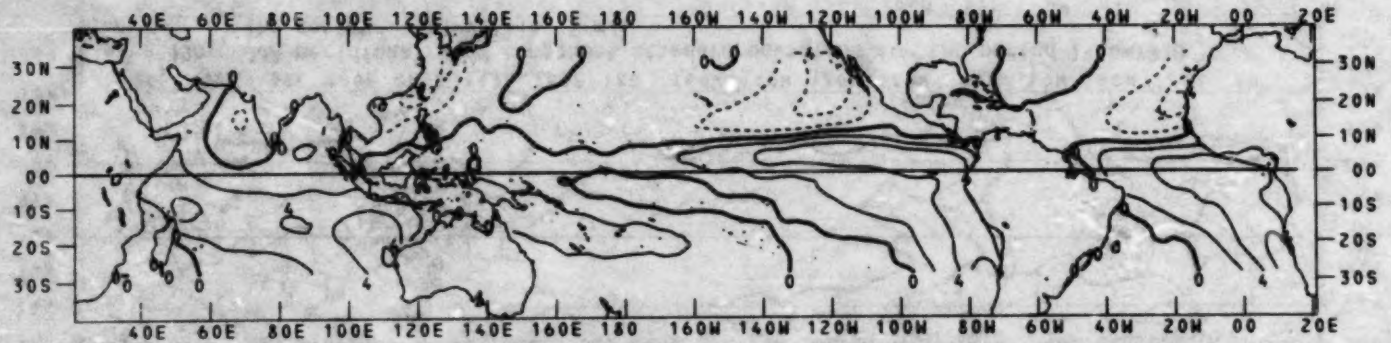

Figure 50a. SON meridional wind component mean for the period 1950-1979. The contour interval is 2 m/s. Negative values (northerlies) are dashed; positive values (southerlies) are solid.

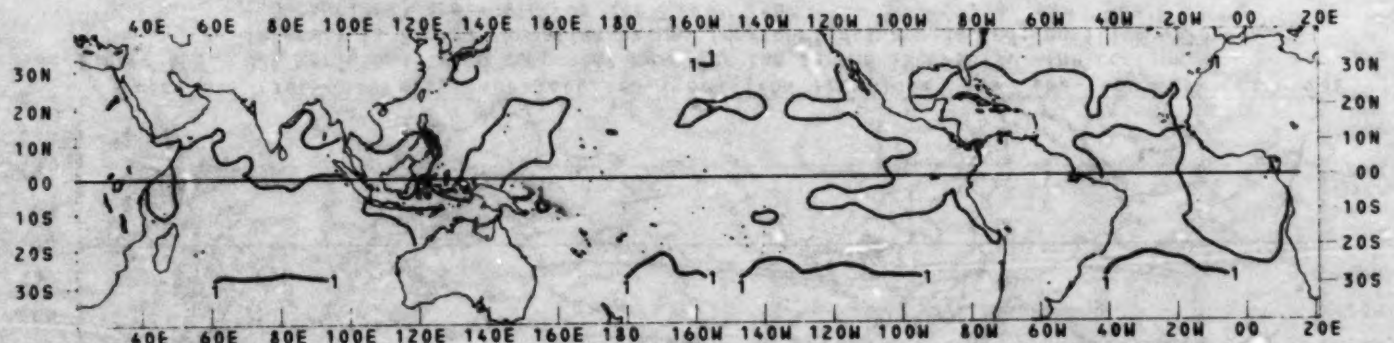

Figure 50b. SON meridional wind component standard deviation for the period 1950-1979. The contour interval is .5 m/s.

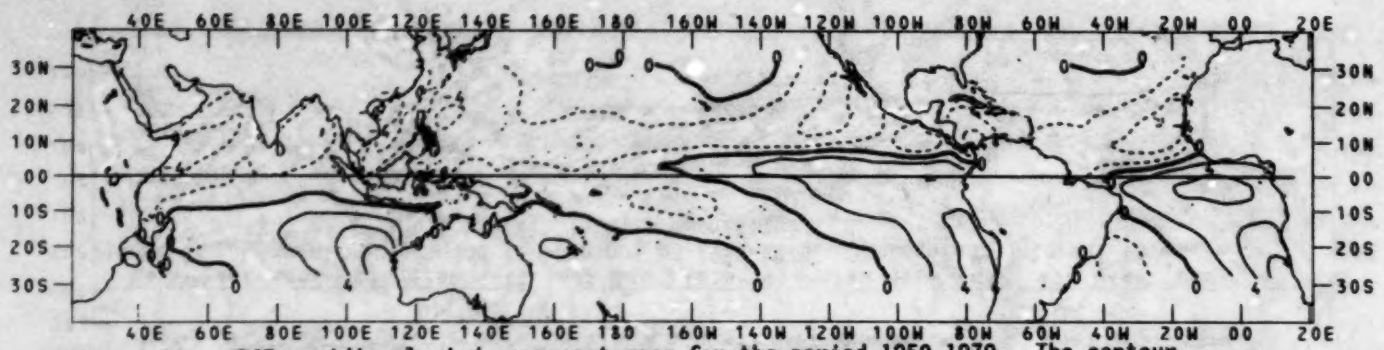

Figure 51a. DJF meridional wind component mean for the period 1950-1979. The contour interval is 2 m/s. Negative values (northerlies) are dashed; positive values (southerlies) are solid.

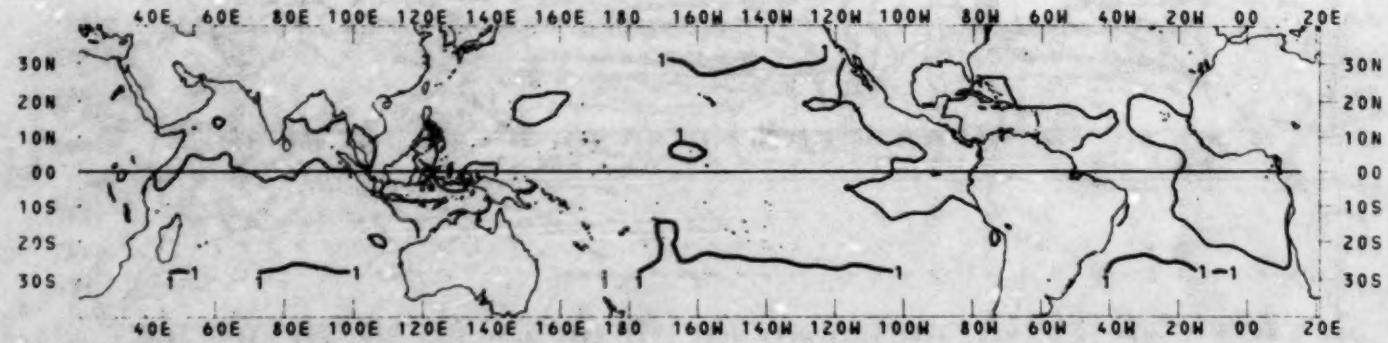

Figure 51b. DJF meridional wind component standard deviation for the period 1950-1979. The contour interval is .5 m/s.

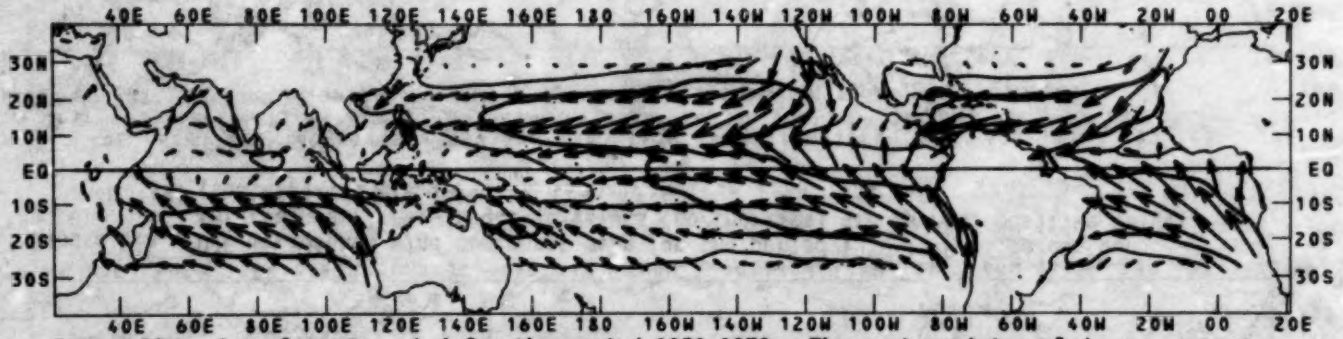

Figure 52. Annual vector wind for the period 1950-1979. The contour interval is 2.5 m/s. The 5 m/s isopleth is emphasized.

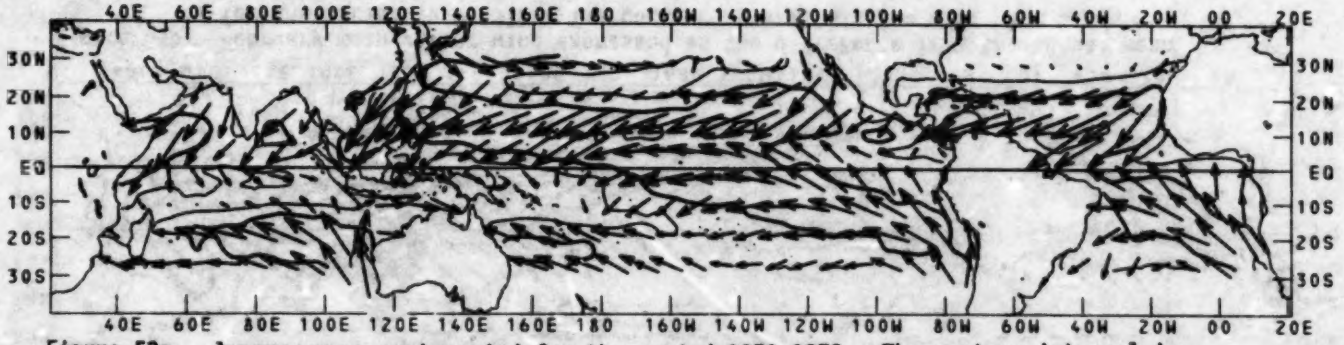

Figure 53a. January mean vector wind for the period 1950-1979. The contour interval is 2.5 m/s. The 5 m/s isopleth is emphasized.

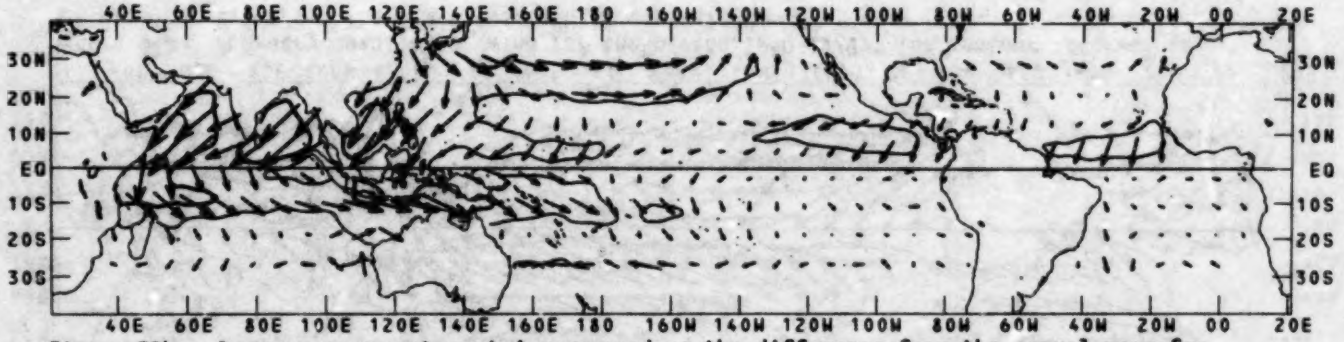

Figure 53b. January mean vector wind expressed as the difference from the annual mean for the period 1950-1979. The contour interval is 2.5 m/s. The 5 m/s isopleth is emphasized.

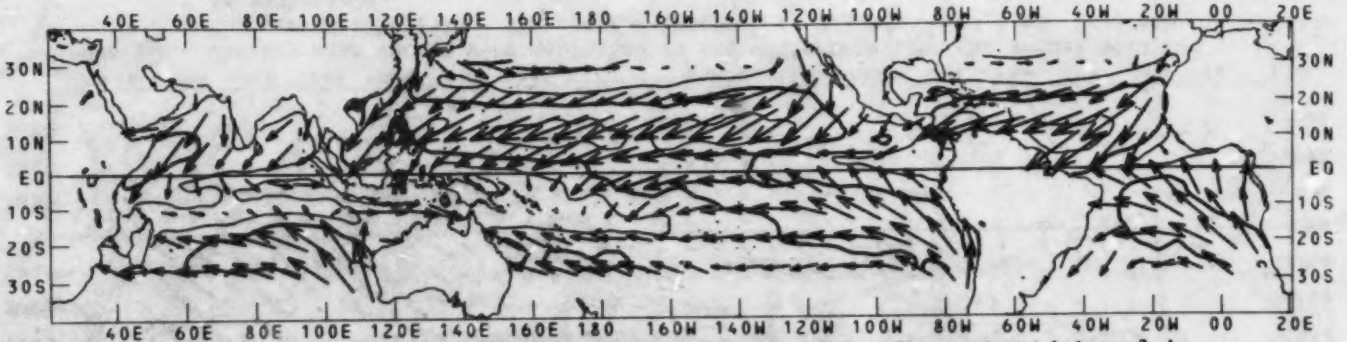

Figure 54a. February mean vector wind for the period 1950-1979. The contour interval is 2.5 m/s. The 5 m/s isopleth is emphasized.

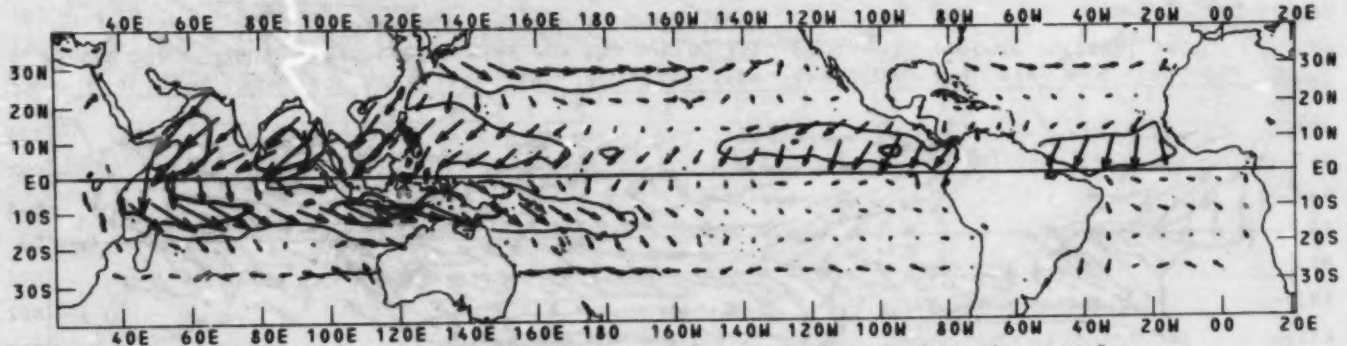

Figure 54b. February mean vector wind expressed as the difference from the annual mean for the period 1950-1979. The contour interval is 2.5 m/s. The 5 m/s isopleth is emphasized.

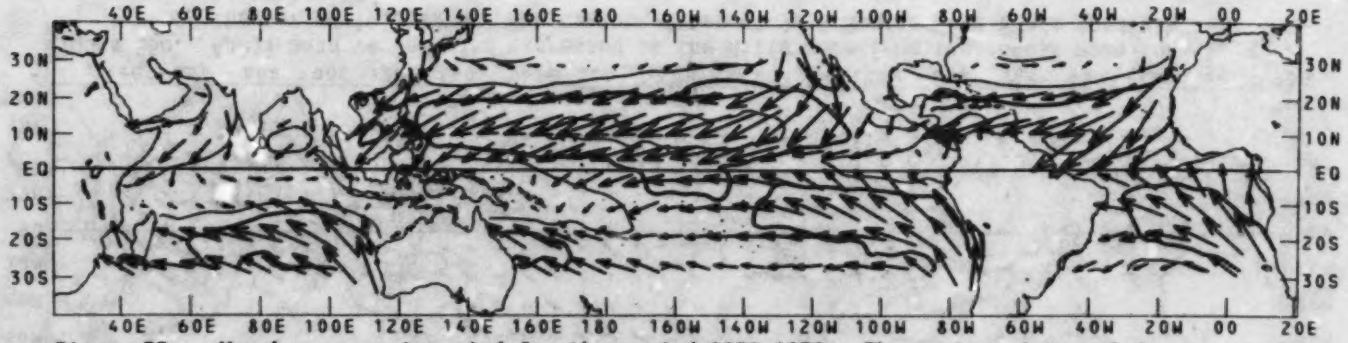

Figure 55a. March mean vector wind for the period 1950-1979. The contour interval is 2.5 m/s. The 5 m/s isopleth is emphasized.

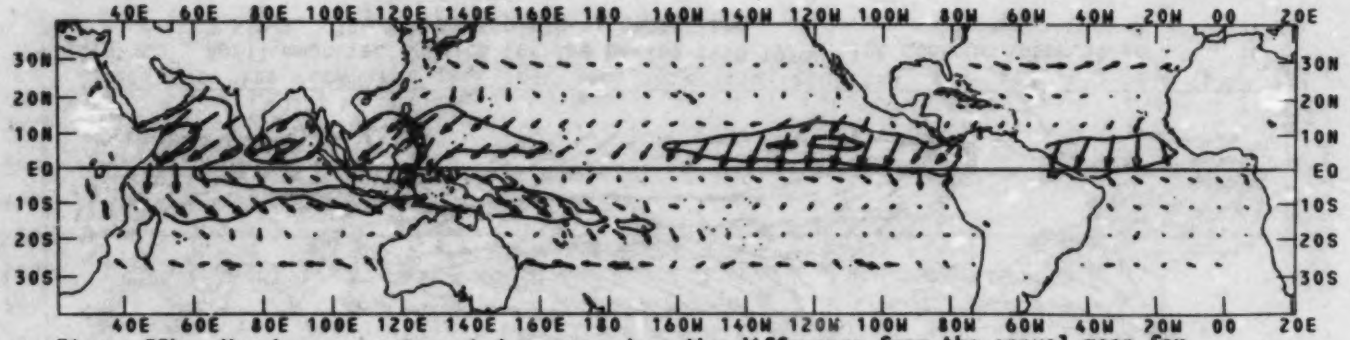

Figure 55b. March mean vector wind expressed as the difference from the annual mean for the period 1950-1979. The contour interval is 2.5 m/s. The 5 m/s isopleth is emphasized.

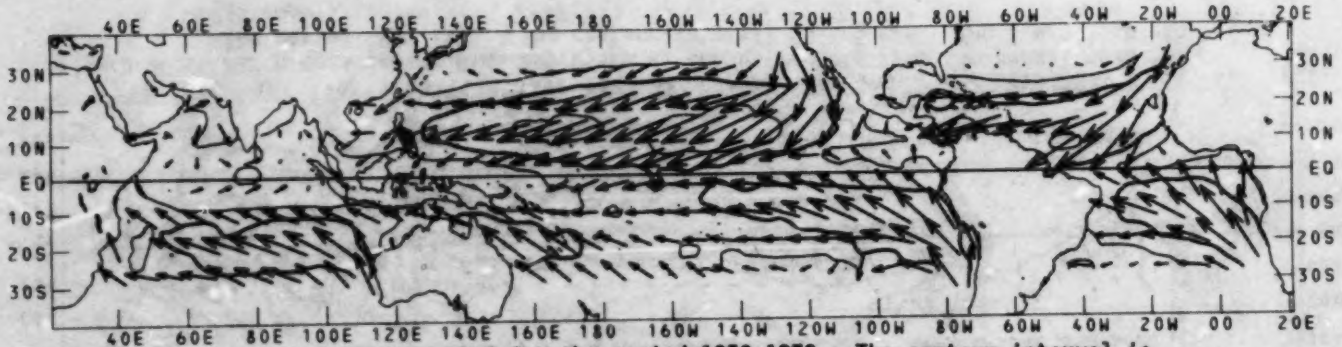

Figure 56a. April mean vector wind for the period 1950-1979. The contour interval is 2.5 m/s. The 5 m/s isopleth is emphasized.

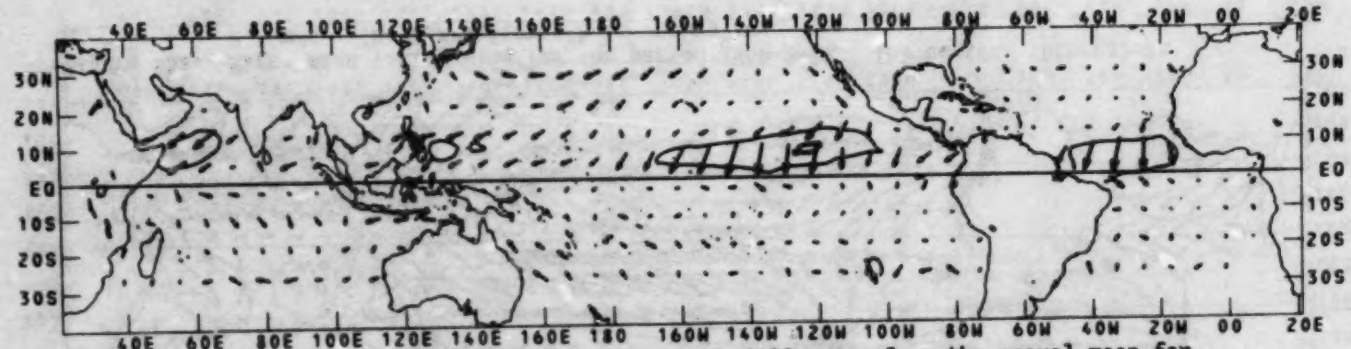

Figure 56b. April mean vector wind expressed as the difference from the annual mean for the period 1950-1979. The contour interval is 2.5 m/s. The 5 m/s isopleth is emphasized.

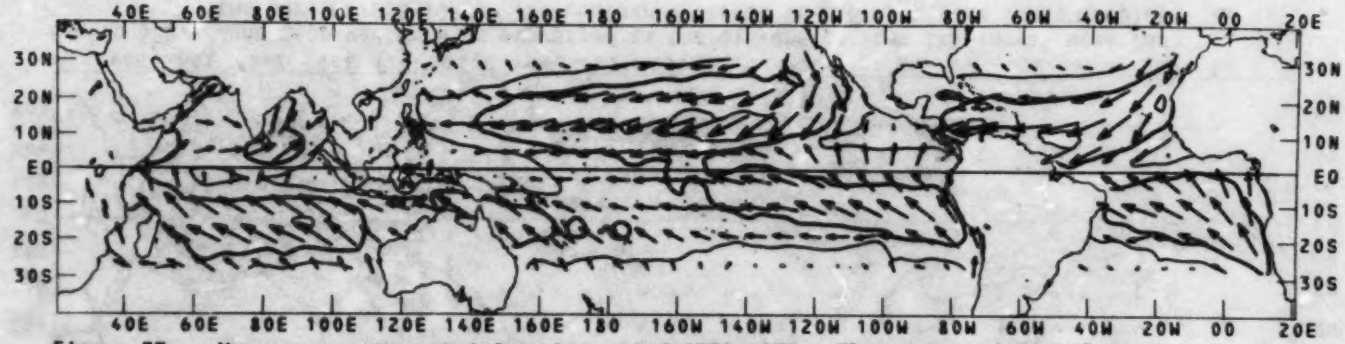

Figure 57a. May mean vector wind for the period 1950-1979. The contour interval is 2.5 m/s. The 5 m/s isopleth is emphasized.

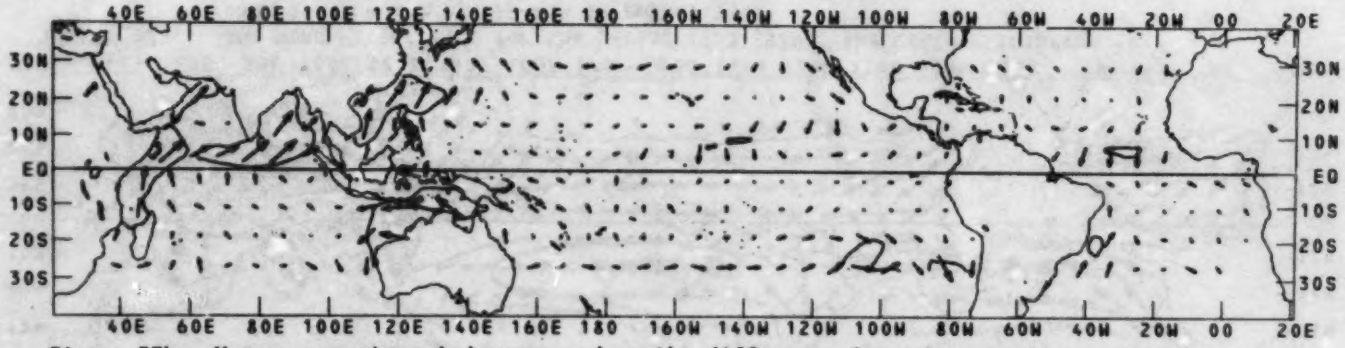

Figure 57b. May mean vector wind expressed as the difference from the annual mean for the period 1950-1979. The contour interval is 2.5 m/s. The 5 m/s isopleth is emphasized.

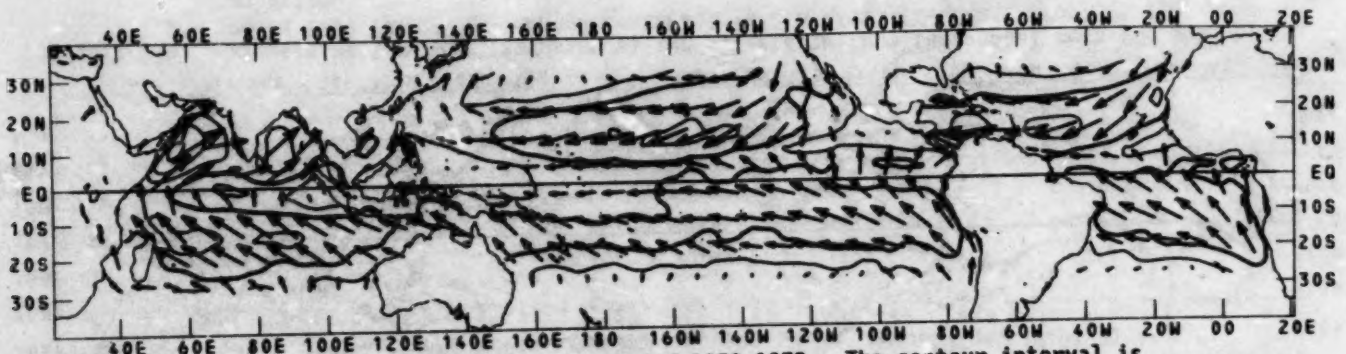

Figure 58a. June mean vector wind for the period 1950-1979. The contour interval is 2.5 m/s. The 5 m/s isopleth is emphasized.

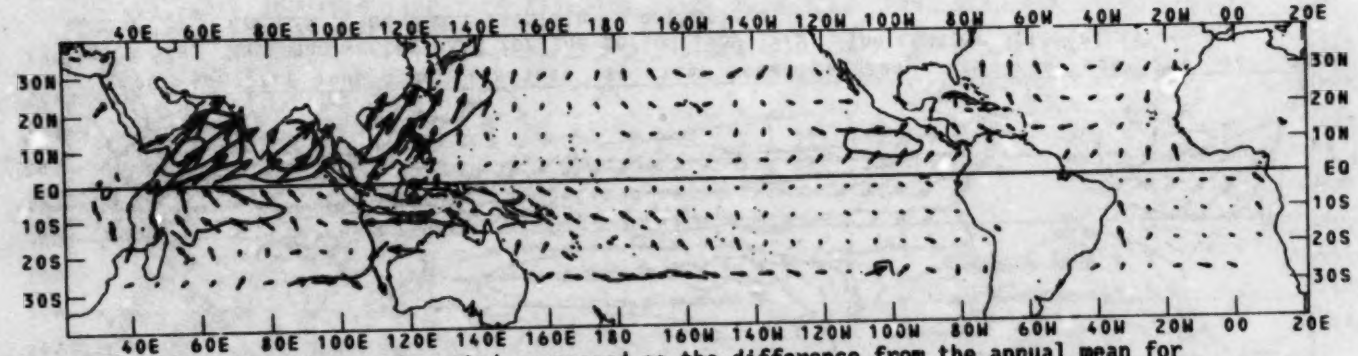

Figure 58b. June mean vector wind expressed as the difference from the annual mean for the period 1950-1979. The contour interval is 2.5 m/s. The 5 m/s isopleth is emphasized.

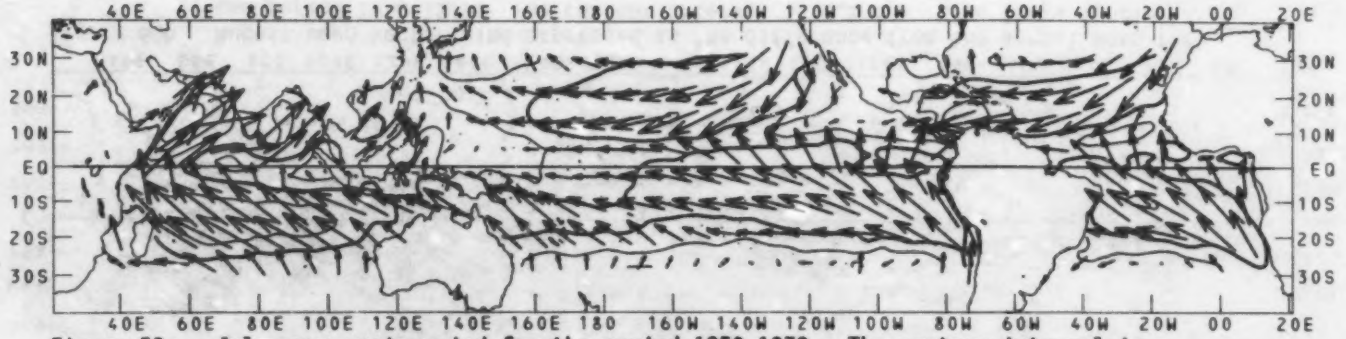

Figure 59a. July mean vector wind for the period 1950-1979. The contour interval is 2.5 m/s. The 5 m/s isopleth is emphasized.

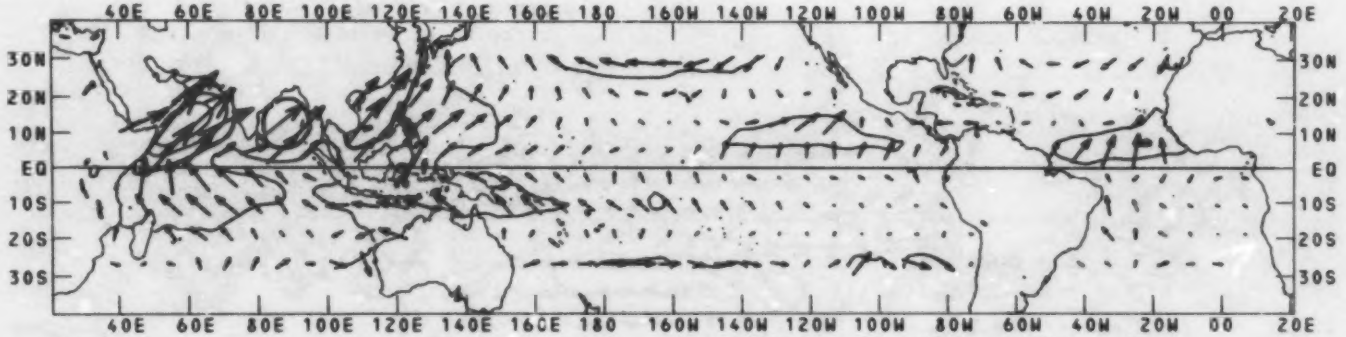

Figure 59b. July mean vector wind expressed as the difference from the annual mean for the period 1950-1979. The contour interval is 2.5 m/s. The 5 m/s isopleth is emphasized.

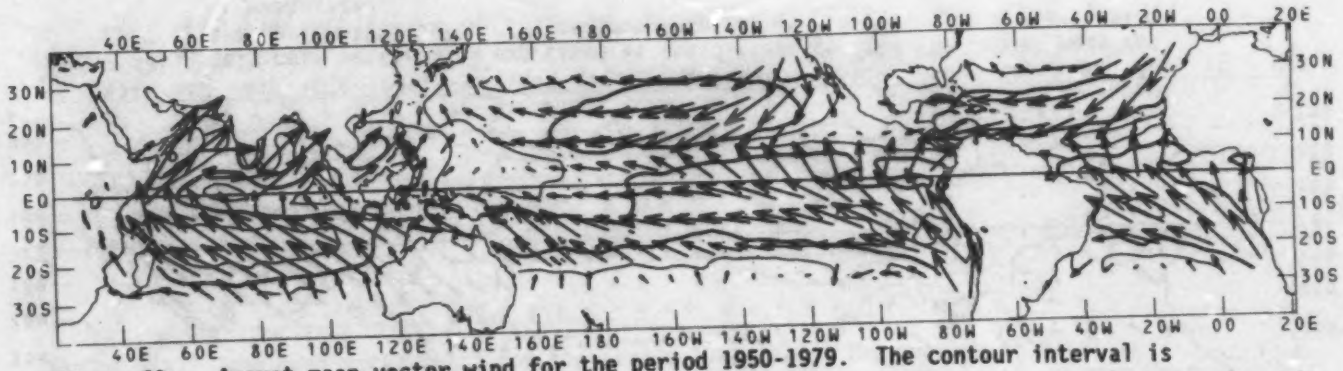

Figure 60a. August mean vector wind for the period 1950-1979. The contour interval is 2.5 m/s. The 5 m/s isopleth is emphasized.

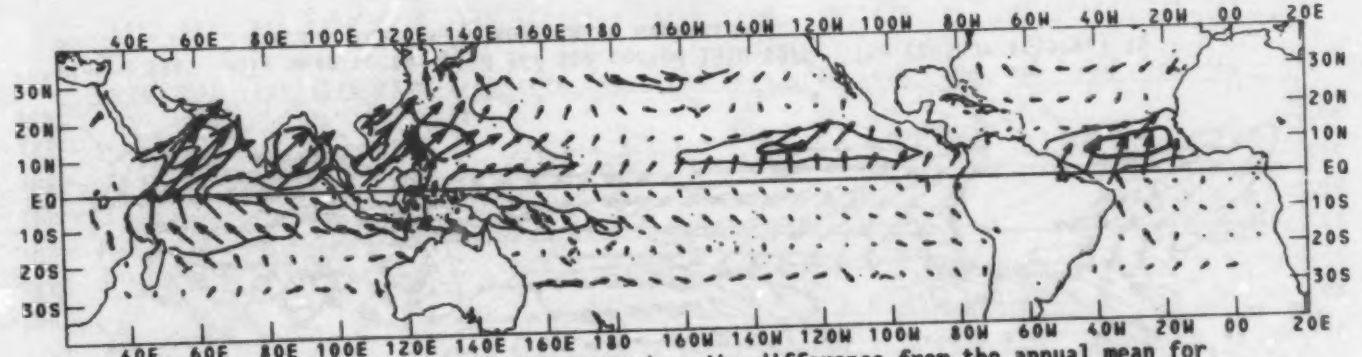

Figure 60b. August mean vector wind expressed as the difference from the annual mean for the period 1950-1979. The contour interval is 2.5 m/s. The 5 m/s isopleth is emphasized.

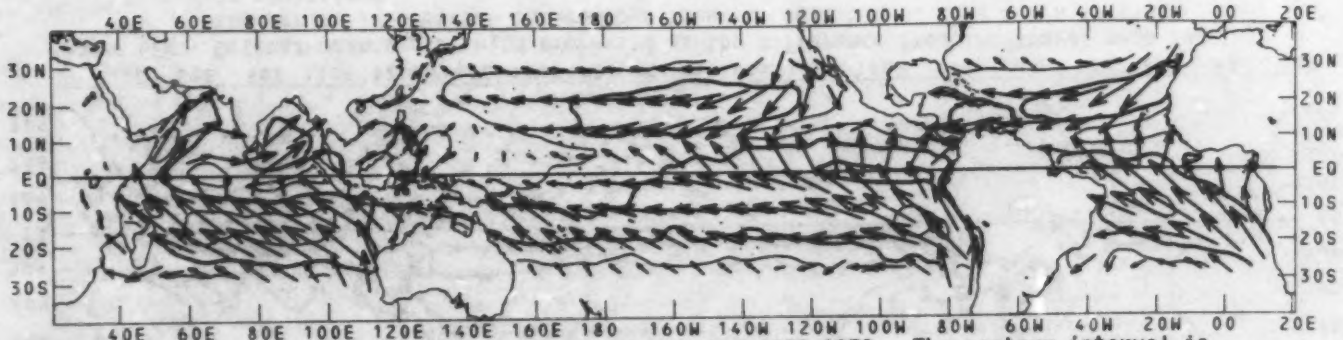

Figure 61a. September mean vector wind for the period 1950-1979. The contour interval is 2.5 m/s. The 5 m/s isopleth is emphasized.

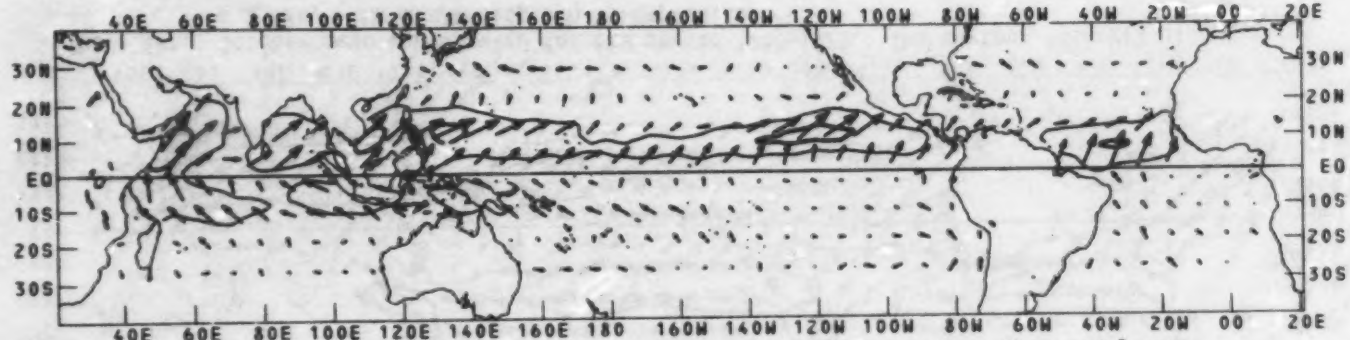

Figure 61b. September mean vector wind expressed as the difference from the annual mean for the period 1950-1979. The contour interval is 2.5 m/s. The 5 m/s isopleth is emphasized.

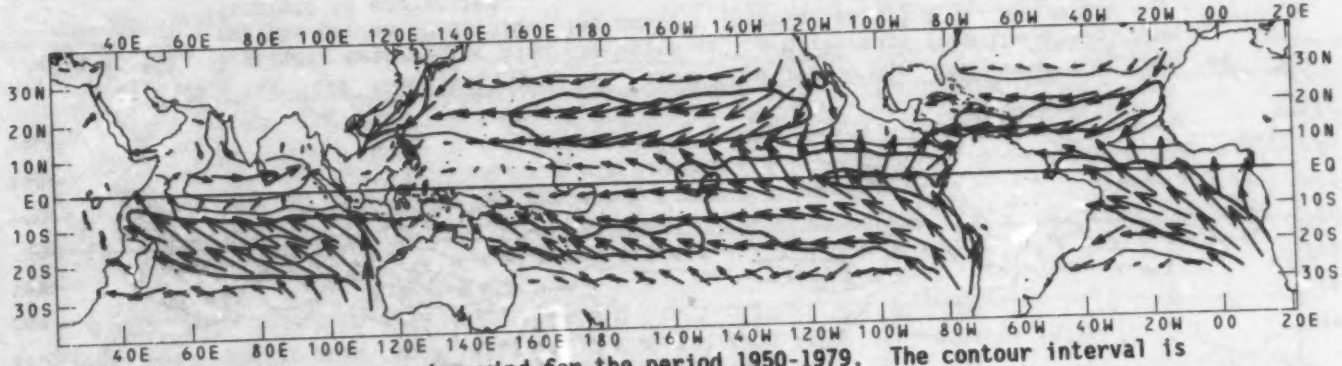

Figure 62a. October mean vector wind for the period 1950-1979. The contour interval is 2.5 m/s. The 5 m/s isopleth is emphasized.

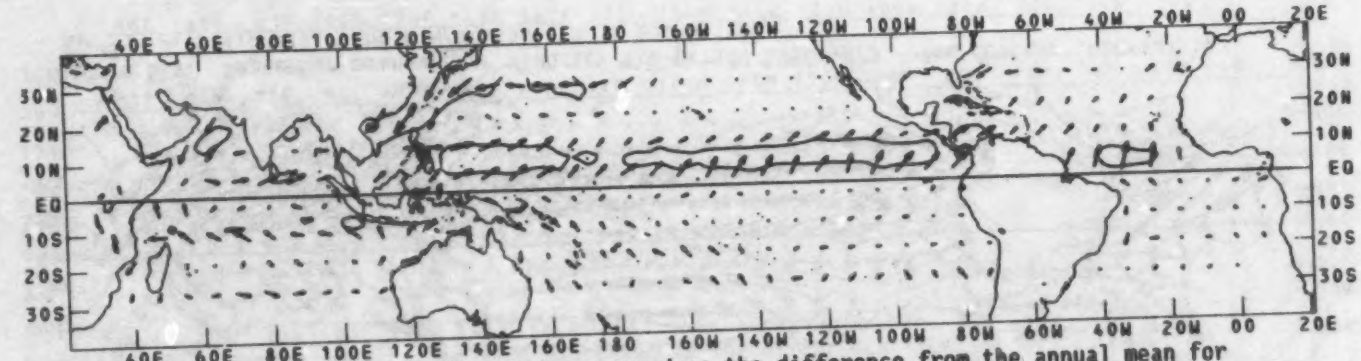

Figure 62b. October mean vector wind expressed as the difference from the annual mean for the period 1950-1979. The contour interval is 2.5 m/s. The 5 m/s isopleth is emphasized.

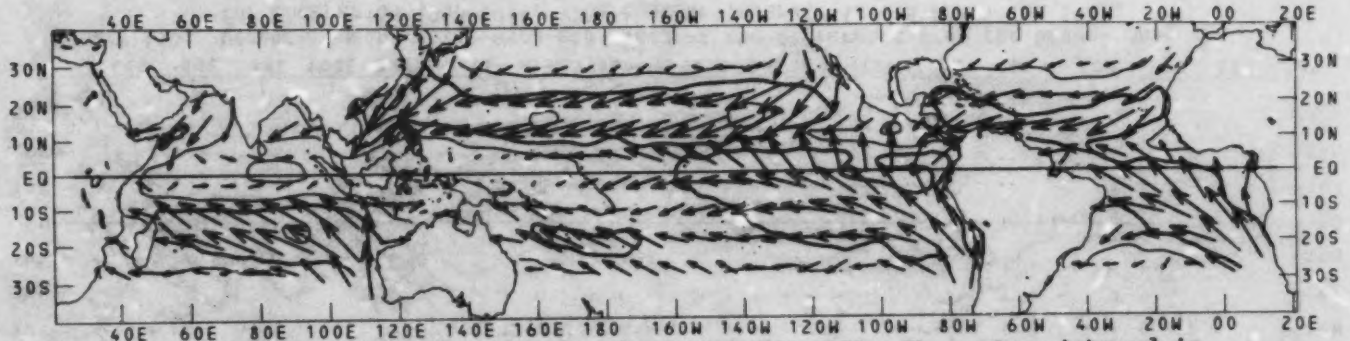

Figure 63a. November mean vector wind for the period 1950-1979. The contour interval is 2.5 m/s. The 5 m/s isopleth is emphasized.

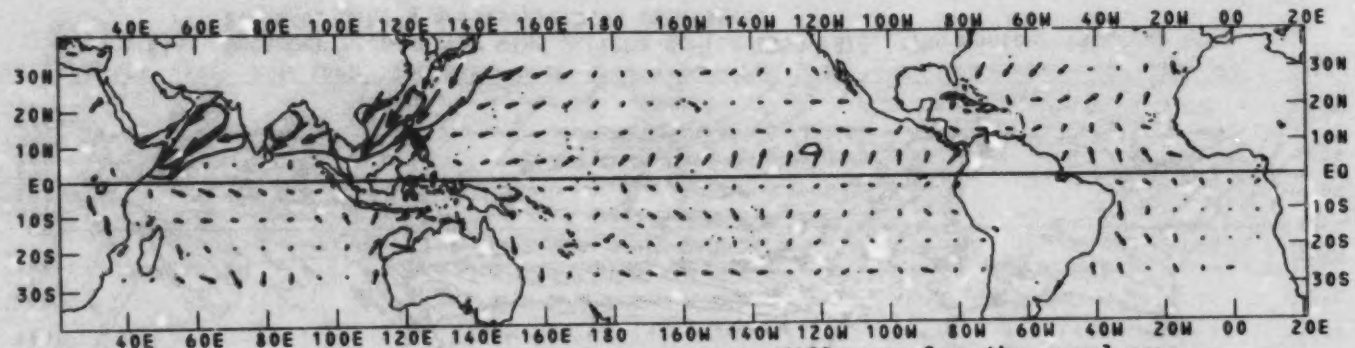

Figure 63b. November mean vector wind expressed as the difference from the annual mean for the period 1950-1979. The contour interval is 2.5 m/s. The 5 m/s isopleth is emphasized.

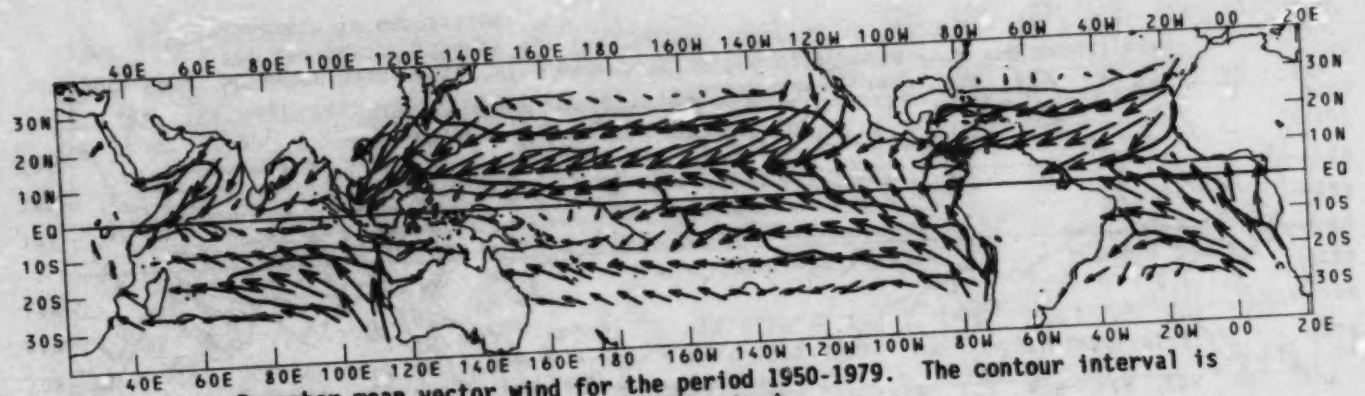

Figure 64a. December mean vector wind for the period 1950-1979. The contour interval is 2.5 m/s. The 5 m/s isopleth is emphasized.

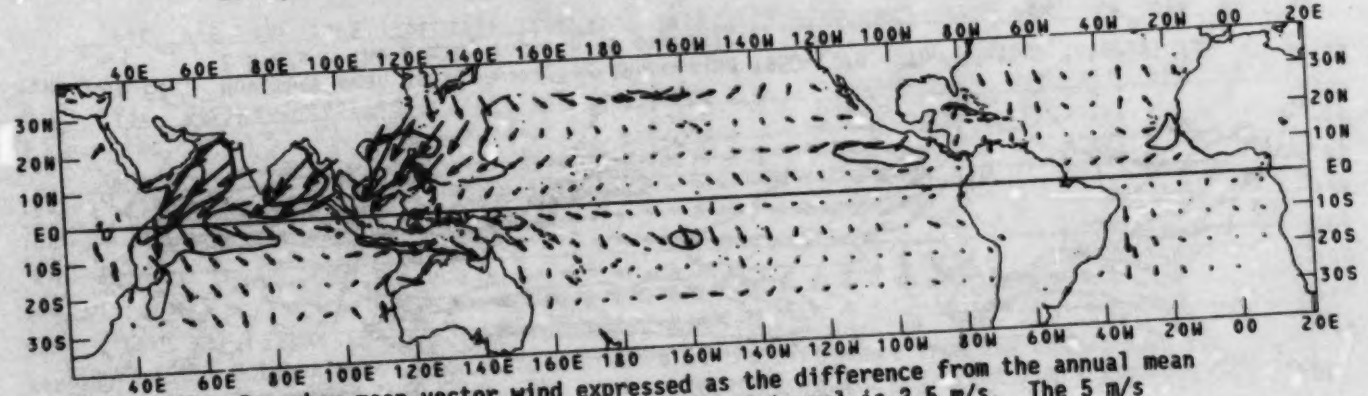

Figure 64b. December mean vector wind expressed as the difference from the annual mean for the period 1950-1979. The contour interval is 2.5 m/s. The 5 m/s isopleth is emphasized.

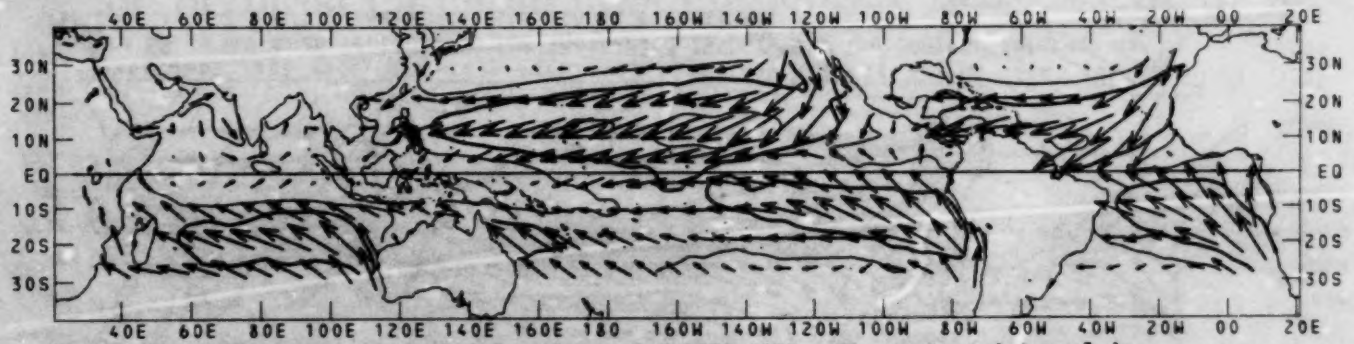

Figure 65. MAM mean vector wind for the period 1950-1979. The contour interval is 2.5 m/s. The 5 m/s isopleth is emphasized.

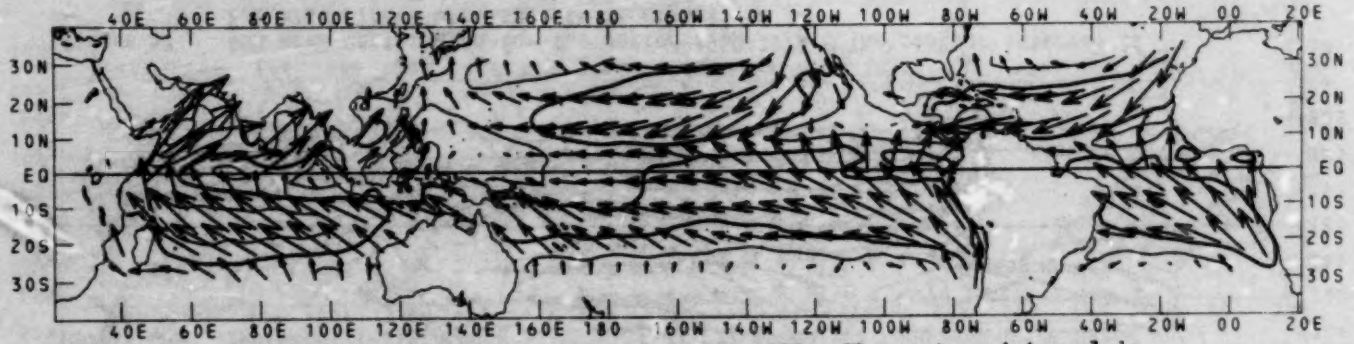

Figure 66. JJA mean vector wind for the period 1950-1979. The contour interval is 2.5 m/s. The 5 m/s isopleth is emphasized.

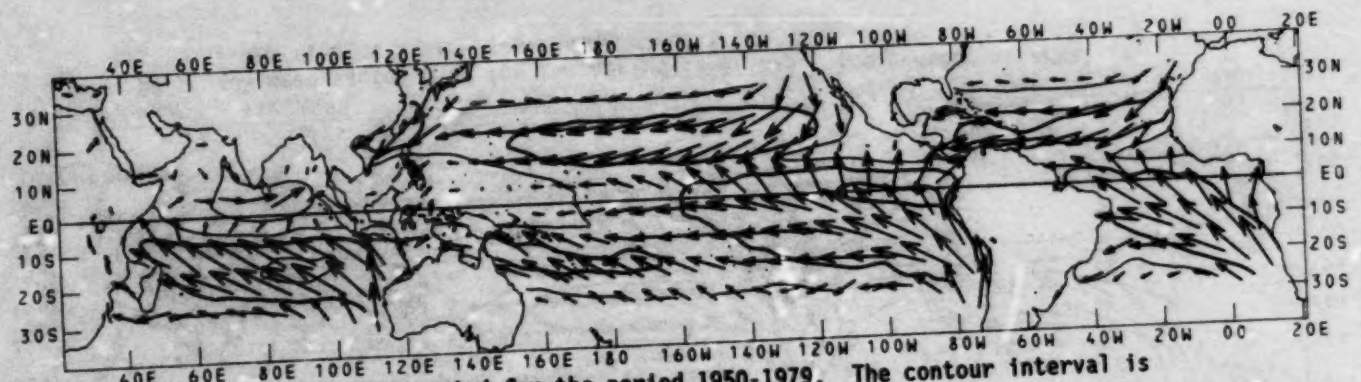

Figure 67. SON mean vector wind for the period 1950-1979. The contour interval is 2.5 m/s. The 5 m/s isopleth is emphasized.

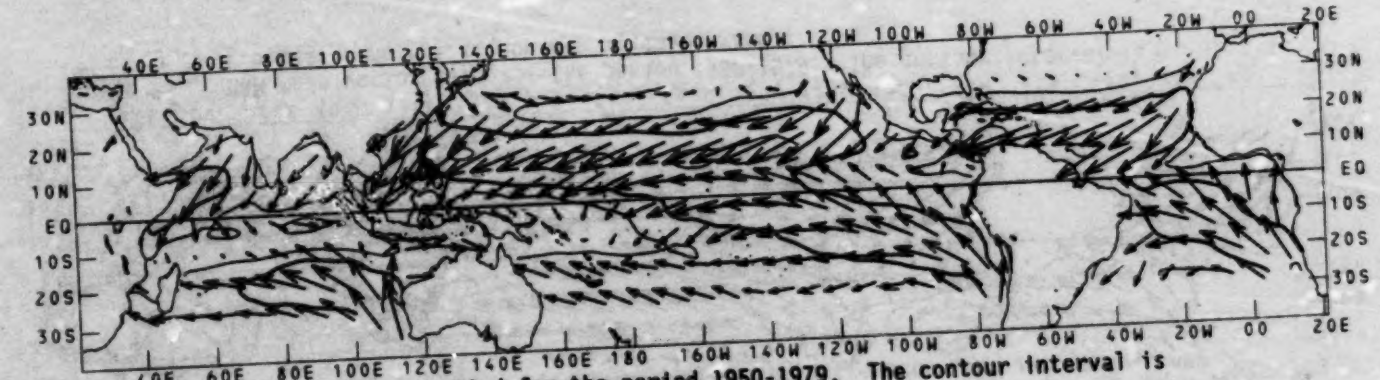

Figure 68. DJF mean vector wind for the period 1950-1979. The contour interval is 2.5 m/s. The 5 m/s isopleth is emphasized.

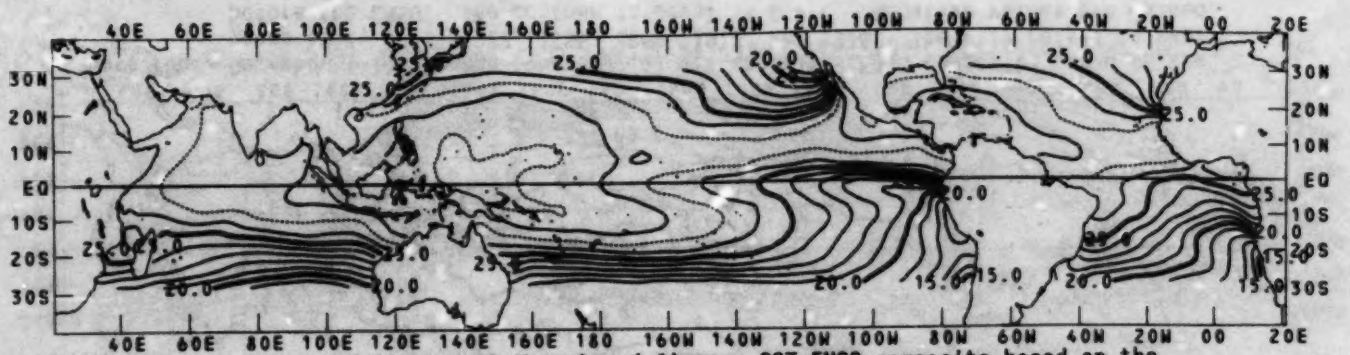

Figure 69a. September (-1) through November (-1) mean SST ENSO composite based on the years 1951, 1953, 1957, 1965, 1969, 1972, and 1976. The (-1) refers to the year before the ENSO. The contour interval is 1°C. The 27°C and 29°C isopleth is dashed.

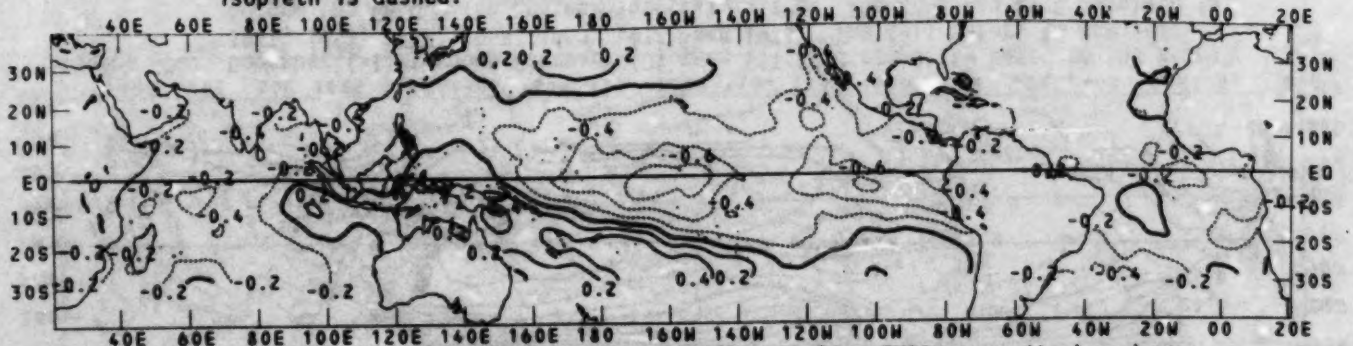

Figure 69b. September (-1) through November (-1) SST anomalies ENSO composite based on the years 1951, 1953, 1957, 1965, 1969, 1972, and 1976. The (-1) refers to year before the ENSO. The contour interval is 0.2°C. Negative values are dashed.

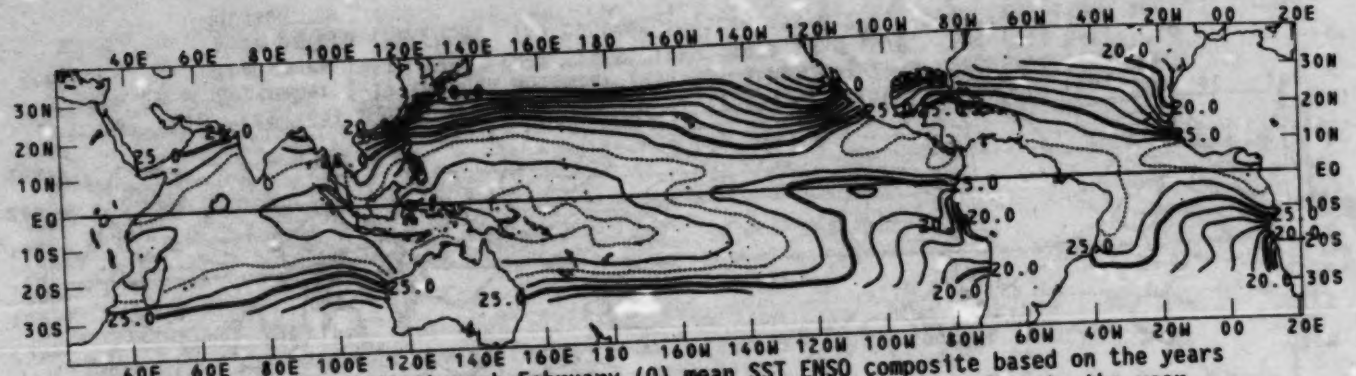

Figure 70a. December (-1) through February (0) mean SST ENSO composite based on the years 1951, 1953, 1957, 1965, 1969, 1972, and 1976. The (-1) refers to the year before the ENSO. The contour interval is 1°C. The 27°C and 29°C isopleth is dashed.

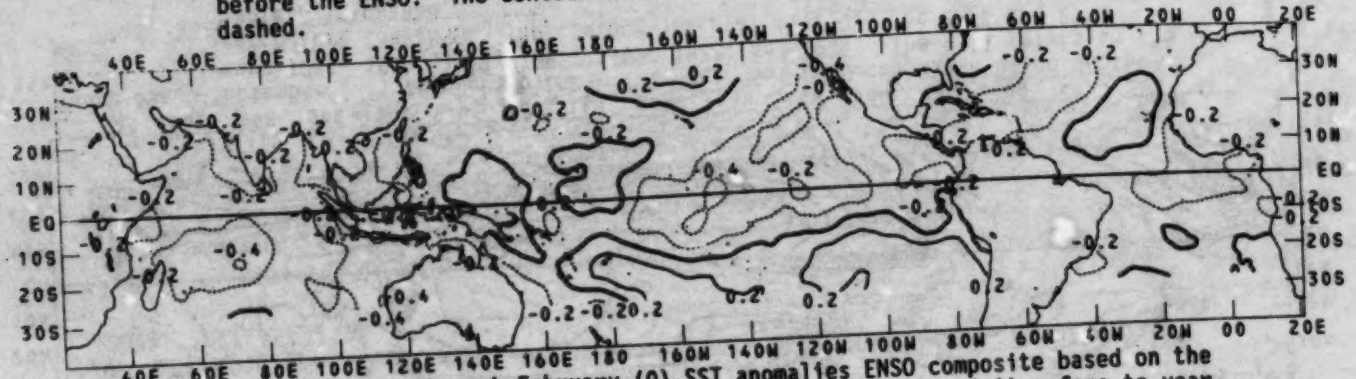

Figure 70b. December (-1) through February (0) SST anomalies ENSO composite based on the years 1951, 1953, 1957, 1965, 1969, 1972, and 1976. The (-1) refers to year before the ENSO. The contour interval is 0.2°C. Negative values are dashed.

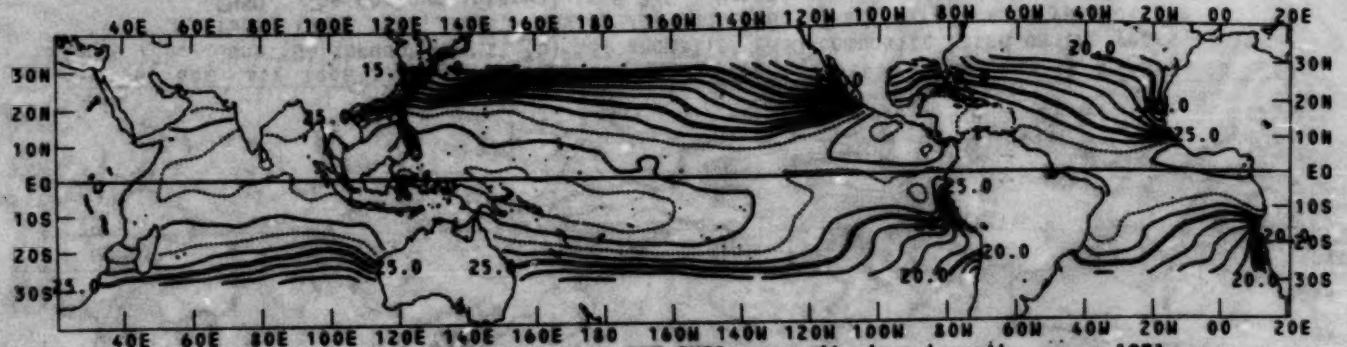

Figure 71a. March (0) through May (0) mean SST ENSO composite based on the years 1951, 1953, 1957, 1965, 1969, 1972, and 1976. The (0) refers to the year of the ENSO. The contour interval is 1°C. The 27°C and 29°C isopleth is dashed.

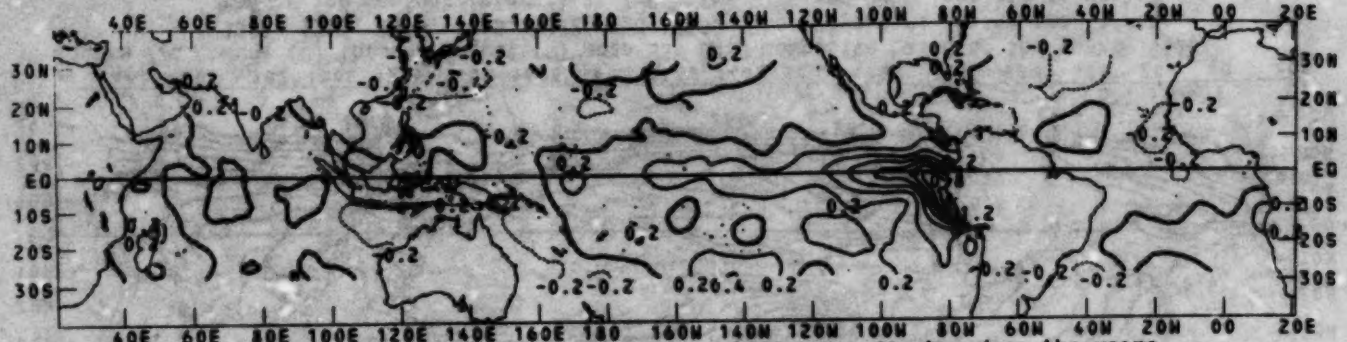

Figure 71b. March (0) through May (0) SST anomalies ENSO composite based on the years 1951, 1953, 1957, 1965, 1969, 1972, and 1976. The (0) refers to year of the ENSO. The contour interval is 0.2°C. Negative values are dashed.

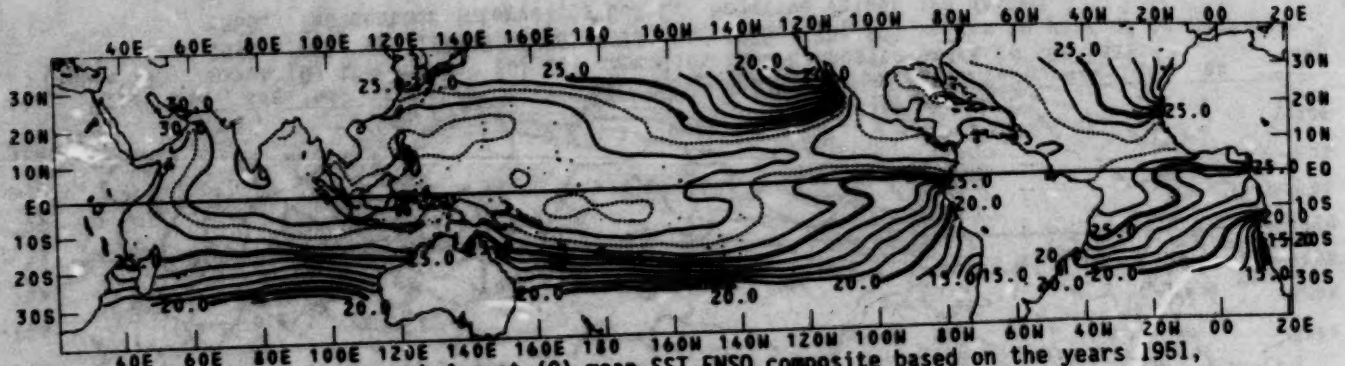

Figure 72a. June (0) through August (0) mean SST ENSO composite based on the years 1951, 1953, 1957, 1965, 1969, 1972, and 1976. The (0) refers to the year of the ENSO. The contour interval is 1°C. The 27°C and 29°C isopleth is dashed.

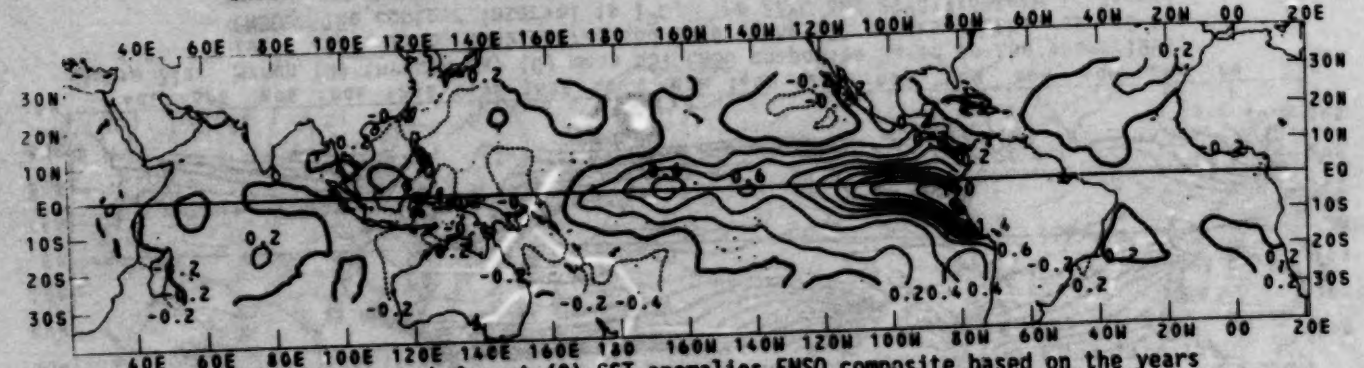

Figure 72b. June (0) through August (0) SST anomalies ENSO composite based on the years 1951, 1953, 1957, 1965, 1969, 1972, and 1976. The (0) refers to year of the ENSO. The contour interval is 0.2°C. Negative values are dashed.

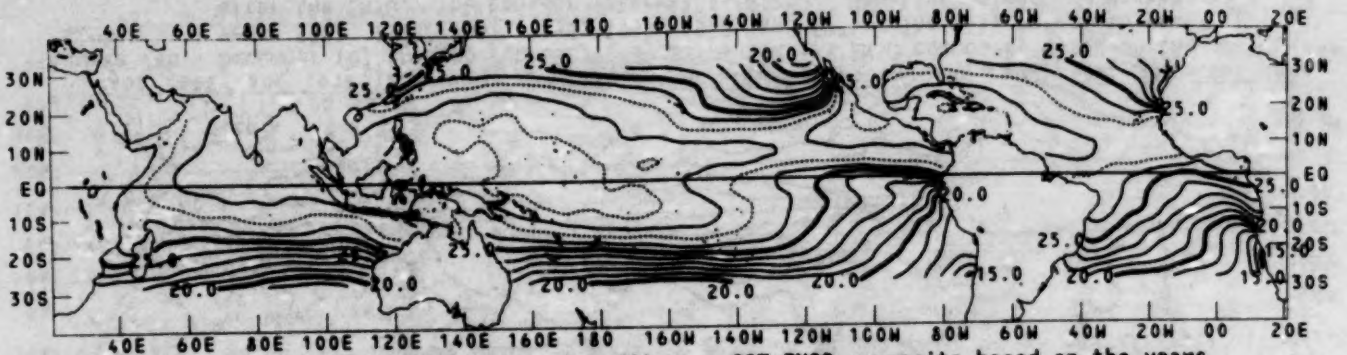

Figure 73a. September (0) through November (0) mean SST ENSO composite based on the years 1951, 1953, 1957, 1965, 1969, 1972, and 1976. The (0) refers to the year of the ENSO. The contour interval is 1°C. The 27°C and 29°C isopleth is dashed.

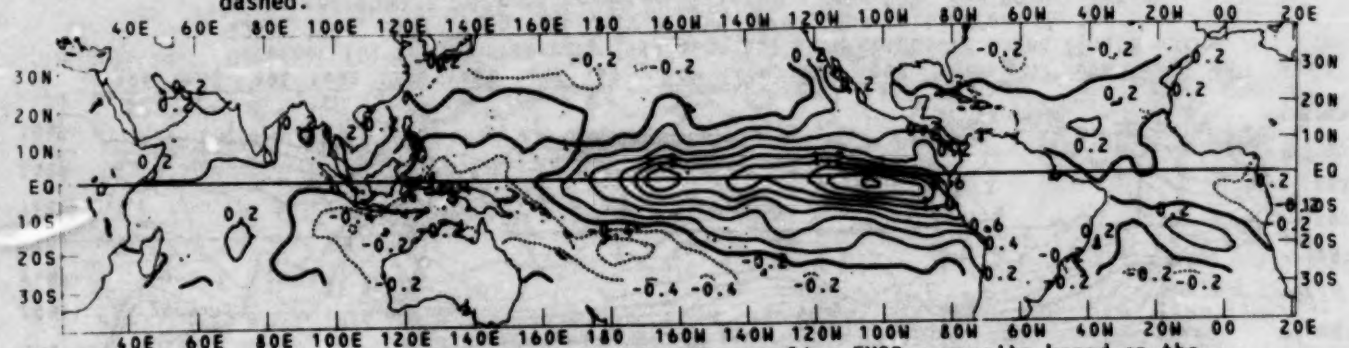

Figure 73b. September (0) through November (0) SST anomalies ENSO composite based on the years 1951, 1953, 1957, 1965, 1969, 1972, and 1976. The (0) refers to year of the ENSO. The contour interval is 0.2°C. Negative values are dashed.

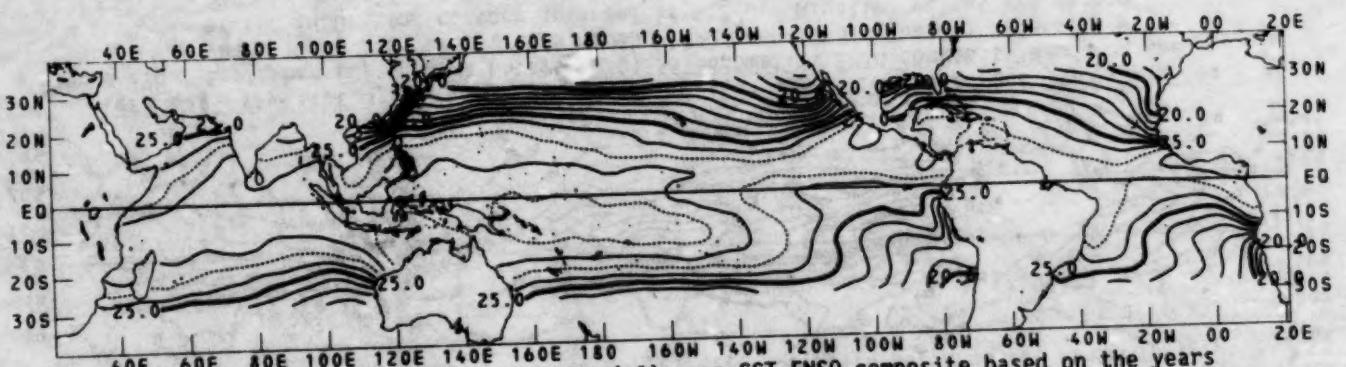

Figure 74a. December (0) through February (+1) mean SST ENSO composite based on the years 1951, 1953, 1957, 1965, 1969, 1972, and 1976. The (+1) refers to the year after the ENSO. The contour interval is 1°C. The 27°C and 29°C isopleth is dashed.

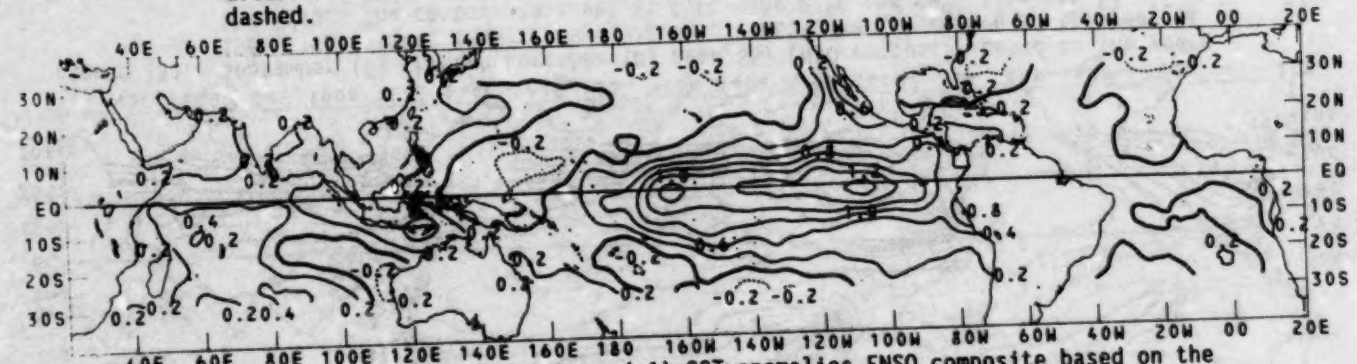

Figure 74b. December (0) through February (+1) SST anomalies ENSO composite based on the years 1951, 1953, 1957, 1965, 1969, 1972, and 1976. The (+1) refers to year after the ENSO. The contour interval is 0.2°C. Negative values are dashed.

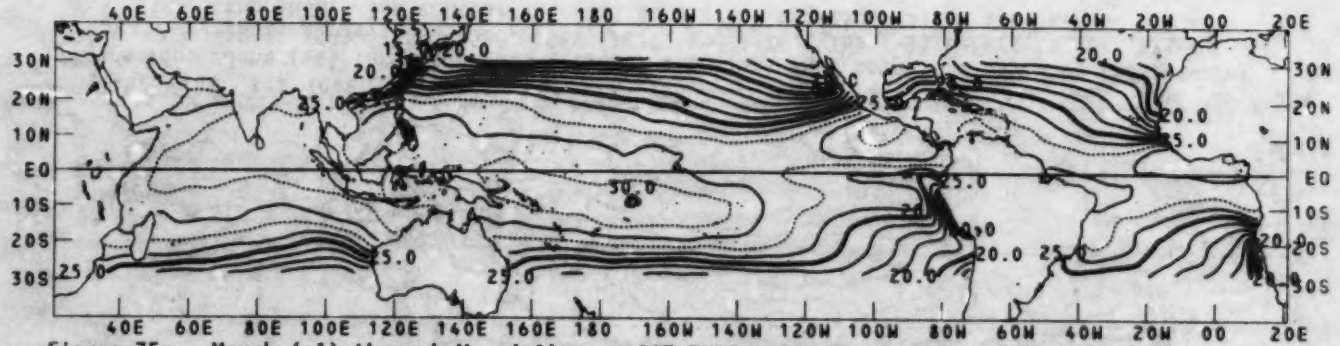

Figure 75a. March (+1) through May (+1) mean SST ENSO composite based on the years 1951, 1953, 1957, 1965, 1969, 1972, and 1976. The (+1) refers to the year after the ENSO. The contour interval is 1°C. The 27°C and 29°C isopleth is dashed.

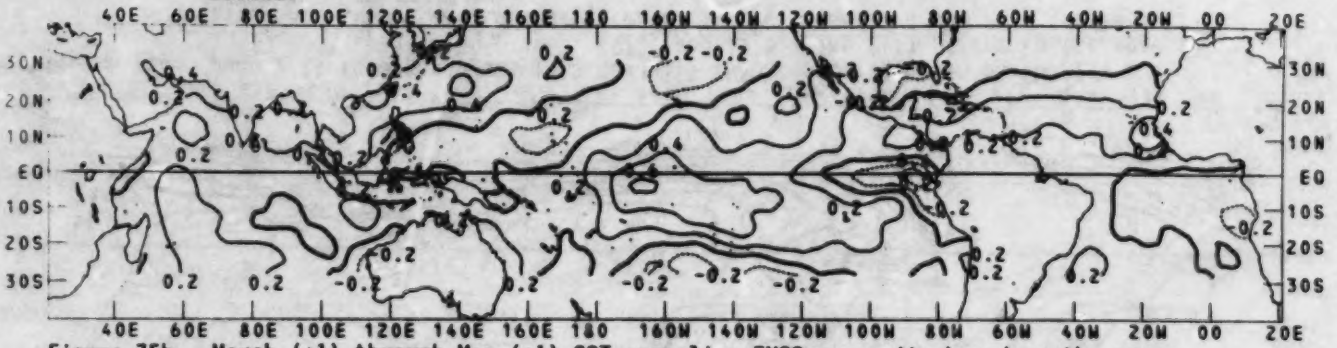

Figure 75b. March (+1) through May (+1) SST anomalies ENSO composite based on the years 1951, 1953, 1957, 1965, 1969, 1972, and 1976. The (+1) refers to year before the ENSO. The contour interval is 0.2°C. Negative values are dashed.

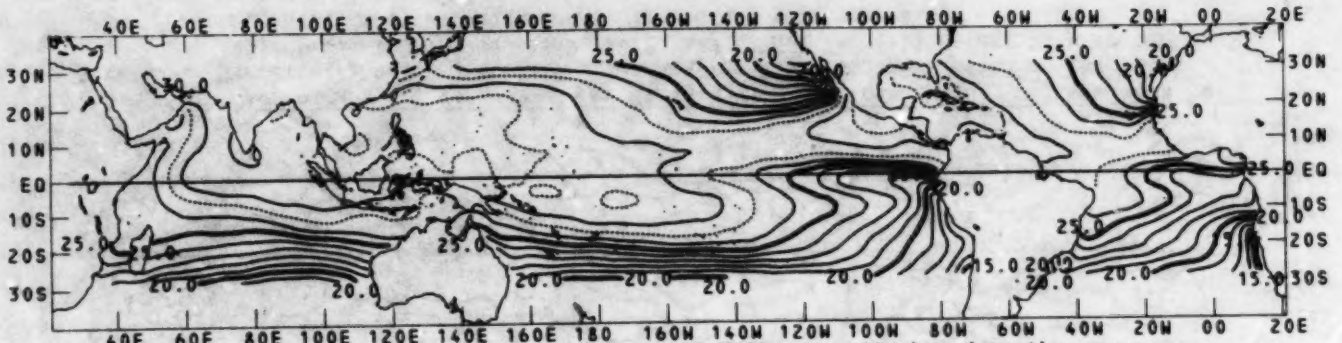

Figure 76a. June (+1) through August (+1) mean SST ENSO composite based on the years 1951, 1953, 1957, 1965, 1969, 1972, and 1976. The (+1) refers to the year after the ENSO. The contour interval is 1°C. The 27°C and 29°C isopleth is dashed.

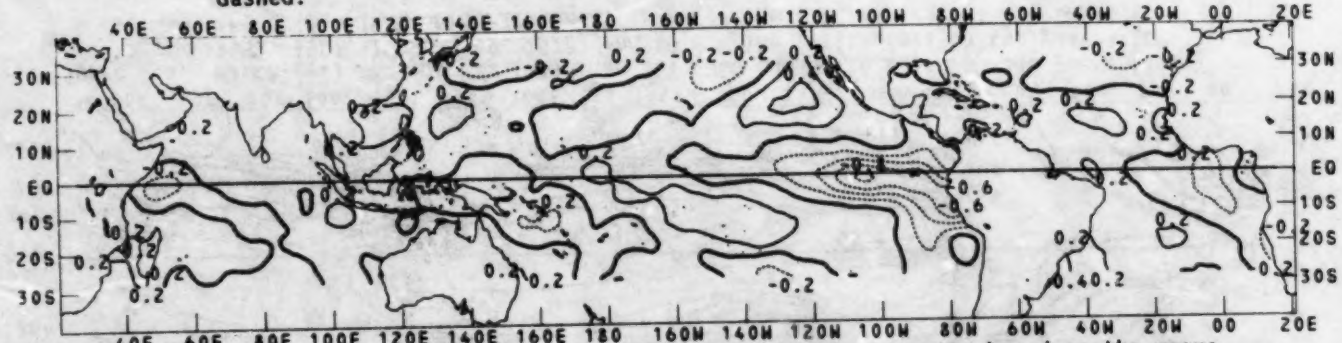

Figure 76b. June (+1) through August (+1) SST anomalies ENSO composite based on the years 1951, 1953, 1957, 1965, 1969, 1972, and 1976. The (+1) refers to year after the ENSO. The contour interval is 0.2°C. Negative values are dashed.

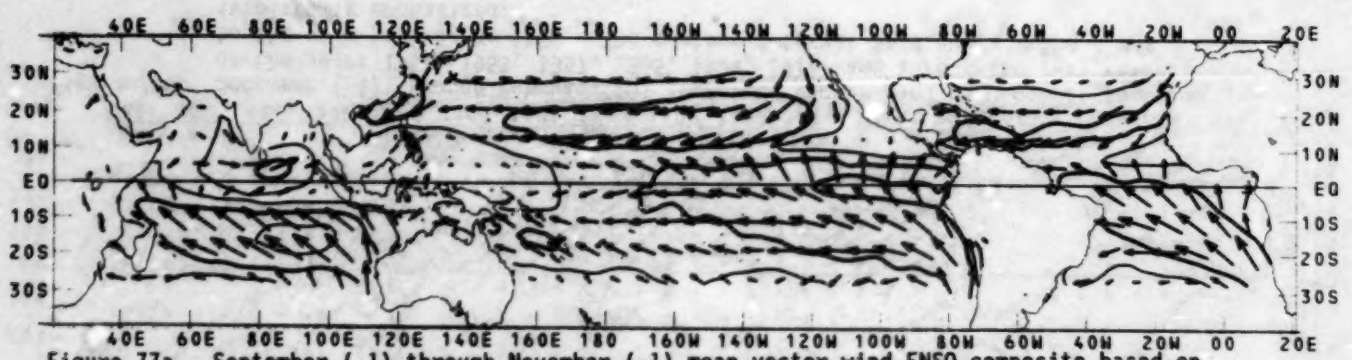

Figure 77a. September (-1) through November (-1) mean vector wind ENSO composite based on the years 1951, 1953, 1957, 1965, 1969, 1972, and 1976. The (-1) refers to the year before the ENSO. The contour interval is 2.5 m/s. The 5 m/s isopleth is emphasized.

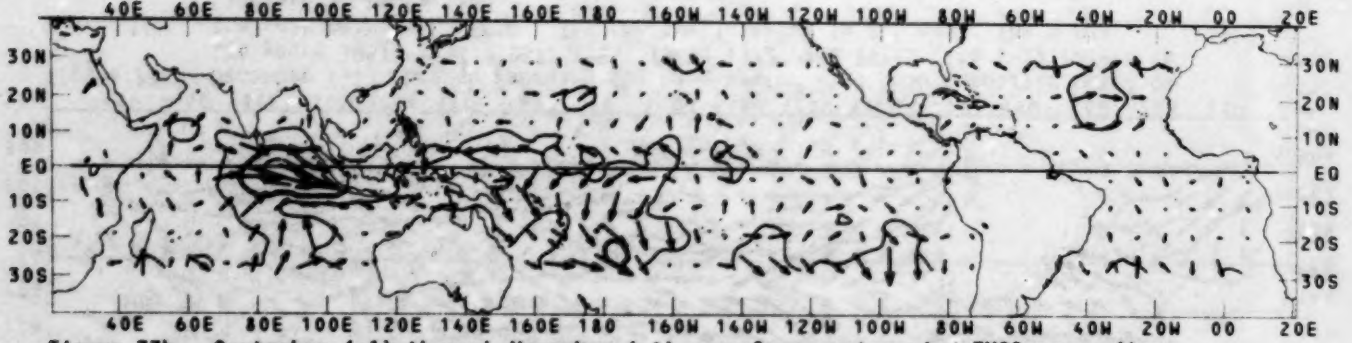

Figure 77b. September (-1) through November (-1) anomalous vector wind ENSO composite based on the years 1951, 1953, 1957, 1965, 1969, 1972, and 1976. The (-1) refers to the year before the ENSO. The contour interval is 0.5 m/s. The 1 m/s isopleth is emphasized.

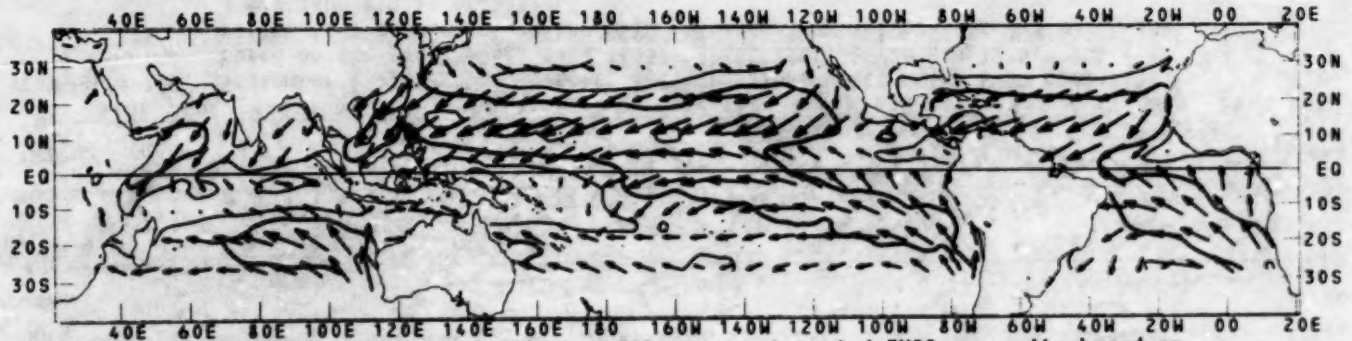

Figure 78a. December (-1) through February (0) mean vector wind ENSO composite based on the years 1951, 1953, 1957, 1965, 1969, 1972, and 1976. The (-1) refers to the year before the ENSO. The contour interval is 2.5 m/s. The 5 m/s isopleth is emphasized.

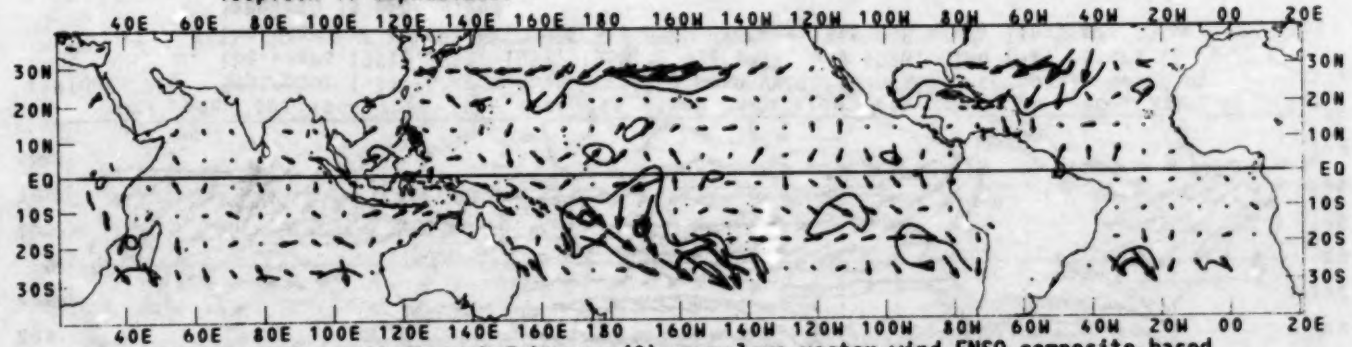

Figure 78b. December (-1) through February (0) anomalous vector wind ENSO composite based on the years 1951, 1953, 1957, 1965, 1969, 1972, and 1976. The (-1) refers to the year before the ENSO. The contour interval is 0.5 m/s. The 1 m/s isopleth is emphasized.

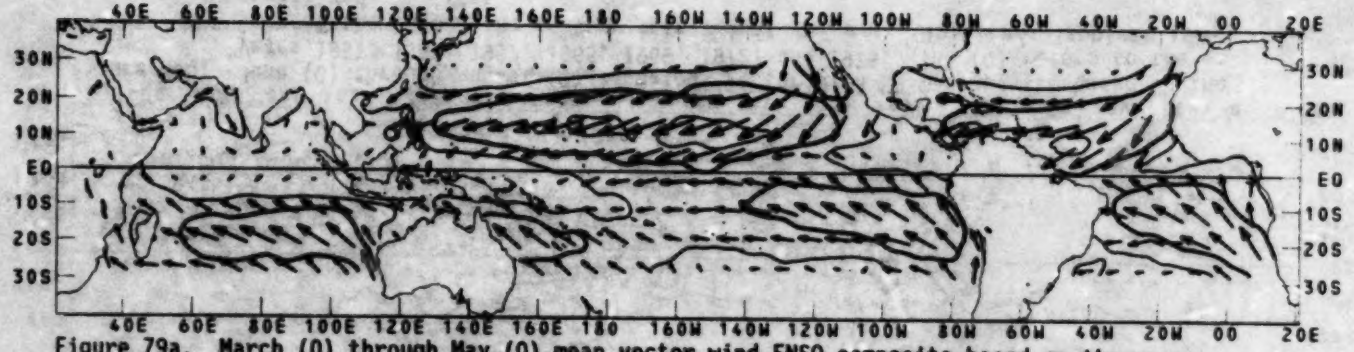

Figure 79a. March (0) through May (0) mean vector wind ENSO composite based on the years 1951, 1953, 1957, 1965, 1969, 1972, and 1976. The (0) refers to the year of the ENSO. The contour interval is 2.5 m/s. The 5 m/s isopleth is emphasized.

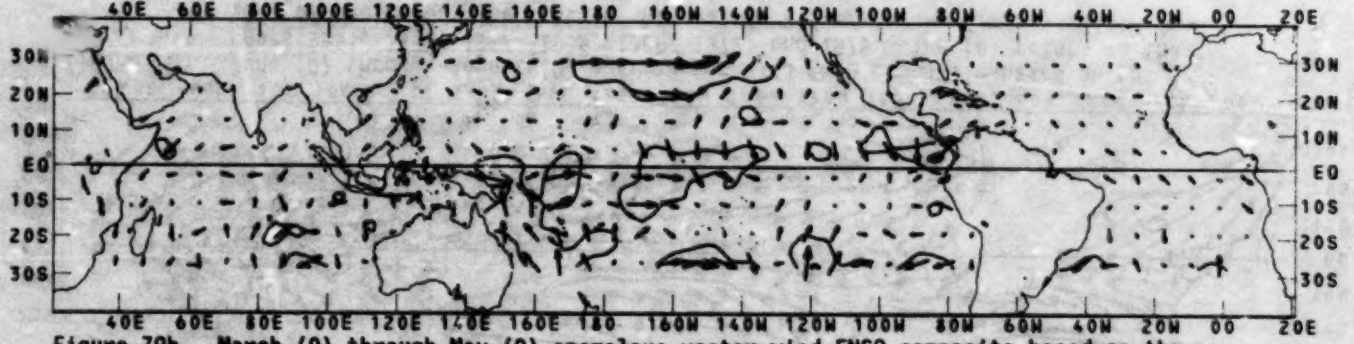

Figure 79b. March (0) through May (0) anomalous vector wind ENSO composite based on the years 1951, 1953, 1957, 1965, 1969, 1972, and 1976. The (0) refers to the year of the ENSO. The contour interval is 0.5 m/s. The 1 m/s isopleth is emphasized.

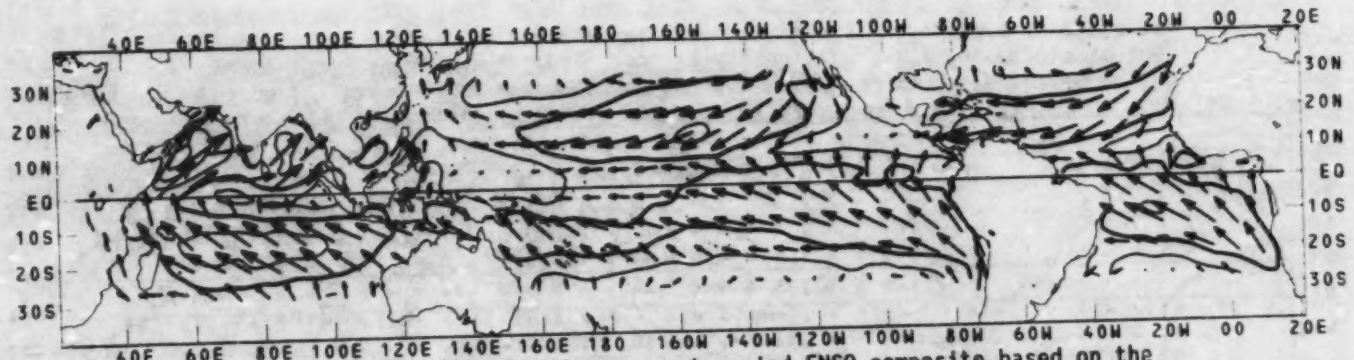

Figure 80a. June (0) through August (0) mean vector wind ENSO composite based on the years 1951, 1953, 1957, 1965, 1969, 1972, and 1976. The (0) refers to the year of the ENSO. The contour interval is 2.5 m/s. The 5 m/s isopleth is emphasized.

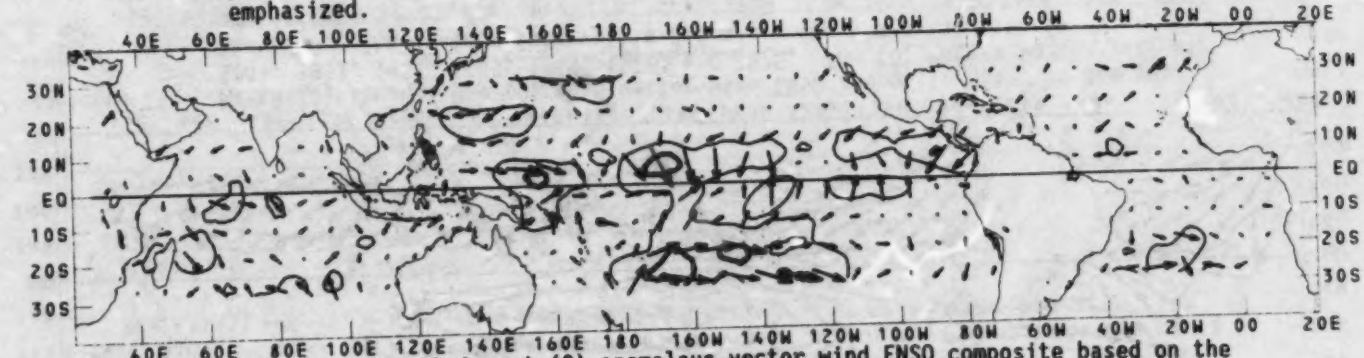

Figure 80b. June (0) through August (0) anomalous vector wind ENSO composite based on the years 1951, 1953, 1957, 1965, 1969, 1972, and 1976. The (0) refers to the year of the ENSO. The contour interval is 0.5 m/s. The 1 m/s isopleth is emphasized.

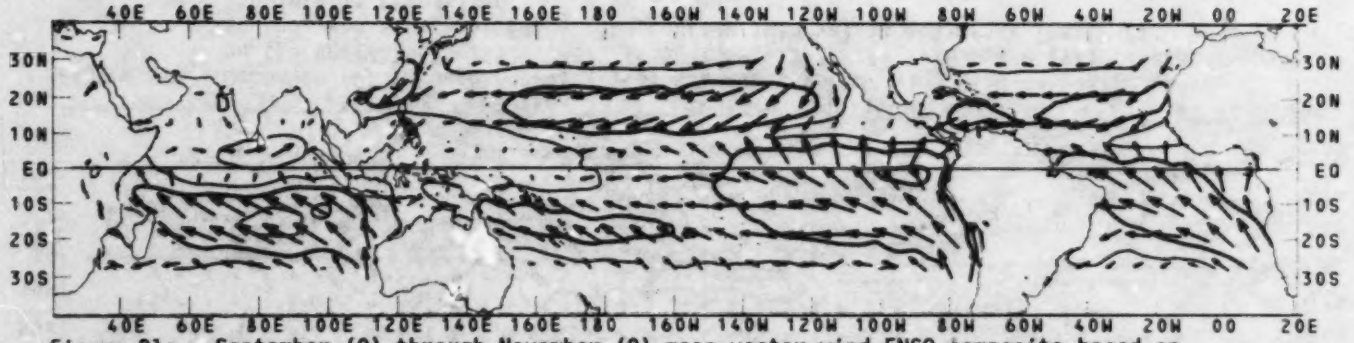

Figure 81a. September (0) through November (0) mean vector wind ENSO composite based on the years 1951, 1953, 1957, 1965, 1969, 1972, and 1976. The (0) refers to the year of the ENSO. The contour interval is 2.5 m/s. The 5 m/s isopleth is emphasized.

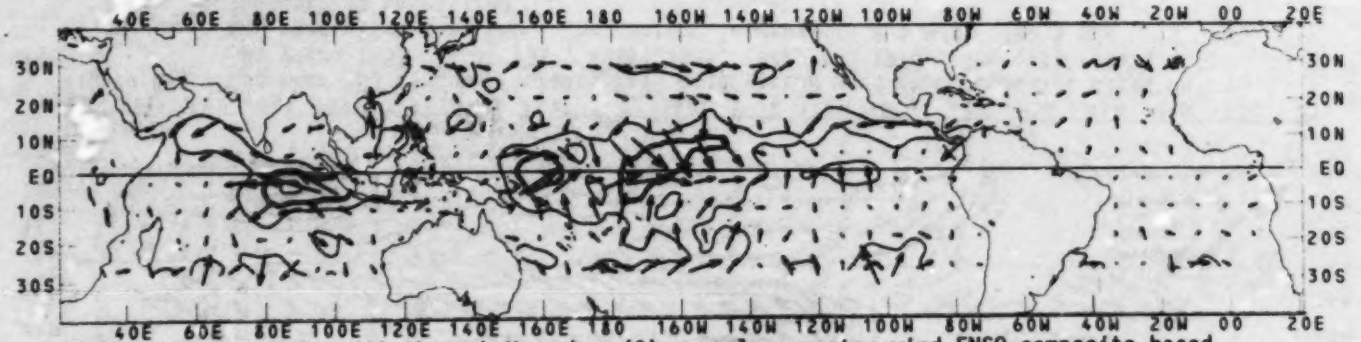

Figure 81b. September (0) through November (0) anomalous vector wind ENSO composite based on the years 1951, 1953, 1957, 1965, 1969, 1972, and 1976. The (0) refers to the year of the ENSO. The contour interval is 0.5 m/s. The 1 m/s isopleth is emphasized.

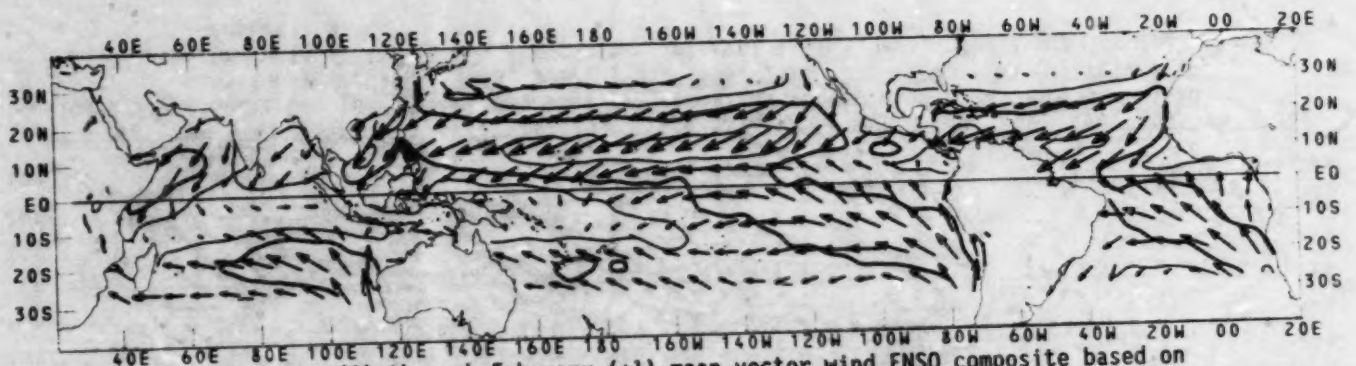

Figure 82a. December (0) through February (+1) mean vector wind ENSO composite based on the years 1951, 1953, 1957, 1965, 1969, 1972, and 1976. The (+1) refers to the year after the ENSO. The contour interval is 2.5 m/s. The 5 m/s isopleth is emphasized.

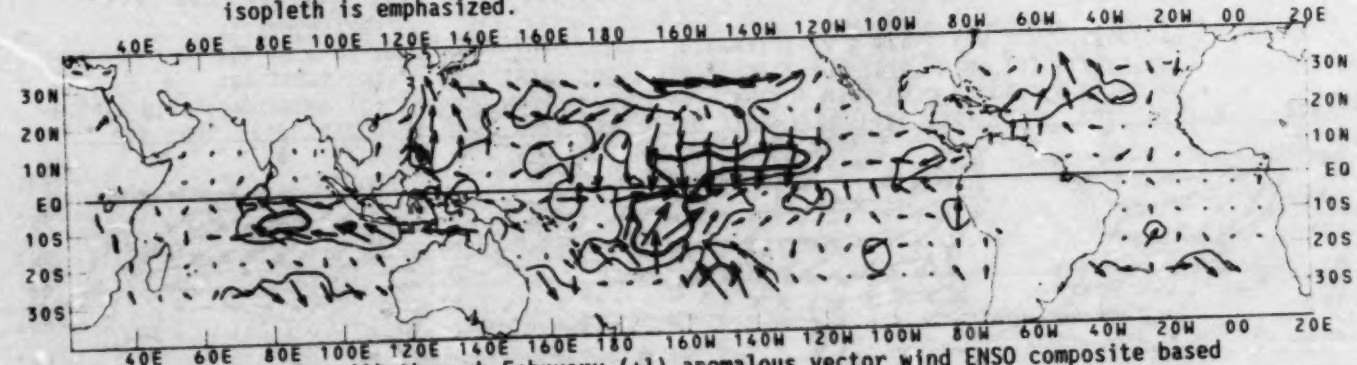

Figure 82b. December (0) through February (+1) anomalous vector wind ENSO composite based on the years 1951, 1953, 1957, 1965, 1969, 1972, and 1976. The (+1) refers to the year after the ENSO. The contour interval is 0.5 m/s. The 1 m/s isopleth is emphasized.

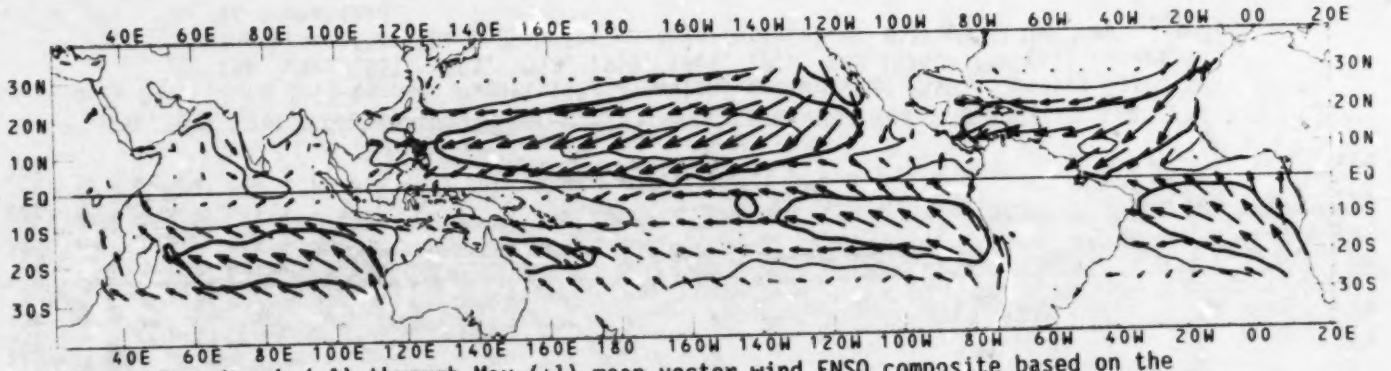

Figure 83a. March (+1) through May (+1) mean vector wind ENSO composite based on the years 1951, 1953, 1957, 1965, 1969, 1972, and 1976. The (+1) refers to the year after the ENSO. The contour interval is 2.5 m/s. The 5 m/s isopleth is emphasized.

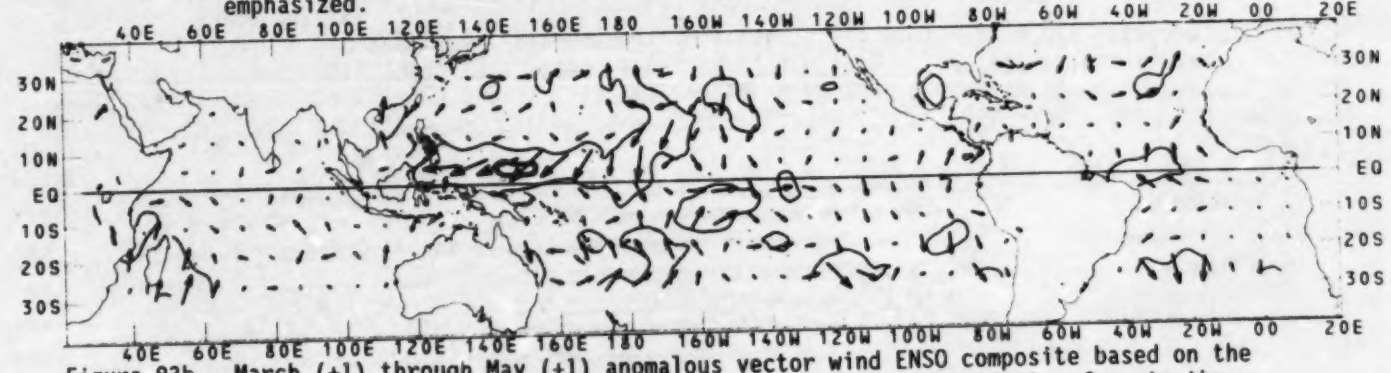

Figure 83b. March (+1) through May (+1) anomalous vector wind ENSO composite based on the years 1951, 1953, 1957, 1965, 1969, 1972, and 1976. The (+1) refers to the year after the ENSO. The contour interval is 0.5 m/s. The 1 m/s isopleth is emphasized.

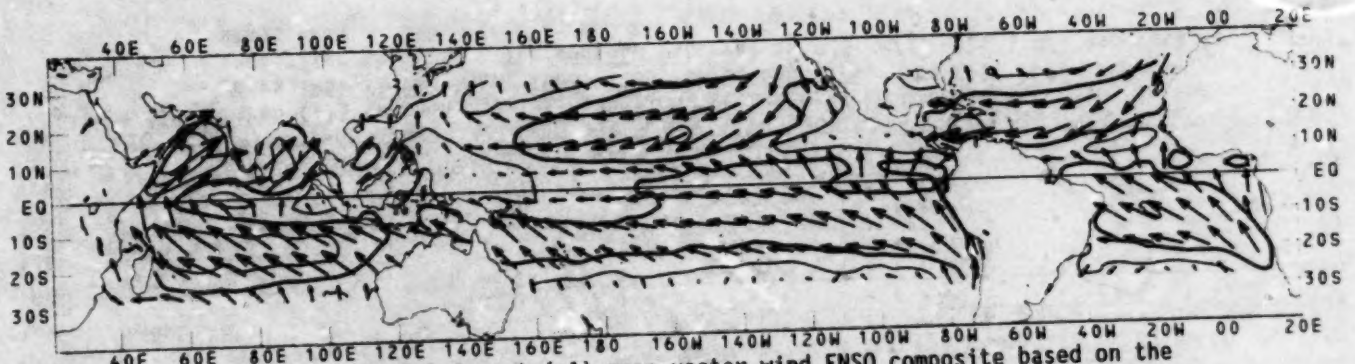

Figure 84a. June (+1) through August (+1) mean vector wind ENSO composite based on the years 1951, 1953, 1957, 1965, 1969, 1972, and 1976. The (+1) refers to the year after the ENSO. The contour interval is 2.5 m/s. The 5 m/s isopleth is emphasized.

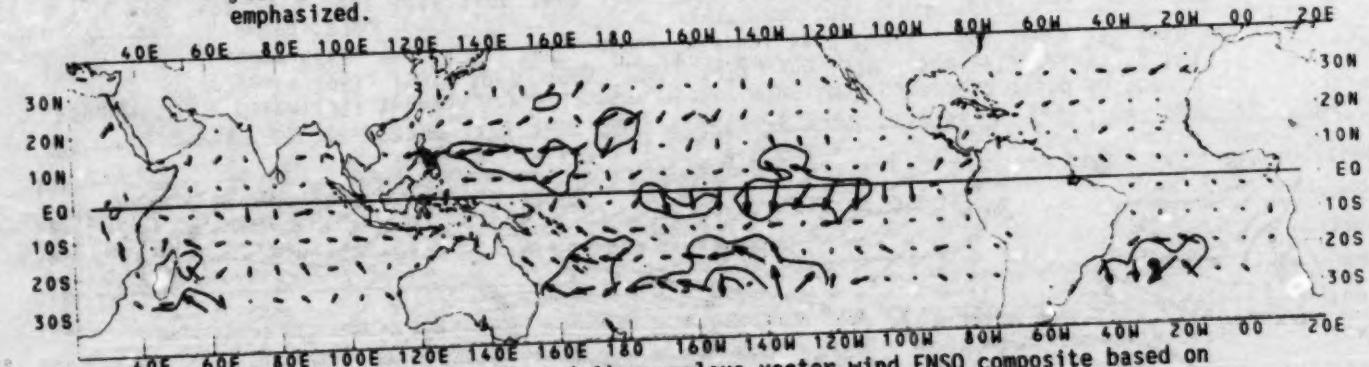

Figure 84b. June (+1) through August (+1) anomalous vector wind ENSO composite based on the years 1951, 1953, 1957, 1965, 1969, 1972, and 1976. The (+1) refers to the year after the ENSO. The contour interval is 0.5 m/s. The 1 m/s isopleth is emphasized.

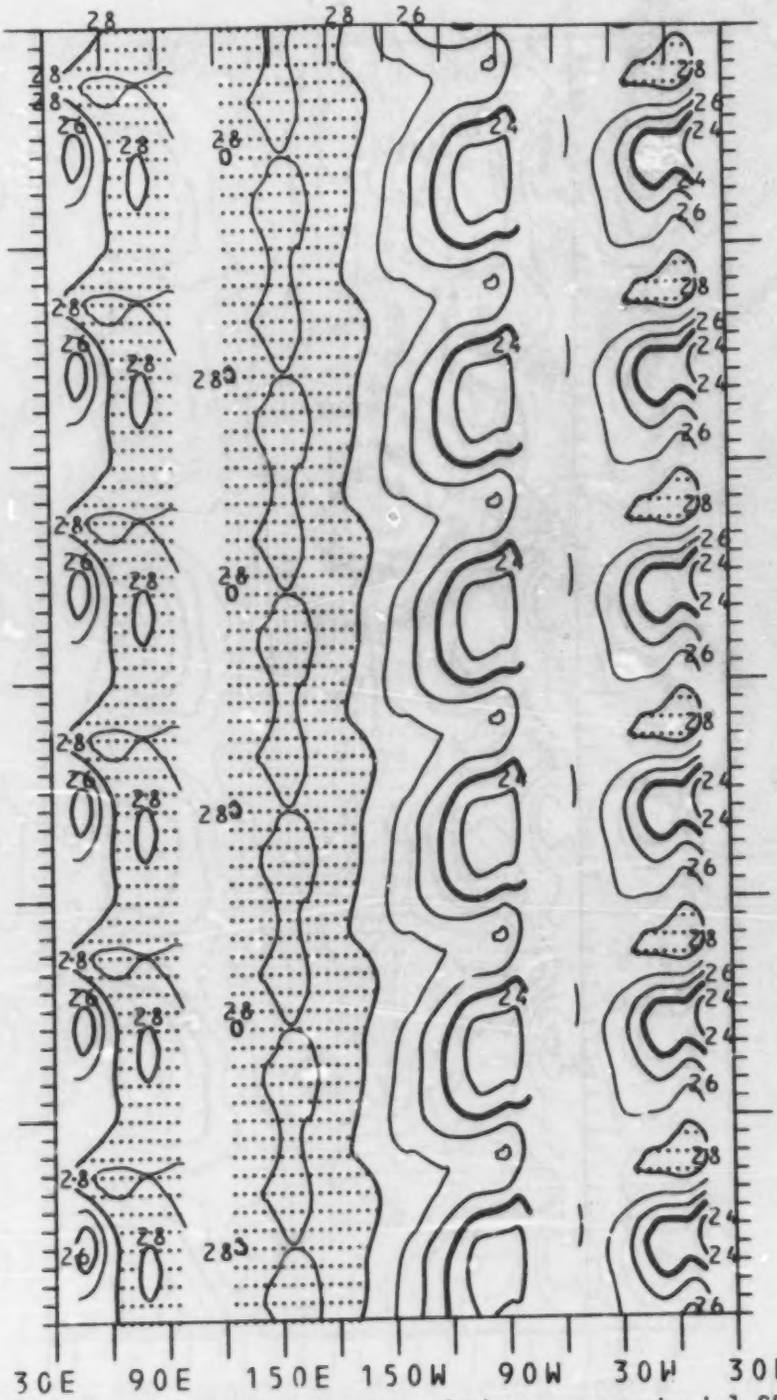

Figure 85. Time-longitude cross-section of the mean equatorial SST based on the period 1950-1979. The contour interval is 1°C. The 25°C isotherm is emphasized. Values greater than 28°C are shaded.

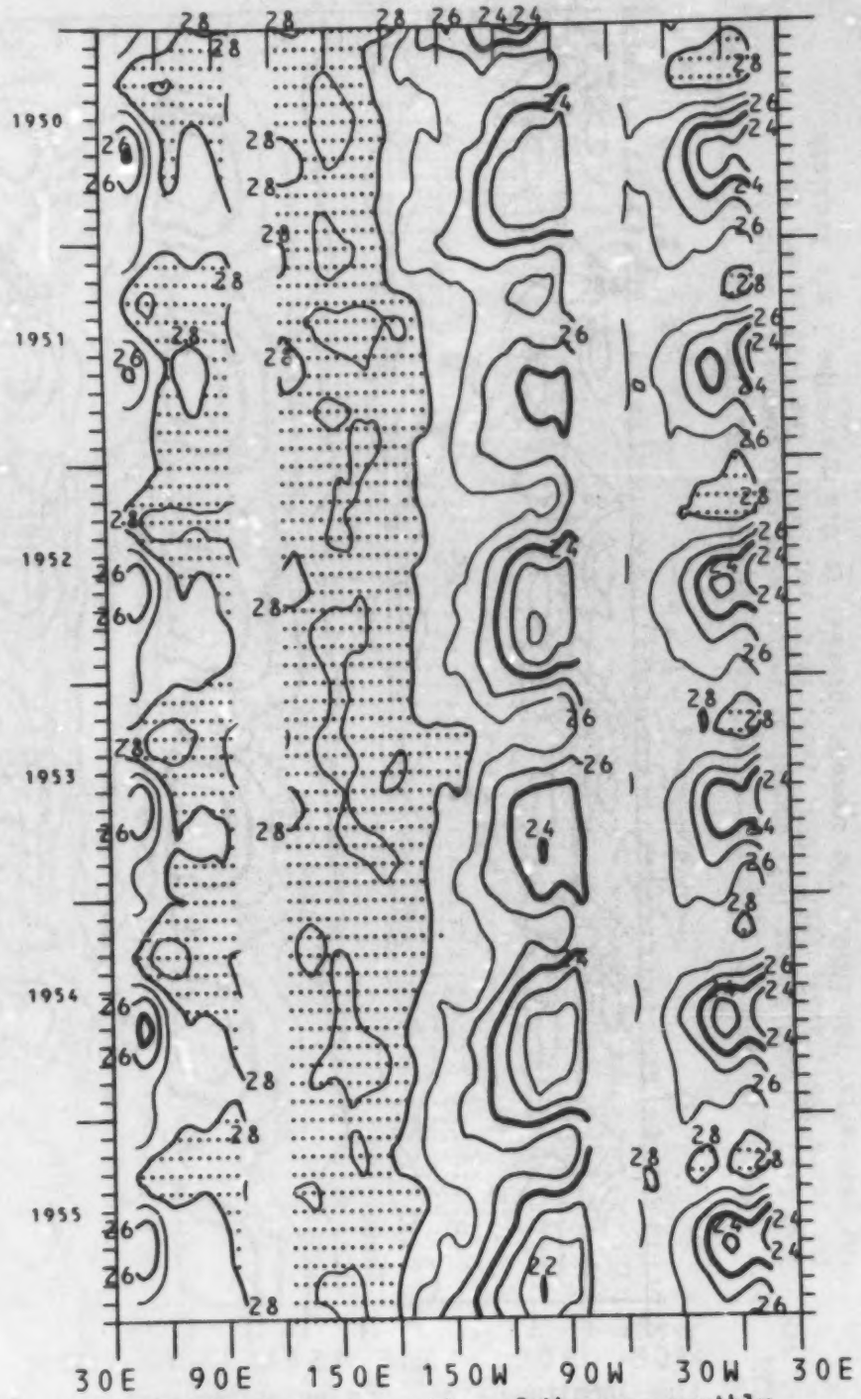

Figure 86. Time-longitude cross-section of the mean monthly equatorial SST for the years 1950-1955. The contour interval is $1^{o}C$. The $25^{o}C$ isotherm is emphasized. Values greater than $28^{o}C$ are shaded.

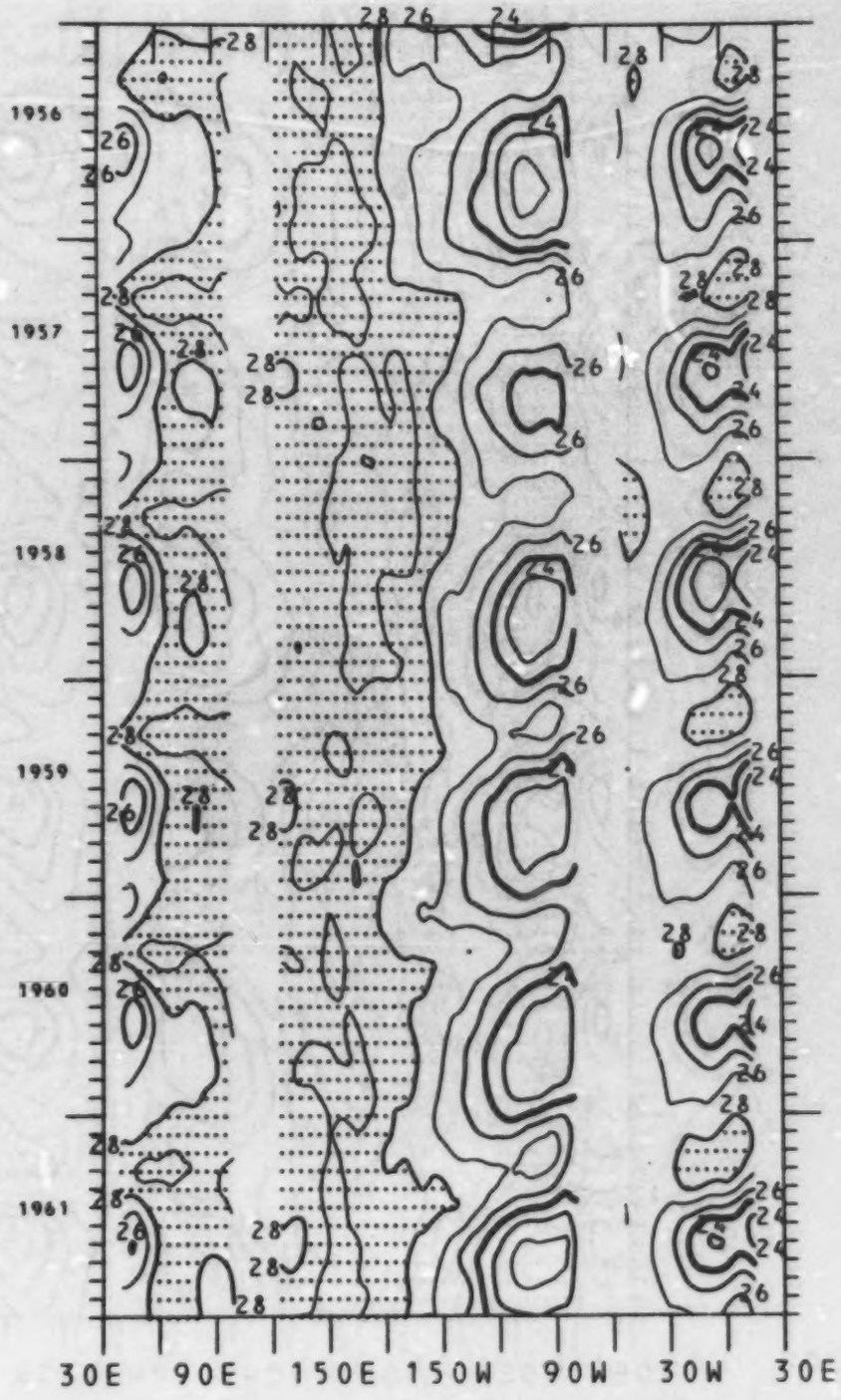

Figure 87. Time-longitude cross-section of the mean monthly equatorial SST for the years 1956-1961. The contour interval is 1°C. The 25°C isotherm is emphasized. Values greater than 28°C are shaded.

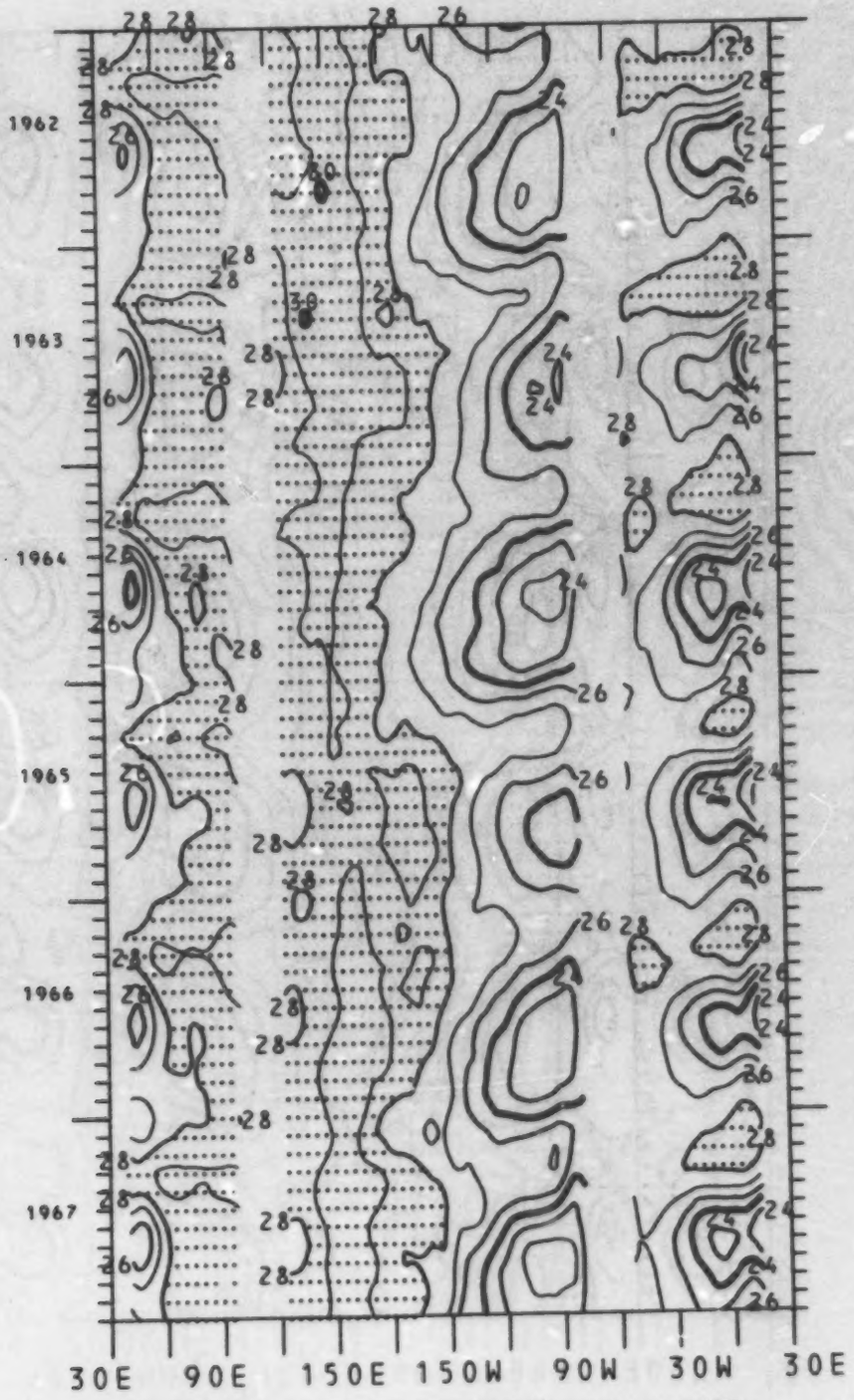

Figure 88. Time-longitude cross-section of the mean monthly equatorial SST for the years 1962-1967. The contour interval is $1^{o}C$. The $25^{o}C$ isotherm is emphasized. Values greater than $28^{o}C$ are shaded.

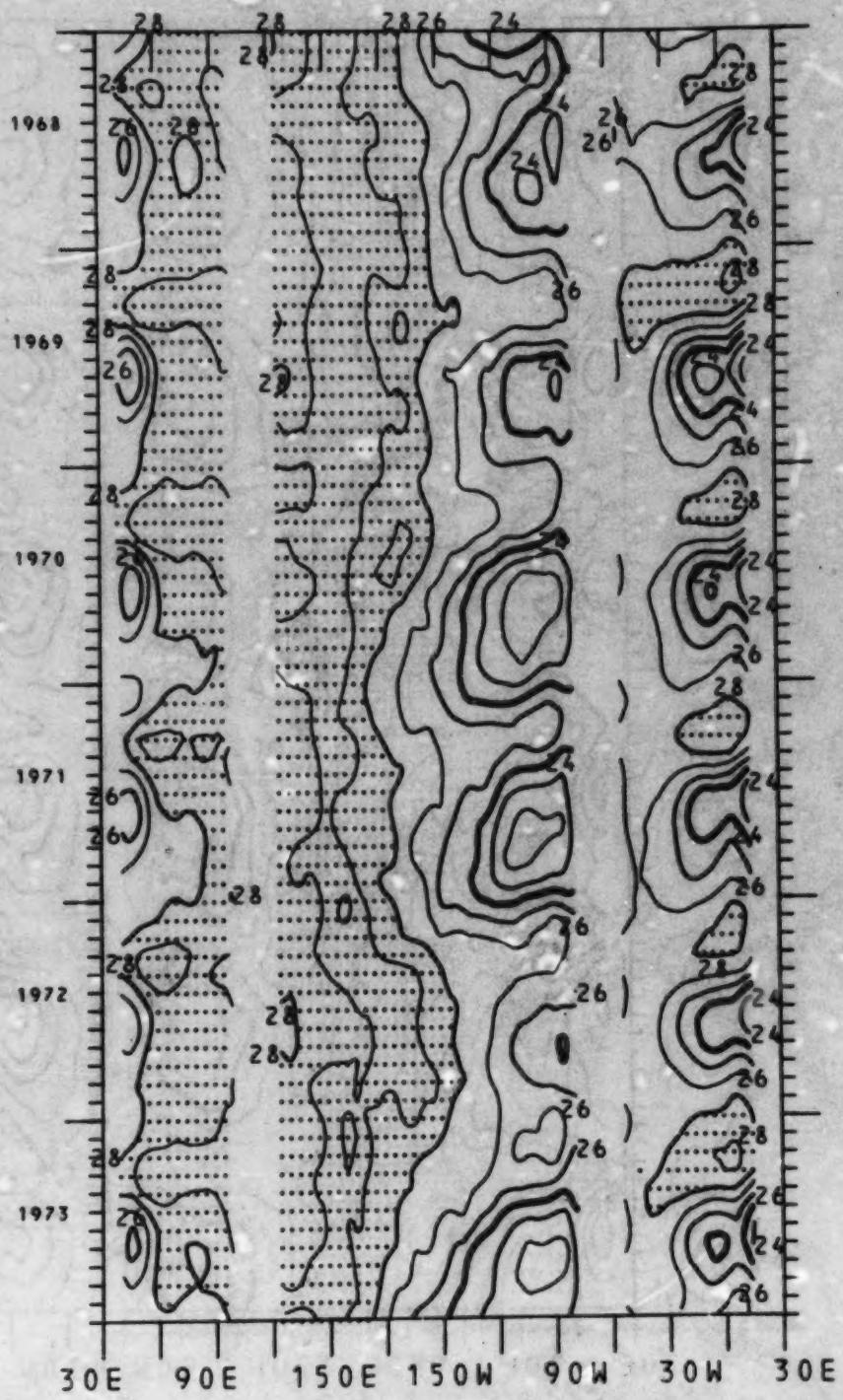

Figure 89. Time-longitude cross-section of the mean monthly equatorial SST for the years 1968-1973. The contour interval is 1°C. The 25°C isotherm is emphasized. Values greater than 28°C are shaded.

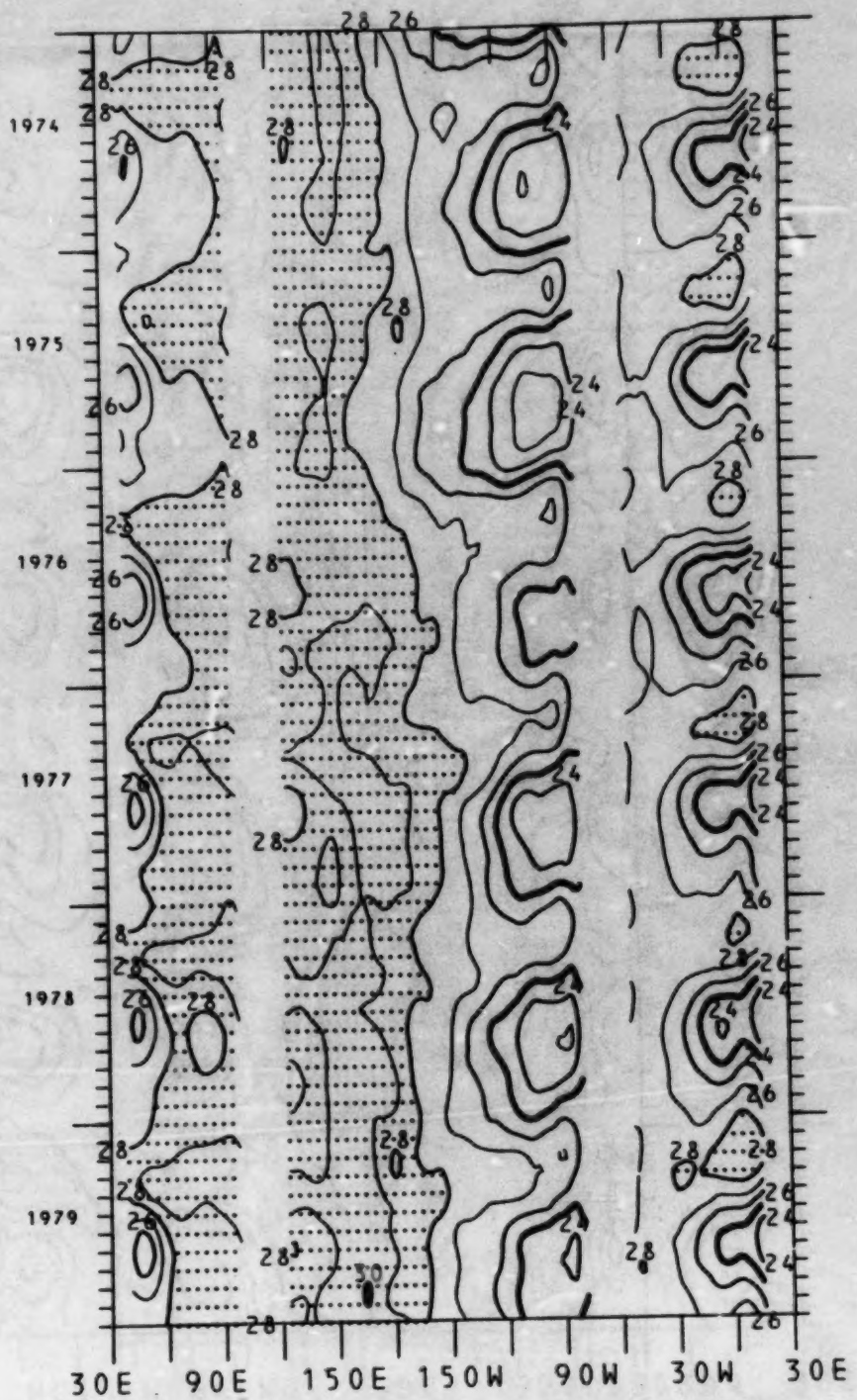

Figure 90. Time-longitude cross-section of the mean monthly equatorial SST for the years 1974-1979. The contour interval is 1°C. The 25°C isotherm is emphasized. Values greater than 28°C are shaded.

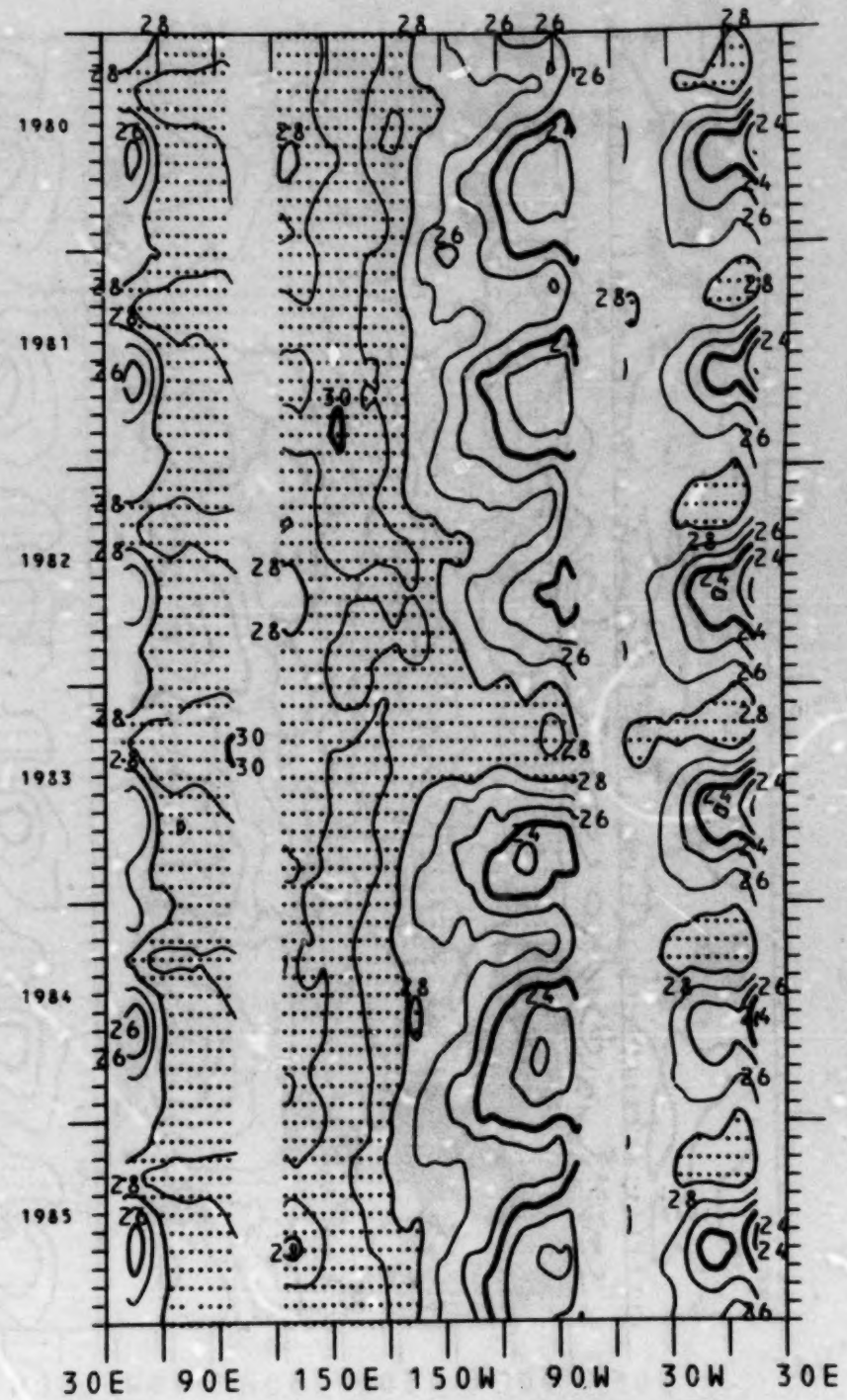

Figure 91. Time-longitude cross-section of the mean monthly equatorial SST for the years 1980-1985. The contour interval is 1°C. The 25°C isotherm is emphasized. Values greater than 28°C are shaded.

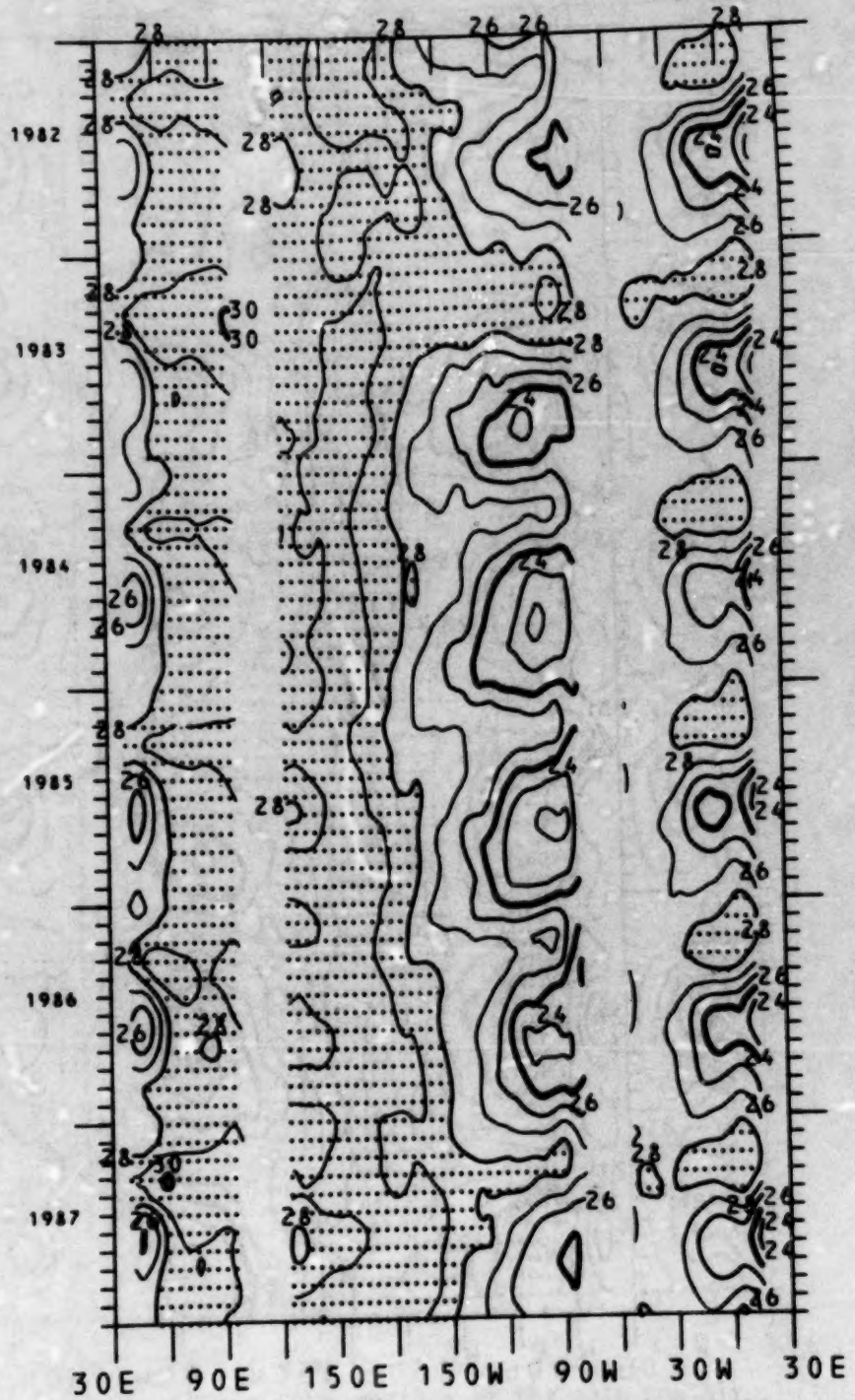

Figure 92. Time-longitude cross-section of the mean monthly equatorial SST for the years 1982-1987. The contour interval is $1^{o}C$. The $25^{o}C$ isotherm is emphasized. Values greater than $28^{o}C$ are shaded.

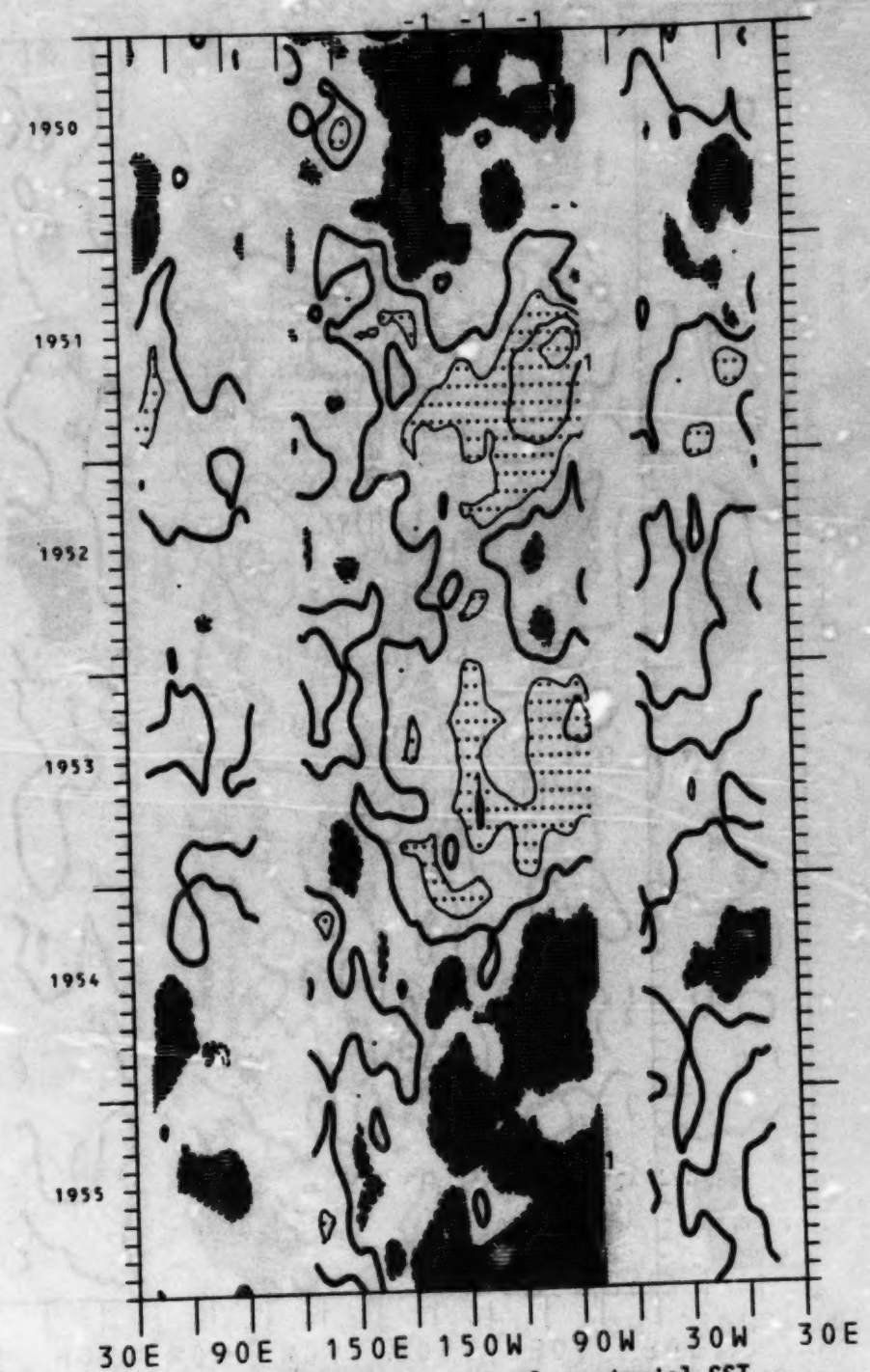

Figure 93. Time-longitude cross-section of equatorial SST anomalies for the years 1950-1955. The contour interval is .5°C. The zero isotherm is emphasized. Negative values are dashed. Light shading is greater than 0.5°C; dark shading is less than -0.5°C.

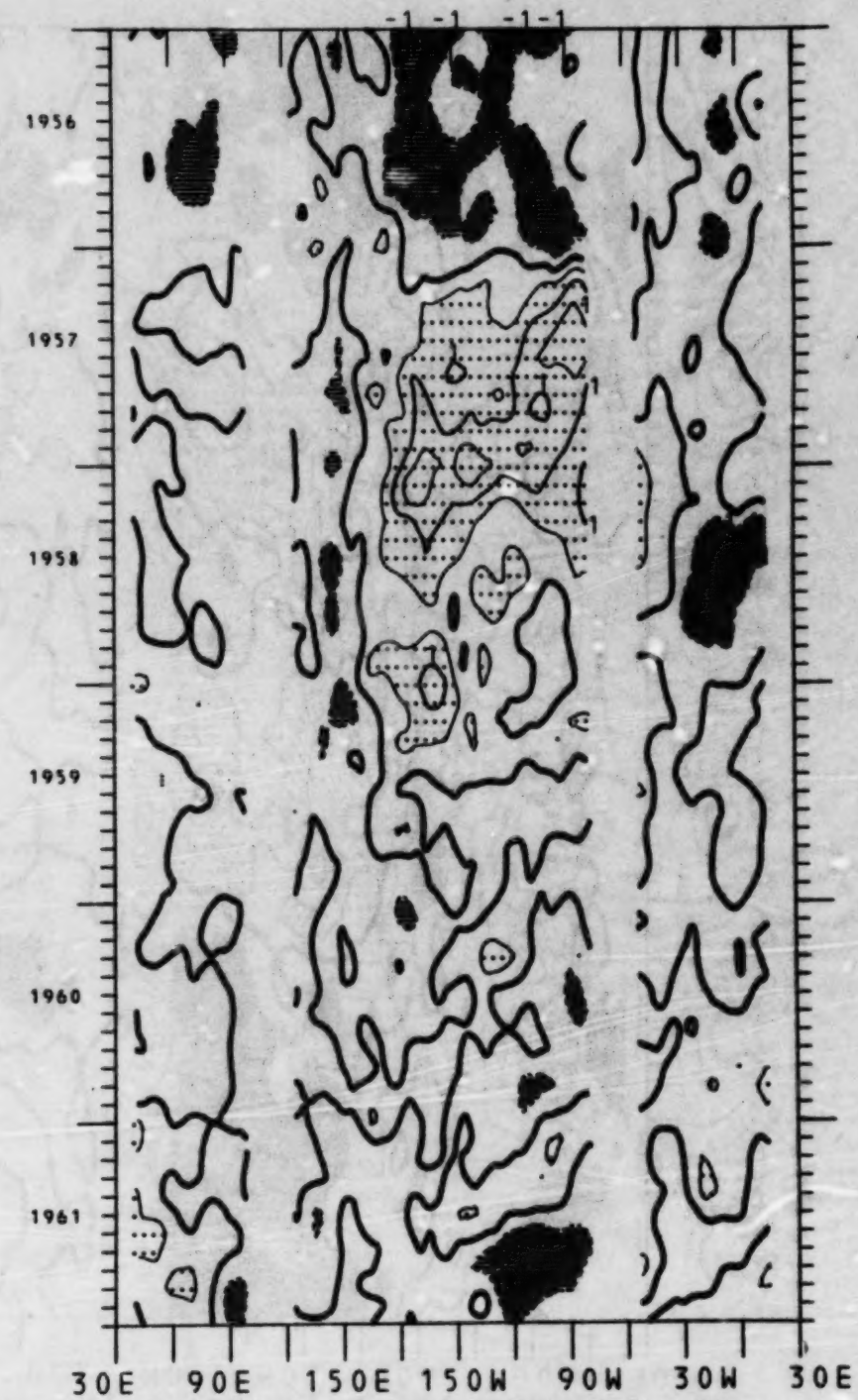

Figure 94. Time-longitude cross-section of equatorial SST anomalies for the years 1956-1961. The contour interval is .5°C. The zero isotherm is emphasized. Negative values are dashed. Light shading is greater than 0.5°C; dark shading is less than -0.5°C.

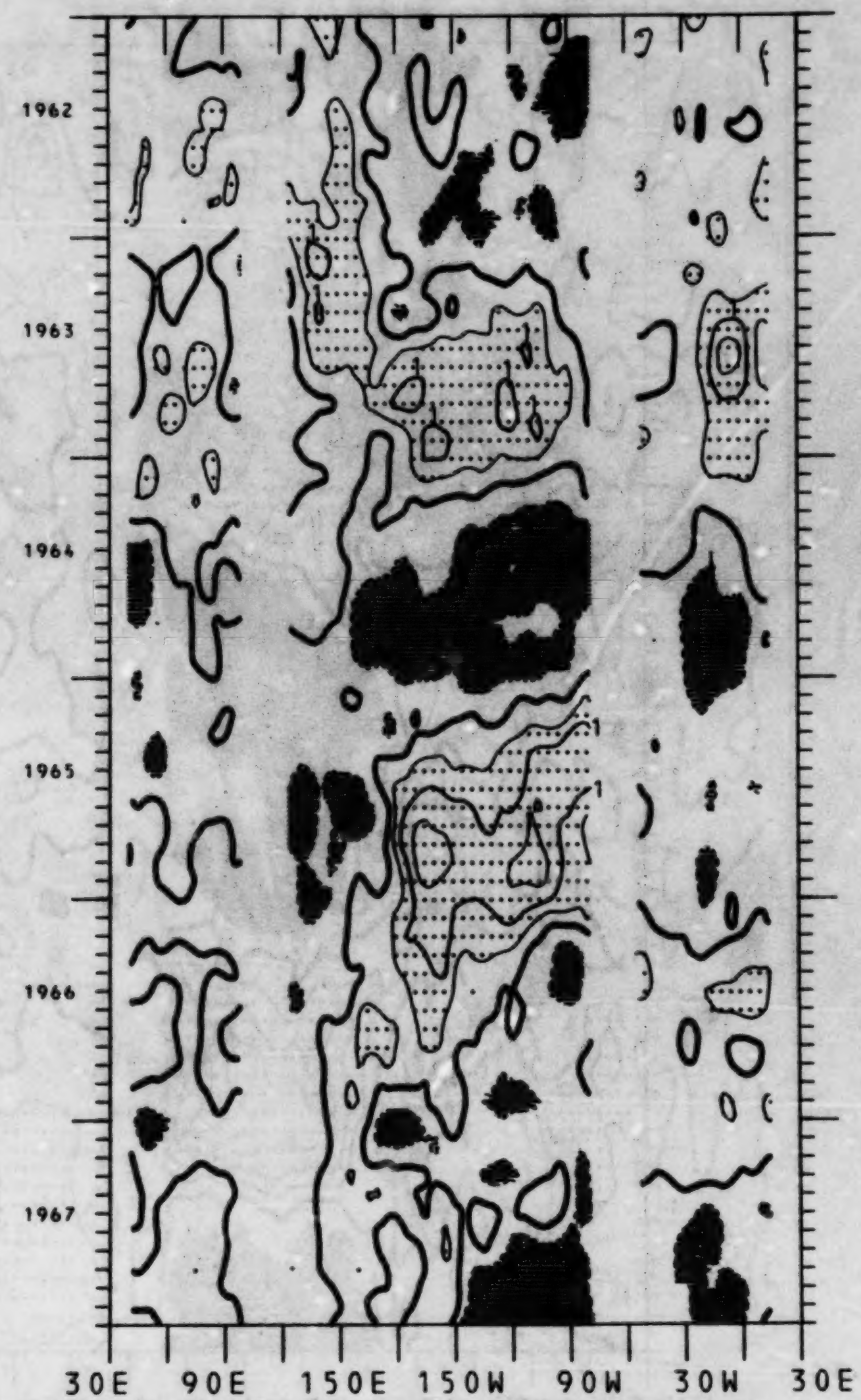

Figure 95. Time-longitude cross-section of equatorial SST anomalies for the years 1962-1967. The contour interval is .5°C. The zero isotherm is emphasized. Negative values are dashed. Light shading is greater than 0.5°C; dark shading is less than -0.5°C.

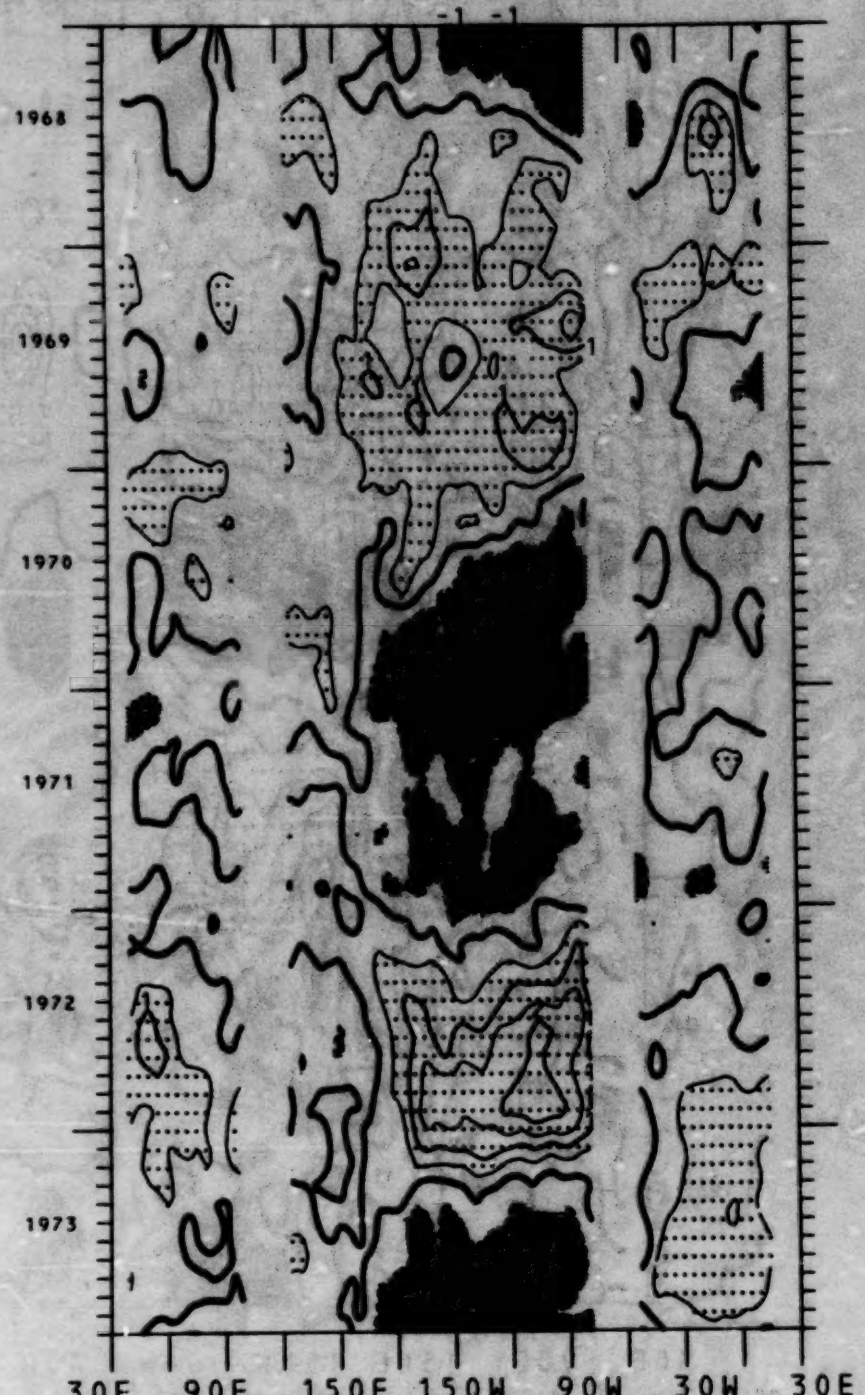

Figure 96. Time-longitude cross-section of equatorial SST anomalies for the years 1968-1973. The contour interval is .5°C. The zero isotherm is emphasized. Negative values are dashed. Light shading is greater than 0.5°C; dark shading is less than -0.5°C.

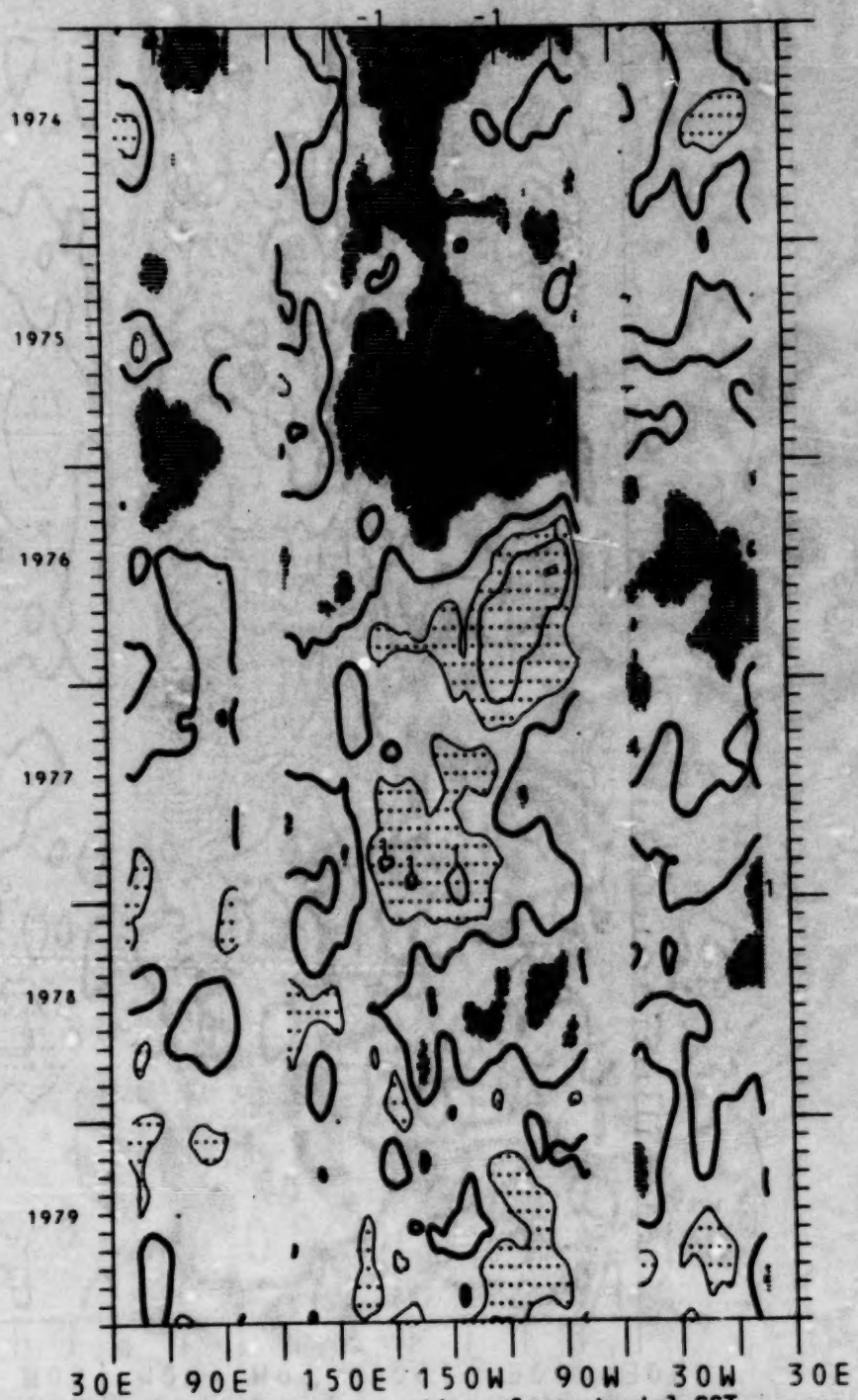

Figure 97. Time-longitude cross-section of equatorial SST anomalies for the years 1974-1979. The contour interval is .5°C. The zero isotherm is emphasized. Negative values are dashed. Light shading is greater than 0.5°C; dark shading is less than -0.5°C.

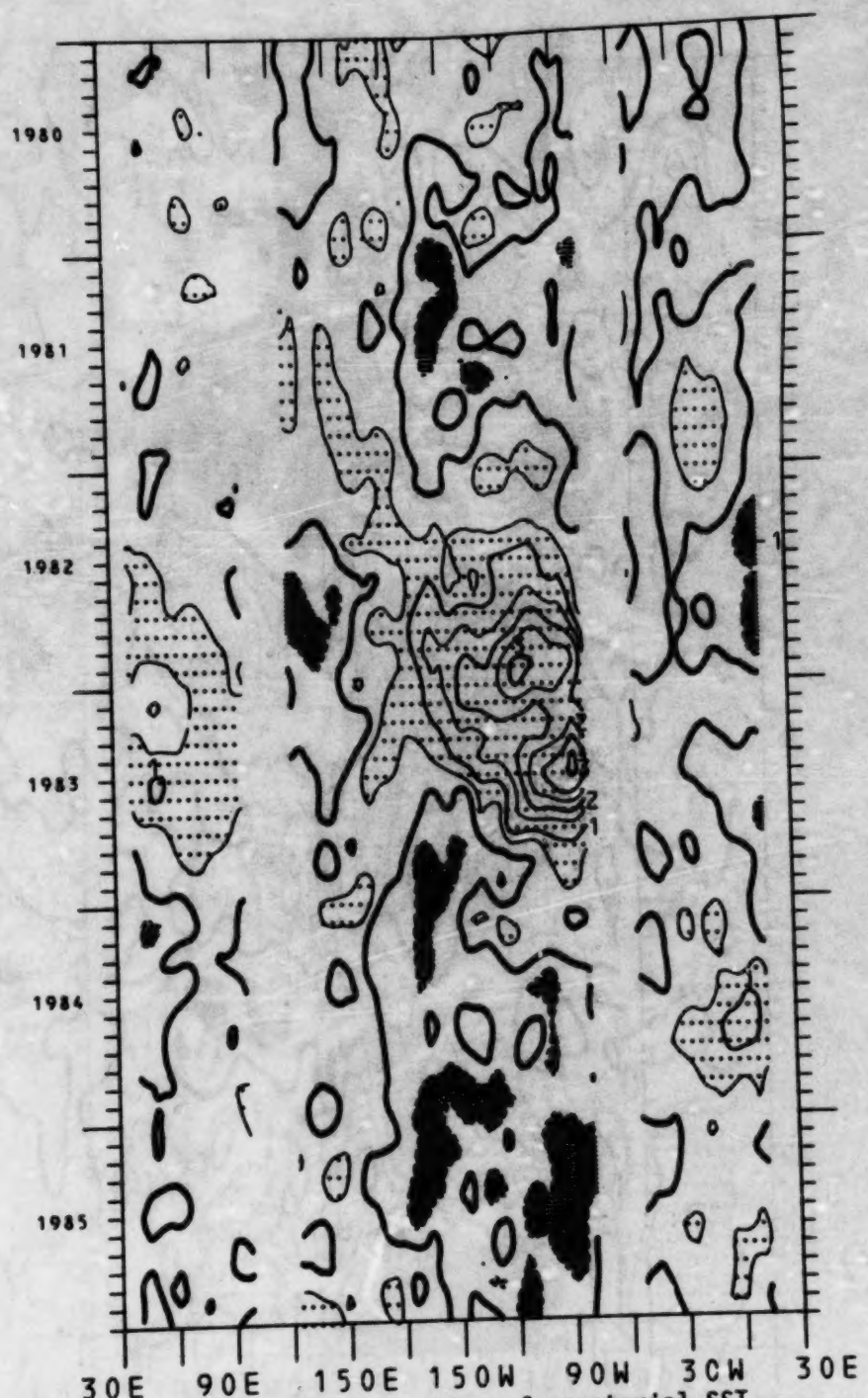

Figure 98. Time-longitude cross-section of equatorial SST anomalies for the years 1980-1985. The contour interval is .5°C. The zero isotherm is emphasized. Negative values are dashed. Light shading is greater than 0.5°C; dark shading is less than -0.5°C.

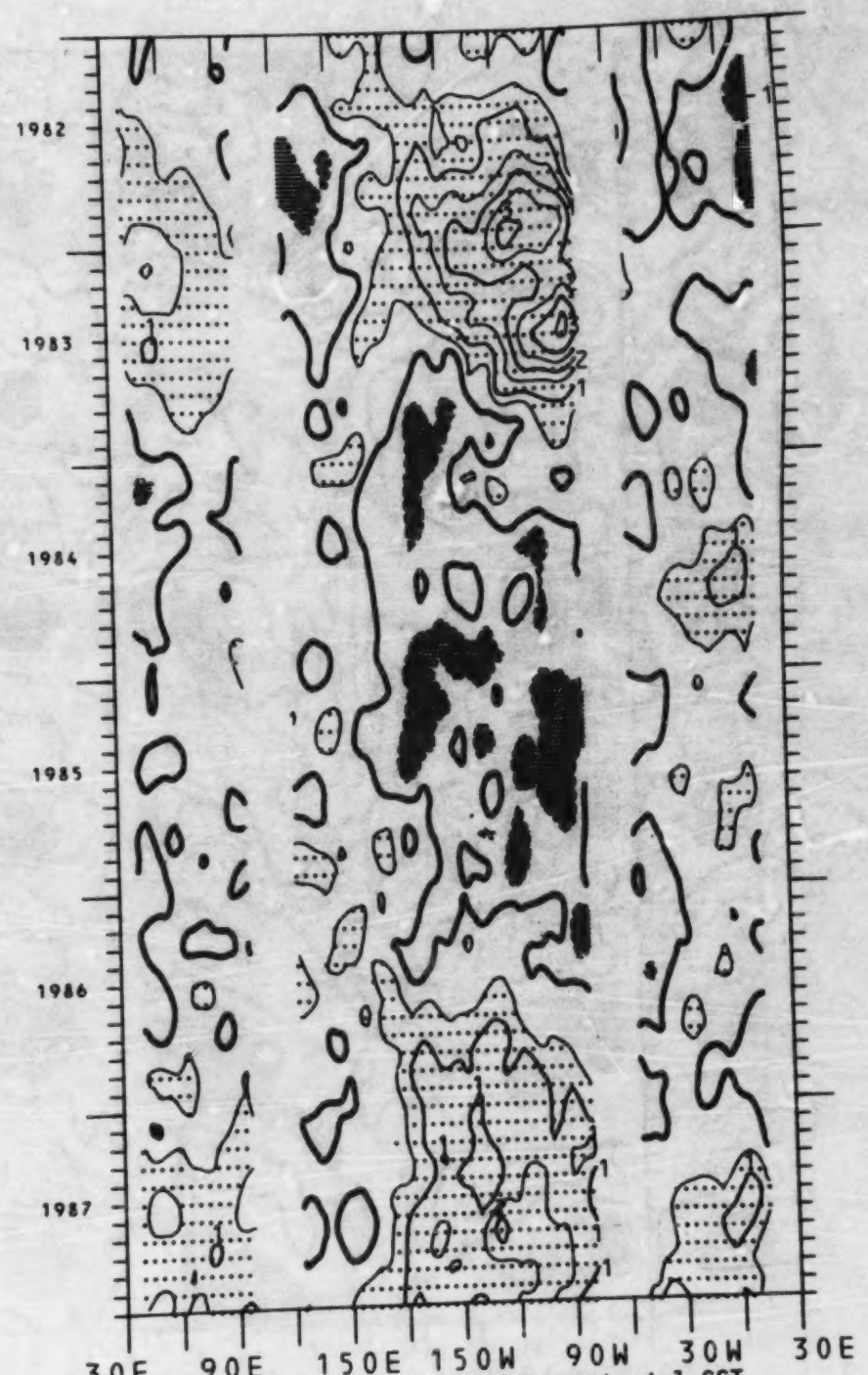

Figure 99. Time-longitude cross-section of equatorial SST anomalies for the years 1982-1987. The contour interval is .5°C. The zero isotherm is emphasized. Negative values are dashed. Light shading is greater than 0.5°C; dark shading is less than -0.5°C.

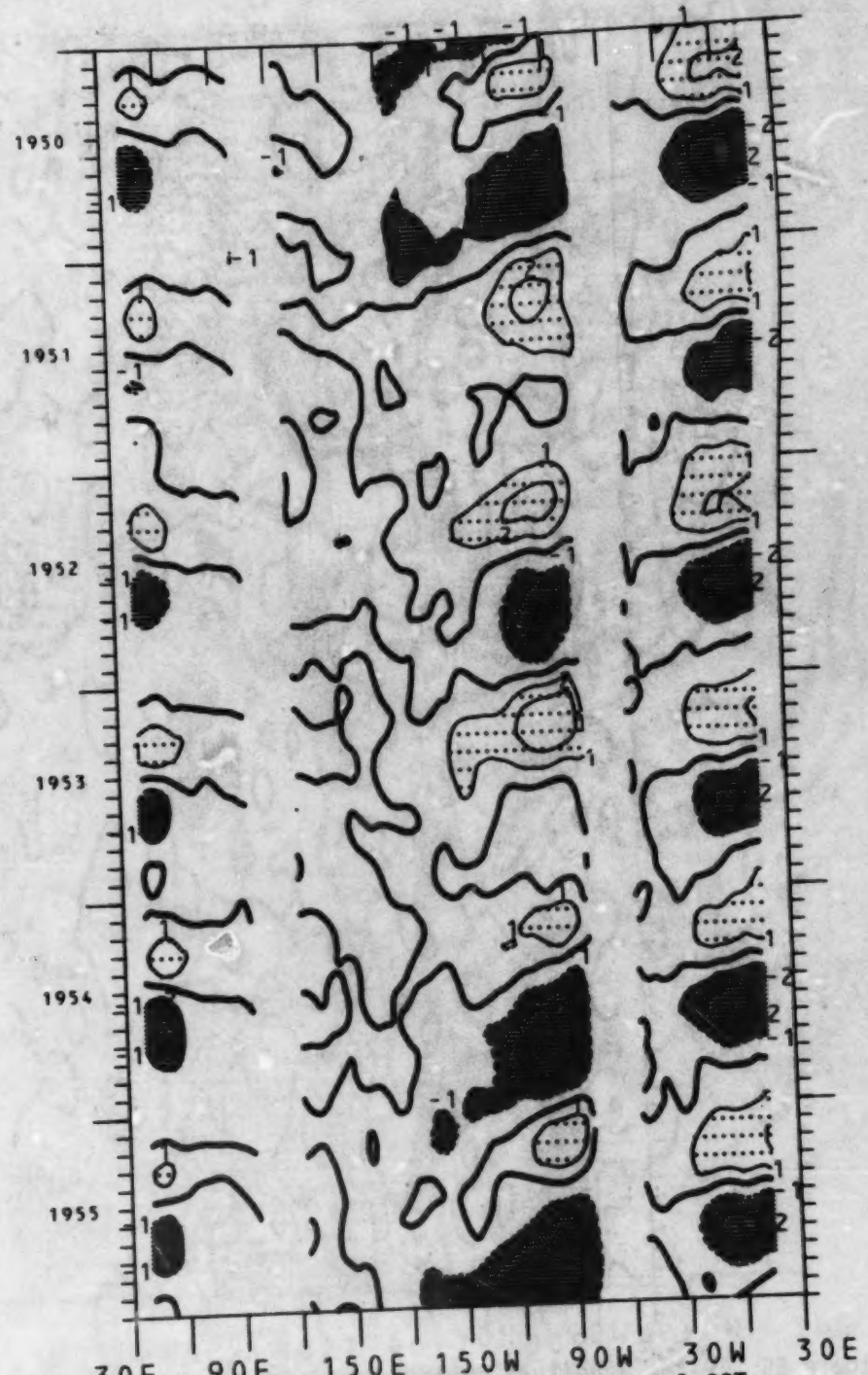

Figure 100. Time-longitude cross-section of equatorial SST expressed as the difference from the annual mean for the years 1950-1955. The contour interval is 1.0°C. The zero isotherm is emphasized. Negative values are dashed. Light shading is greater than 1.0°C; dark shading is less than -1.0°C.

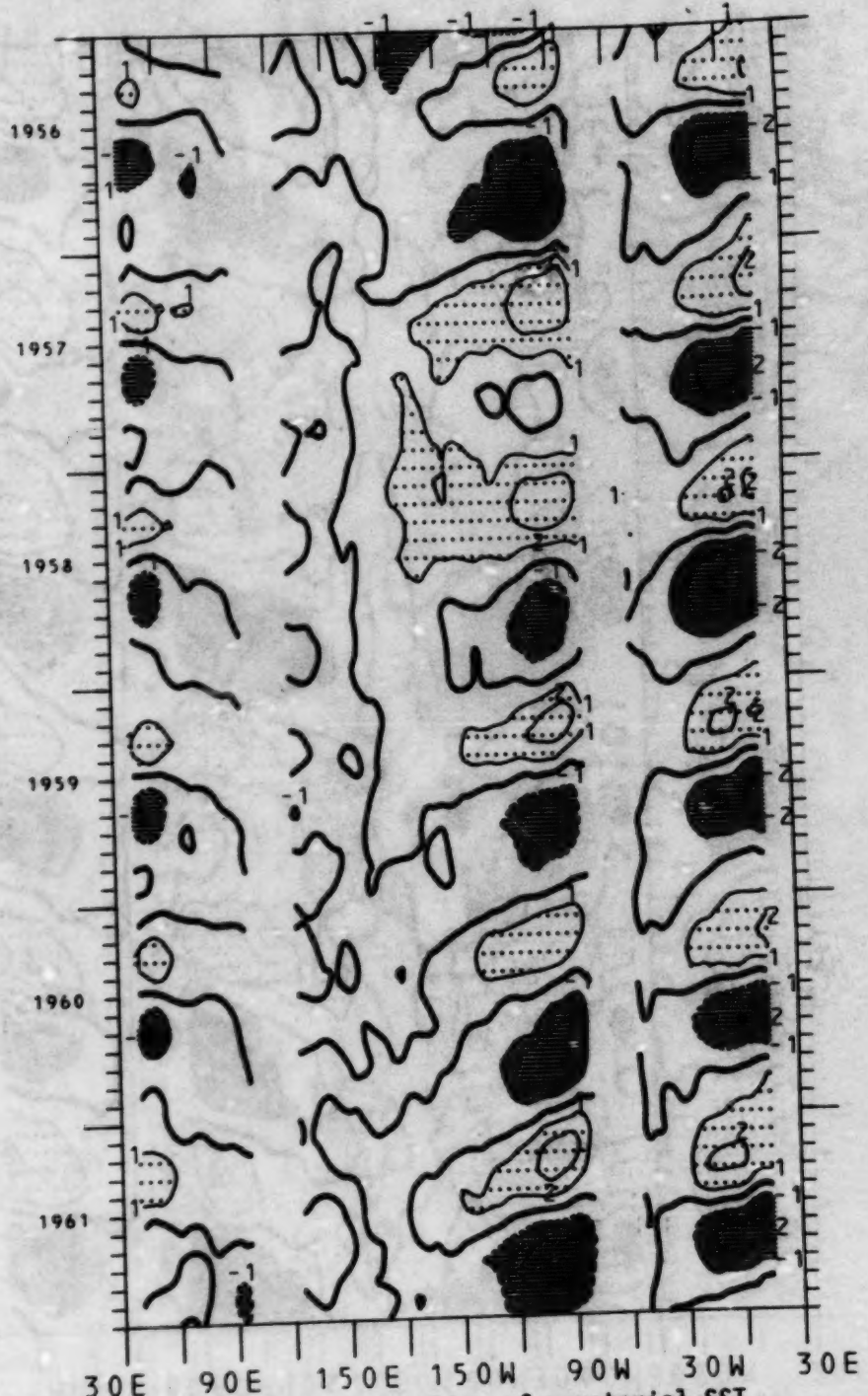

Figure 101. Time-longitude cross-section of equatorial SST expressed as the difference from the annual mean for the years 1956-1961. The contour interval is 1.0°C. The zero isotherm is emphasized. Negative values are dashed. Light shading is greater than 1.0°C; dark shading is less than -1.0°C.

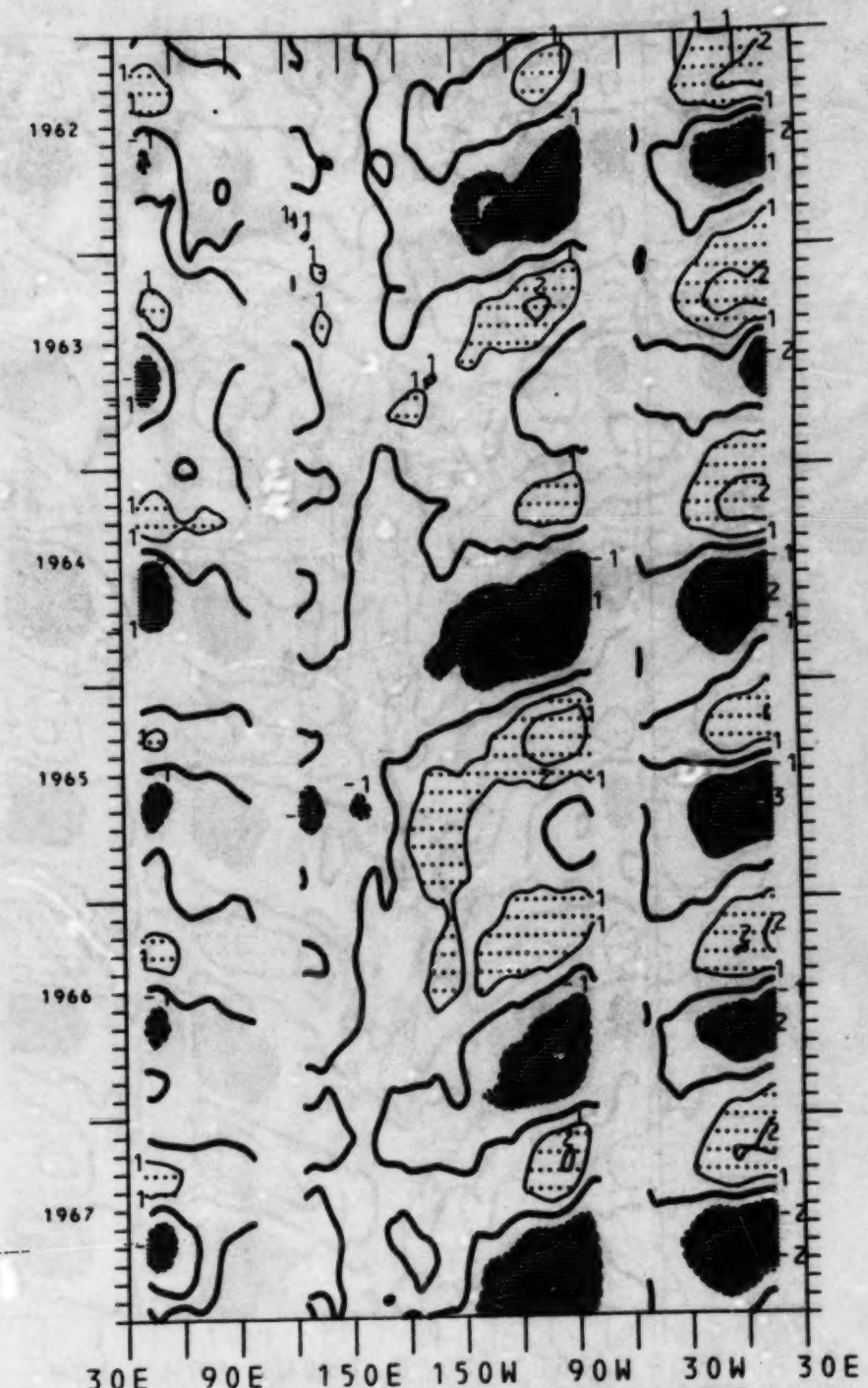

Figure 102. Time-longitude cross-section of equatorial SST expressed as the difference from the annual mean for the years 1962-1967. The contour interval is 1.0°C. The zero isotherm is emphasized. Negative values are dashed. Light shading is greater than 1.0°C; dark shading is less than -1.0°C.

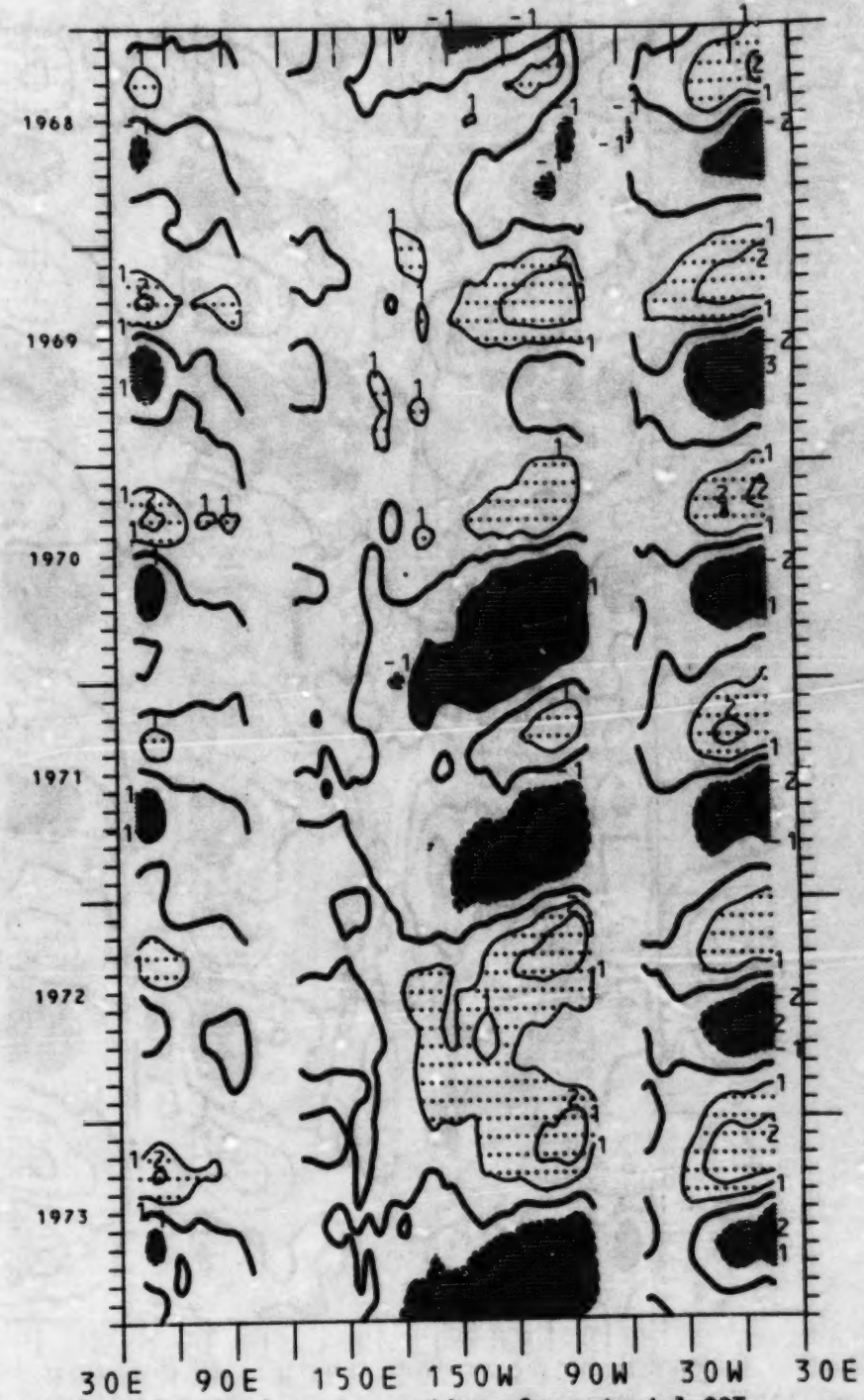

Figure 103. Time-longitude cross-section of equatorial SST expressed as the difference from the annual mean for the years 1968-1973. The contour interval is 1.0°C. The zero isotherm is emphasized. Negative values are dashed. Light shading is greater than 1.0°C; dark shading is less than -1.0°C.

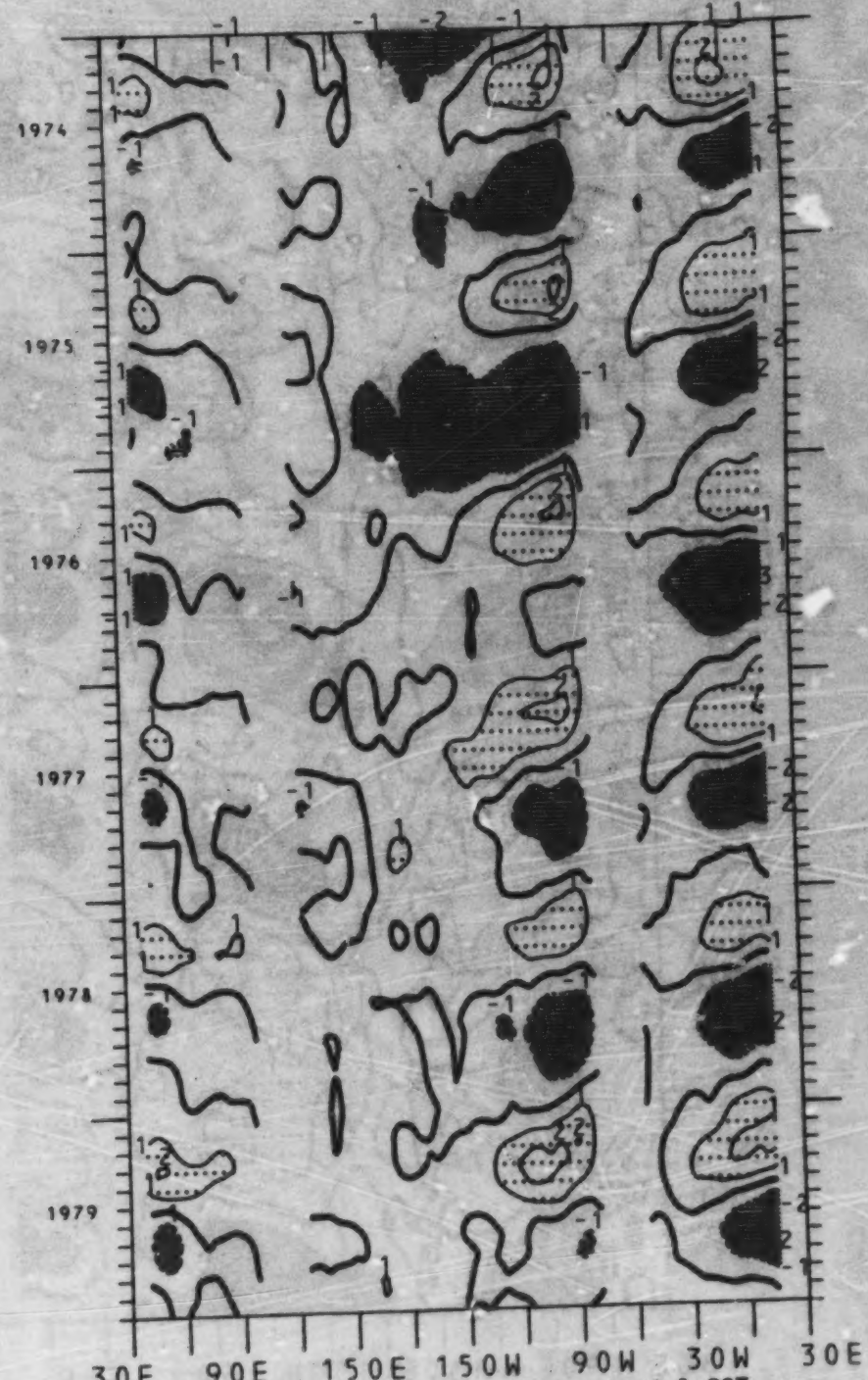

Figure 104. Time-longitude cross-section of equatorial SST expressed as the difference from the annual mean for the years 1974-1979. The contour interval is 1.0°C. The zero isotherm is emphasized. Negative values are dashed. Light shading is greater than 1.0°C; dark shading is less than -1.0°C.

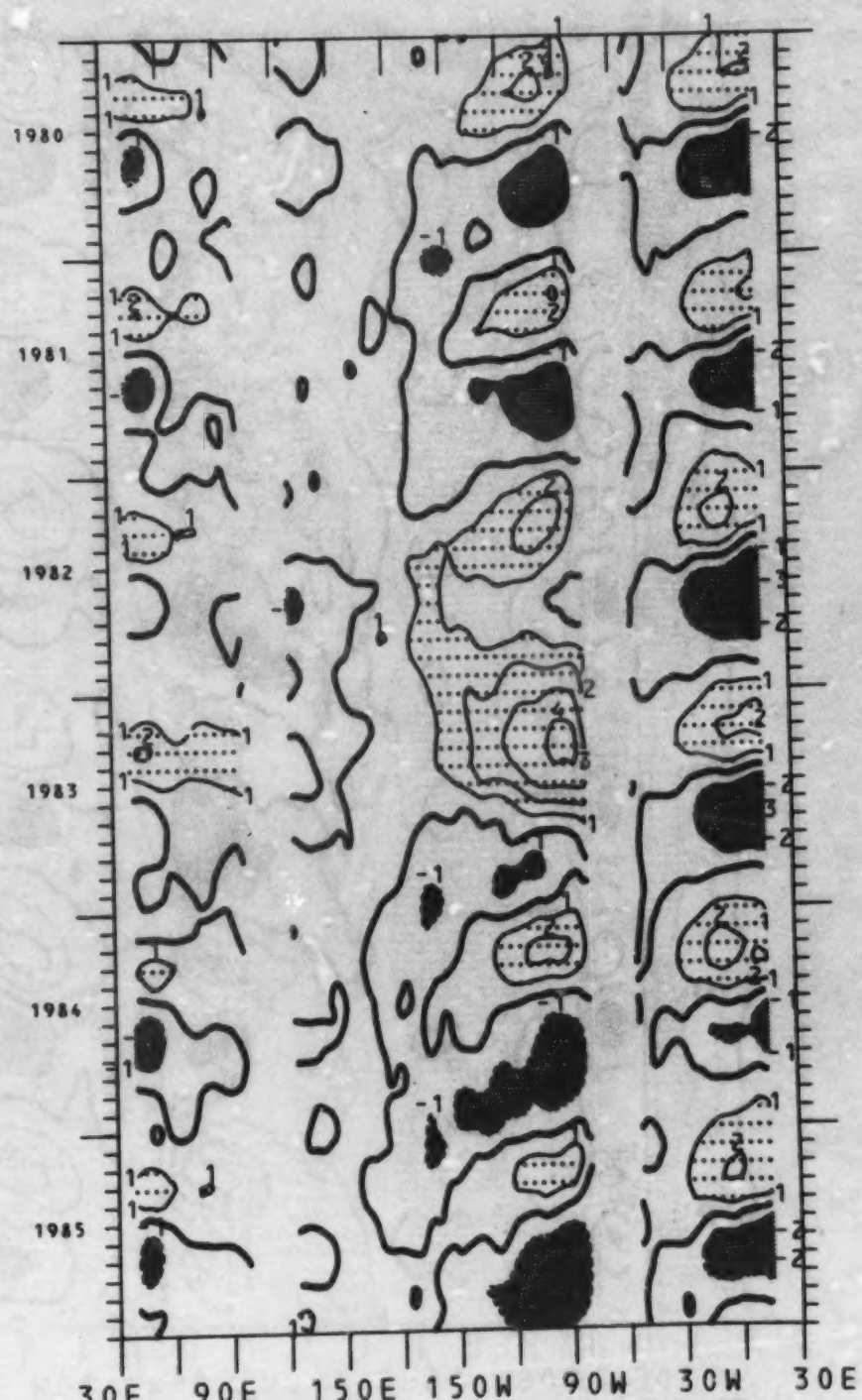

Figure 105. Time-longitude cross-section of equatorial SST expressed as the difference from the annual mean for the years 1980-1985. The contour interval is 1.0°C. The zero isotherm is emphasized. Negative values are dashed. Light shading is greater than 1.0°C; dark shading is less than -1.0°C.

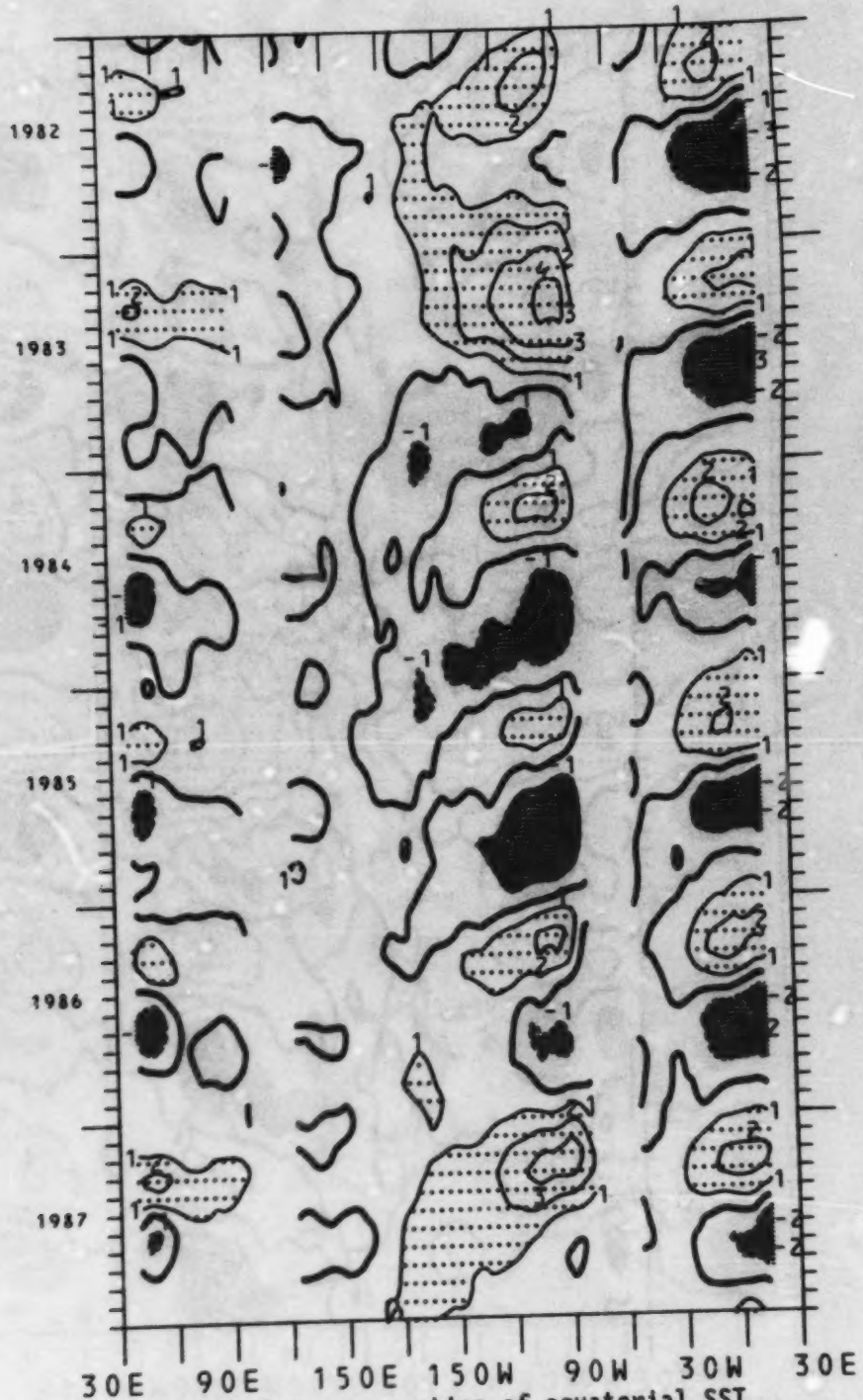

Figure 106. Time-longitude cross-section of equatorial SST expressed as the difference from the annual mean for the years 1982-1987. The contour interval is 1.0°C. The zero isotherm is emphasized. Negative values are dashed. Light shading is greater than 1.0°C; dark shading is less than -1.0°C.

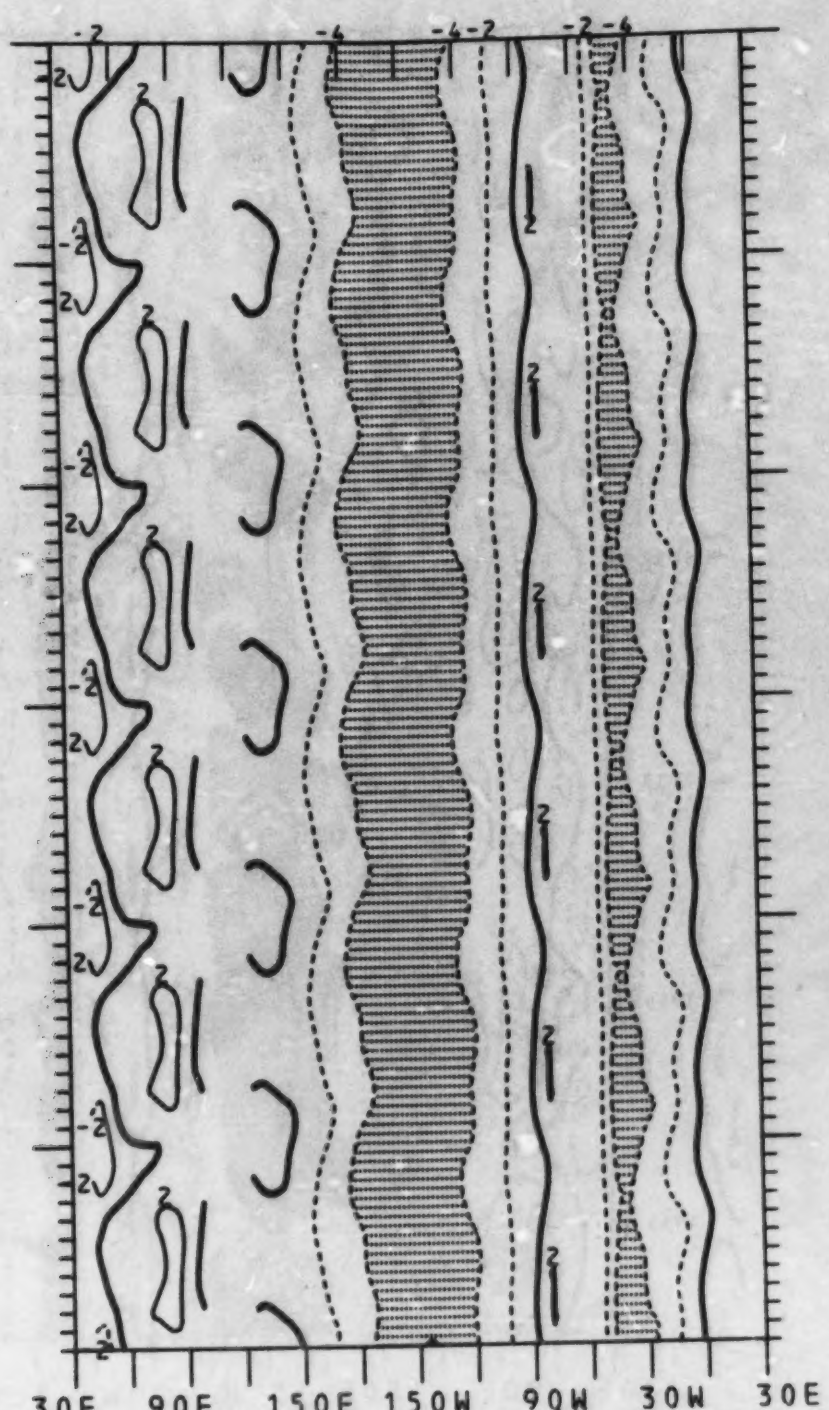

Figure 107. Time-longitude cross-section of the mean equatorial zonal wind component based on the period 1950-1979. The contour interval is 2.0 m/s. The zero isotherm is emphasized. Negative values (easterlies) are dashed. Values less than -4.0 m/s are shaded.

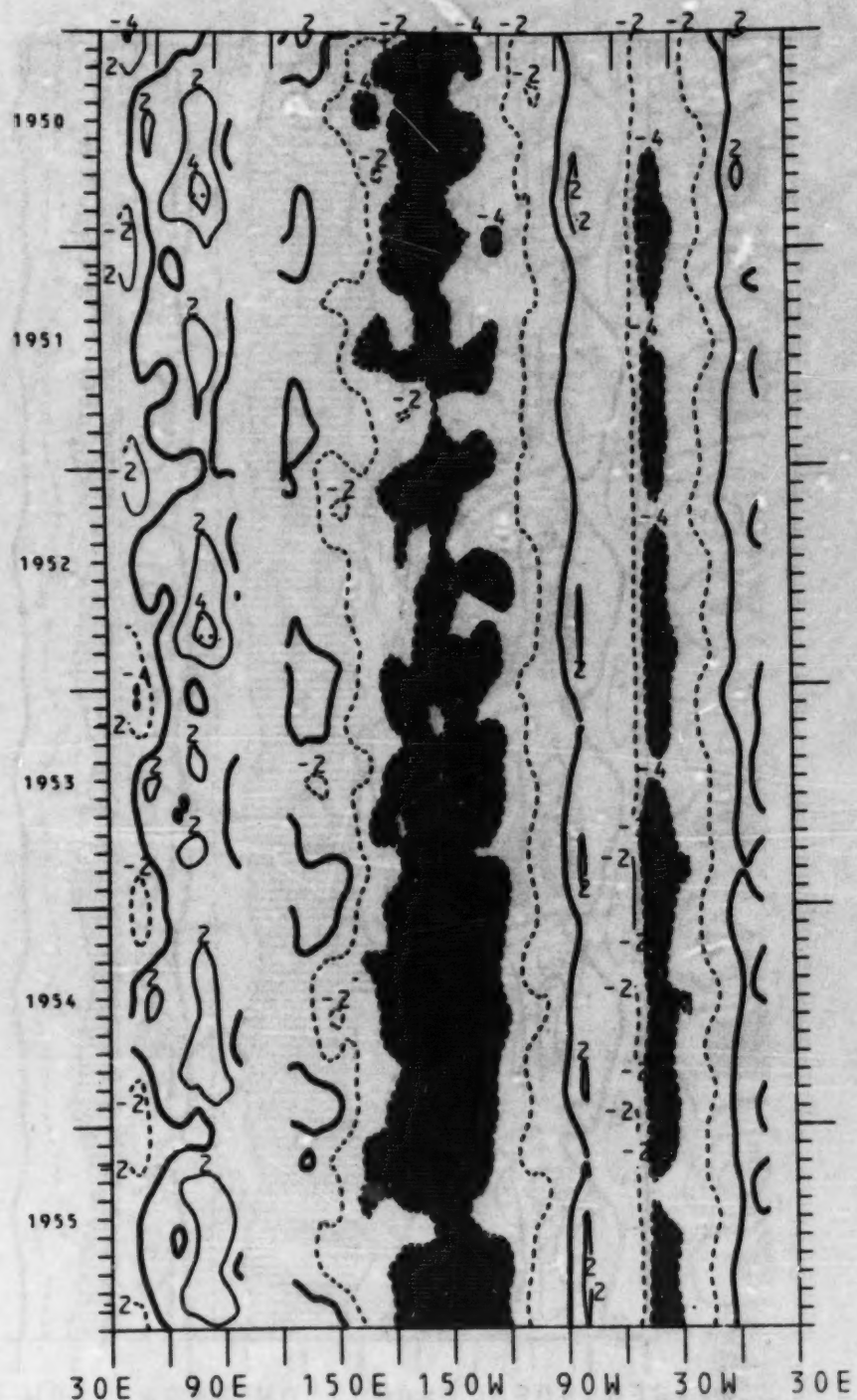

Figure 108. Time-longitude cross-section of the mean monthly equatorial zonal wind component for the years 1950-1955. The contour interval is 2.0 m/s. The zero isotherm is emphasized. Negative values (easterlies) are dashed. Light shading is greater than 4.0 m/s; dark shading is less than -4.0 m/s.

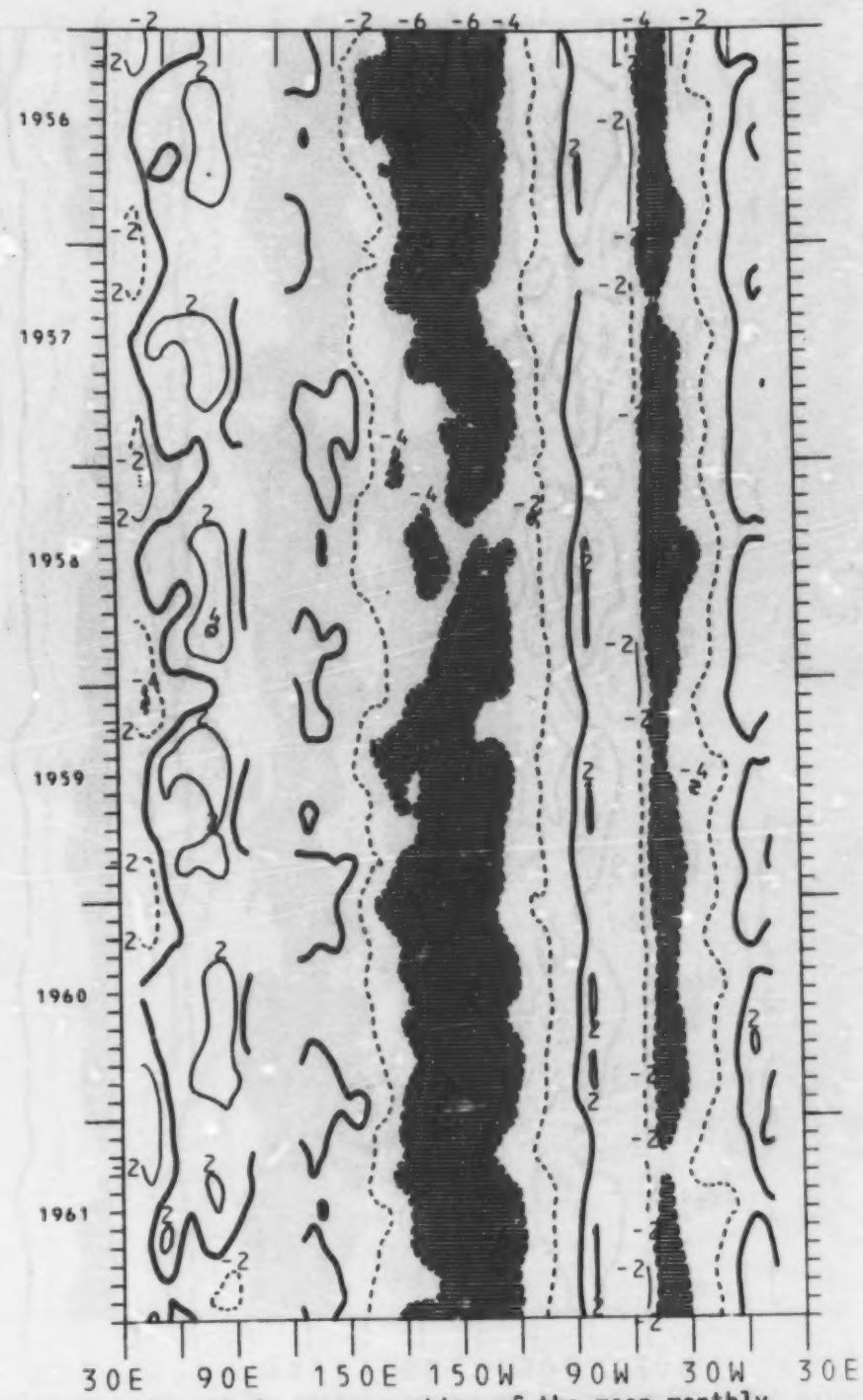

Figure 109. Time-longitude cross-section of the mean monthly equatorial zonal wind component for the years 1956-1961. The contour interval is 2.0 m/s. The zero isotherm is emphasized. Negative values (easterlies) are dashed. Light shading is greater than 4.0 m/s; dark shading is less than -4.0 m/s.

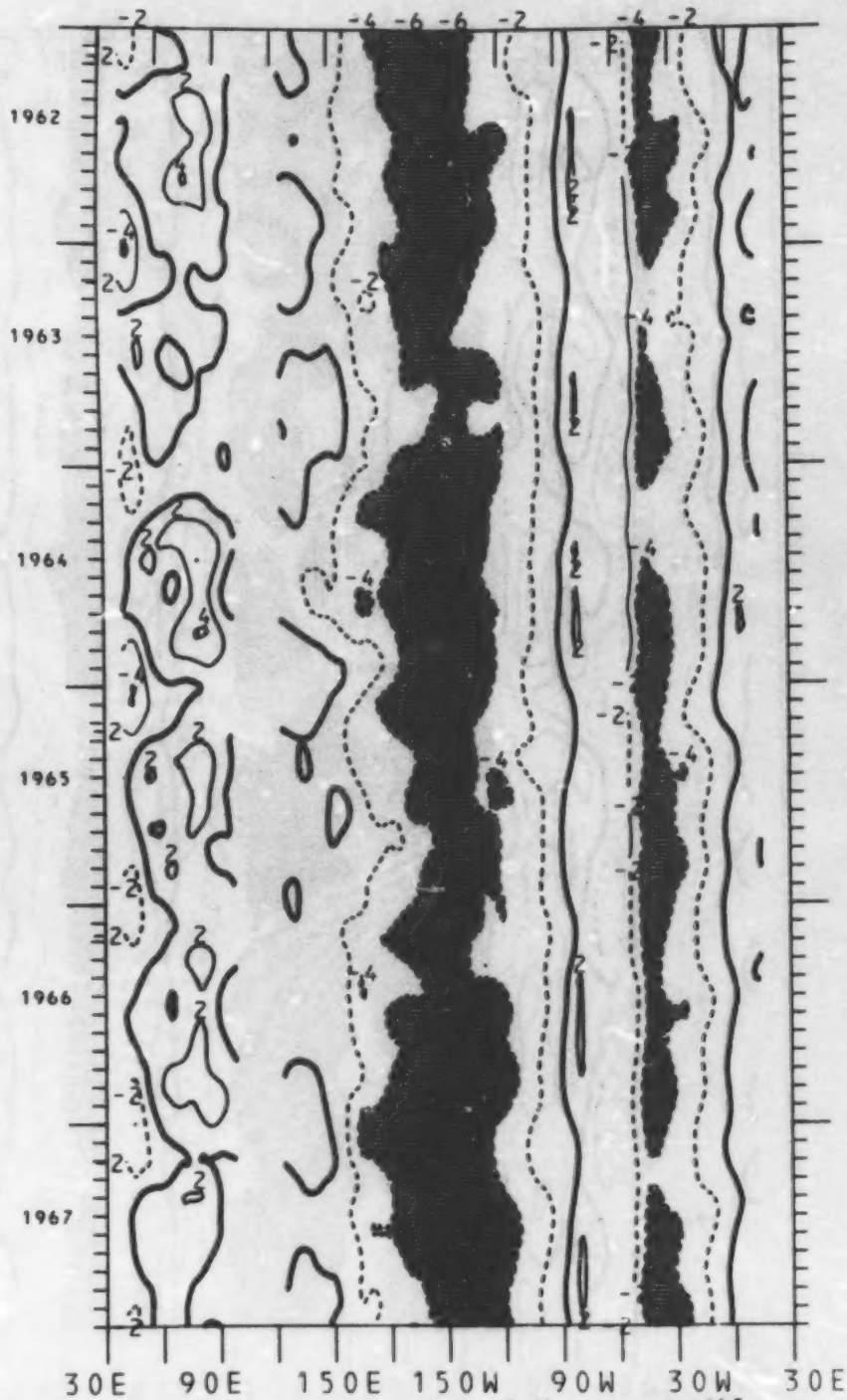

Figure 110. Time-longitude cross-section of the mean monthly equatorial zonal wind component for the years 1962-1967. The contour interval is 2.0 m/s. The zero isotherm is emphasized. Negative values (easterlies) are dashed. Light shading is greater than 4.0 m/s; dark shading is less than -4.0 m/s.

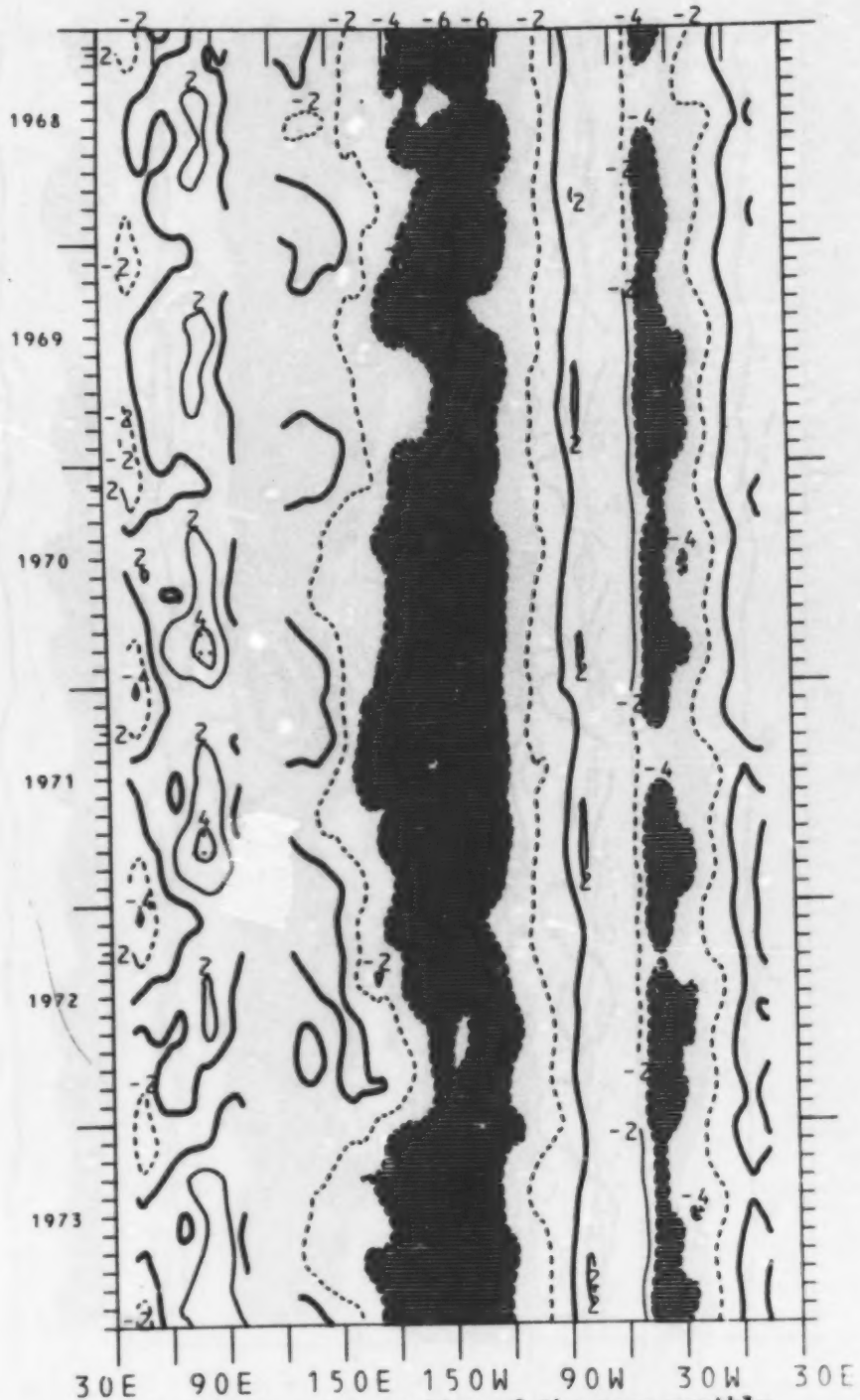

Figure 111. Time-longitude cross-section of the mean monthly equatorial zonal wind component for the years 1968-1973. The contour interval is 2.0 m/s. The zero isotherm is emphasized. Negative values (easterlies) are dashed. Light shading is greater than 4.0 m/s; dark shading is less than -4.0 m/s.

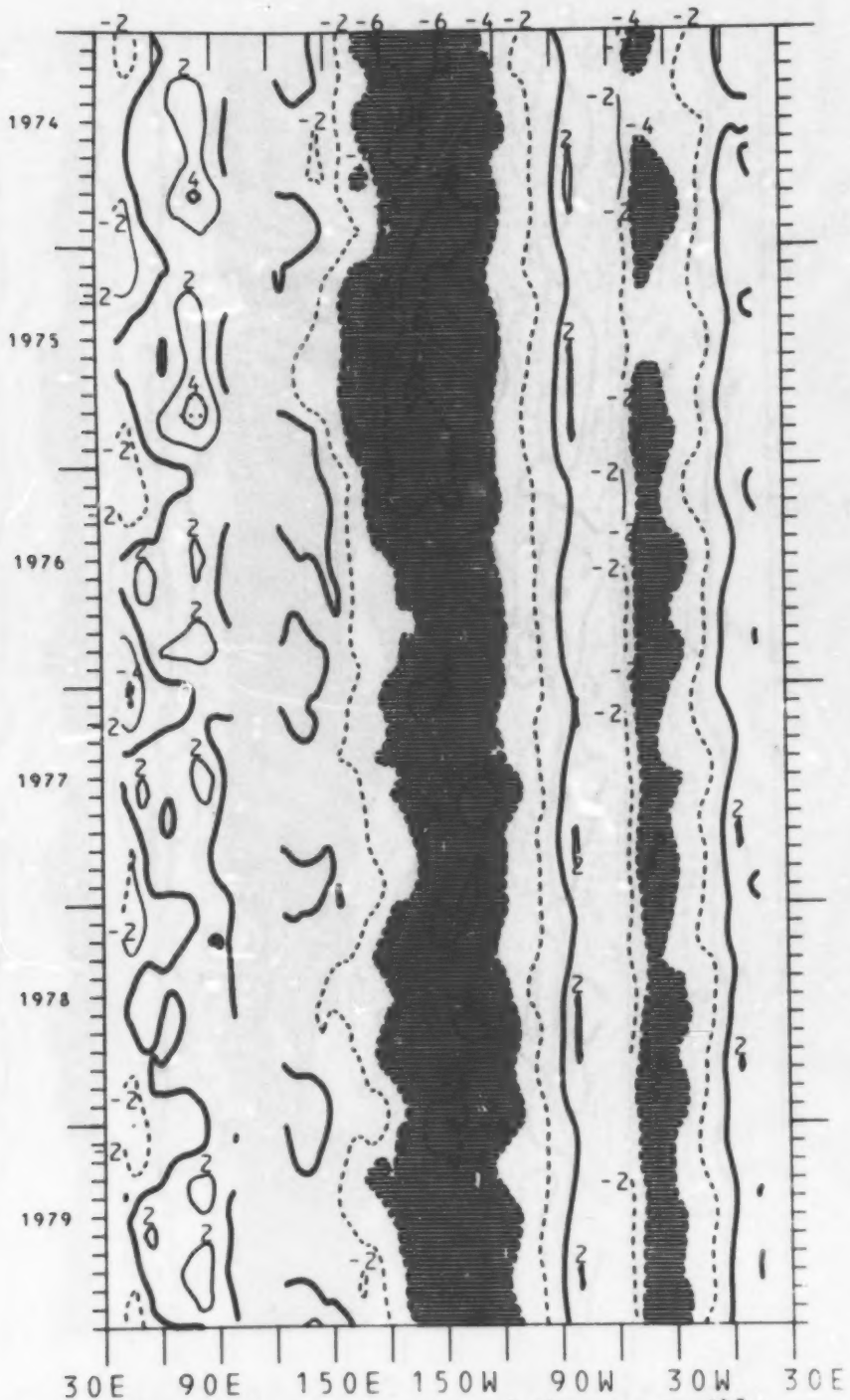

Figure 112. Time-longitude cross-section of the mean monthly equatorial zonal wind component for the years 1974-1979. The contour interval is 2.0 m/s. The zero isotherm is emphasized. Negative values (easterlies) are dashed. Light shading is greater than 4.0 m/s; dark shading is less than -4.0 m/s.

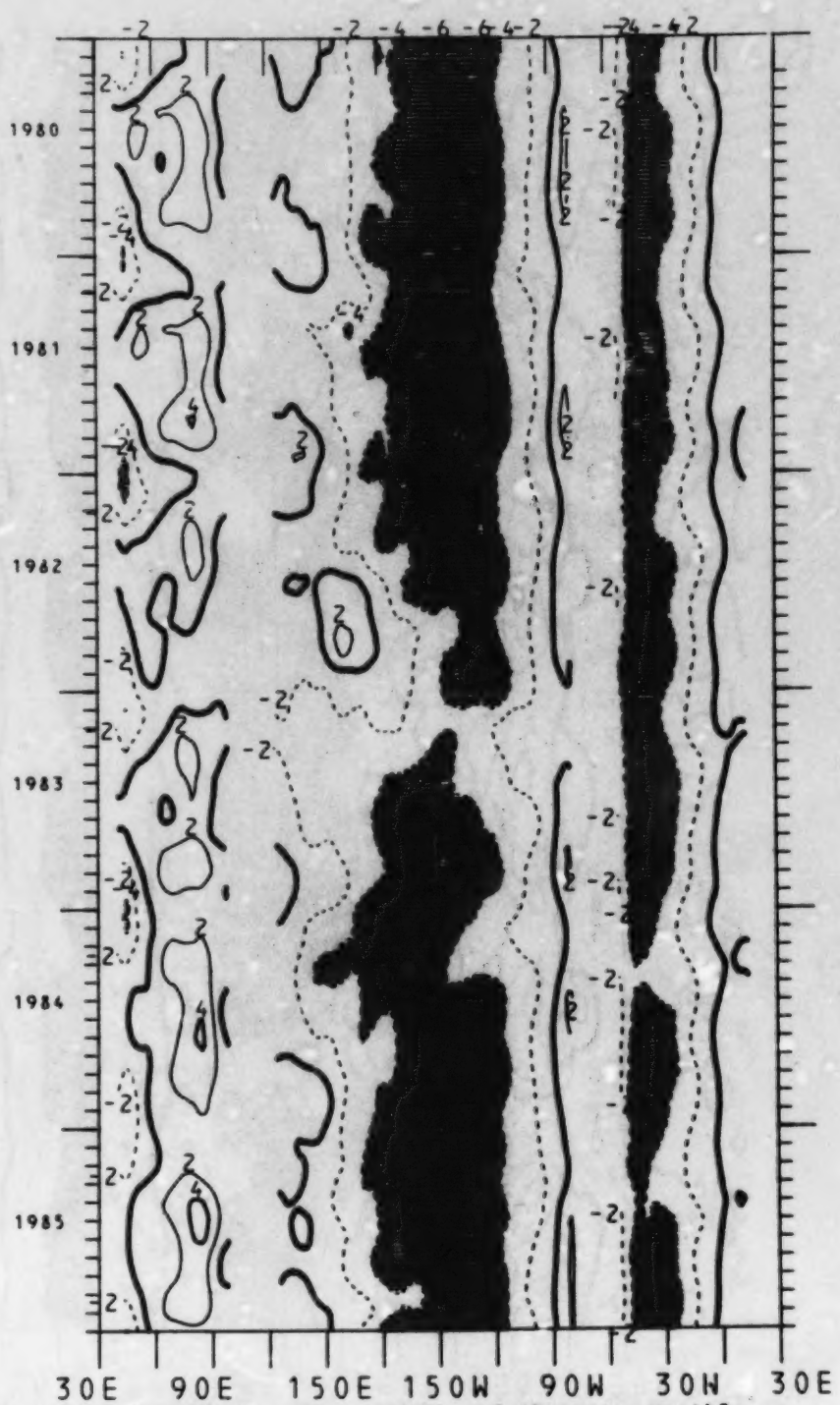

Figure 113. Time-longitude cross-section of the mean monthly equatorial zonal wind component for the years 1980-1985. The contour interval is 2.0 m/s. The zero isotherm is emphasized. Negative values (easterlies) are dashed. Light shading is greater than 4.0 m/s; dark shading is less than -4.0 m/s.

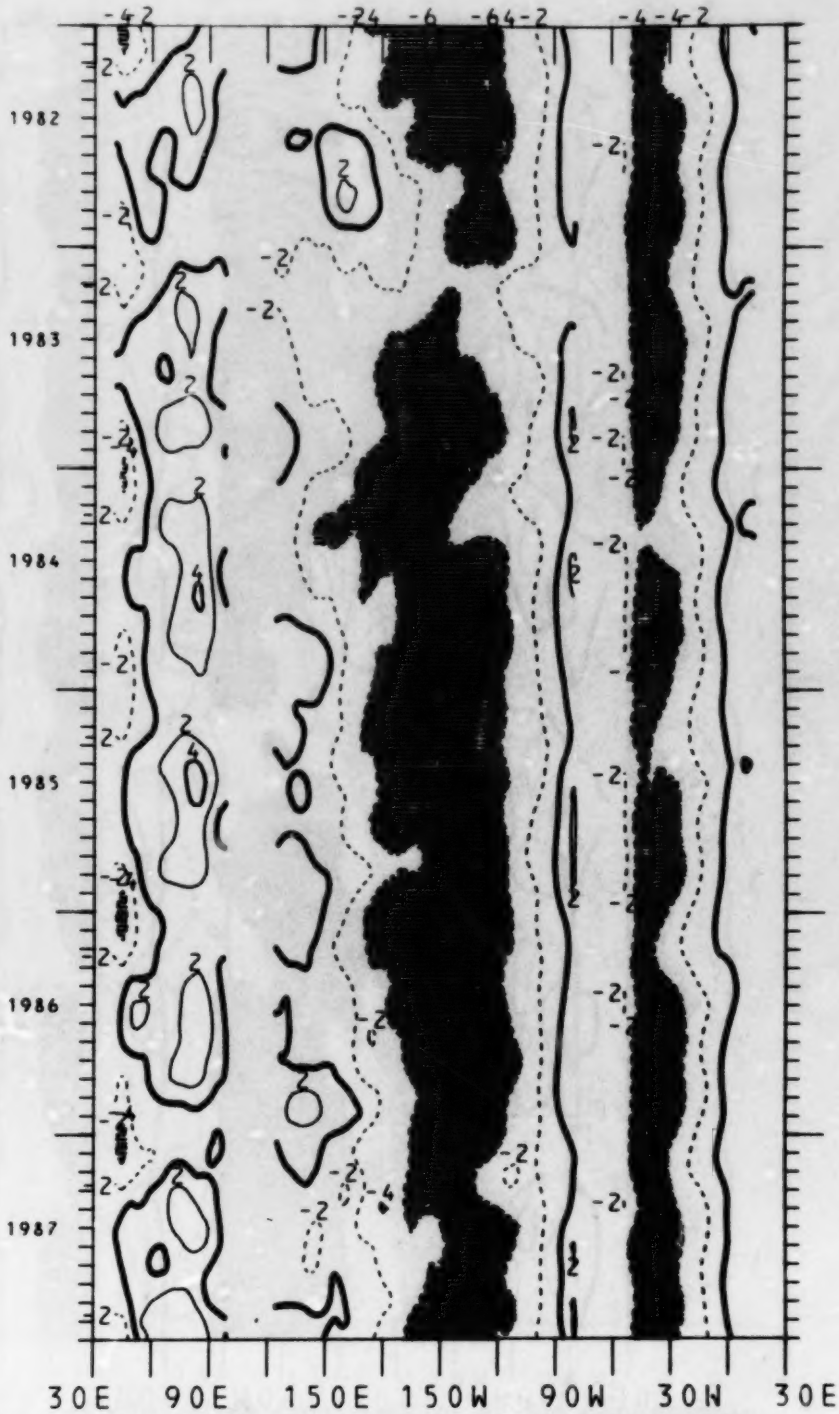

Figure 114. Time-longitude cross-section of the mean monthly equatorial zonal wind component for the years 1982-1987. The contour interval is 2.0 m/s. The zero isotherm is emphasized. Negative values (easterlies) are dashed. Light shading is greater than 4.0 m/s; dark shading is less than -4.0 m/s.

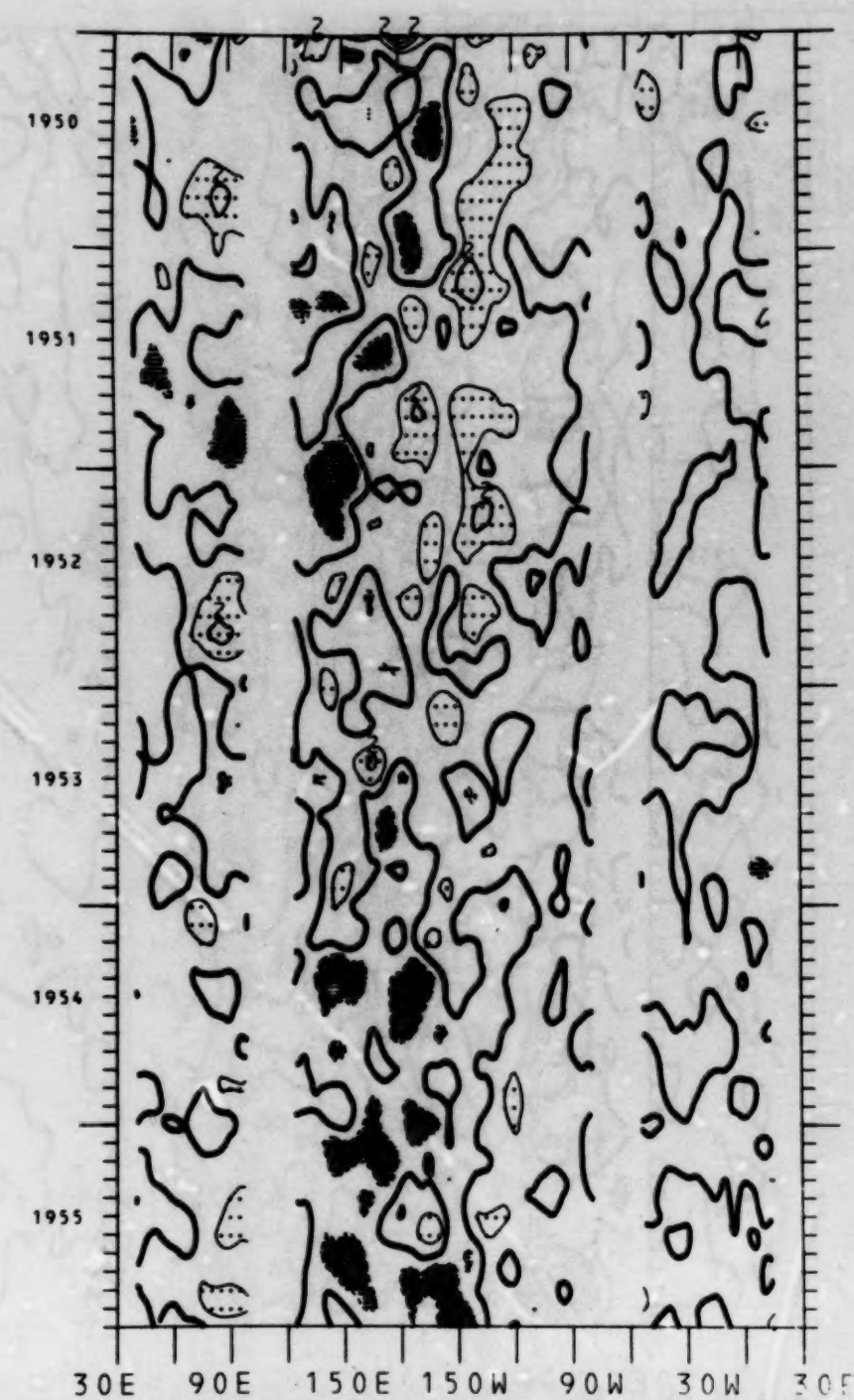

Figure 115. Time-longitude cross-section of equatorial zonal wind component anomalies for the years 1950-1955. The contour interval is 1.0 m/s. The zero isotherm is emphasized. Light shading is greater than 1.0 m/s; dark shading is less than -1.0 m/s.

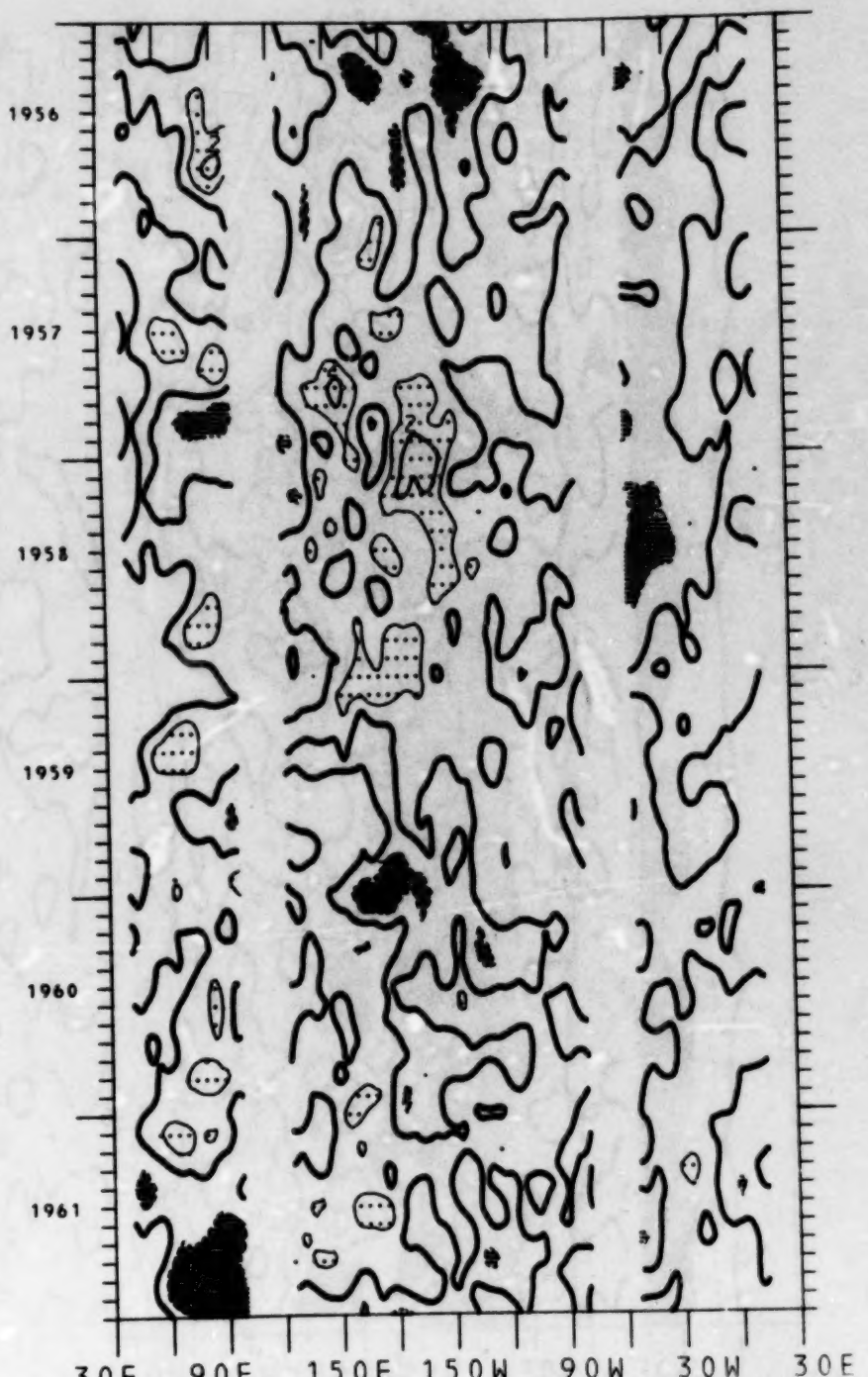

Figure 116. Time-longitude cross-section of equatorial zonal wind component anomalies for the years 1956-1961. The contour interval is 1.0 m/s. The zero isotherm is emphasized. Light shading is greater than 1.0 m/s; dark shading is less than -1.0 m/s.

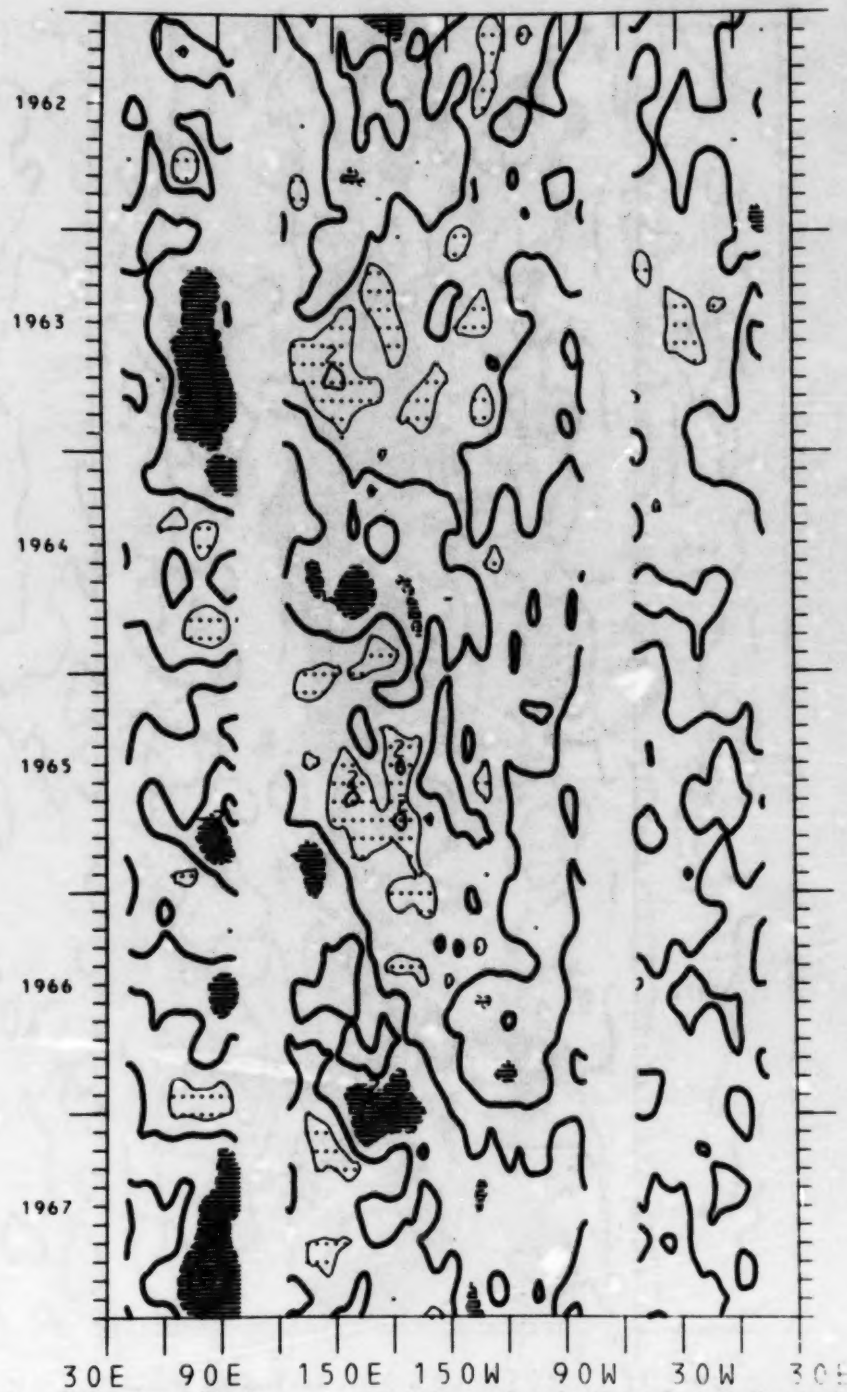

Figure 117. Time-longitude cross-section of equatorial zonal wind component anomalies for the years 1962-1967. The contour interval is 1.0 m/s. The zero isotherm is emphasized. Light shading is greater than 1.0 m/s; dark shading is less than -1.0 m/s.

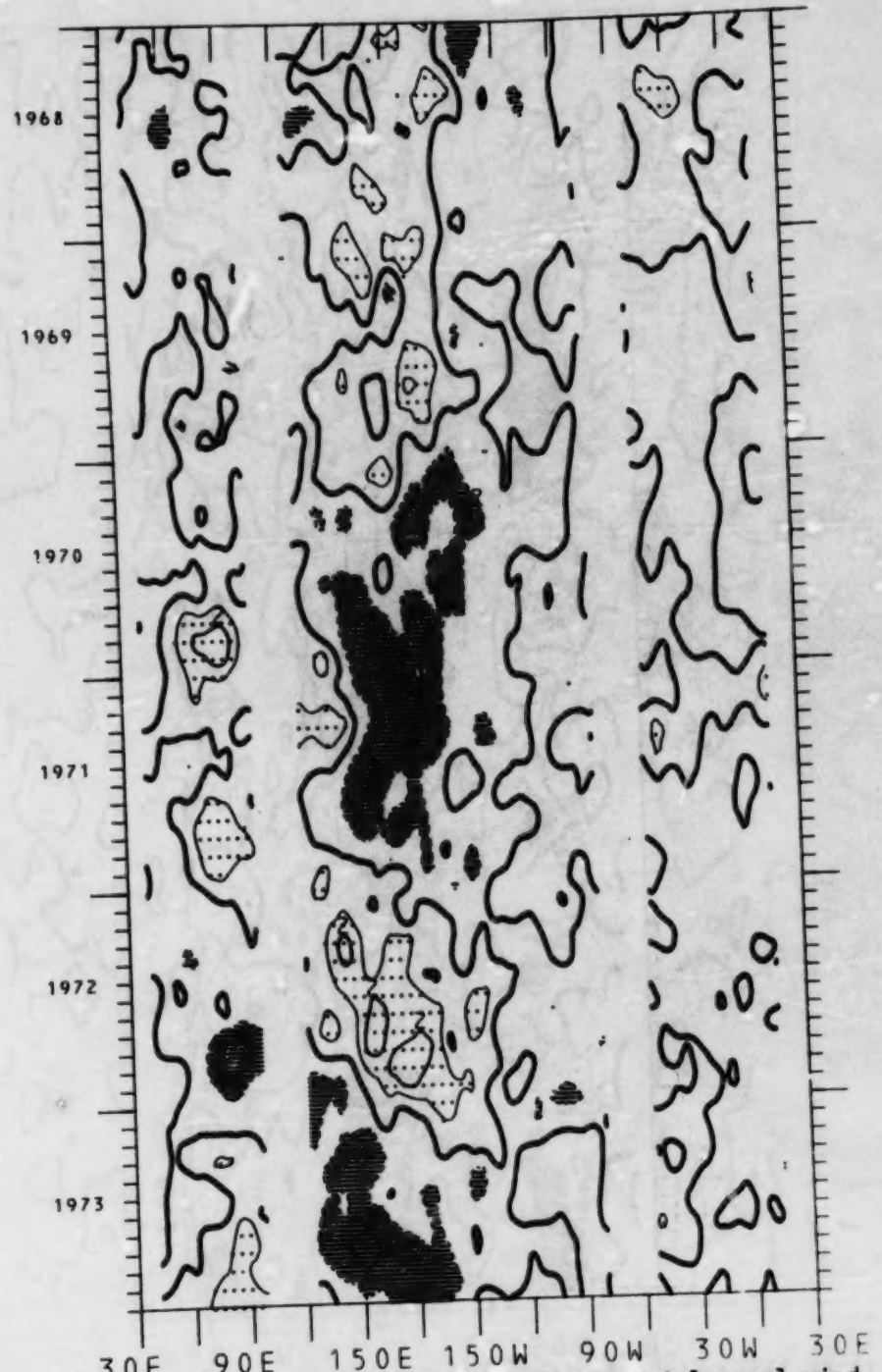

Figure 118. Time-longitude cross-section of equatorial zonal wind component anomalies for the years 1968-1973. The contour interval is 1.0 m/s. The zero isotherm is emphasized. Light shading is greater than 1.0 m/s; dark shading is less than -1.0 m/s.

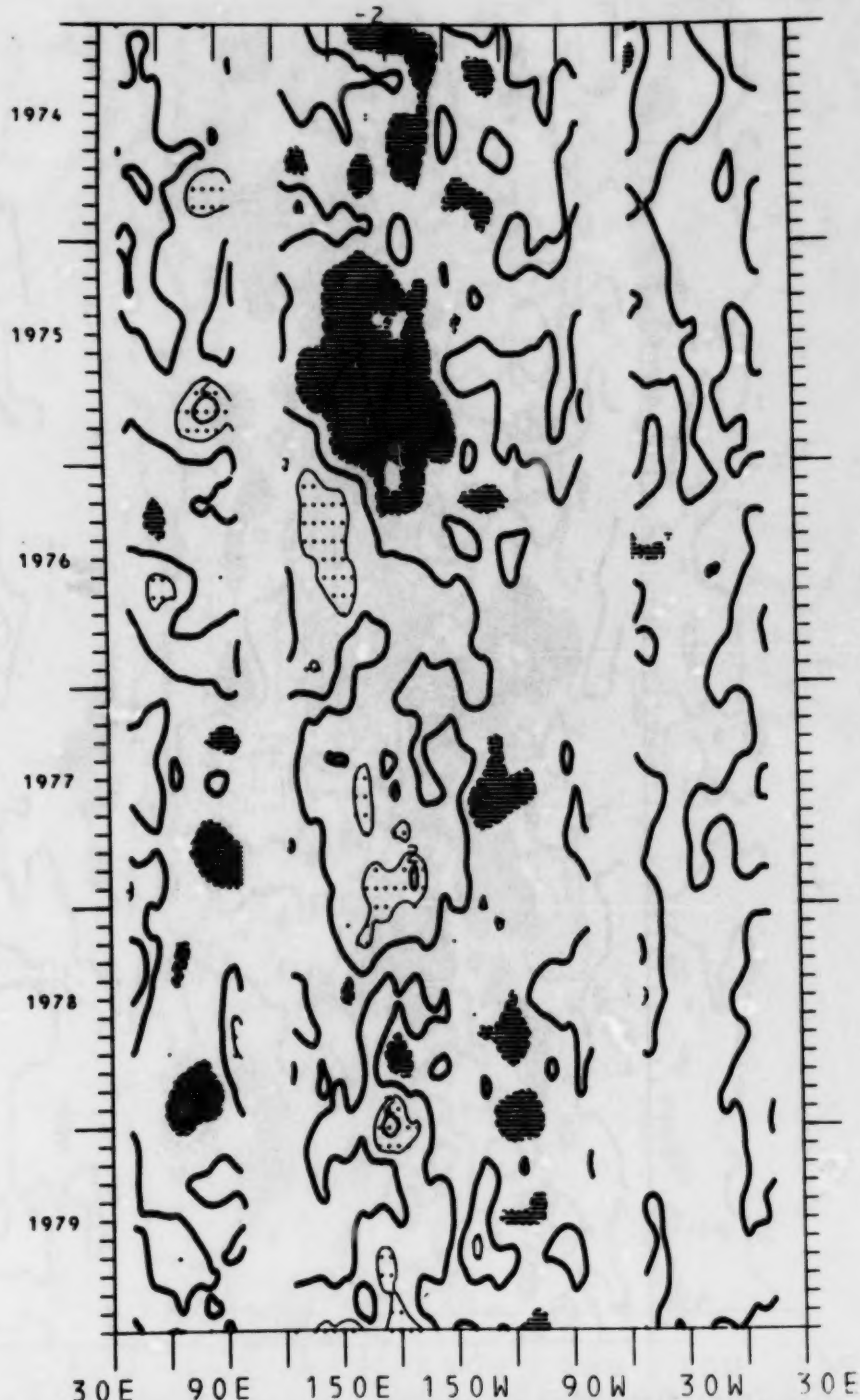

Figure 119. Time-longitude cross-section of equatorial zonal wind component anomalies for the years 1974-1979. The contour interval is 1.0 m/s. The zero isotherm is emphasized. Light shading is greater than 1.0 m/s; dark shading is less than -1.0 m/s.

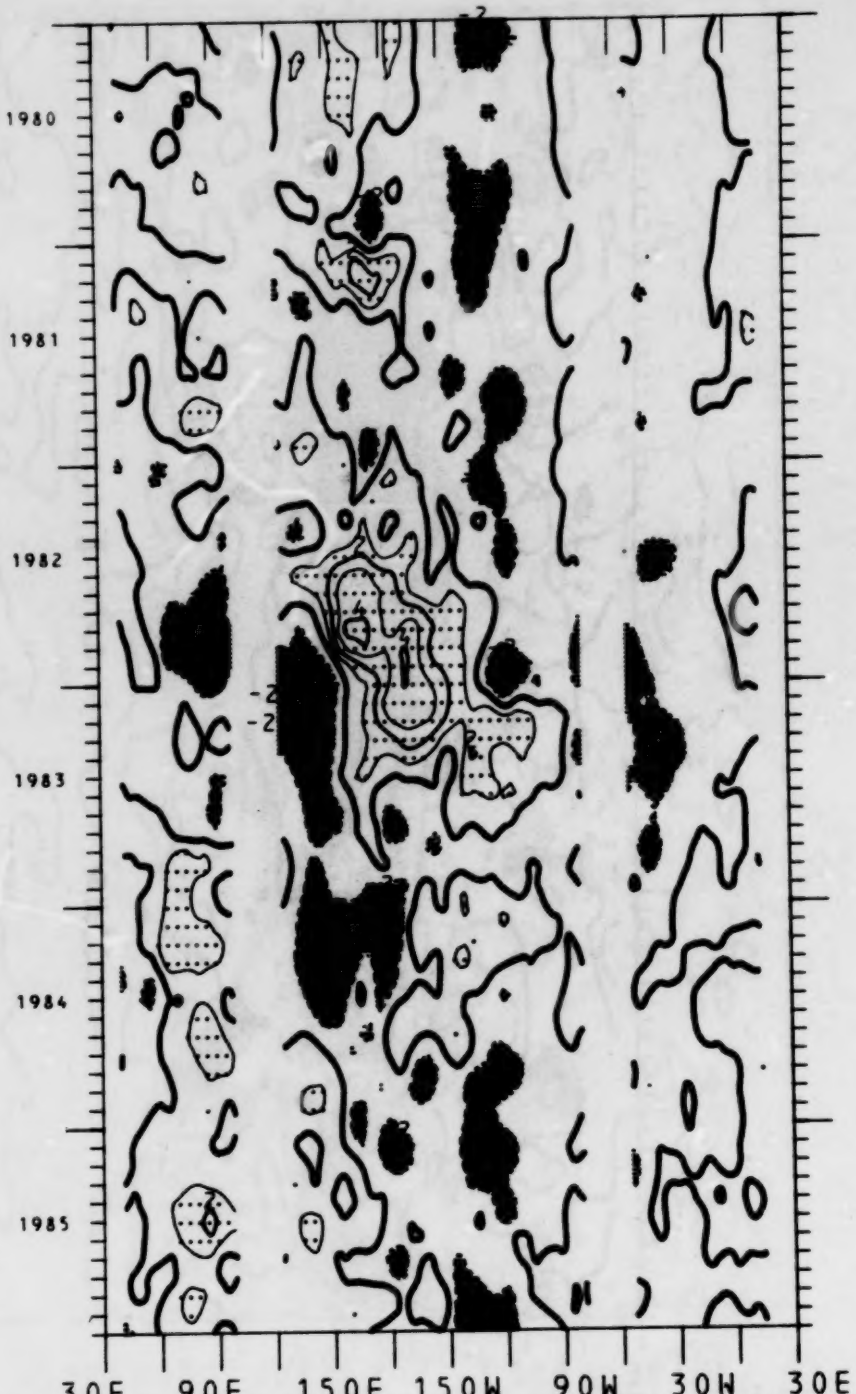

Figure 120. Time-longitude cross-section of equatorial zonal wind component anomalies for the years 1980-1985. The contour interval is 1.0 m/s. The zero isotherm is emphasized. Light shading is greater than 1.0 m/s; dark shading is less than -1.0 m/s.

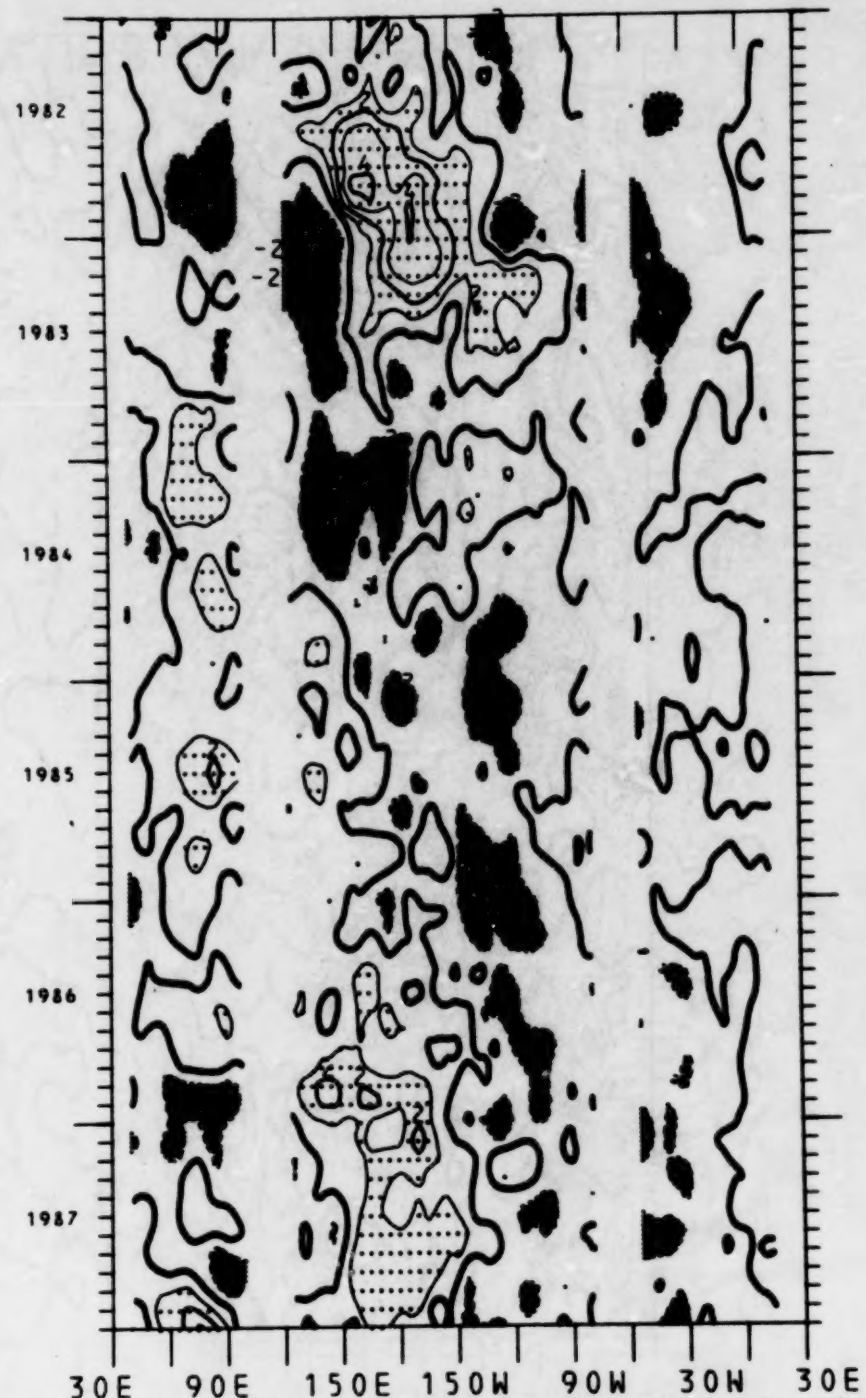

Figure 121. Time-longitude cross-section of equatorial zonal wind component anomalies for the years 1982-1987. The contour interval is 1.0 m/s. The zero isotherm is emphasized. Light shading is greater than 1.0 m/s; dark shading is less than -1.0 m/s.

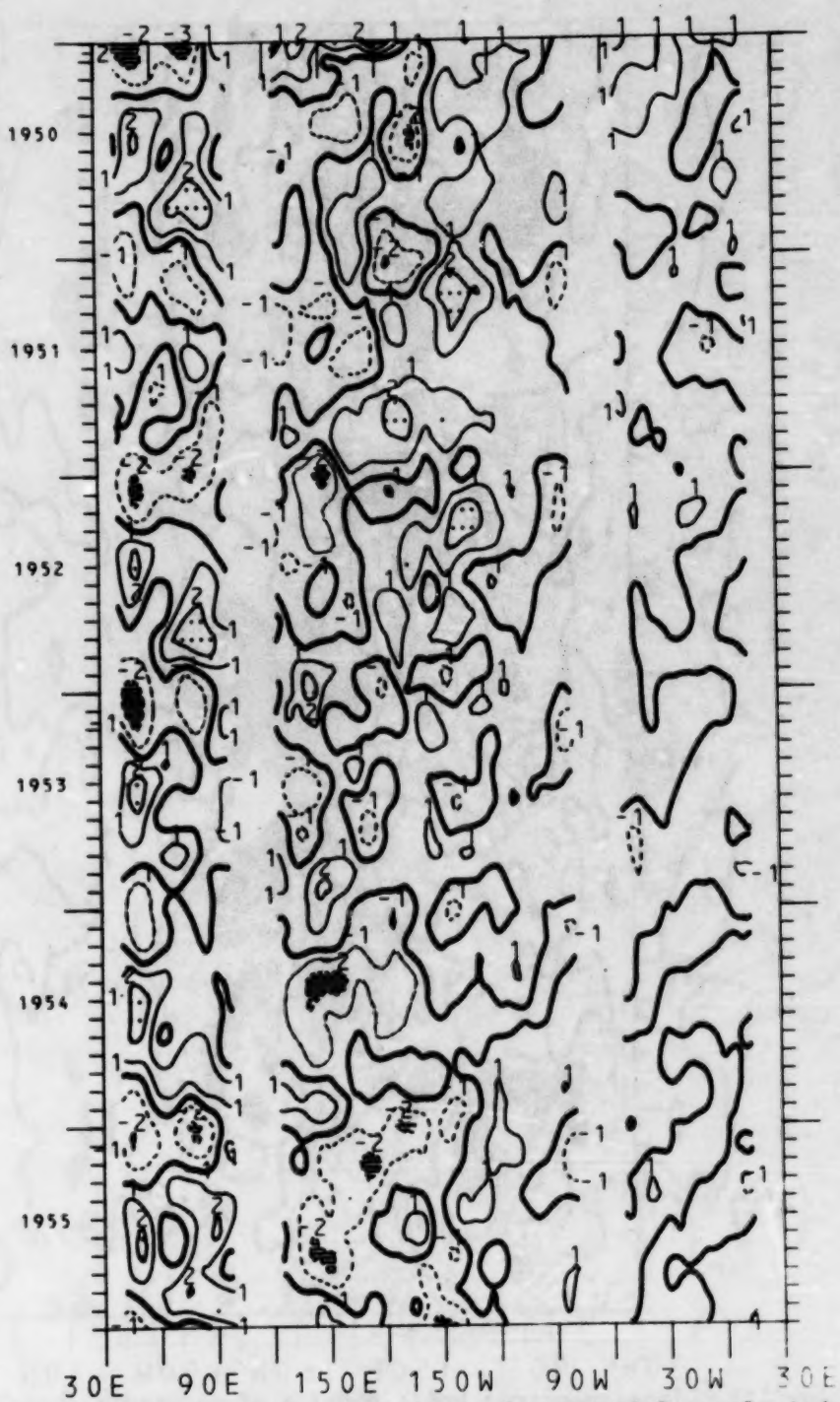

Figure 122. Time-longitude cross-section of equatorial zonal wind component expressed as the difference from the annual mean for the years 1950-1955. The contour interval is 1.0 m/s. The zero isotherm is emphasized. Light shading is greater than 2.0 m/s; dark shading is less than -2.0 m/s.

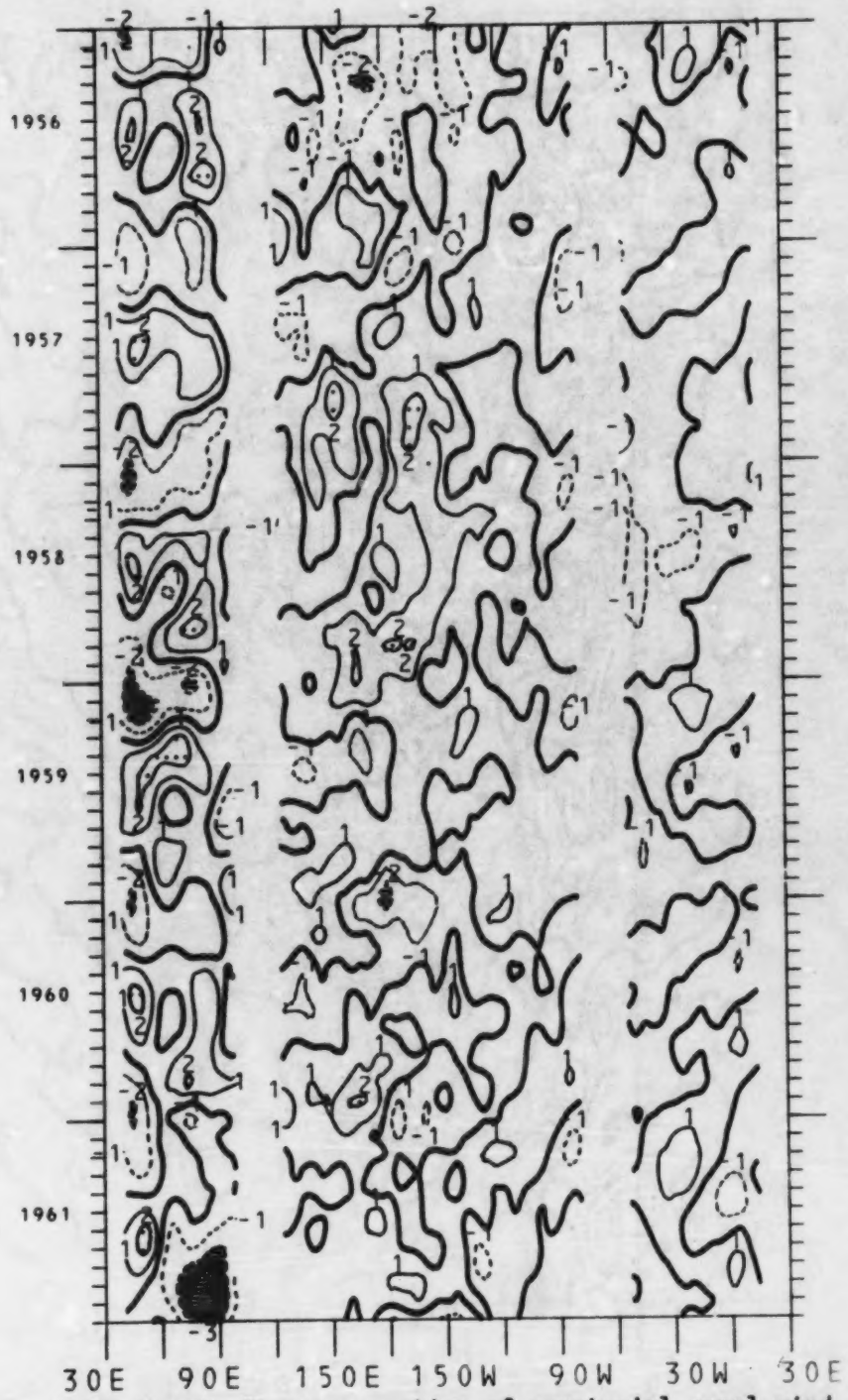

Figure 123. Time-longitude cross-section of equatorial zonal wind component expressed as the difference from the annual mean for the years 1956-1961. The contour interval is 1.0 m/s. The zero isotherm is emphasized. Light shading is greater than 2.0 m/s; dark shading is less than -2.0 m/s.

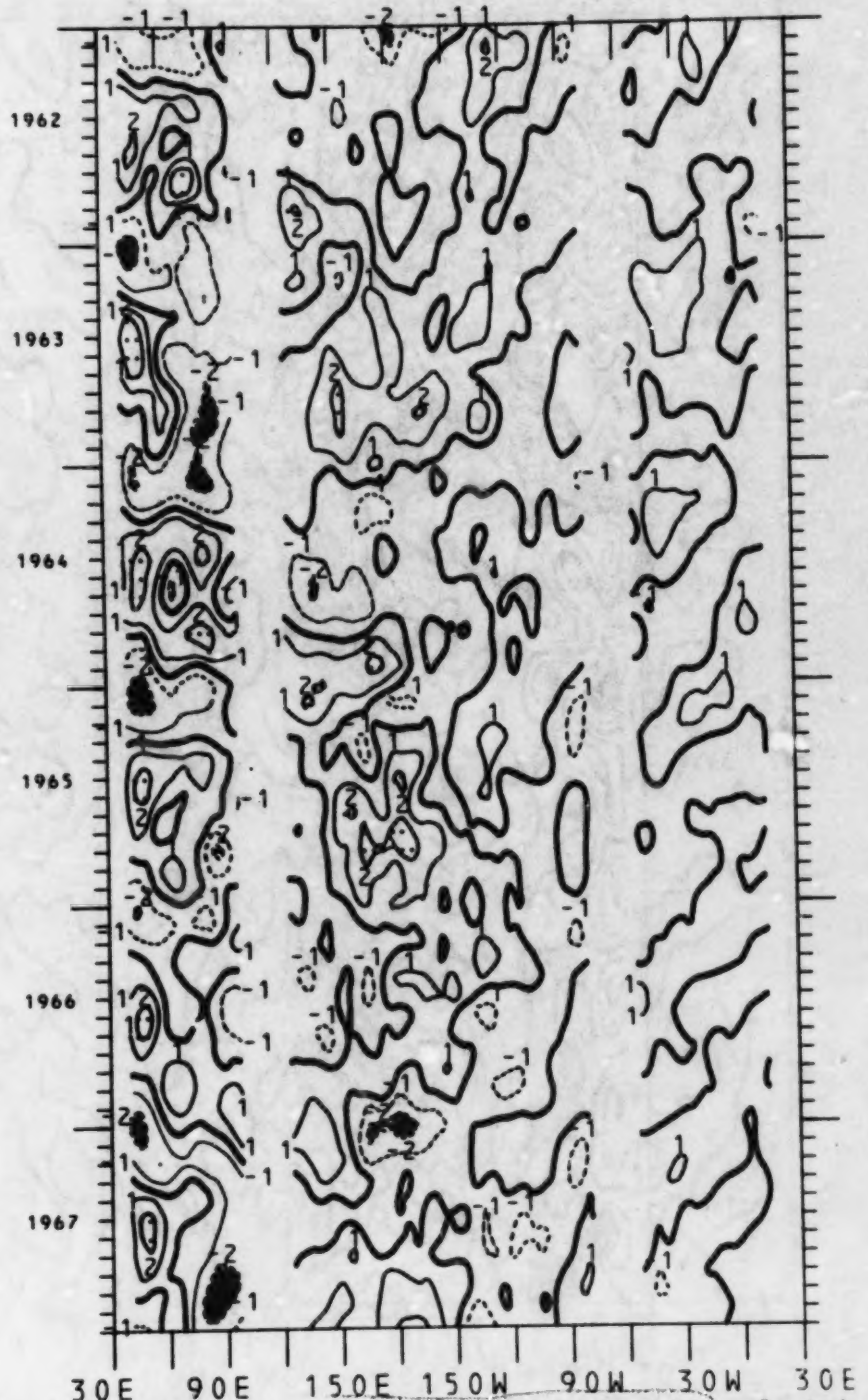

Figure 124. Time-longitude cross-section of equatorial zonal wind component expressed as the difference from the annual mean for the years 1962-1967. The contour interval is 1.0 m/s. The zero isotherm is emphasized. Light shading is greater than 2.0 m/s; dark shading is less than -2.0 m/s.

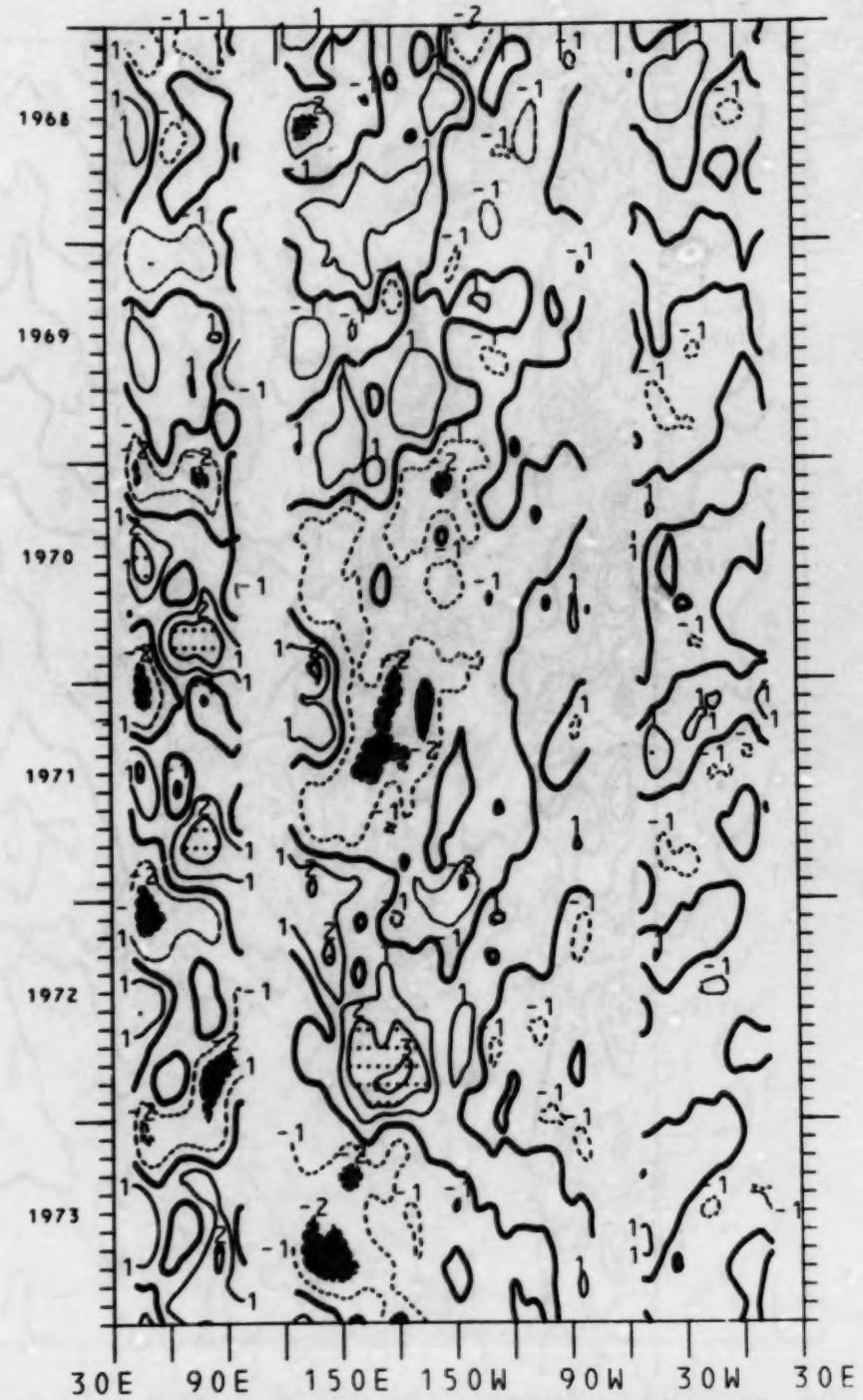

Figure 125. Time-longitude cross-section of equatorial zonal wind component expressed as the difference from the annual mean for the years 1968-1973. The contour interval is 1.0 m/s. The zero isotherm is emphasized. Light shading is greater than 2.0 m/s; dark shading is less than -2.0 m/s.

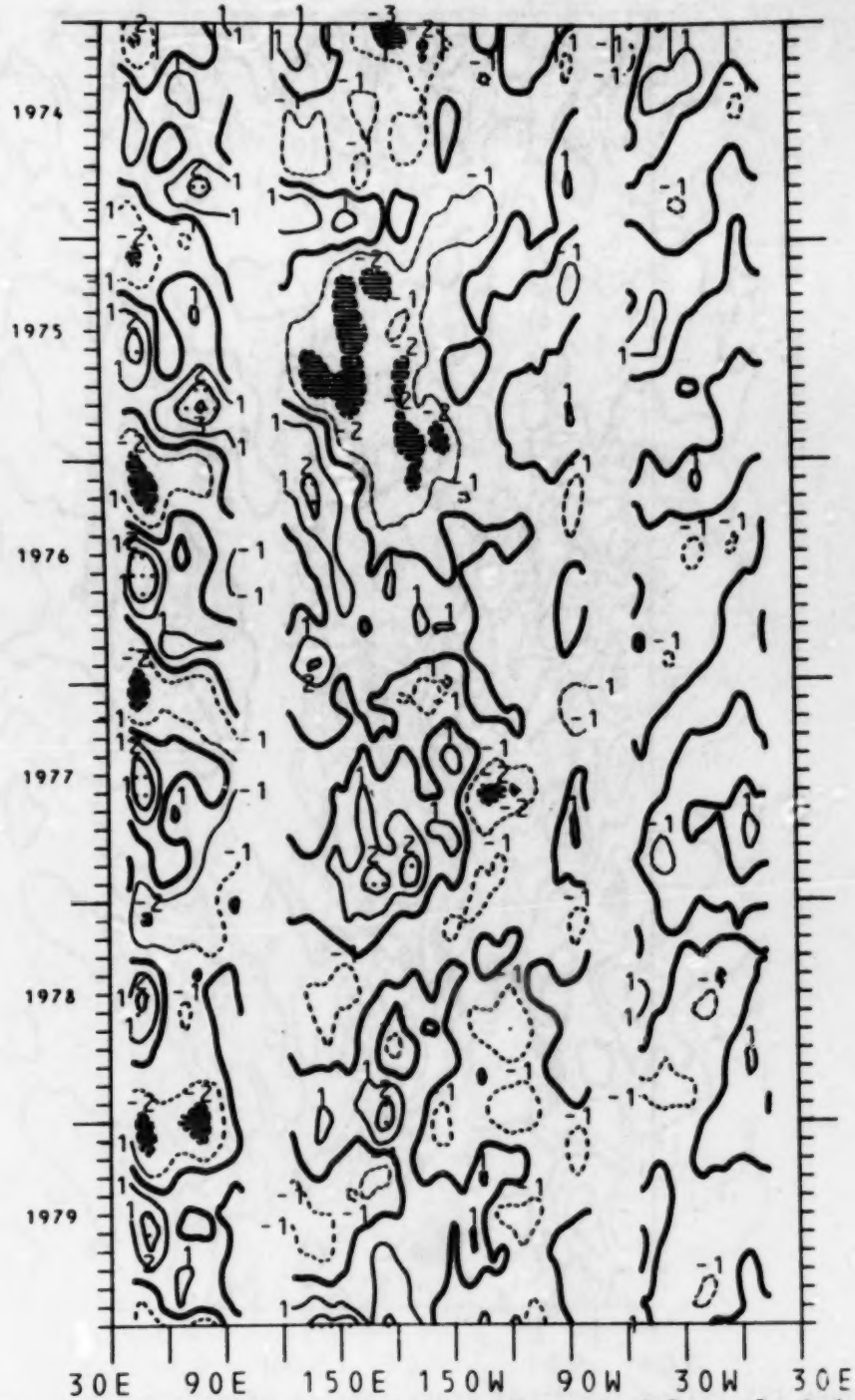

Figure 126. Time-longitude cross-section of equatorial zonal wind component expressed as the difference from the annual mean for the years 1974-1979. The contour interval is 1.0 m/s. The zero isotherm is emphasized. Light shading is greater than 2.0 m/s; dark shading is less than -2.0 m/s.

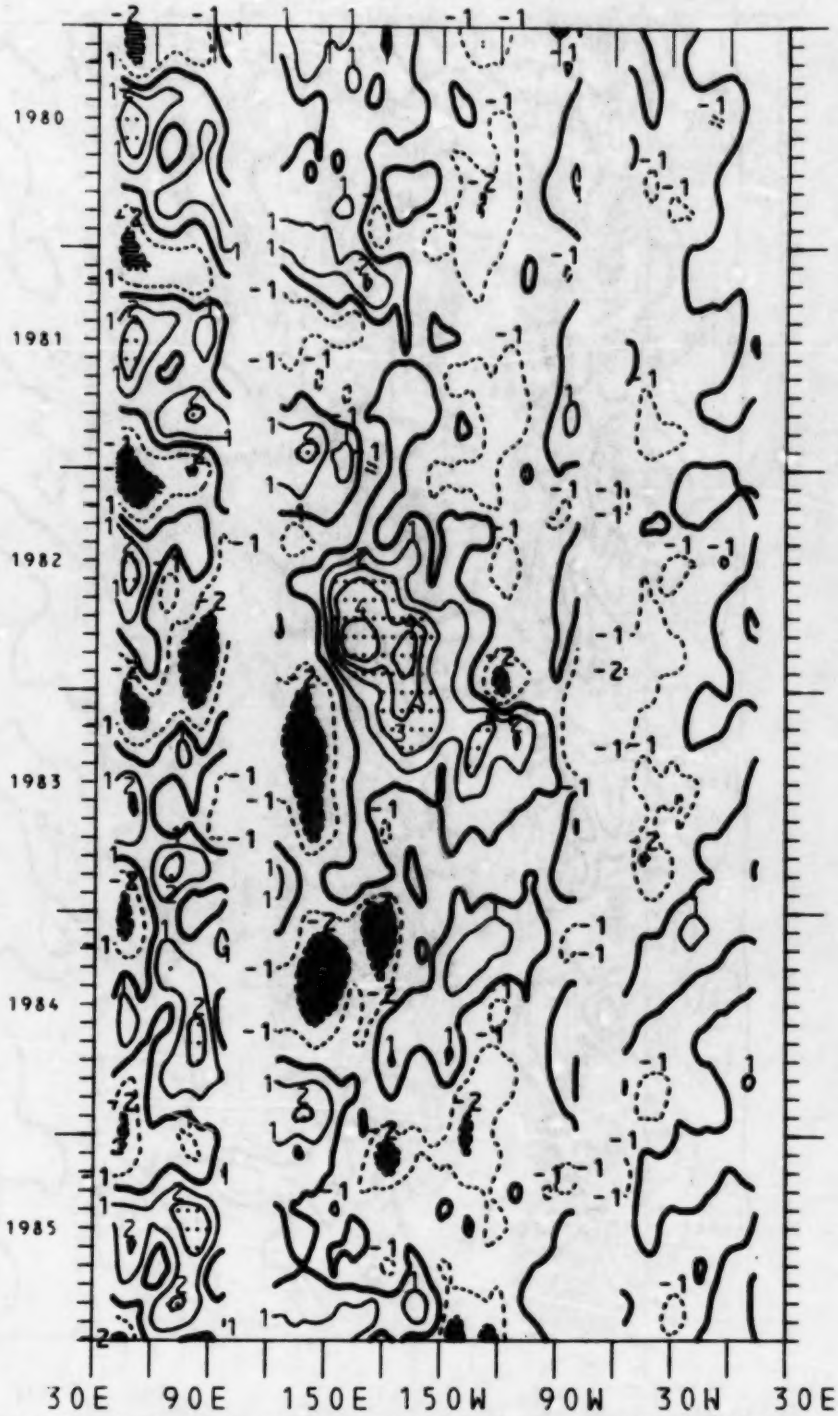

Figure 127. Time-longitude cross-section of equatorial zonal wind component expressed as the difference from the annual mean for the years 1980-1985. The contour interval is 1.0 m/s. The zero isotherm is emphasized. Light shading is greater than 2.0 m/s; dark shading is less than -2.0 m/s.

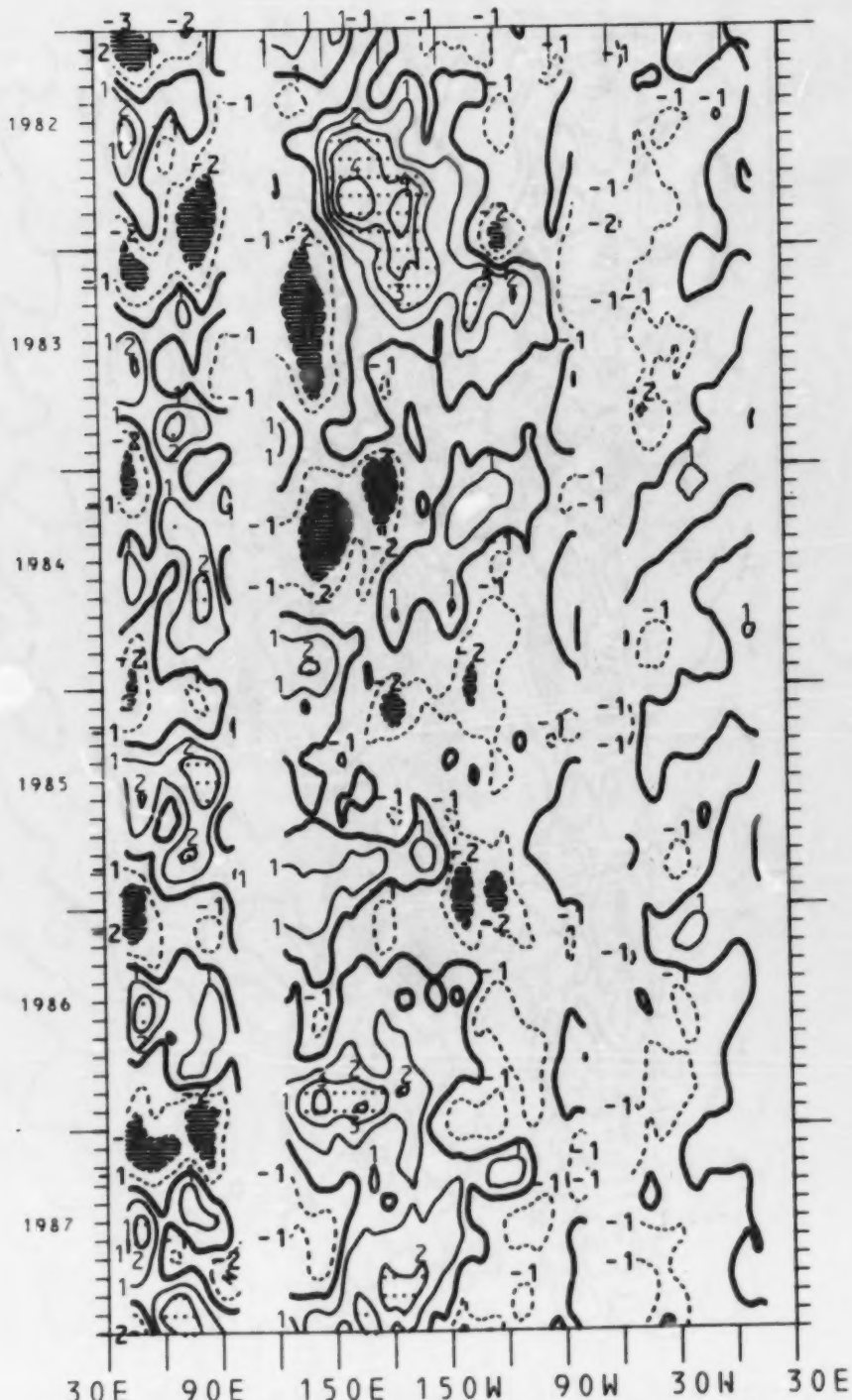

Figure 128. Time-longitude cross-section of equatorial zonal wind component expressed as the difference from the annual mean for the years 1982-1987. The contour interval is 1.0 m/s. The zero isotherm is emphasized. Light shading is greater than 2.0 m/s; dark shading is less than -2.0 m/s.

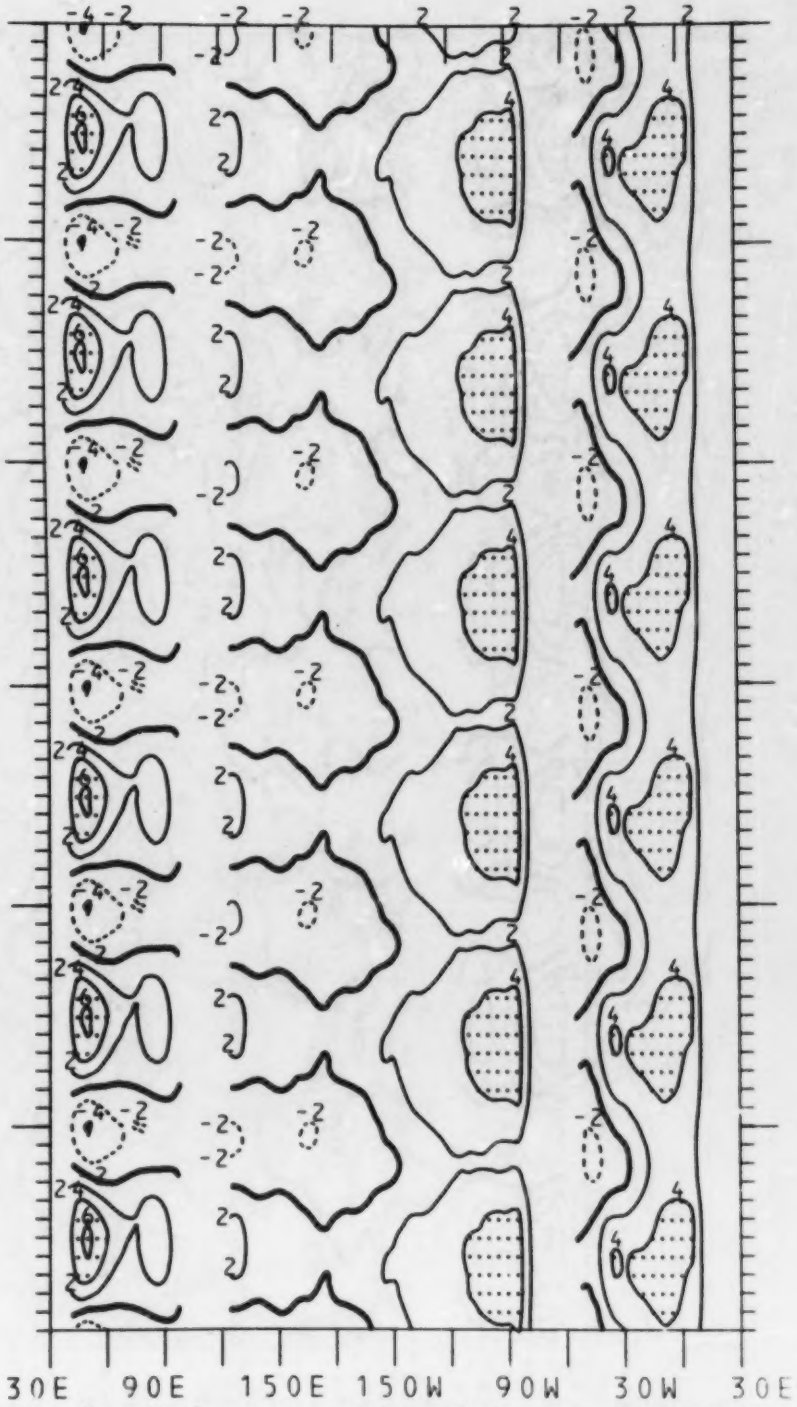

Figure 129. Time-longitude cross-section of the mean equatorial meridional wind component based on the period 1950-1979. The contour interval is 2.0 m/s. The zero isotherm is emphasized. Negative values (northerlies) are dashed. Light shading is greater than 4.0 m/s; dark shading is less than -4.0 m/s.

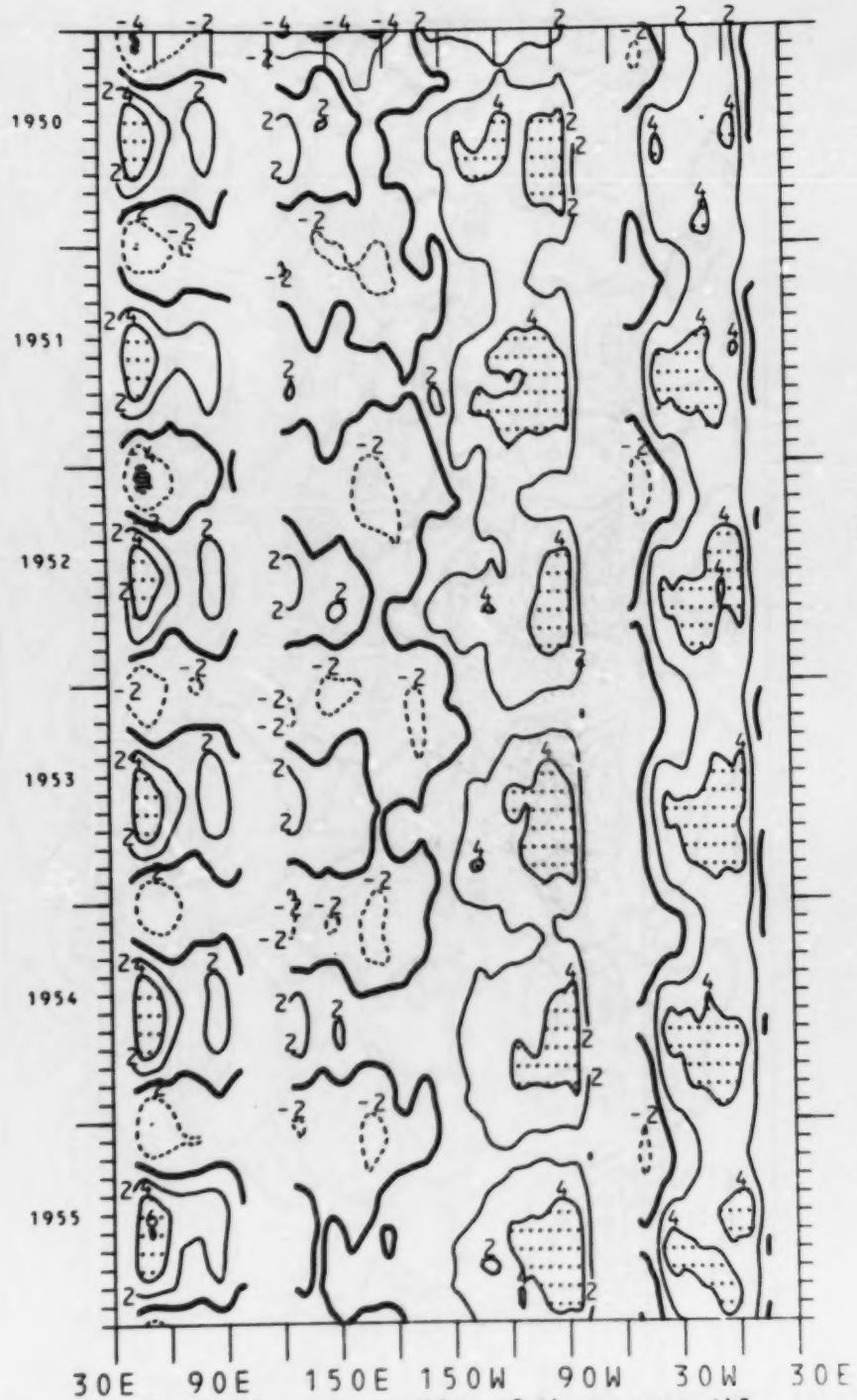

Figure 130. Time-longitude cross-section of the mean monthly equatorial meridional wind component for the years 1950-1955. The contour interval is 2.0 m/s. The zero isotherm is emphasized. Negative values (northerlies) are dashed. Light shading is greater than 4.0 m/s; dark shading is less than -4.0 m/s.

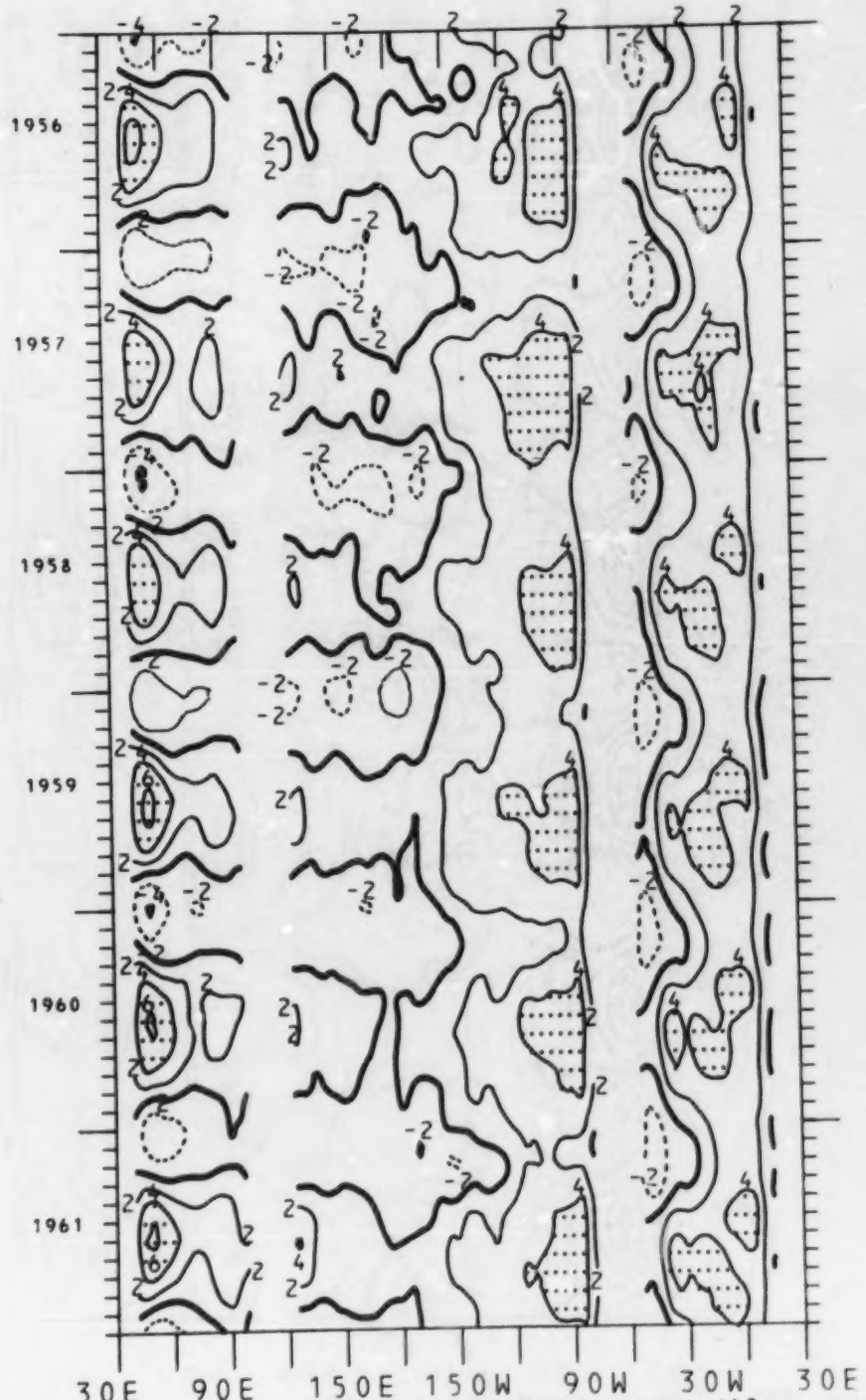

Figure 131. Time-longitude cross-section of the mean monthly equatorial meridional wind component for the years 1956-1961. The contour interval is 2.0 m/s. The zero isotherm is emphasized. Negative values (northerlies) are dashed. Light shading is greater than 4.0 m/s; dark shading is less than -4.0 m/s.

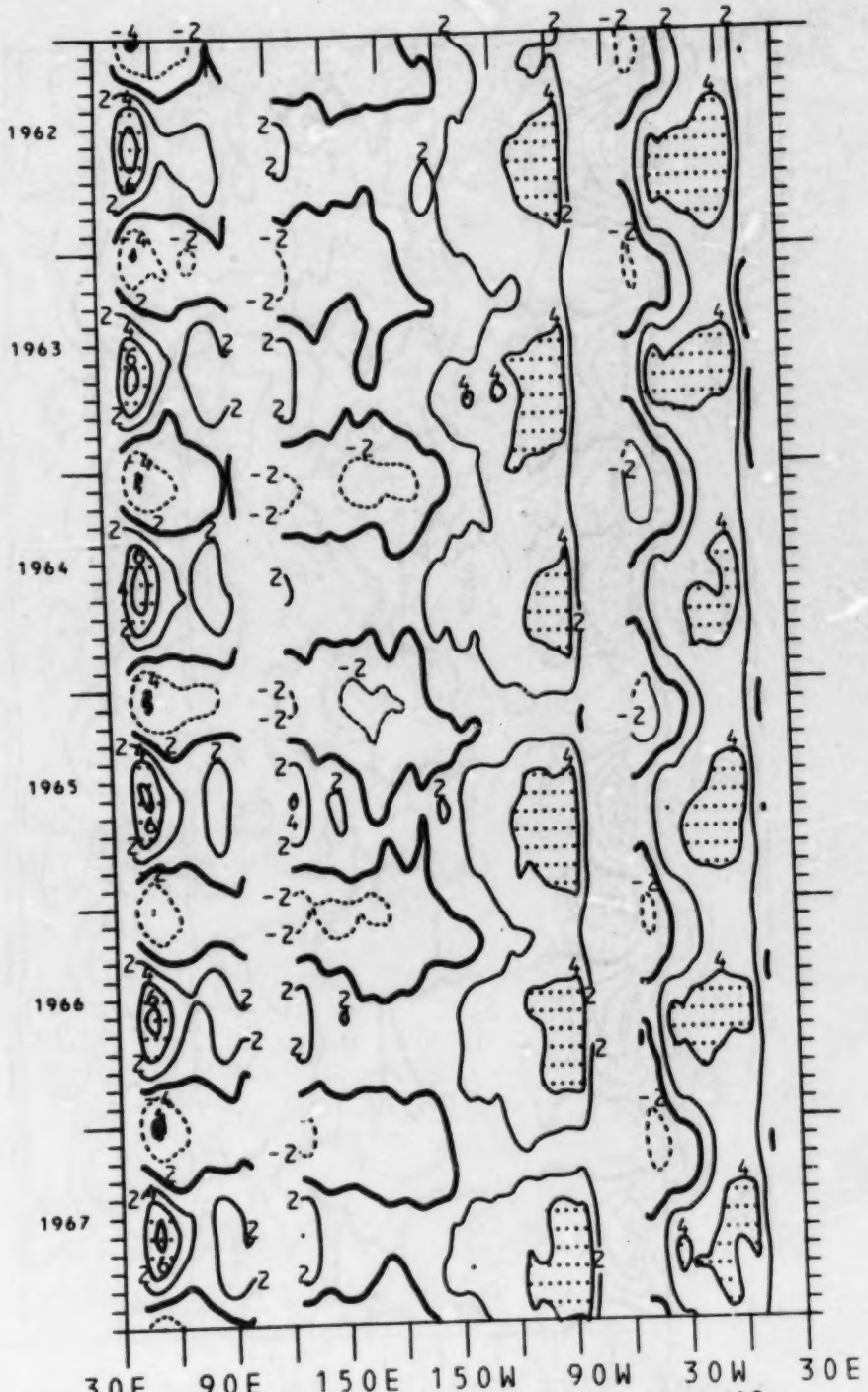

Figure 132. Time-longitude cross-section of the mean monthly equatorial meridional wind component for the years 1962-1967. The contour interval is 2.0 m/s. The zero isotherm is emphasized. Negative values (northerlies) are dashed. Light shading is greater than 4.0 m/s; dark shading is less than -4.0 m/s.

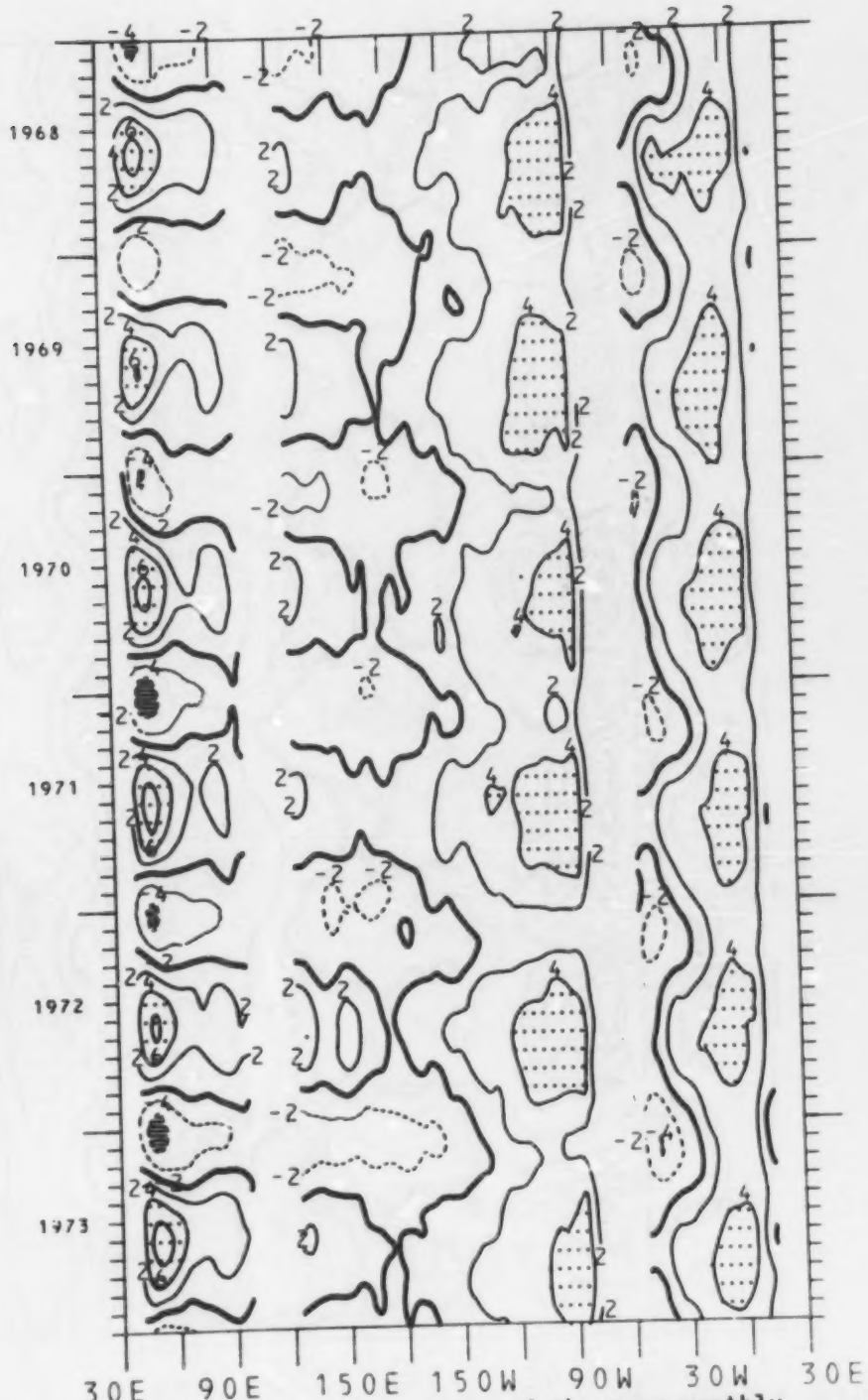

Figure 133. Time-longitude cross-section of the mean monthly equatorial meridional wind component for the years 1968-1973. The contour interval is 2.0 m/s. The zero isotherm is emphasized. Negative values (northerlies) are dashed. Light shading is greater than 4.0 m/s; dark shading is less than -4.0 m/s.

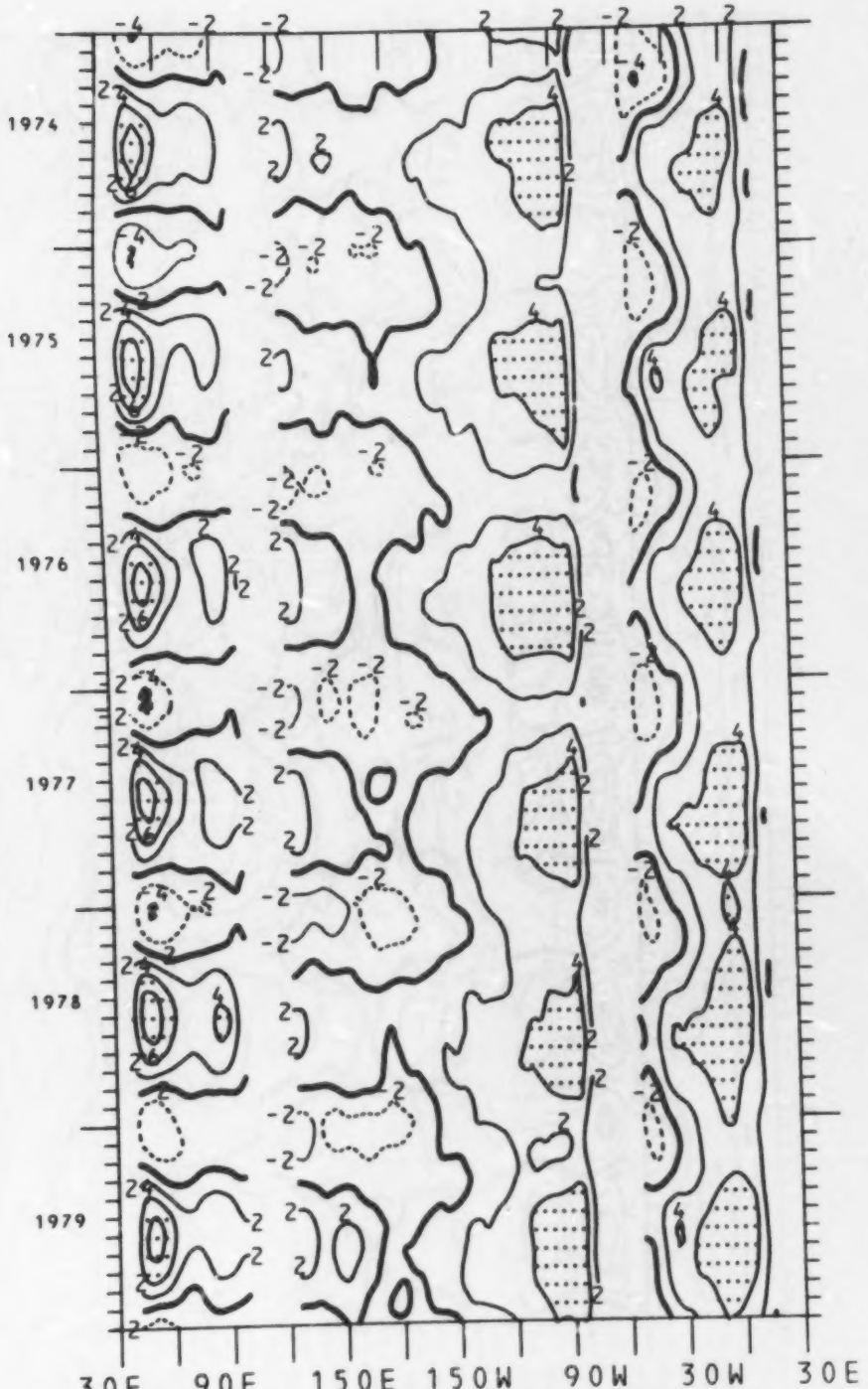

Figure 134. Time-longitude cross-section of the mean monthly equatorial meridional wind component for the years 1974-1979. The contour interval is 2.0 m/s. The zero isotherm is emphasized. Negative values (northerlies) are dashed. Light shading is greater than 4.0 m/s; dark shading is less than -4.0 m/s.

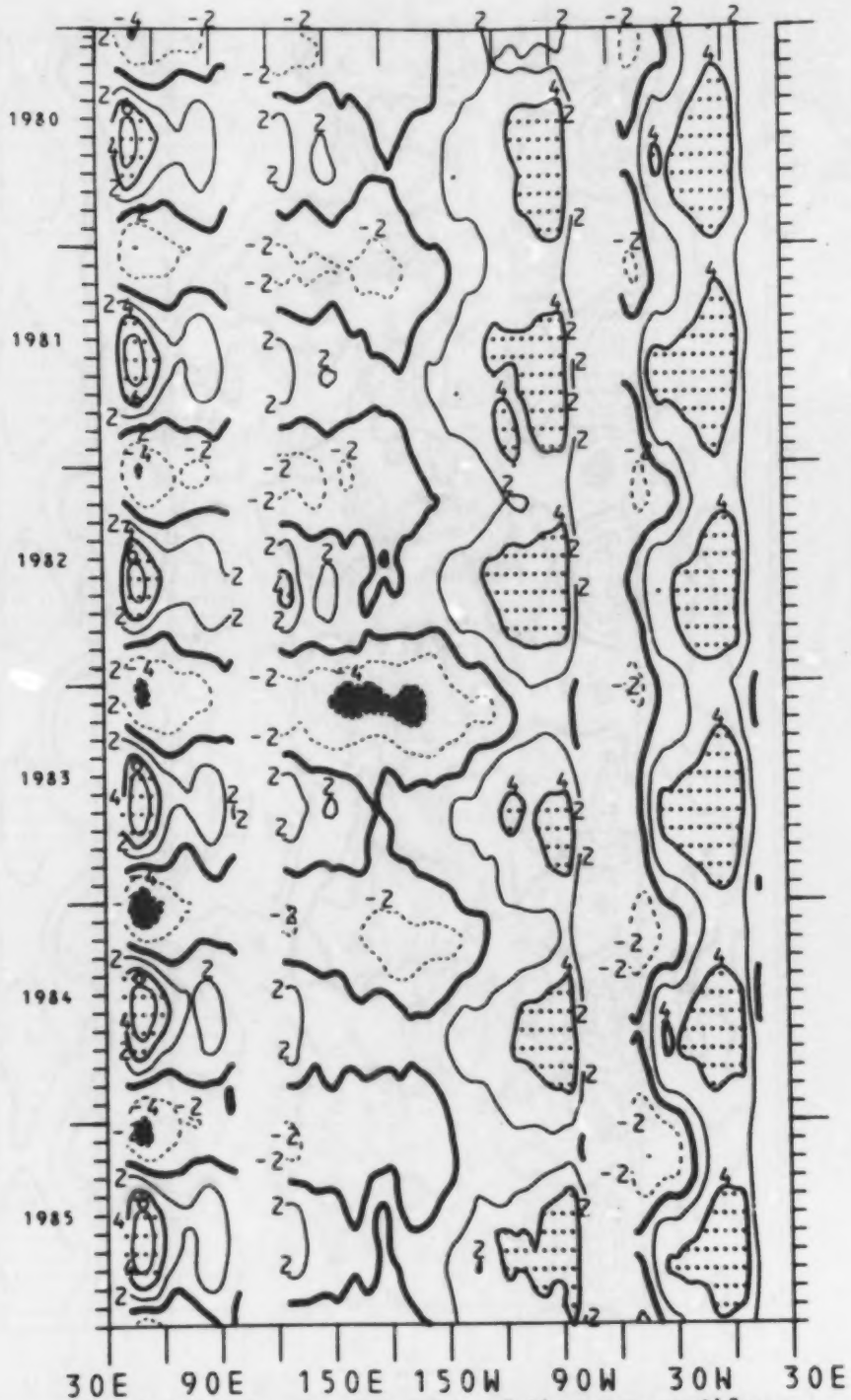

Figure 135. Time-longitude cross-section of the mean monthly equatorial meridional wind component for the years 1980-1985. The contour interval is 2.0 m/s. The zero isotherm is emphasized. Negative values (northerlies) are dashed. Light shading is greater than 4.0 m/s; dark shading is less than -4.0 m/s.

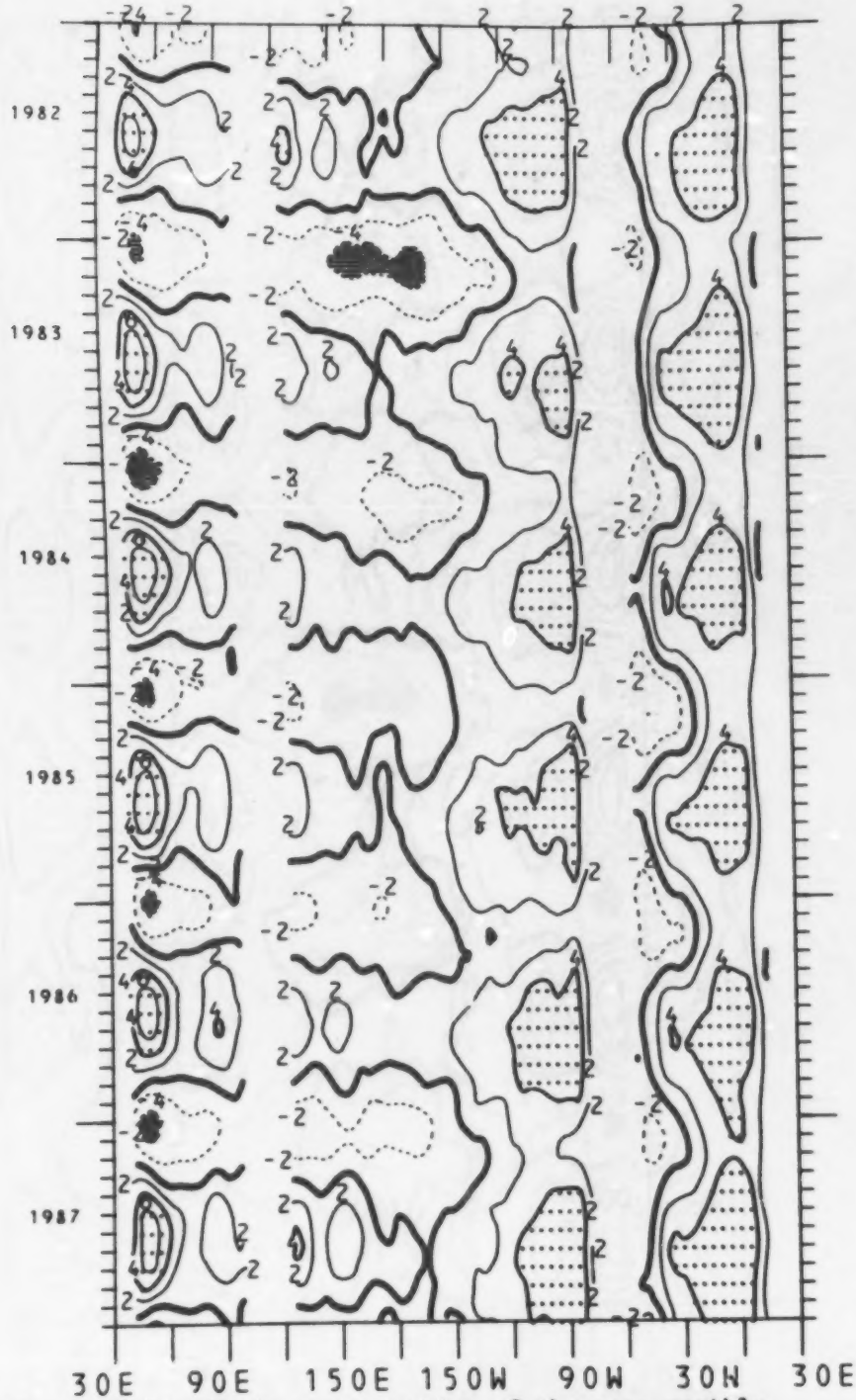

Figure 136. Time-longitude cross-section of the mean monthly equatorial meridional wind component for the years 1982-1987. The contour interval is 2.0 m/s. The zero isotherm is emphasized. Negative values (northerlies) are dashed. Light shading is greater than 4.0 m/s; dark shading is less than -4.0 m/s.

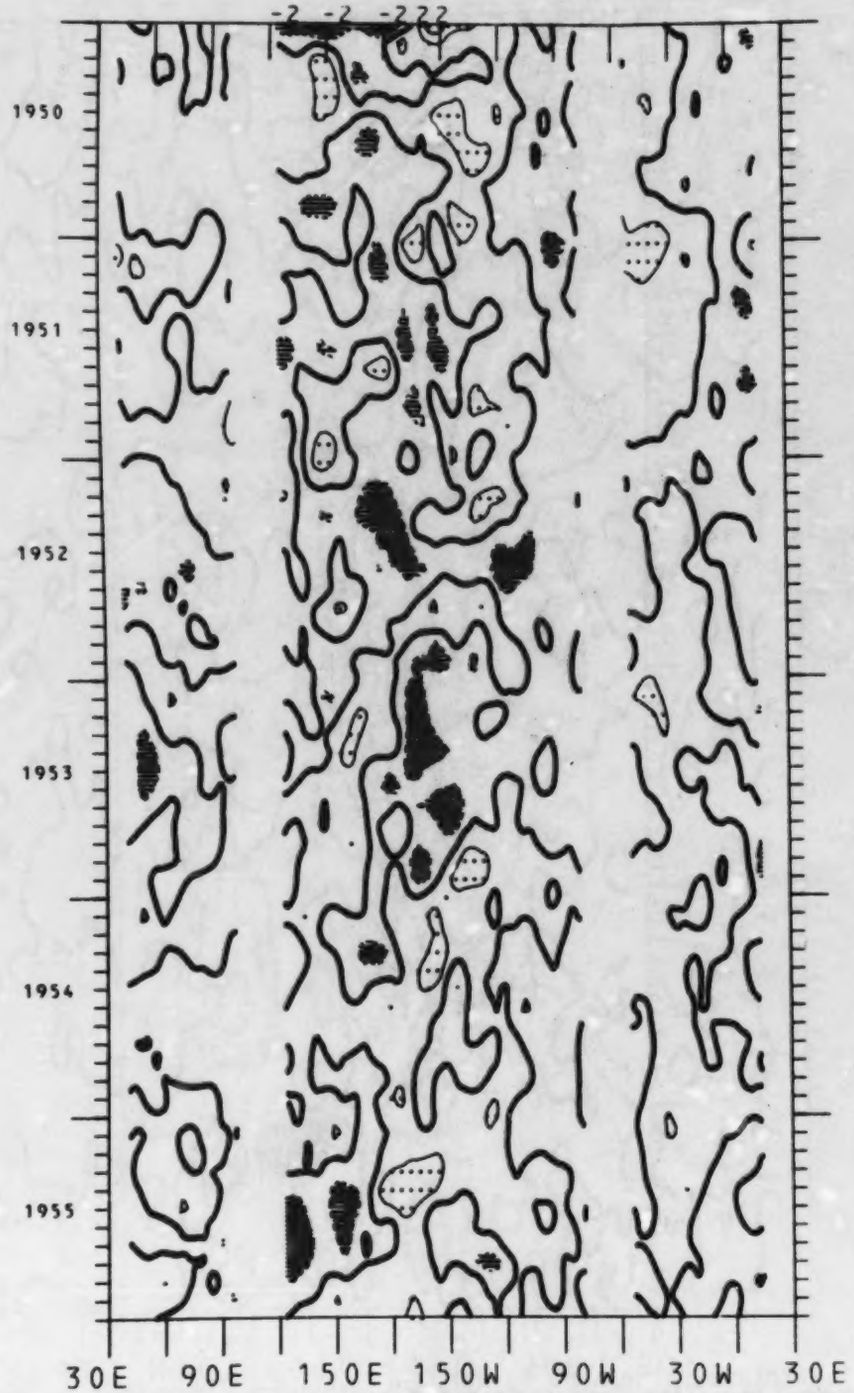

Figure 137. Time-longitude cross-section of equatorial meridional wind component anomalies for the years 1950-1955. The contour interval is 1.0 m/s. The zero isotherm is emphasized. Light shading is greater than 1.0 m/s; dark shading is less than -1.0 m/s.

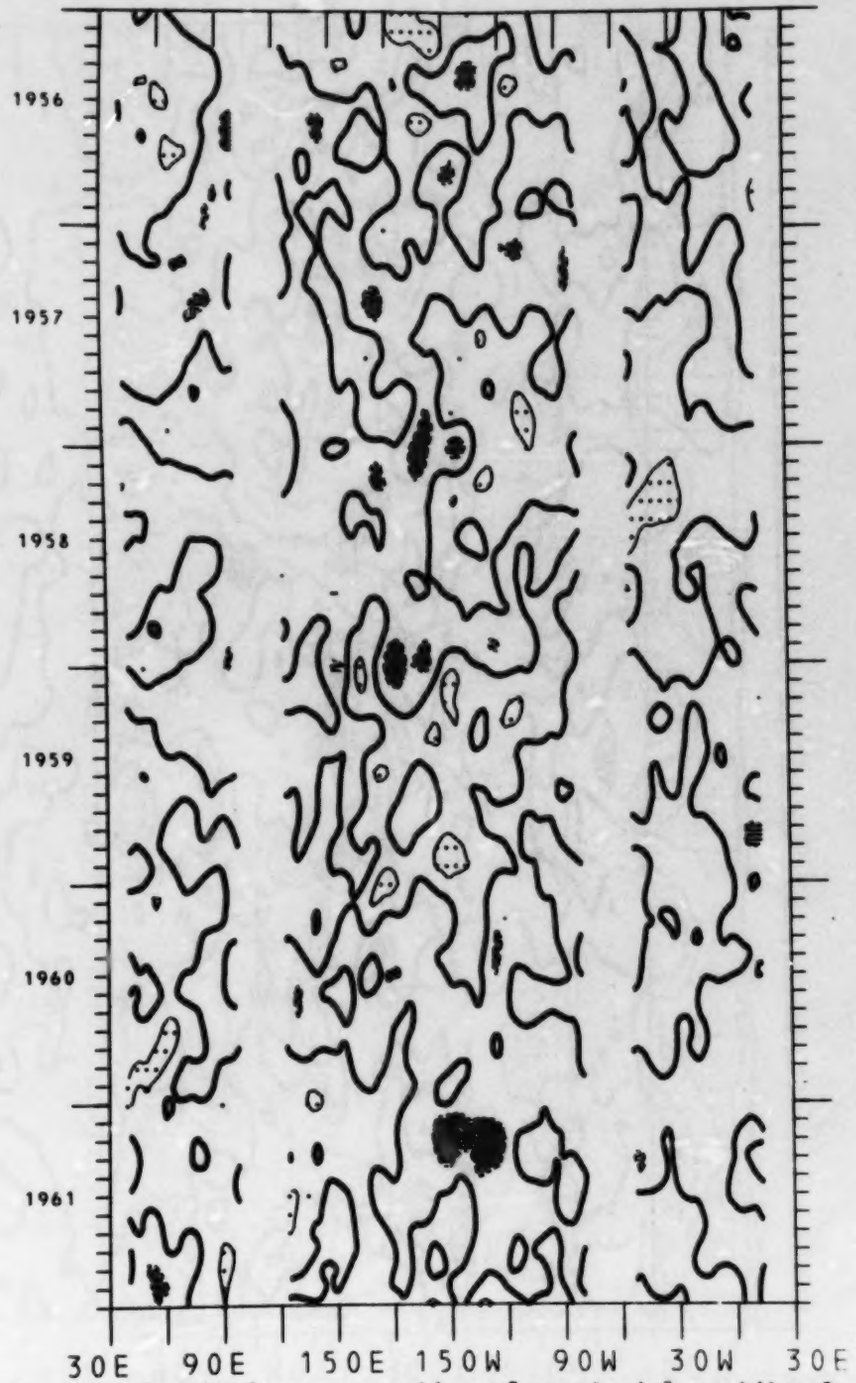

Figure 138. Time-longitude cross-section of equatorial meridional wind component anomalies for the years 1956-1961. The contour interval is 1.0 m/s. The zero isotherm is emphasized. Light shading is greater than 1.0 m/s; dark shading is less than -1.0 m/s.

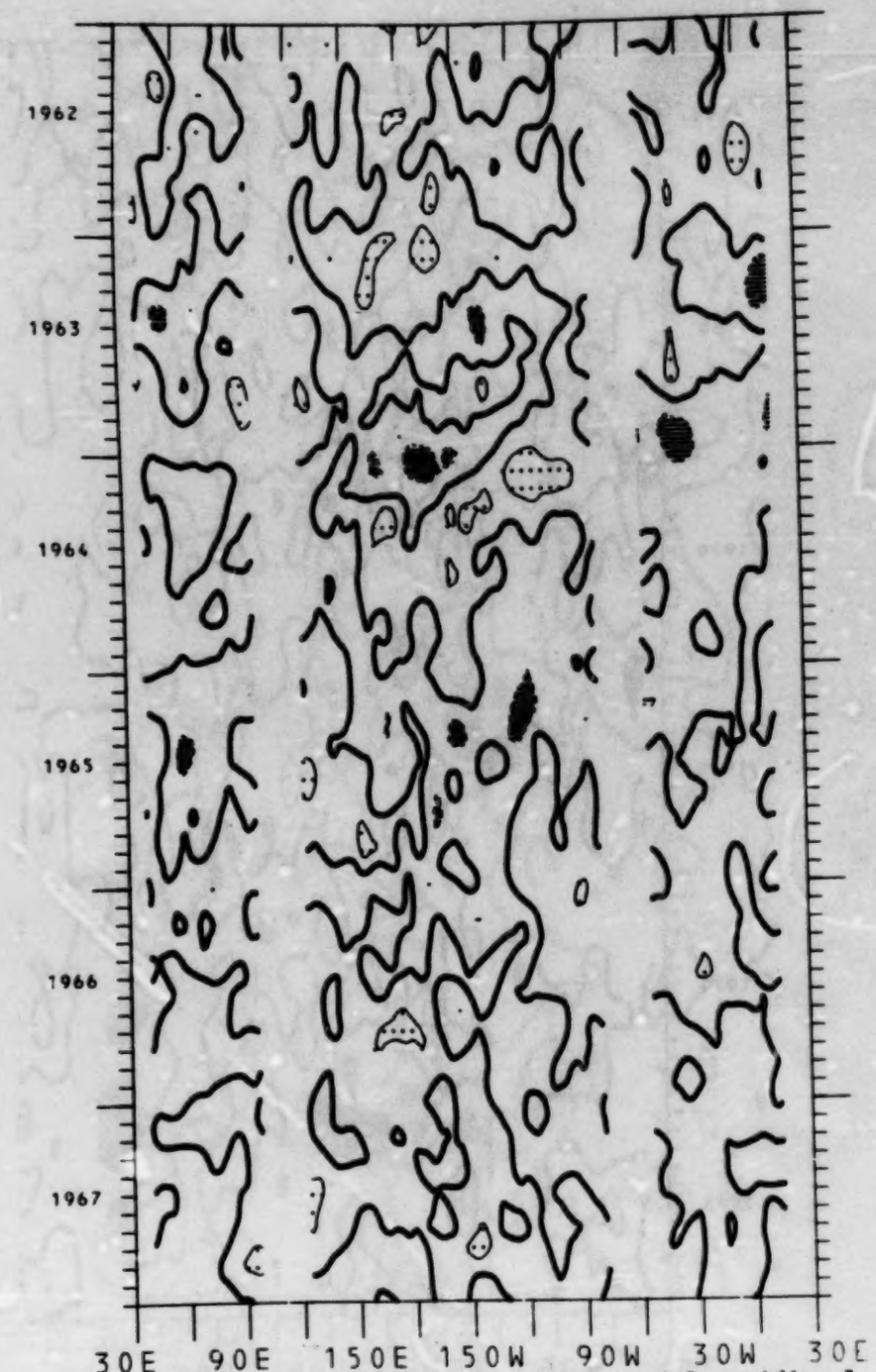

Figure 139. Time-longitude cross-section of equatorial meridional wind component anomalies for the years 1962-1967. The contour interval is 1.0 m/s. The zero isotherm is emphasized. Light shading is greater than 1.0 m/s; dark shading is less than -1.0 m/s.

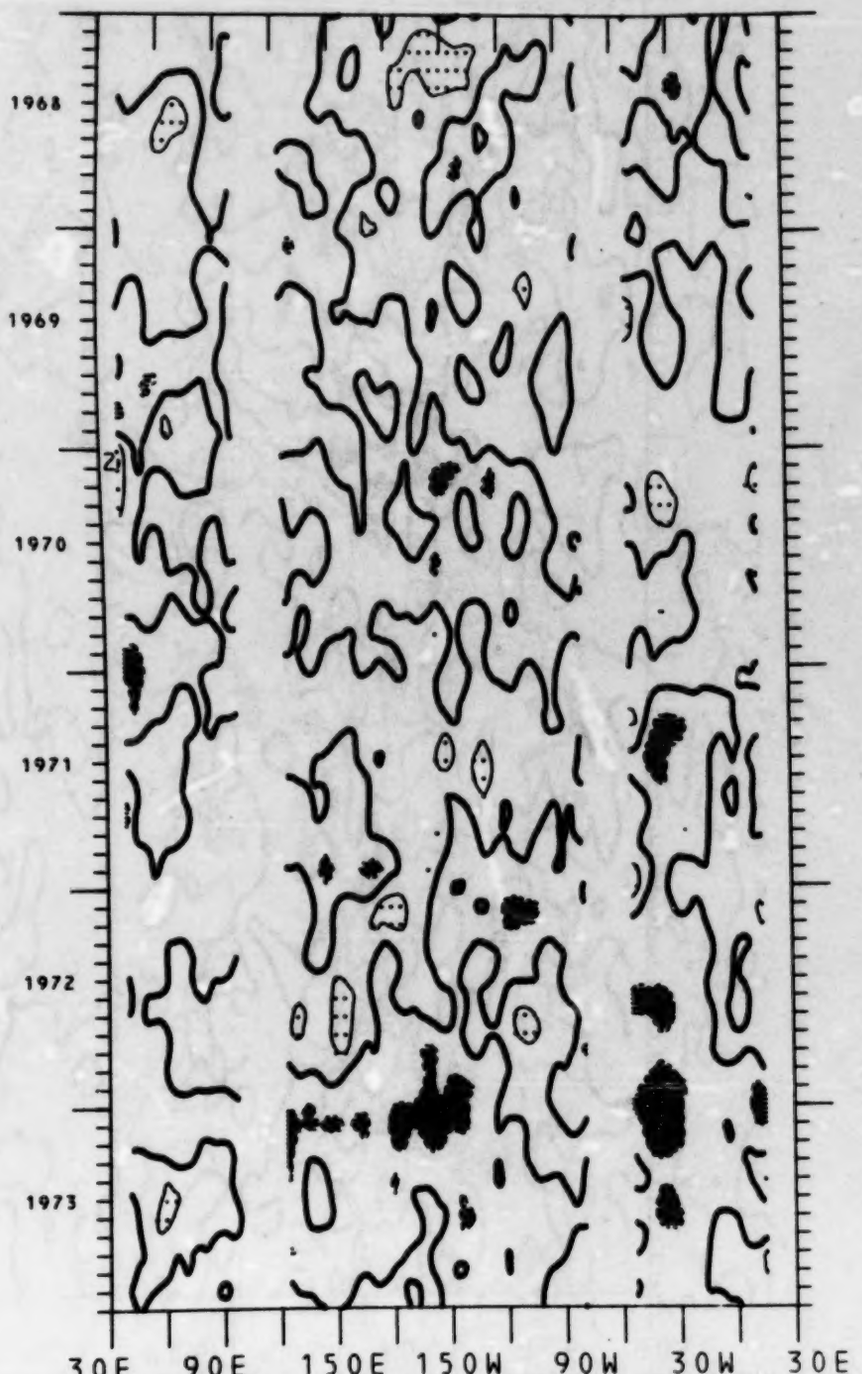

Figure 140. Time-longitude cross-section of equatorial meridional wind component anomalies for the years 1968-1973. The contour interval is 1.0 m/s. The zero isotherm is emphasized. Light shading is greater than 1.0 m/s; dark shading is less than -1.0 m/s.

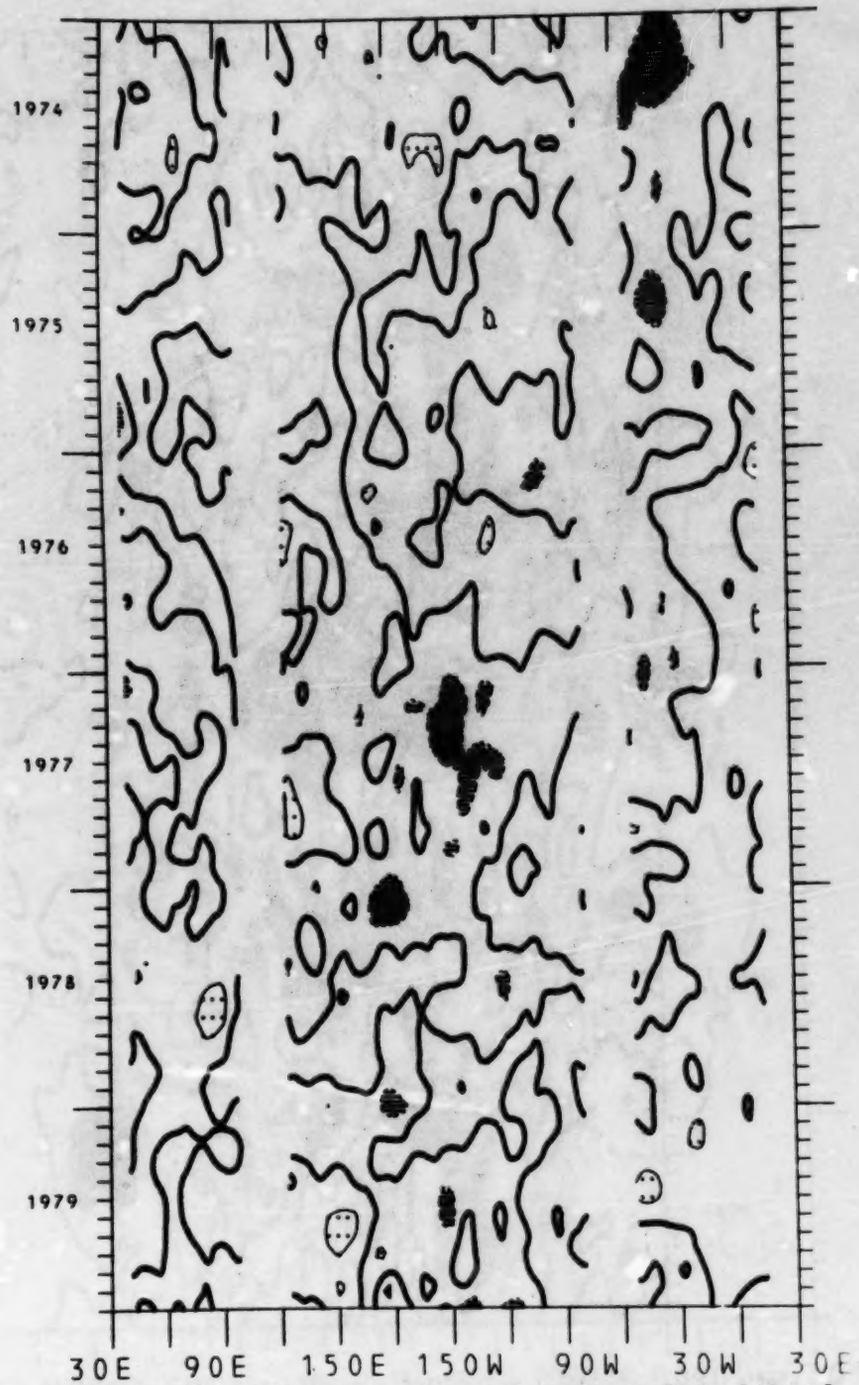

Figure 141. Time-longitude cross-section of equatorial meridional wind component anomalies for the years 1974-1979. The contour interval is 1.0 m/s. The zero isotherm is emphasized. Light shading is greater than 1.0 m/s; dark shading is less than -1.0 m/s.

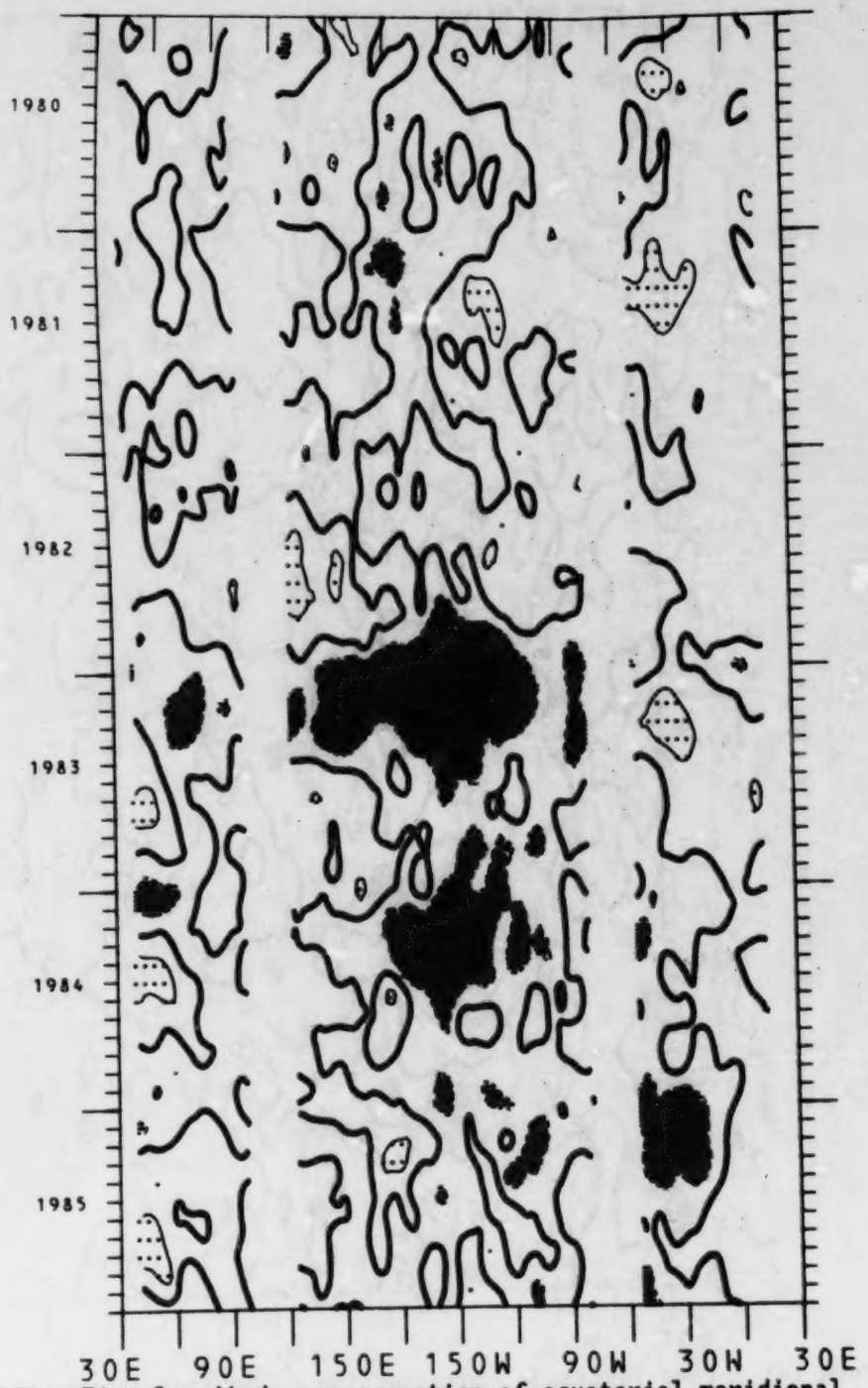

Figure 142. Time-longitude cross-section of equatorial meridional wind component anomalies for the years 1980-1985. The contour interval is 1.0 m/s. The zero isotherm is emphasized. Light shading is greater than 1.0 m/s; dark shading is less than -1.0 m/s.

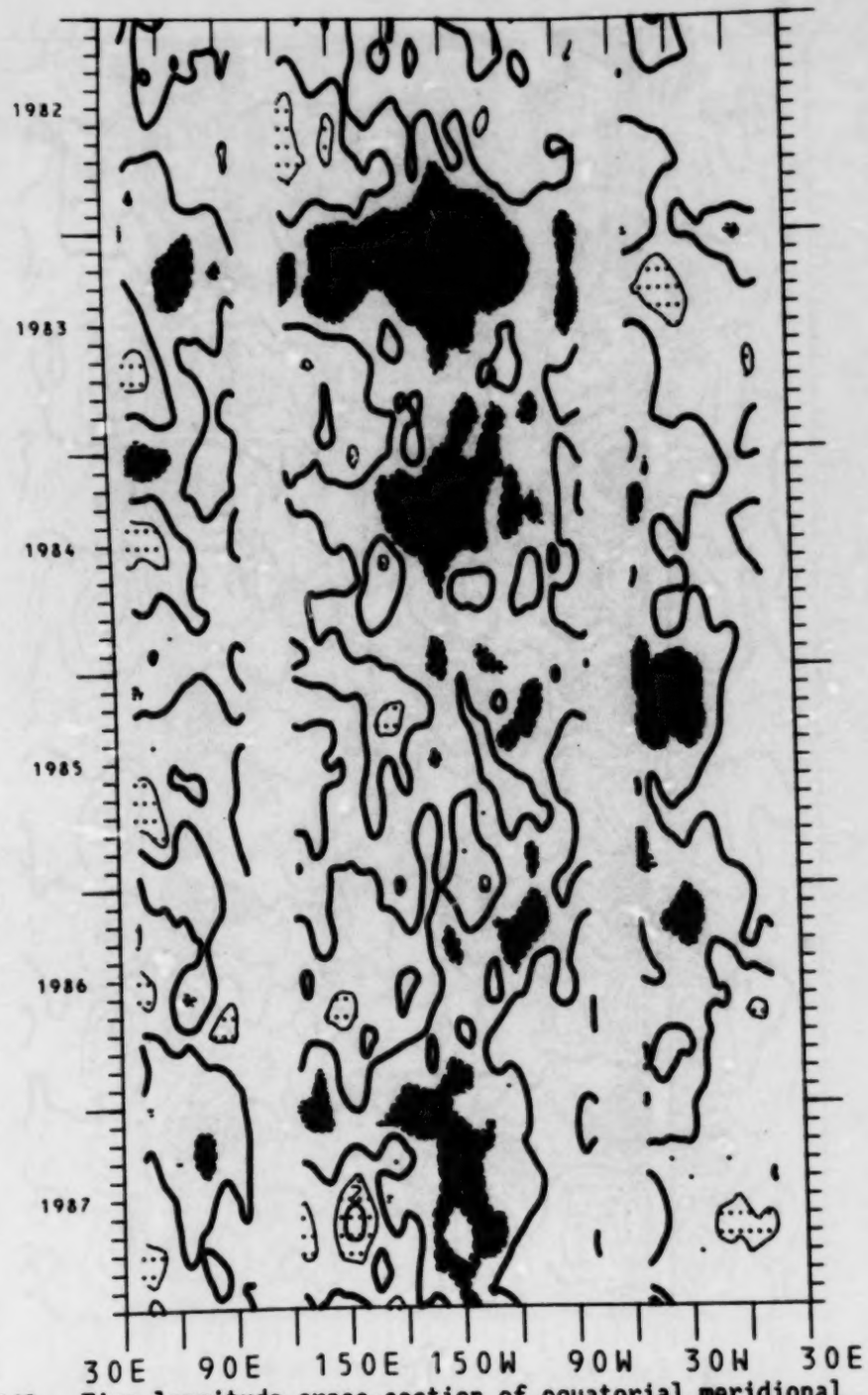

Figure 143. Time-longitude cross-section of equatorial meridional wind component anomalies for the years 1982-1987. The contour interval is 1.0 m/s. The zero isotherm is emphasized. Light shading is greater than 1.0 m/s; dark shading is less than -1.0 m/s.

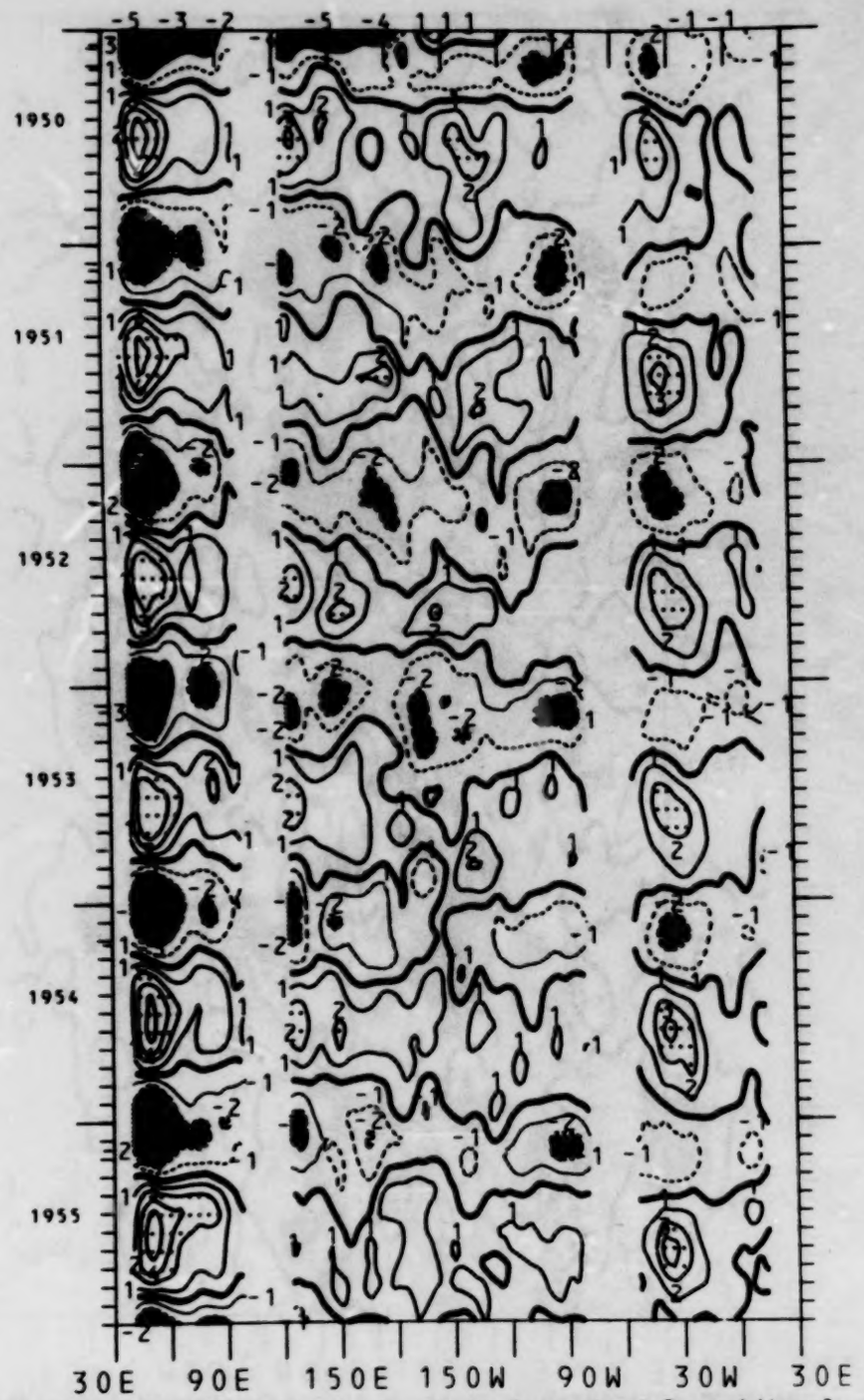

Figure 144. Time-longitude cross-section of equatorial meridional wind component expressed as the difference from the annual mean for the years 1950-1955. The contour interval is 1.0 m/s. The zero isotherm is emphasized. Light shading is greater than 2.0 m/s; dark shading is less than -2.0 m/s.

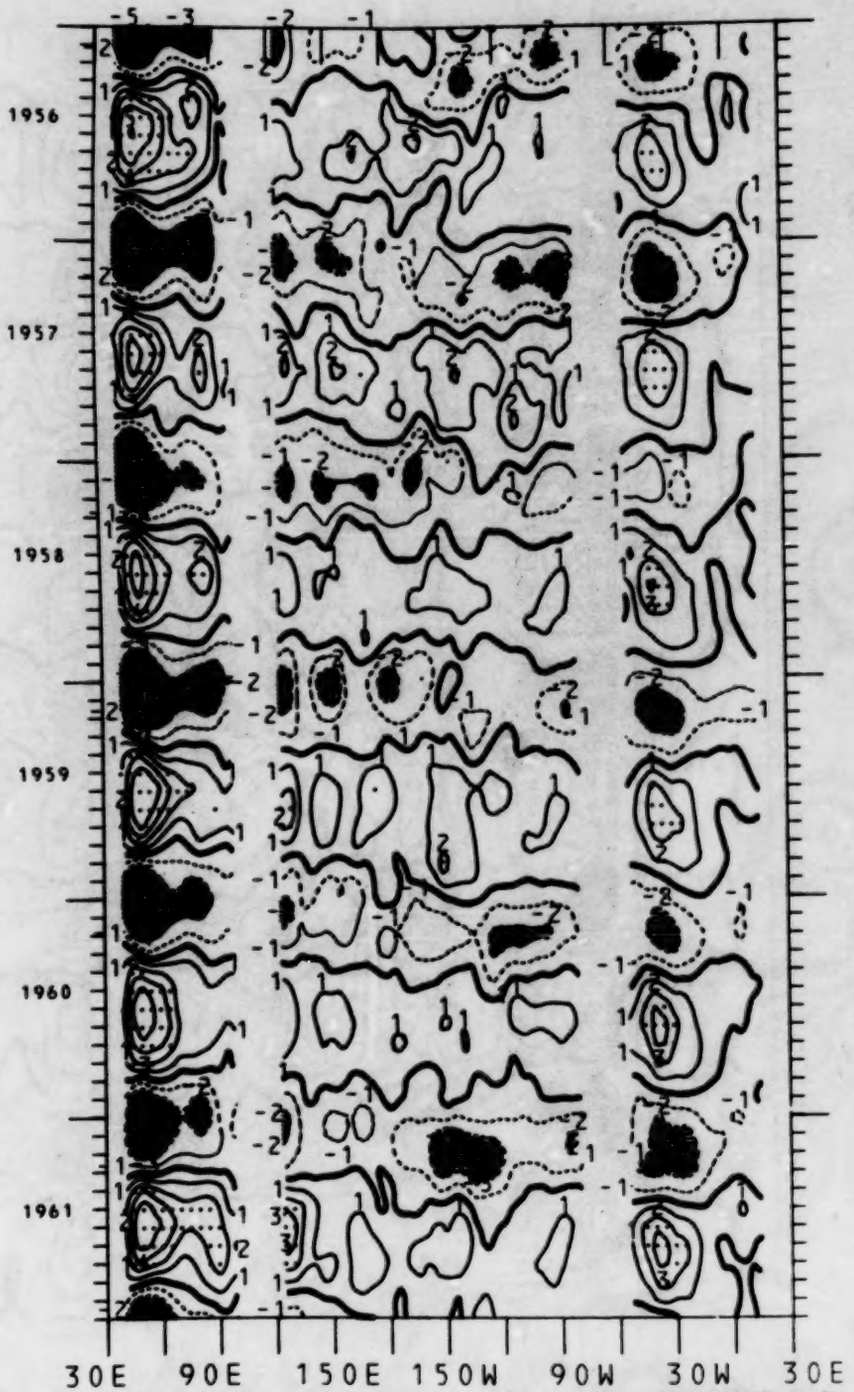

Figure 145 Time-longitude cross-section of equatorial meridional wind component expressed as the difference from the annual mean for the years 1956-1961. The contour interval is 1.0 m/s. The zero isotherm is emphasized. Light shading is greater than 2.0 m/s; dark shading is less than -2.0 m/s.

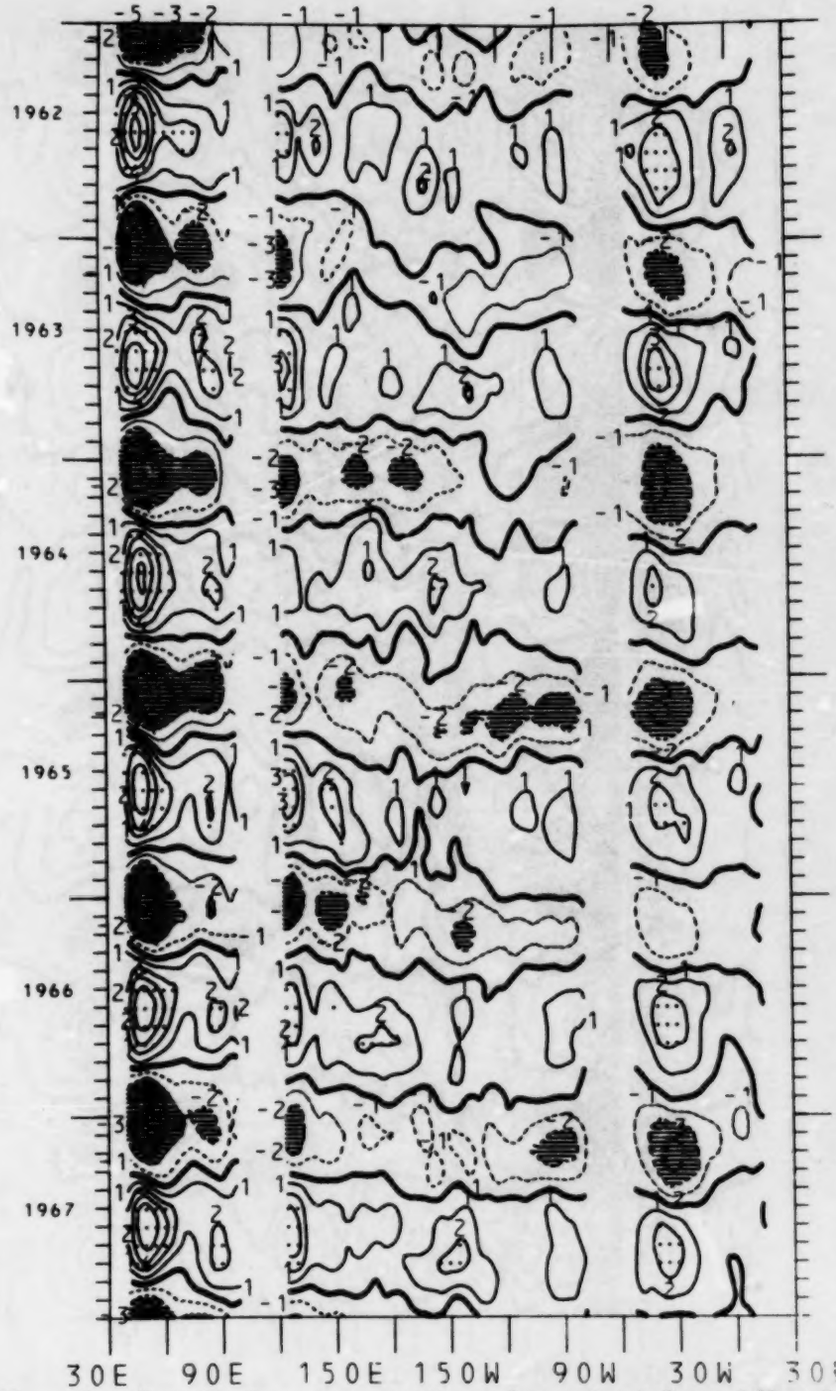

Figure 146. Time-longitude cross-section of equatorial meridional wind component expressed as the difference from the annual mean for the years 1962-1967. The contour interval is 1.0 m/s. The zero isotherm is emphasized. Light shading is greater than 2.0 m/s; dark shading is less than -2.0 m/s.

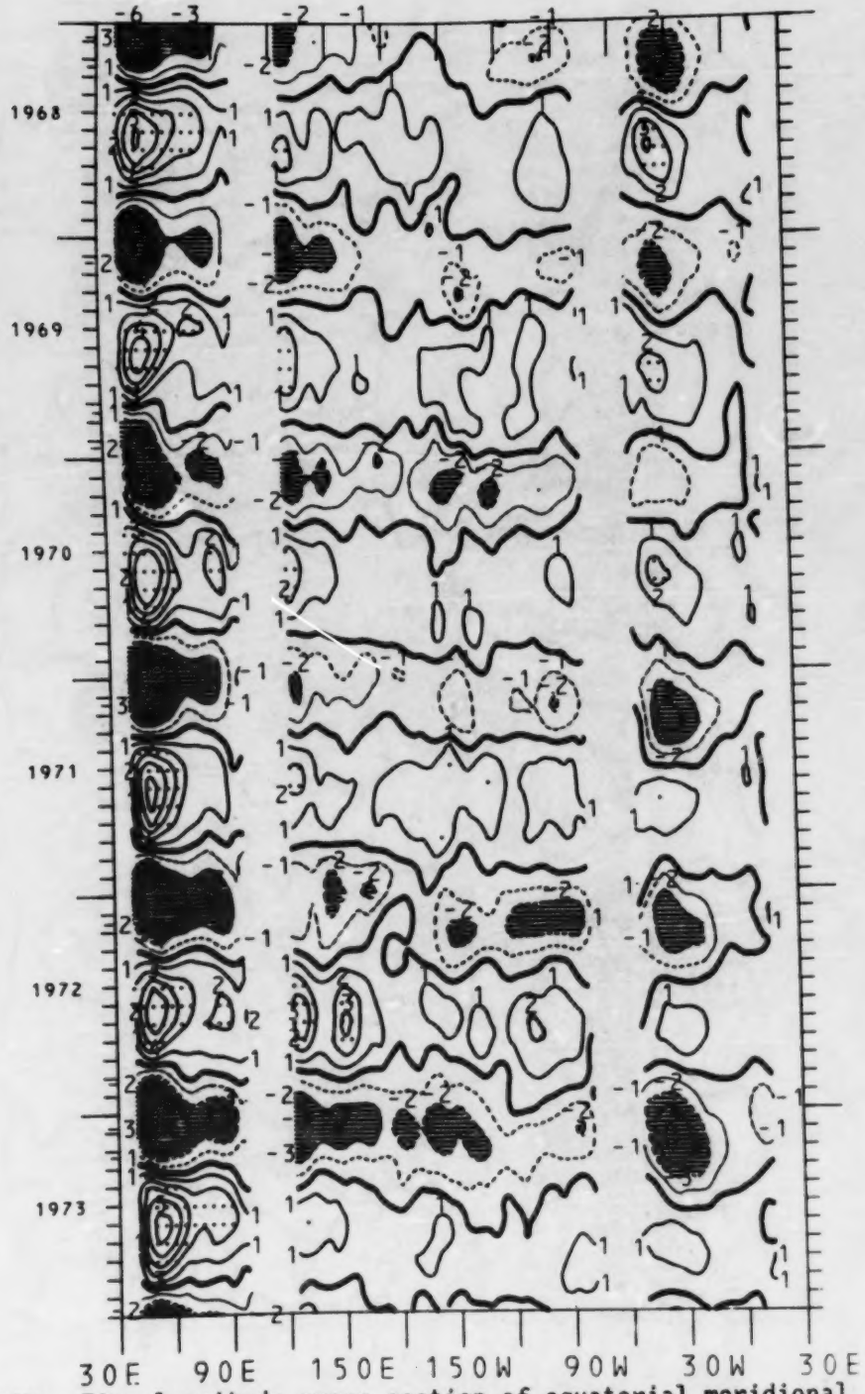

Figure 147. Time-longitude cross-section of equatorial meridional wind component expressed as the difference from the annual mean for the years 1968-1973. The contour interval is 1.0 m/s. The zero isotherm is emphasized. Light shading is greater than 2.0 m/s; dark shading is less than -2.0 m/s.

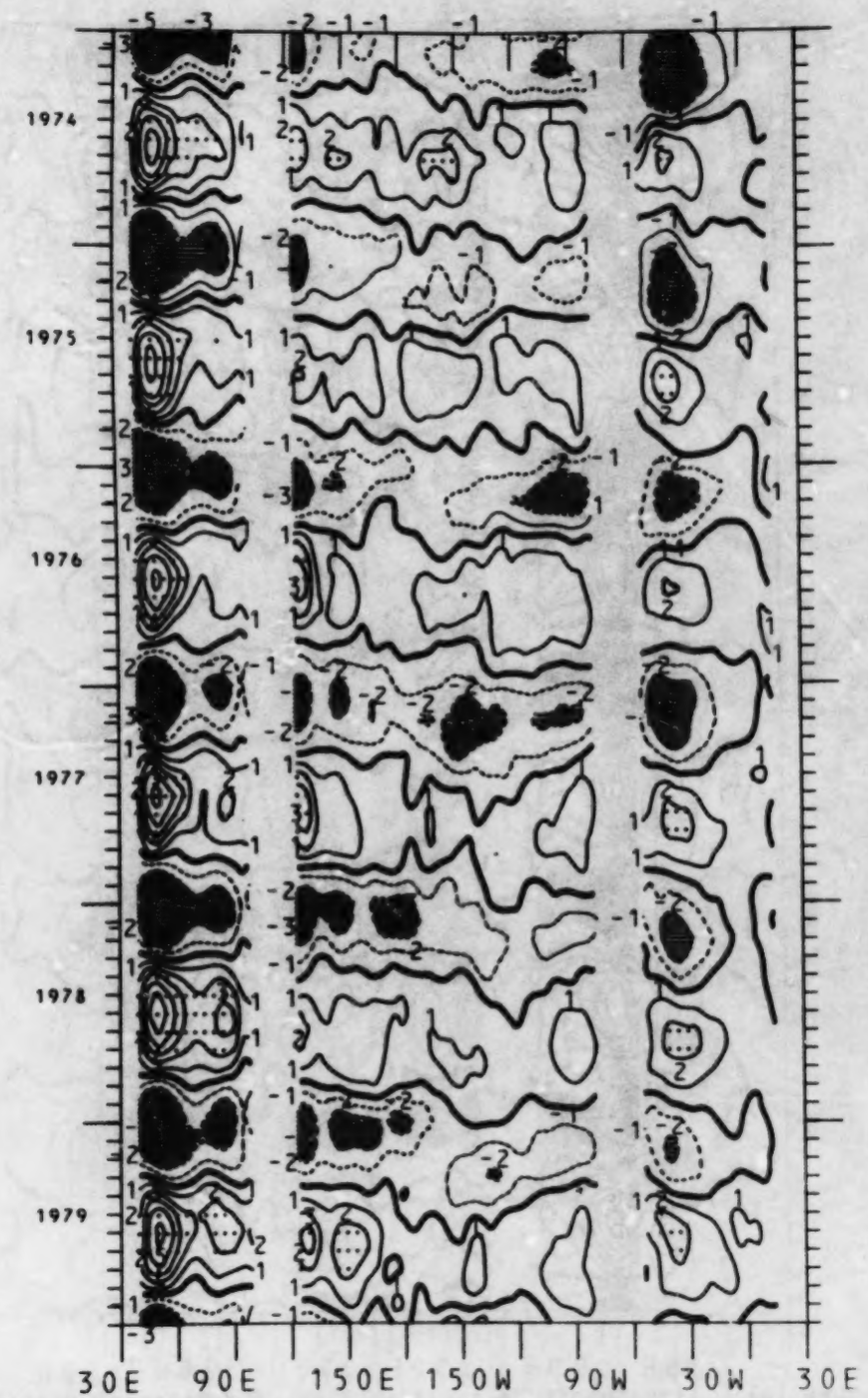

Figure 148. Time-longitude cross-section of equatorial meridional wind component expressed as the difference from the annual mean for the years 1974-1979. The contour interval is 1.0 m/s. The zero isotherm is emphasized. Light shading is greater than 2.0 m/s; dark shading is less than -2.0 m/s.

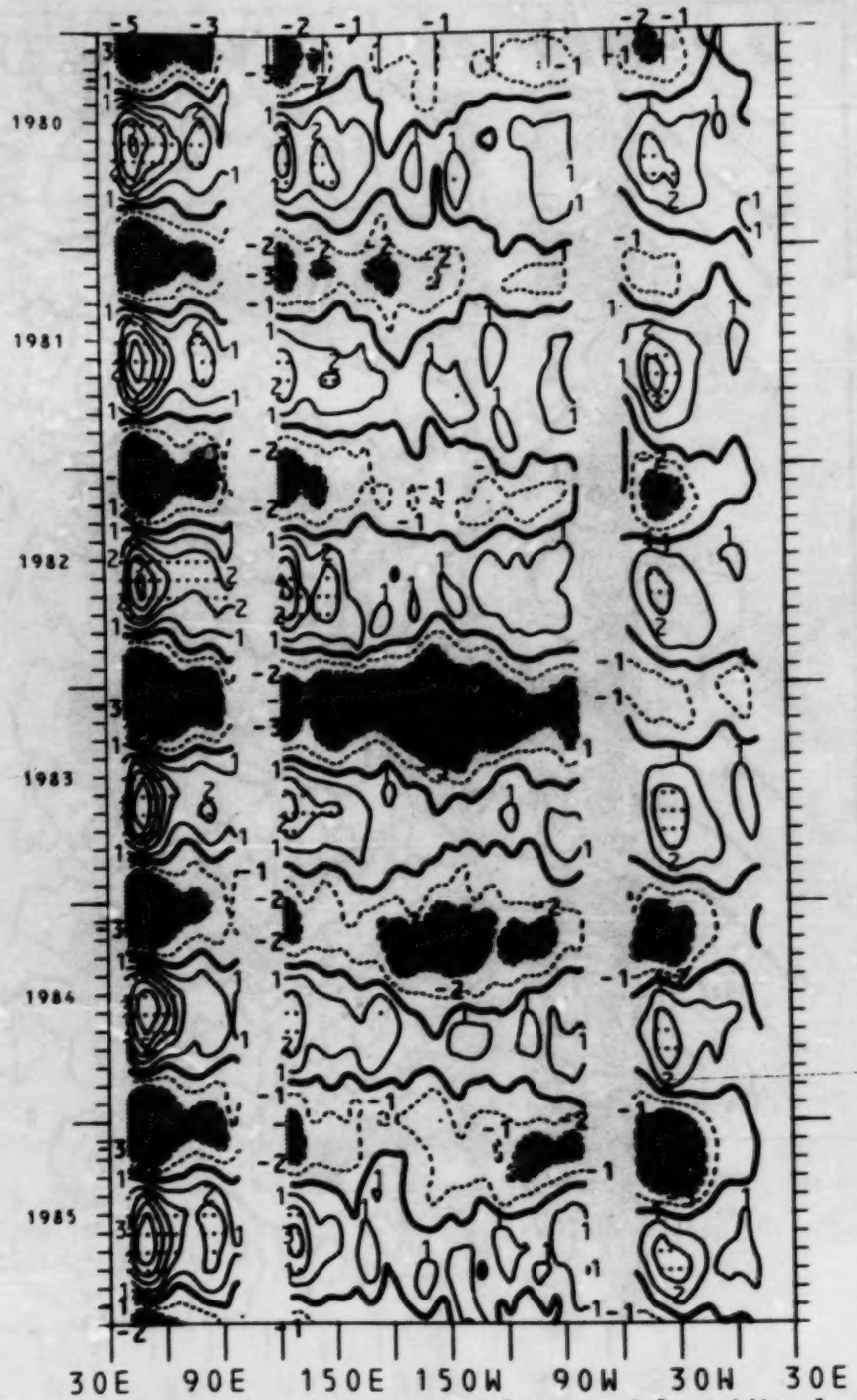

Figure 149. Time-longitude cross-section of equatorial meridional wind component expressed as the difference from the annual mean for the years 1980-1985. The contour interval is 1.0 m/s. The zero isotherm is emphasized. Light shading is greater than 2.0 m/s; dark shading is less than -2.0 m/s.

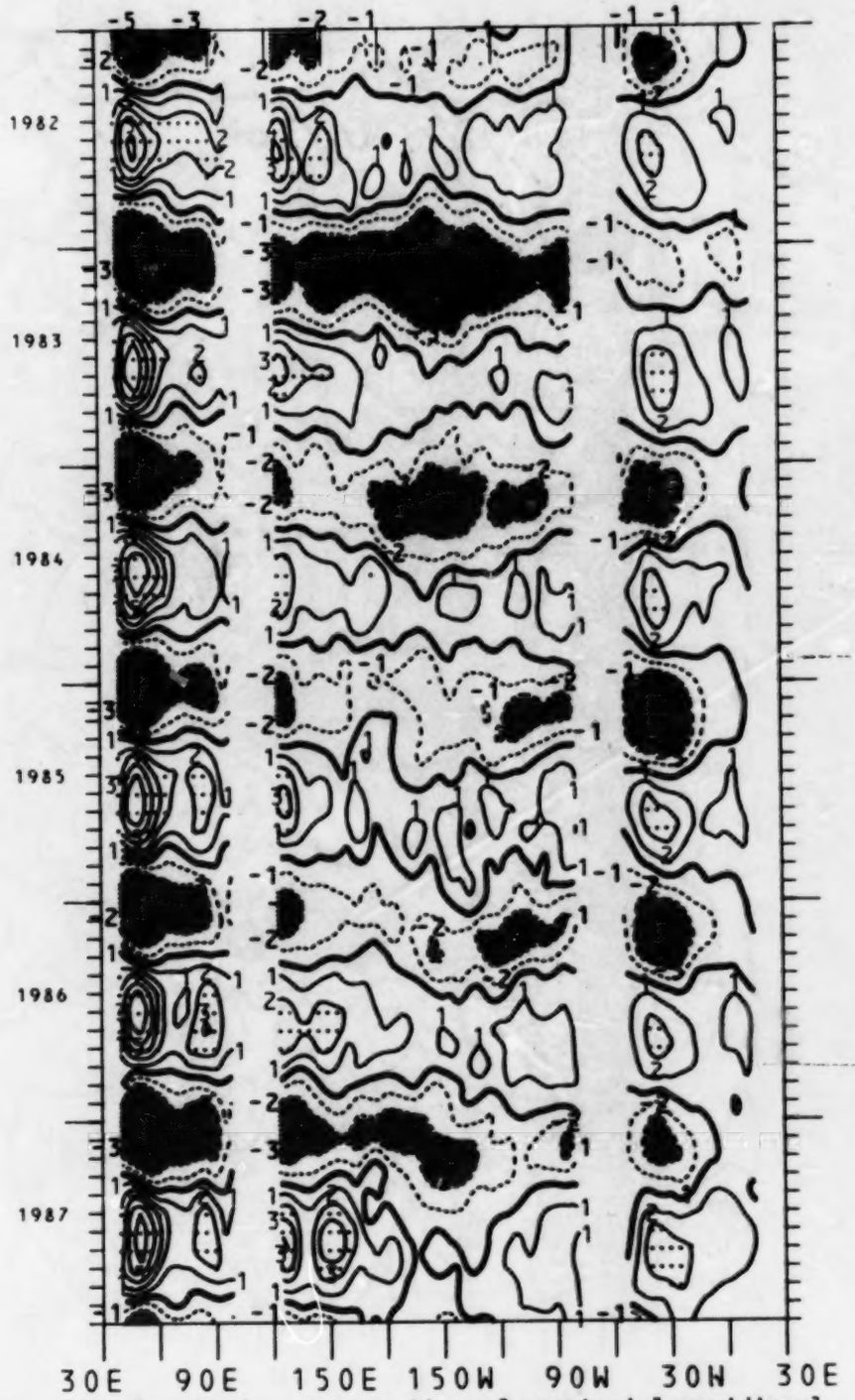

Figure 150. Time-longitude cross-section of equatorial meridional wind component expressed as the difference from the annual mean for the years 1982-1987. The contour interval is 1.0 m/s. The zero isotherm is emphasized. Light shading is greater than 2.0 m/s; dark shading is less than -2.0 m/s.

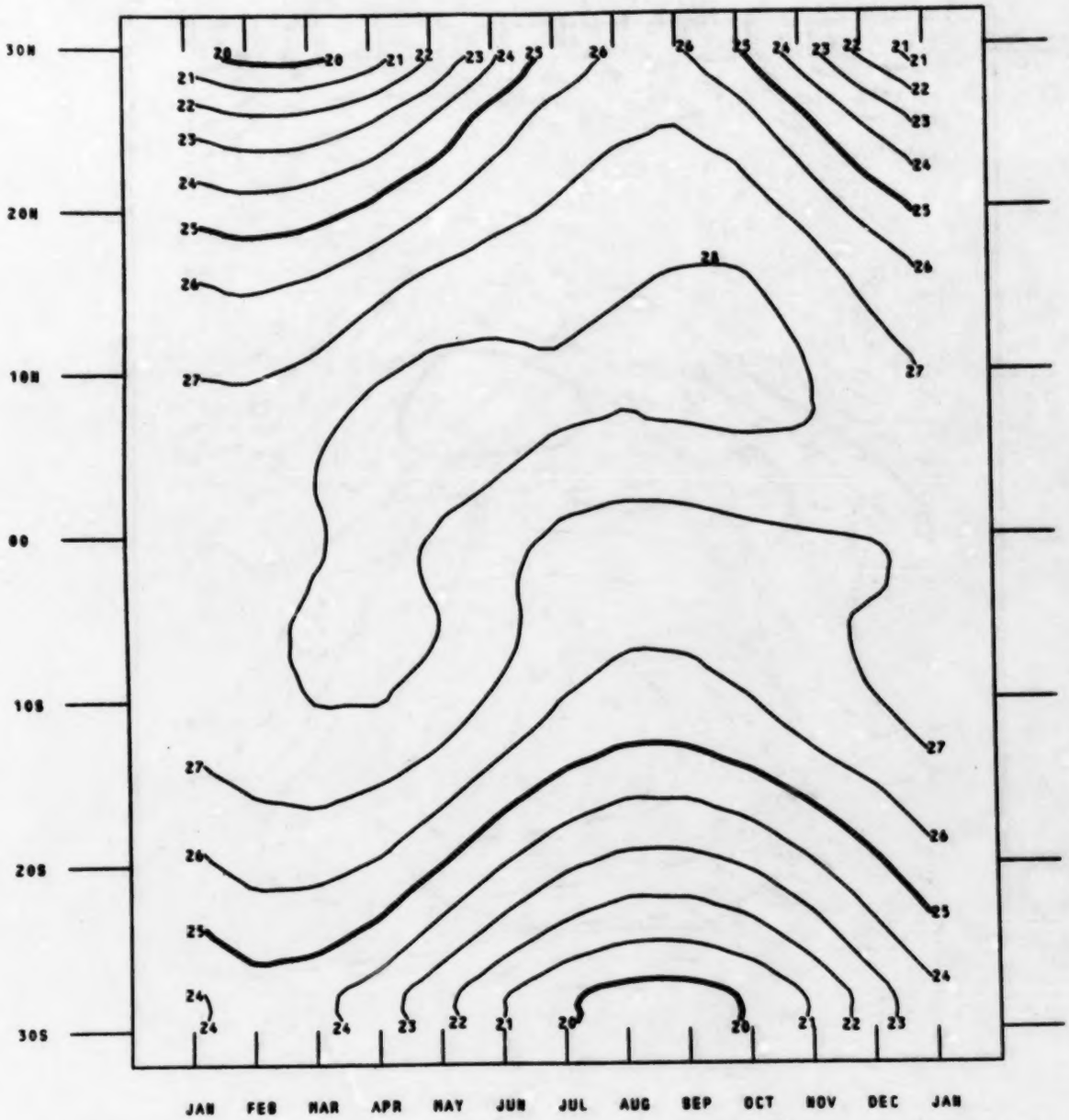

Figure 151. Time-latitude cross-section of the zonally averaged SST. The contour interval is $1^{o}C$.

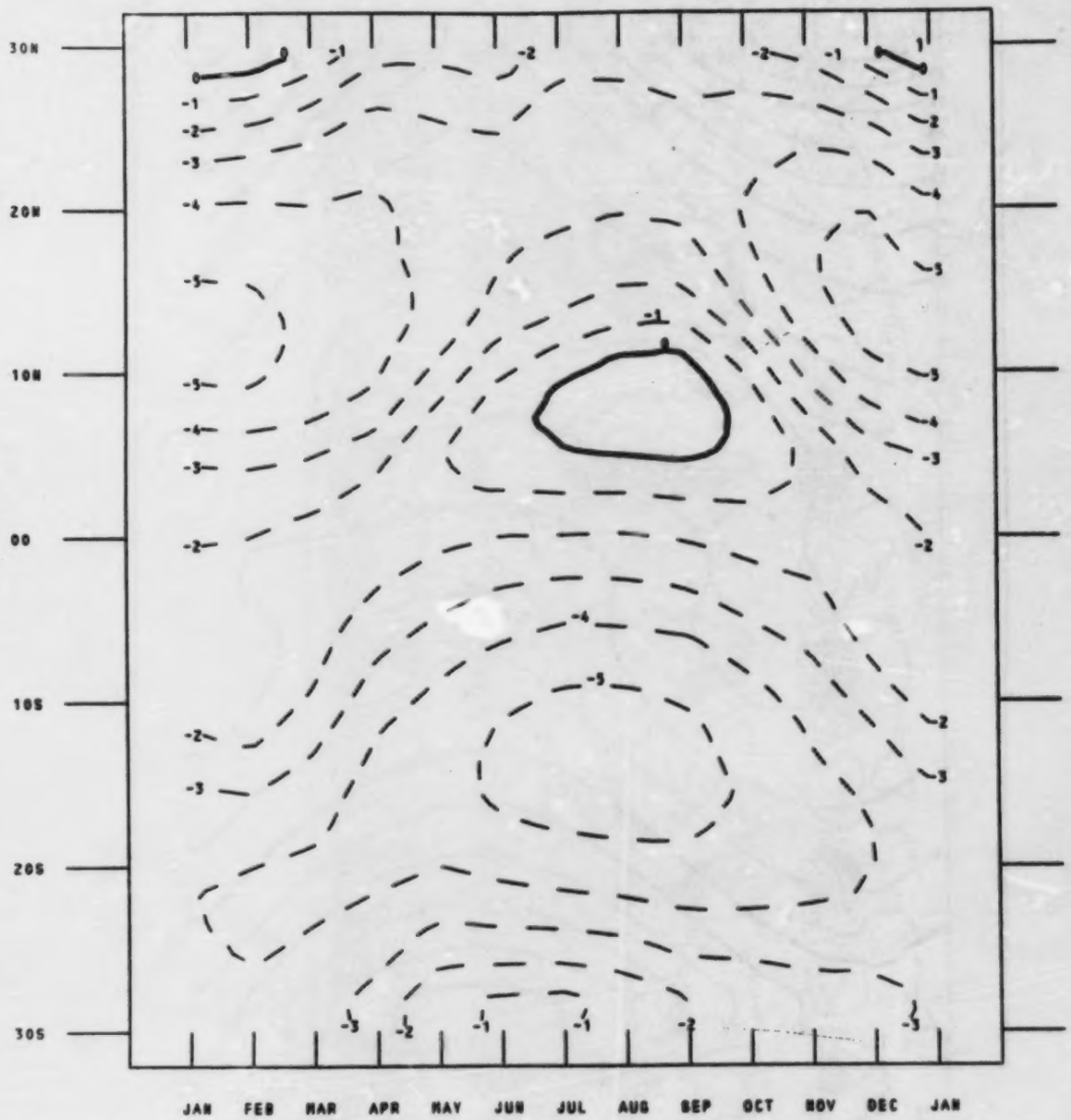

Figure 152. Time-latitude cross-section of the zonally averaged zonal wind. The contour interval is 1 m/s. Negative values (easterlies) are dashed.

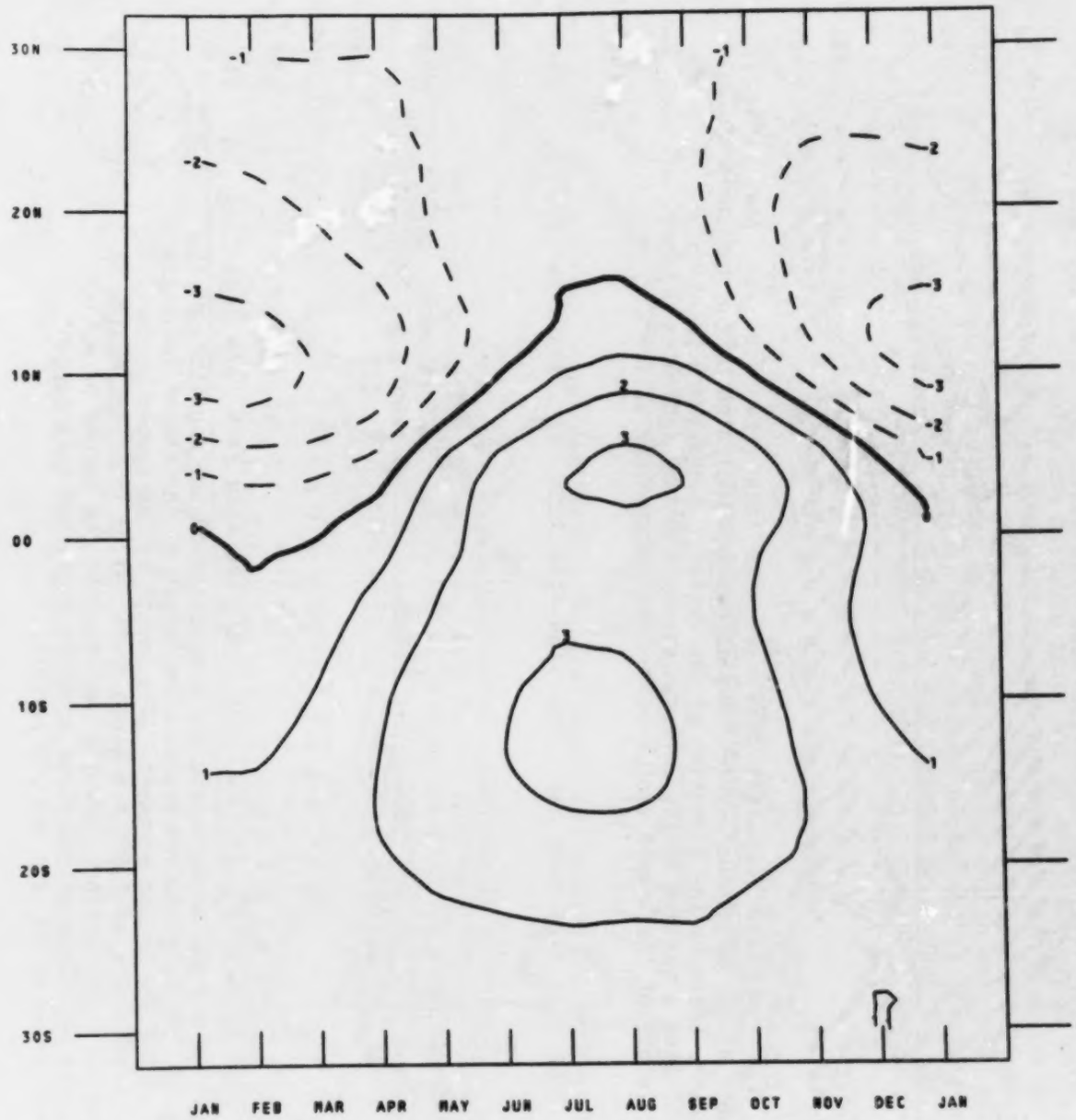

Figure 153. Time-latitude cross-section of the zonally averaged meridional wind. The contour interval is 1 m/s. Negative values (northerlies) are dashed.

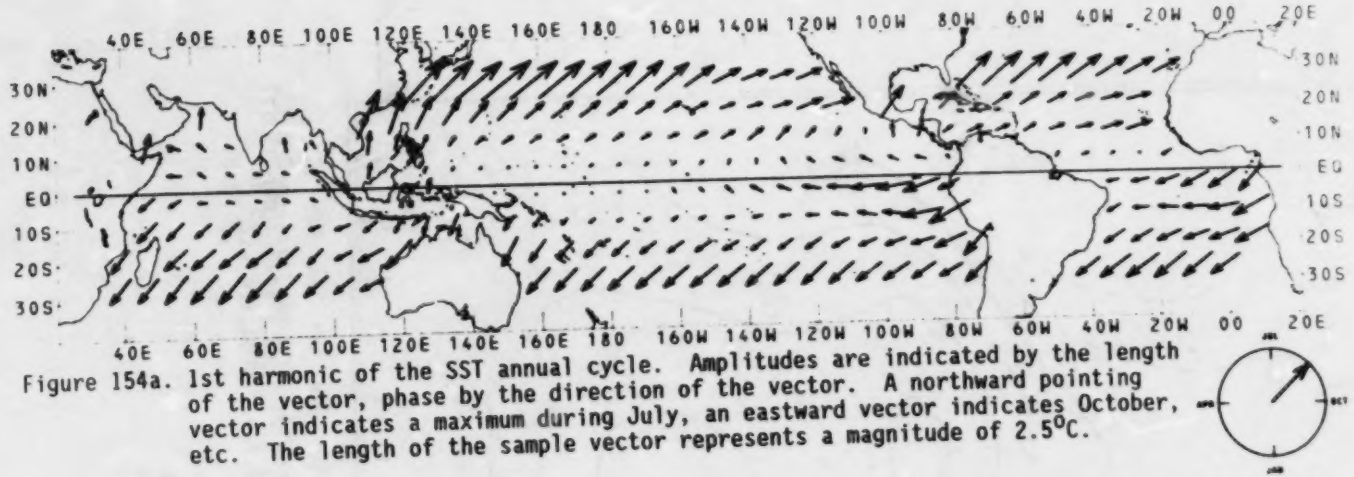

Figure 154a. 1st harmonic of the SST annual cycle. Amplitudes are indicated by the length of the vector, phase by the direction of the vector. A northward pointing vector indicates a maximum during July, an eastward vector indicates October, etc. The length of the sample vector represents a magnitude of 2.5°C.

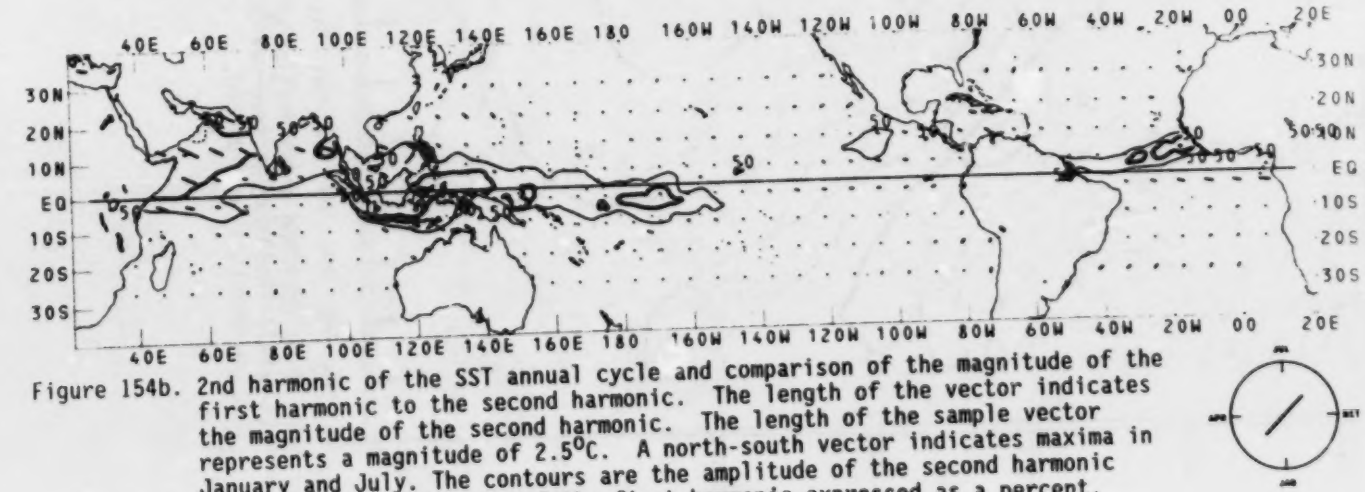

Figure 154b. 2nd harmonic of the SST annual cycle and comparison of the magnitude of the first harmonic to the second harmonic. The length of the vector indicates the magnitude of the second harmonic. The length of the sample vector represents a magnitude of 2.5°C. A north-south vector indicates maxima in January and July. The contours are the amplitude of the second harmonic divided by the amplitude of the first harmonic expressed as a percent. Contours are drawn at 50, 100 and 200 percent.

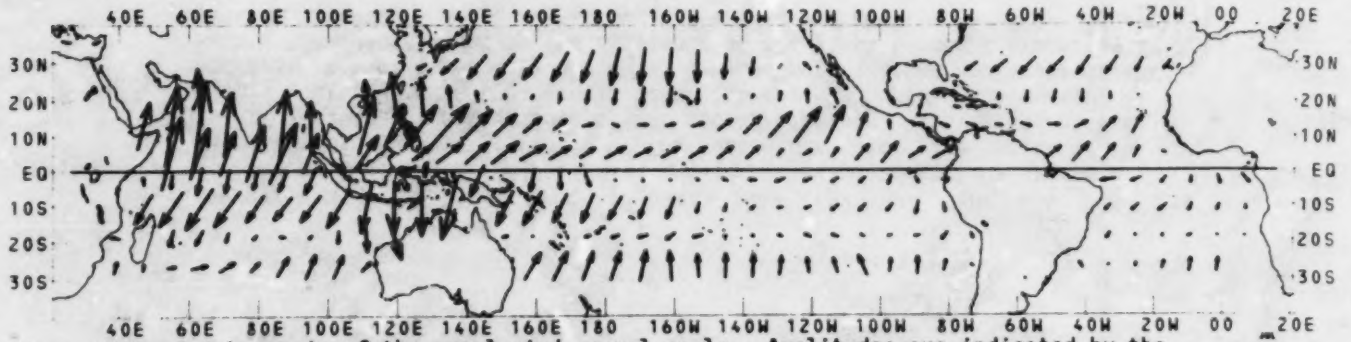

Figure 155a. 1st harmonic of the zonal wind annual cycle. Amplitudes are indicated by the length of the vector, phase by the direction of the vector. A northward pointing vector indicates a maximum during July, an eastward vector indicates October, etc. The length of the sample vector represents a magnitude of 2.5 m/s.

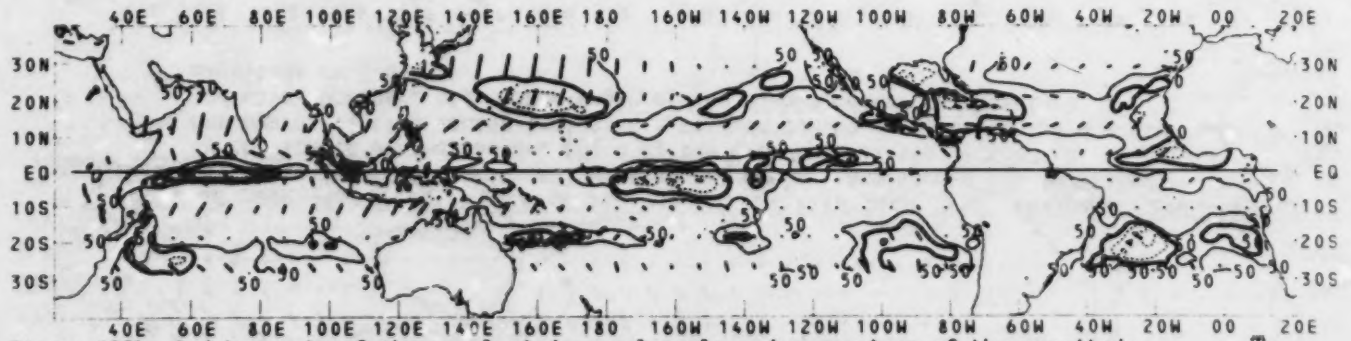

Figure 155b. 2nd harmonic of the zonal wind annual cycle and comparison of the magnitude of the first harmonic to the second harmonic. The length of the vector indicates the magnitude of the second harmonic. The length of the sample vector represents a magnitude of 2.5 m/s. A north-south vector indicates maxima in January and July. The contours are the amplitude of the second harmonic divided by the amplitude of the first harmonic expressed as a percent. Contours are drawn at 50, 100 and 200 percent.

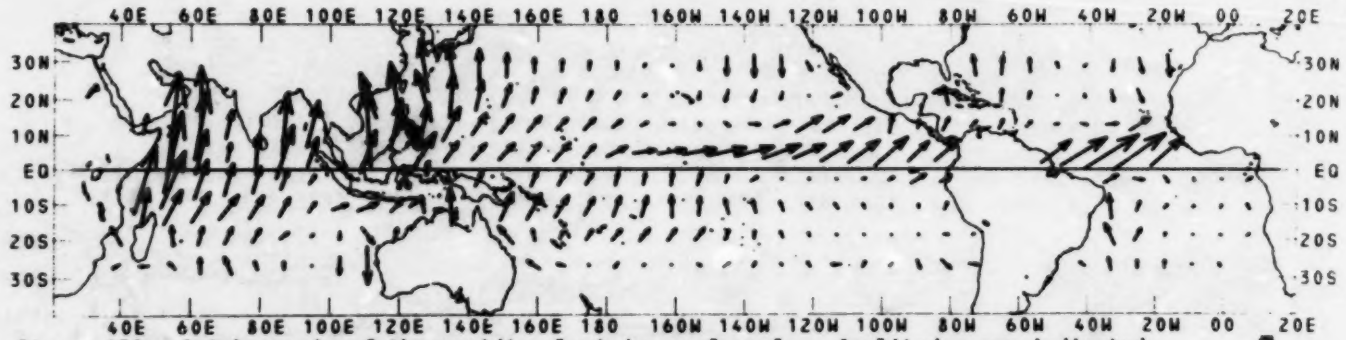

Figure 156a. 1st harmonic of the meridional wind annual cycle. Amplitudes are indicated by the length of the vector, phase by the direction of the vector. A northward pointing vector indicates a maximum during July, an eastward vector indicates October, etc. The length of the sample vector represents a magnitude of 2.5 m/s.

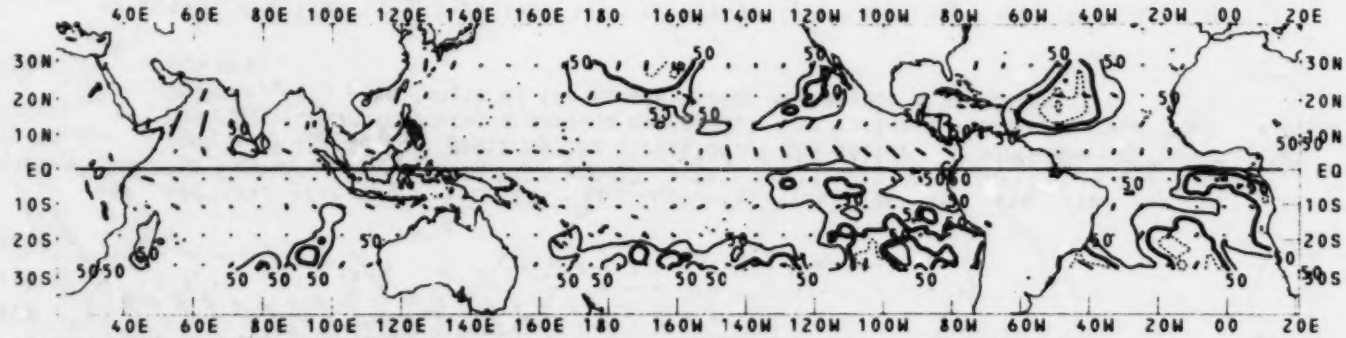

Figure 156b. 2nd harmonic of the meridional wind annual cycle and comparison of the magnitude of the first harmonic to the second harmonic. The length of the vector indicates the magnitude of the second harmonic. The length of the sample vector represents a magnitude of 2.5 m/s. A north-south vector indicates maxima in January and July. The contours are the amplitude of the second harmonic divided by the amplitude of the first harmonic expressed as a percent. Contours are drawn at 50, 100 and 200 percent.

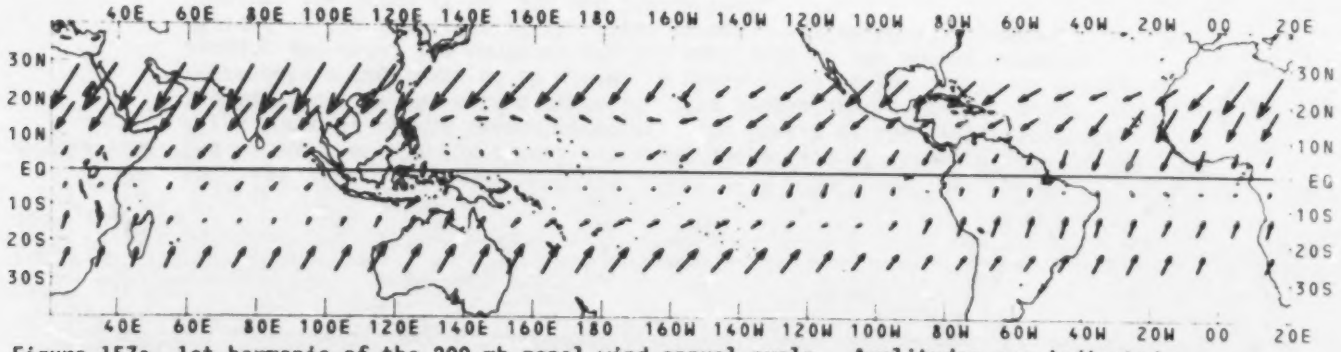

Figure 157a. 1st harmonic of the 200 mb zonal wind annual cycle. Amplitudes are indicated by the length of the vector, phase by the direction of the vector. A northward pointing vector indicates a maximum during July, an eastward vector indicates October, etc. The length of the sample vector represents a magnitude of 10 m/s.

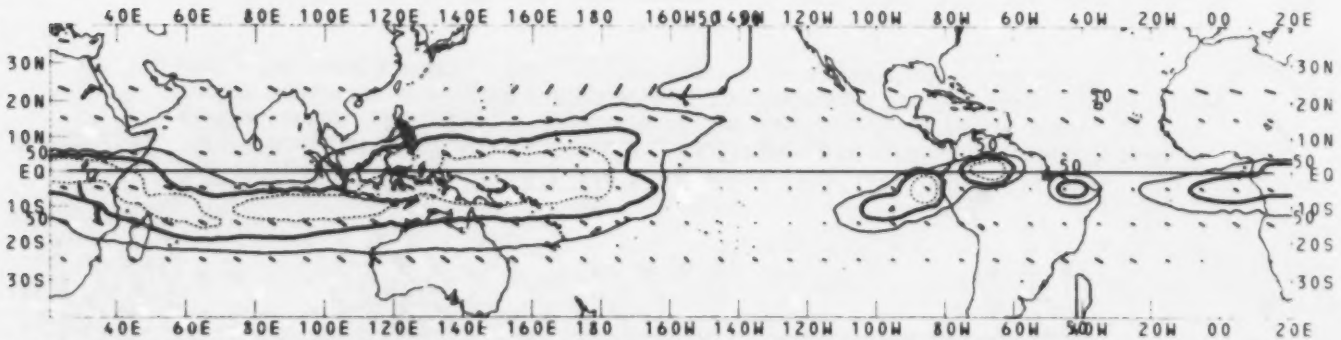

Figure 157b. 2nd harmonic of the 200 mb zonal wind annual cycle and comparison of the magnitude of the first harmonic to the second harmonic. The length of the vector indicates the magnitude of the second harmonic. The length of the sample vector represents a magnitude of 10 m/s. A north-south vector indicates maxima in January and July. The contours are the amplitude of the second harmonic divided by the amplitude of the first harmonic expressed as a percent. Contours are drawn at 50, 100 and 200 percent.

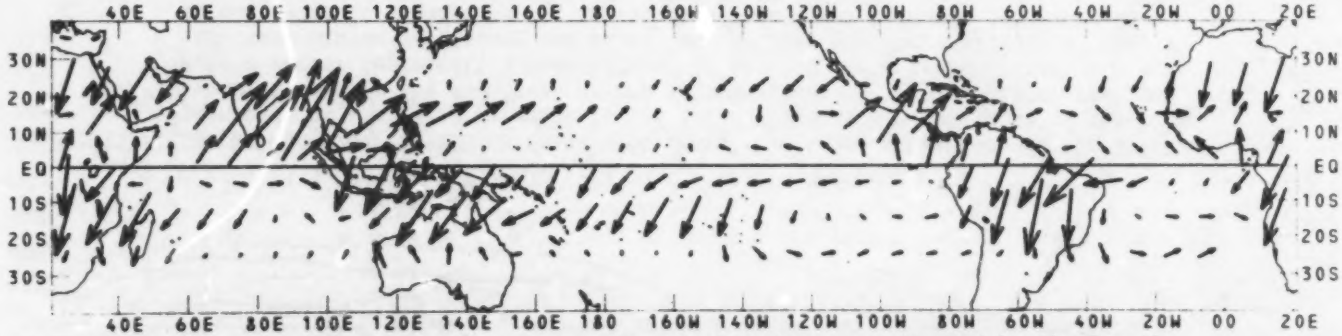

Figure 158a. 1st harmonic of the OLR annual cycle. Amplitudes are indicated by the length of the vector, phase by the direction of the vector. A northward pointing vector indicates a minimum during July, an eastward vector indicates October, etc. The length of the sample vector represents a magnitude of 20 W/m*m.

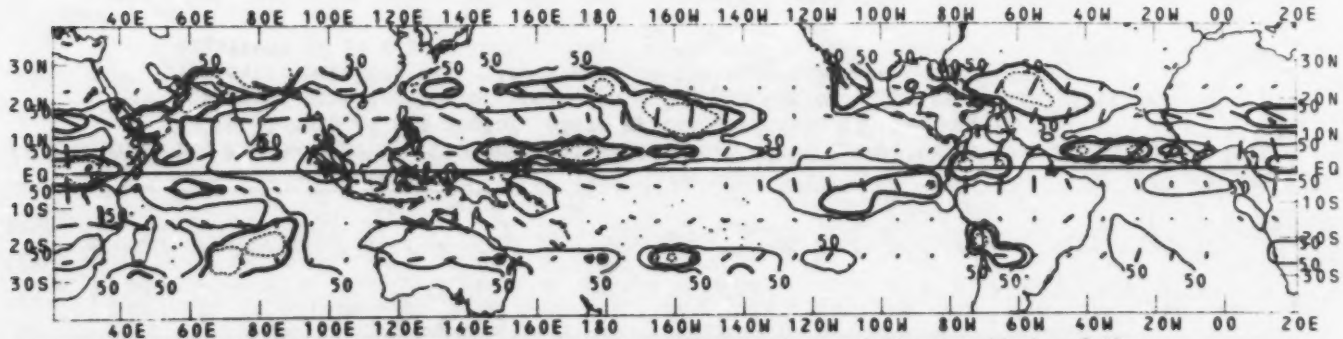

Figure 158b. 2nd harmonic of the OLR annual cycle and comparison of the magnitude of the first harmonic to the second harmonic. The length of the vector indicates the magnitude of the second harmonic. The length of the sample vector represents a magnitude of 20 W/m*m. A north-south vector indicates minima in January and July. The contours are the amplitude of the second harmonic divided by the amplitude of the first harmonic expressed as a percent. Contours are drawn at 50, 100 and 200 percent.

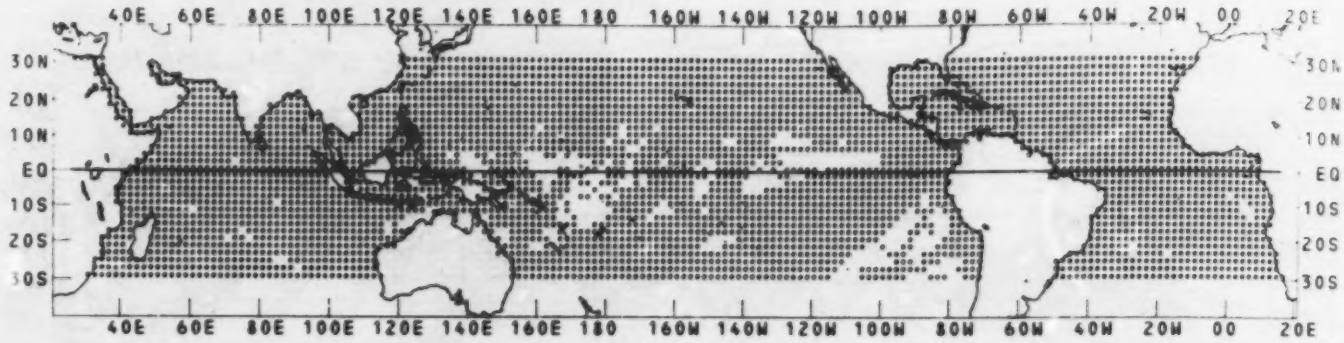

Figure A1. Locations which had at least one observation in a 2^{0} latitude by 2^{0} longitude grid box during any January in the 1950's.

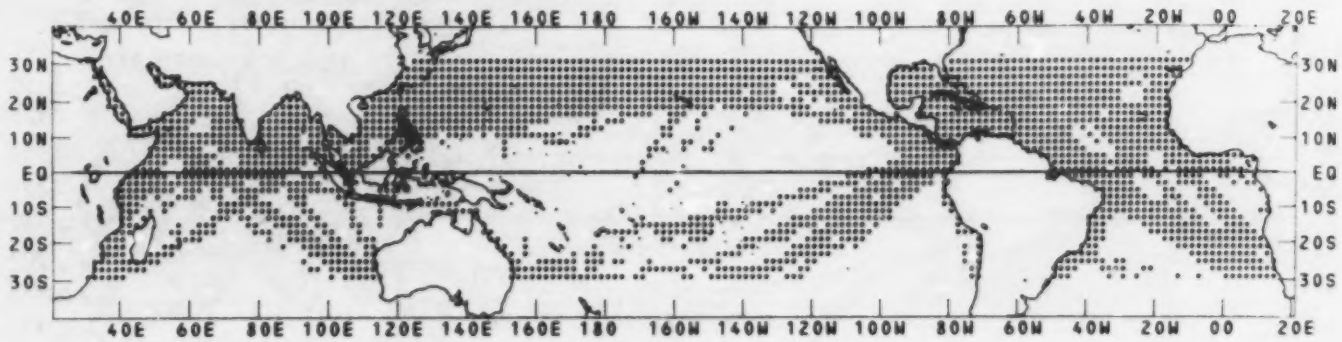

Figure A2. Locations which had data in a 2^{0} latitude by 2^{0} longitude grid box for more than five Januaries during the 1950's.

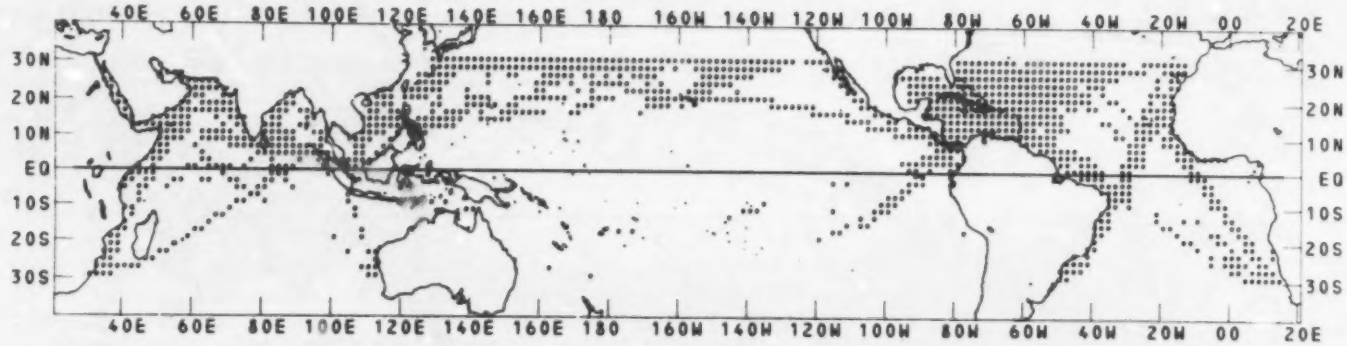

Figure A3. Locations which had data in a 2^{o} latitude by 2^{o} longitude grid box during all ten Januaries during the 1950's.

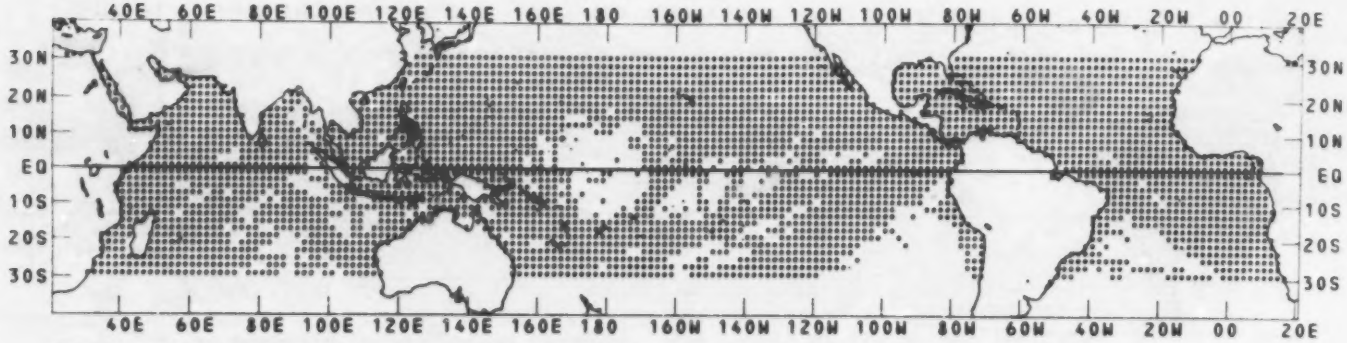

Figure A4. Locations which had data in a 2^{o} latitude by 2^{o} longitude grid box for more than five Januaries during the 1970's.

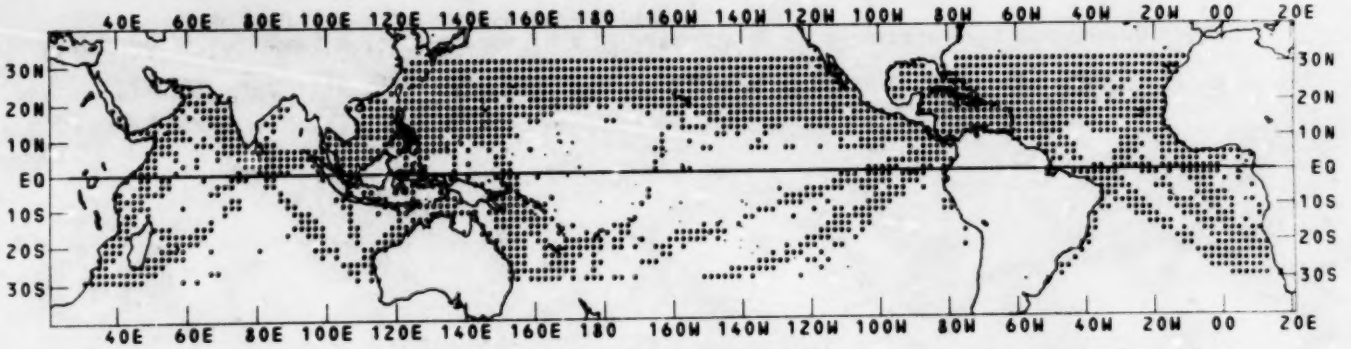

Figure A5. Locations which had data in a 2^{0} latitude by 2^{0} longitude grid box during all ten Januaries during the 1970's.

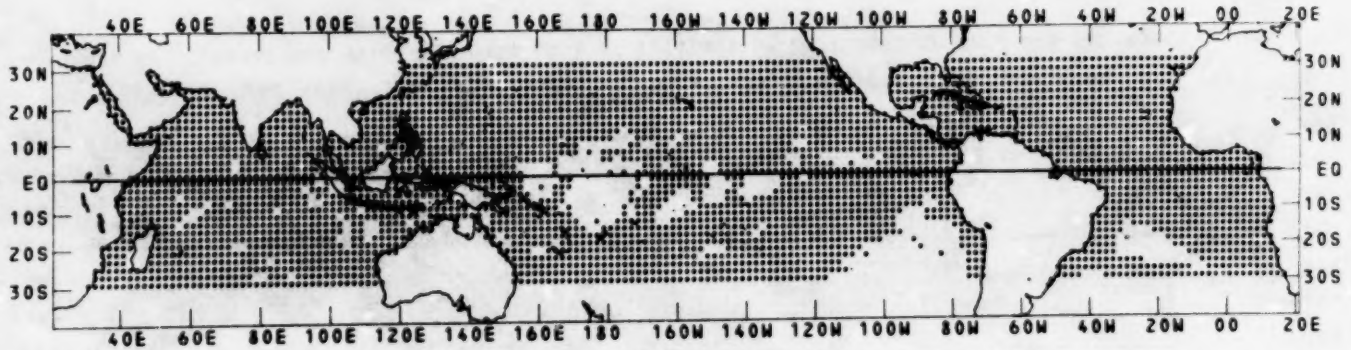

Figure A6. Locations which had data in a 2^{0} latitude by 2^{0} longitude grid box for more than ten Januaries during the 30 year period 1950-1979.

☆ U.S. GOVERNMENT PRINTING OFFICE: 1980—242-312/0408

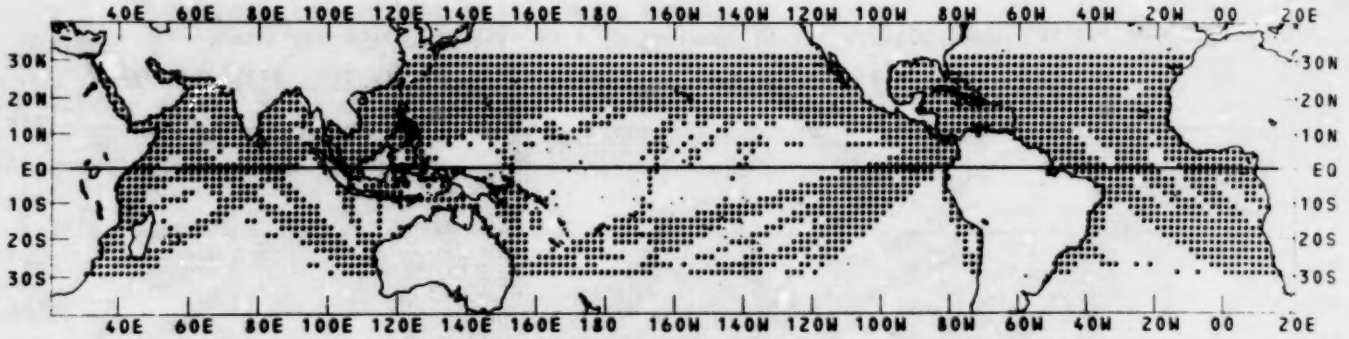

Figure A7. Locations which had data in a 2^{o} latitude by 2^{o} longitude grid box for more than 20 Januaries during the 30 year period 1950-1979.

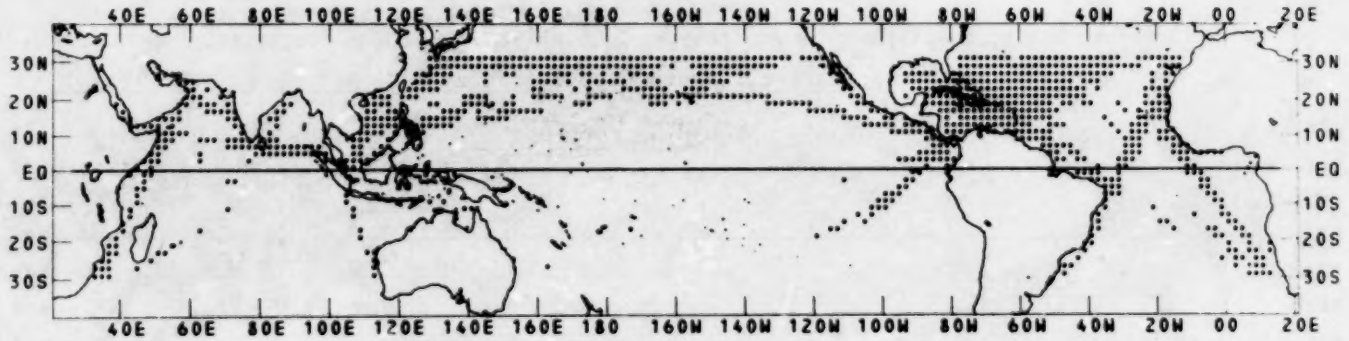

Figure A8. Locations which had data in a 2^{o} latitude by 2^{o} longitude grid box during all 30 years during the 1950-1979 period.